

UNIVERSAL
LIBRARY

OU_160064

UNIVERSAL
LIBRARY

OSMANIA UNIVERSITY LIBRARY

Call No. 551 / A 43 A Accession No. 42784

Author Allen, Lawrence H.

Title Abundance of the elements - 191

This book should be returned on or before the date last marked below.

INTERSCIENCE MONOGRAPHS AND TEXTS IN PHYSICS AND ASTRONOMY

Edited by R. E. MARSHAK

Volume I: E. R. Cohen, K. M. Crowe, and J. W. M. DuMond
THE FUNDAMENTAL CONSTANTS OF PHYSICS

Volume II: G. J. Dienes and G. H. Vineyard
RADIATION EFFECTS IN SOLIDS

Volume III: N. N. Bogoliubov and D. V. Shirkov
**INTRODUCTION TO THE THEORY OF
QUANTIZED FIELDS**

Volume IV: J. B. Marion and J. L. Fowler, *Editors*
FAST NEUTRON PHYSICS In two parts
 Part I: Techniques
 Part II: Experiments and Theory

Volume V: D. M. Ritson, *Editor*
TECHNIQUES OF HIGH ENERGY PHYSICS

Volume VI: R. N. Thomas and R. G. Athay
PHYSICS OF THE SOLAR CHROMOSPHERE

Volume VII: Lawrence H. Aller
THE ABUNDANCE OF THE ELEMENTS

Additional volumes in preparation

INTERSCIENCE MONOGRAPHS AND TEXTS IN PHYSICS AND ASTRONOMY

Edited by R. E. MARSHAK

University of Rochester, Rochester, New York

VOLUME VII

Editorial Advisory Board

- H. ALFVEN, *Royal Institute of Technology, Stockholm, Sweden*
L. V. BERKNER, *Associated Universities, New York, New York*
H. J. BHABHA, *Tata Institute, Bombay, India*
N. N. BOGOLIUBOV, *Academy of Sciences, Moscow, U. S. S. R.*
S. CHANDRASEKHAR, *Yerkes Observatory, Williams Bay, Wisconsin*
J. W. DUMOND, *California Institute of Technology, Pasadena, California*
L. GOLDBERG, *University of Michigan, Ann Arbor, Michigan*
M. GOLDHABER, *Brookhaven National Laboratory, Upton, New York*
C. HERRING, *Bell Telephone Laboratories, Murray Hill, New Jersey*
J. KAPLAN, *University of California, Los Angeles, California*
C. MØLLER, *Institute for Theoretical Physics, Copenhagen, Denmark*
L. NÉEL, *University of Grenoble, Grenoble, France*
W. K. H. PANOFSKY, *Stanford University, Stanford, California*
R. E. PEIERLS, *University of Birmingham, Birmingham, England*
F. PRESS, *California Institute of Technology, Pasadena, California*
B. ROSSI, *Massachusetts Institute of Technology, Cambridge, Massachusetts*
L. SPITZER, Jr., *Princeton Observatory, Princeton, New Jersey*
B. STRÖMGREN, *Institute for Advanced Study, Princeton, New Jersey*
G. TORALDO di FRANCIA, *University of Florence, Florence, Italy*
G. E. UHLENBECK, *University of Michigan, Ann Arbor, Michigan*
V. F. WEISSKOPF, *Cern, Geneva, Switzerland*
H. YUKAWA, *Kyoto University, Kyoto, Japan*

THE ABUNDANCE OF THE ELEMENTS

LAWRENCE H. ALLER

*The Observatory of the University of Michigan,
Ann Arbor, Michigan*



INTERSCIENCE PUBLISHERS, INC., NEW YORK
Interscience Publishers Ltd., London **1961**

Copyright © 1961 by Interscience Publishers, Inc.

ALL RIGHTS RESERVED

Library of Congress Catalog Card Number 61 13870

INTERSCIENCE PUBLISHERS, INC., 250 Fifth Avenue, New York 1, N. Y.

For Great Britain and Northern Ireland

INTERSCIENCE PUBLISHERS LTD., 88/90 Chancery Lane, London W.C. 2

PRINTED IN THE UNITED STATES OF AMERICA

TO THE MEMORY OF:

FRANK WIGGLESWORTH CLARKE

V. M. GOLDSCHMIDT

HENRY NORRIS RUSSELL

Preface

Any attempt to assess abundances of elements is difficult because of the vast variety in types of information available. The earth's crust, meteorites, the sun, stars, and gaseous nebulae all present different problems, require different analytical techniques, and yield results of varying accuracy. Because of its complex geochemical history, the earth's crust has a particularly involved structure. Likewise, meteorites present a host of difficulties in interpretation, although we believe that they are capable of yielding more accurate data concerning the composition of the solar system than the earth's crust.

Accordingly, I have discussed the earth's crust and meteorites in a brief, descriptive way and have concentrated on abundances derived from celestial objects. A short summary of theories of element building in stars is given in the last chapter.

Preparation of this review would have been impossible had it not been for considerable help from chemists, geophysicists, geologists, cosmic-ray and nuclear physicists, and fellow astronomers interested in abundance problems. Valuable comments and advice on the manuscript have been given by S. Bashkin, W. P. Bidelman, Geoffrey Burbidge, Margaret Burbidge, Harrison Brown, A. G. W. Cameron, E. L. Fireman, W. A. Fowler, W. Hazen, G. Hawkins, J. Klarmann, J. F. Lovering, G. J. F. MacDonald, J. B. Marion, R. E. Marshak, D. B. McLaughlin, P. Millman, H. H. Nininger, D. C. Peaslee, B. Peters, A. Poldervaart, K. Rankama, A. E. Ringwood, M. P. Savedoff, S. R. Taylor, H. C. Urey, G. K. Yates, H. Zanstra, the late F. C. Leonard, and others. Helpful discussions with Leo Goldberg, J. L. Greenstein, Edith Müller, and many other astronomers are gratefully recalled. Gratitude is expressed to the University of Chicago Press for permission to use material from the *Astrophysical Journal* and its

Supplement and to the editors of *Reviews of Modern Physics* for permission to reproduce illustrations from the Burbidge, Fowler, and Hoyle article.

April 1961

LAWRENCE H. ALLER

"Lapstone," Glen Road

Emu Plains, New South Wales

Contents

1. The Nature and Scope of the Problem of Elemental Abundances	1
1-1. Introductory Remarks.	1
1-2. Some Definitions.	1
1-3. Sources of Data	3
1-4. Concerning the Luminosities, Color, and Spectra of Stars. .	6
1-5. Element Building in Stars	20
 2 Composition of the Earth and Its Crust	 25
2-1. Introduction.	25
2-2. Concerning the Structure of the Earth	27
2-3. Abundances of Elements in the Earth's Crust	29
2-4. The Internal Structure of the Earth and Its Mean Com- position.	31
2-5. The Structure and Composition of the Planets.	36
 3. Meteorites.	 40
3-1. Introduction	40
3-2. Types of Meteorites.	42
3-3. The Relative Proportions of Different Types of Meteorites	45
3-4. Qualitative Mineralogical and Chemical Features of Mete- orite Compositions.	46
3-5. The Ages and Origins of Meteorites	47
3-6. Loss of Elements by Fractionation.	51
3-7. Abundances in Meteorites.	52
3-8. The Composition of Meteors	57
 4. Abundances Dervied from Gaseous Nebulae.	 60
4-1. Advantages and Disadvantages.	60
4-2. Excitation of the Bright-Line Spectrum	63
4-3. Determination of the Ionic Concentrations.	69
4-4. Estimates of the Ionization.	71
4-5. Composition of the Interstellar Medium.	76

5. Abundances of Elements from Normal Stellar Atmospheres.	79
5-1. The Observational Data	79
5-2. The Continuous Spectra of the Stars	82
5-3. The Coefficient of Line Absorption . .	87
5-4. Transition Probabilities and Damping Constants	91
5-5. The Analysis of Stellar Atmospheres in the Isothermal Approximation	96
5-6. Method of Model Atmospheres	105
5-7. The Application of Model-Atmosphere Methods to the Interpretation of Stellar Atmosphere Compositions .	108
5-8. Stellar Applications of the Model-Atmosphere Techniques	113
5-9. The Composition of the Sun	118
5-10. Deviations from Thermodynamic Equilibrium and Other Complications .	135
5-11. Diffusion	136
5-12. Improvements in the Basic Data and Their Interpretation	138
 6. Abundances from Cosmic Rays	 112
6-1. Introduction	112
6-2. The Energy Spectrum	113
6-3. The Charge Distribution Spectrum	114
6-4. Suggested Abundances in Cosmic Rays	116
6-5. Interpretation of Cosmic-Ray Abundances .	117
 7. Isotope Abundances	 151
7-1. Introduction	151
7-2. Empirical Rules for the Stability of Nuclei.	153
7-3. Terrestrial Isotope Abundances	158
7-4. The Missing Elements	159
7-5. Astrophysical Studies of Isotope Ratios .	160
 8. General Abundance Compilations	 170
8-1. Introduction	170
8-2. The Suess-Urey Semi-Empirical Abundance Tabulation .	174
8-3. Cameron's Abundance Compilation and Nucleogenesis	188
8-4. An Abundance Compilation Based Primarily on Astrophysical Data	190
 9. Composition Differences between Stars	 199
9-1. Introduction	199

9-2. Observable Parameters Influenced by Composition Differences in Stars.....	200
9-3. Population Types and Associated Characteristics.....	202
9-4. Remarks on the Composition of the Spiral-Arm Population	204
9-5. The Composition of the Halo Stars.....	205
9-6. Composition Differences in Intermediate and Disk Stars..	209
9-7. Stars with Abundance Modifications Produced in Their Interiors ..	211
9-8. Carbon Stars and Related Objects. ..	220
9-9. The Heavy-Metal Stars.....	228
9-10. The Peculiar A Star.....	231
9-11. Metallic-Line Stars.....	233
9-12. The Lithium Problem.....	234
9-13. Abundance Differences between Stellar Systems...	236
 10. Theories of the Origin of the Elements.....	 240
10-1. Introduction.....	240
10-2. Earlier Theories of Element Formation...	240
10-3. Formation of Elements in Stars...	243
10-4. Hydrogen Burning ..	246
10-5. Helium-Burning and Alpha-Particle Reactions	249
10-6. The "Equilibrium" Process.....	252
10-7. Neutron-Capture Processes	254
10-8. The Problem of the Synthesis of Deuterium, Lithium, Beryllium, and Boron ..	261
10-9. Element Building in the Atmospheres of Magnetic Stars..	266
10-10. Concluding Remarks	267
 Author Index.....	 271
 Subject Index ..	 276
 Index of Stars, Clusters, and Nebulae ..	 282

The Nature and Scope of the Problem of Elemental Abundances

1-1. Introductory Remarks

The quantitative distribution of the elements in the universe is a classical problem in cosmochemistry and astronomy. When we speak of the chemical composition of the "universe" what we really mean is the composition of the stars and gaseous nebulae in the neighborhood of the sun, of the various objects in the solar system, and particularly that of the sun itself. As far as we have been able to test the hypothesis, the chemical composition of our part of the galaxy seems to be representative of that of the observable part of the astronomical universe.

At the outset, let us enumerate the reasons why we are interested in the abundances of the chemical elements:

1. We should like to know the primordial composition of the solar system and its relation to the present composition of the earth and other planets. Such data might throw some light on vexing problems connected with the origin and chemical history of the earth.

2. A knowledge of the composition of the local part of our galaxy is needed for the construction of models of the sun and stars and for a complete understanding of physical and chemical processes taking place in stellar atmospheres and in the interstellar medium.

3. The observed abundance distribution of elements, and particularly of the individual nuclides, enables us to test the hypotheses that have been proposed for element formation.

1-2. Some Definitions

The methods of geochemistry and of astrophysics emphasize the determination of abundances of *elements*, i.e., the atoms are grouped according to their atomic numbers. Since the abundance distribution

of the elements is a function of the stability of the various atomic nuclei and of their evolution, the data of most fundamental importance are the abundance values of the individual nuclear species or nuclides.

Any given nucleus is described by two parameters: Z = charge on nucleus (i.e., the proton number) and A = atomic weight or mass number. Alternately, one may use in place of A , N , the number of neutrons. More than 700 nuclides have been recognized in nature or have been prepared artificially. Suess and Urey list 347 of them in their abundance table. In addition, there exist several nuclides that are found in nature in radioactive decay series.

Isotopes have the same value of Z , the proton number, but different atomic weights,¹ A , and numbers of neutrons. *Isobars* have the same A 's but different values of N and Z ; therefore they comprise different elements. *Isotones* have the same number of neutrons, N , but different values of A and Z . Another quantity of importance is the neutron excess, $I = N - Z$. Nuclides with the same neutron excess are called *isodiaspheres* by some writers. A nucleus in an excited state of measurable lifetime is an *isomer*. Thus, In^{115} is the most abundant isotope of indium. It has an excited state, In^{115*} , with an energy of 0.335 Mev and a half-life of 4.5 hr. Some of the atoms in this isomeric state decay to the lightest odd- A isotope of tin, Sn^{115} , by β^+ decay.

Table 1-1 gives examples of isotones, isotopes, isobars, and isodiaspheres for elements in the neighborhood of calcium. The percentages refer to the fraction that a particular isotope contributes to the total number of the atoms of a given element. The relative abundances of the isotopes of a given element can be measured with high accuracy by means of the mass spectrograph.

With terrestrial samples and meteorites it is possible to get the relative isotopic abundances with a mass spectrometer, but to get the

¹ We must distinguish between the chemical and physical systems of atomic weights. In the chemical system the atomic weight of atmospheric oxygen has been taken traditionally as 16.000, whereas the physical system sets the atomic weight of the most abundant isotope of oxygen, ^{16}O , as 16.000. Hence, atomic weights in the physical system are greater than those in the chemical system. Recently, the IUPAP decided to adopt a scale based on $\text{C}^{12} = 12.000$. This convention will change the chemical scale hardly at all, but will slightly influence the physical scale.

Table 1-1. Illustration of Isotones, Isotopes, Isobars, and Isodiaspheres

Isotones $N = 20$				Isotopes $Z = 20$ (calcium)		
Element	Z	A	% of element	N	A	% of element
Sulfur	16	36	0.0136	20	40	96.97
Chlorine	17	37	24.471	22	42	0.64
Argon	18	38	0.063	23	43	0.145
Potassium	19	39	93.10	24	44	2.06
Calcium	20	40	96.97	26	46	0.0033
				28	48	0.185

Isobars $A = 40$				Isodiaspheres $I = 4$			
Element	Z	N	% of element	Element	A	N	Z
Argon	18	22	99.61	Sulfur	36	20	16
Potassium	19	21	0.0119	Argon	40	22	18
Calcium	20	20	96.97	Calcium	44	24	20

relative abundances of isotones or isobars requires a knowledge of the relative abundances of the elements themselves.

1-3. Sources of Data

Our first task in this project is to ascertain the "normal" or average composition of our part of the universe, and our second task is to try to see, although briefly, how the present distribution of elemental abundances came into being. Our sources of data are: (1) the sun and the stars, (2) the gaseous nebulae and the interstellar medium, (3) cosmic rays, (4) the earth's crust, and (5) meteorites.

From the outset there is one fact that we must emphasize and keep constantly in mind. The observable data with which we shall be dealing are always affected by the specific chemical and physical history the object under consideration has experienced, or by the hindering hand of observational selection. For example, improvement of experimental techniques will permit us to determine relative abundances of the most important of the heavy elements to be found in cosmic rays. Even the somewhat incomplete knowledge available to

us at present indicates that the abundance distribution of the cosmic-ray particles is not typical of the abundance distribution of the atomic species found in the solar system. The differences are to be sought in the mode of production of these high-energy particles.

Again, we can collect the rocks of the earth's crust, have a chemist analyze them, and get a geologist to estimate for us the relative proportions of the various types of our rocks as they occur on the surface of the earth. Likewise, we can analyze the salty waters of the sea and the gases of the air, and from all of this information build up a more or less representative picture of the composition of the uppermost crust of the earth, but what can we say of the mantle which lies below the Mohorovicic discontinuity, and what can we say of the presumably liquid core that lies below the mantle? We have reasons for believing that the mantle and the core have somewhat different compositions, the core having a larger proportion of elements of the iron group. To estimate the composition of the earth as a whole, therefore, is a difficult problem since it involves the composition of the interior concerning which relatively little is known at present.

Many investigators believe that the average composition of the earth may resemble that of certain types of meteorites. Although the meteorites which the observer finds in collections are predominantly of the iron-nickel type, the preponderant type of meteorite falling upon the earth is of the stony variety. Among these stony meteorites or *aerolites*, the *chondrites* comprise the most important class. These objects are believed by some to represent the best sample available to us of the non-volatile materials out of which the solar system has been formed. They are particularly useful for getting relative abundances of elements of roughly similar chemical properties. Nevertheless, since the mechanism for formation of meteorites and the geochemical history of the earth are not known, use of data obtained from either of these sources in the derivation of "cosmic" abundances requires care and judgment.

Our analysis of astronomical objects other than meteorites is restricted to a careful interpretation of the spectra of light which they emit. The stars tell us what they please and we have to deduce from their radiation what information we can about their physical and chemical makeup. In some respects, the gaseous nebulae offer a number of important advantages. All parts of a typical gaseous nebula

are accessible to observation, and mechanisms for the excitation of their spectra appear to be reasonably well understood. On the other hand, the deviations from thermodynamical equilibrium experienced by the attenuated gas are so severe that it is often difficult to go from observable line intensities to the actual abundances of responsible elements.

Both gaseous nebulae and atmospheres of the sun and stars provide a less distorted picture than do other sources in that the relative proportions of light and heavy elements are not affected by selective losses as are the earth and planets, although it is possible that the effects of diffusion may play some role in very ancient stars. On the other hand, the composition of the surface layers is not necessarily the same as that of the interior. In most stars hydrogen is converted into helium in the interior, but there is no mixing between surface layers and deep interior, at least not until the star reaches a very advanced stage in its evolution.

For a number of reasons we shall adopt the atmosphere of the sun as the standard of chemical composition. The sun appears to be a typical star whose atmospheric layers show little evidence of mixing with the deep interior where energy is generated as hydrogen is converted into helium at a temperature of about $15,000,000^{\circ}\text{K}$. Therefore, unless diffusion has seriously modified the abundance values of the heavier elements in its atmosphere, the surface layers of the sun should represent rather well the primordial composition of the solar system. An enormous effort has been expended in analyzing the sun from its spectrum, but we shall see that much more work remains to be done, although very difficult observations and even more difficult terrestrial experiments will be required.

Using the solar atmosphere as a standard composition, we find that the planets are depleted in elements forming volatile compounds. Jupiter and Saturn appear to have retained most of their initial supply of gases, although Uranus and Neptune presumably have lost most of their hydrogen, whereas the terrestrial planets like the earth have lost most of the other permanent gases as well. Evidently the evolution of the solar system has resulted in the physical loss of much of the original material.

Because of their huge masses, the other stars, like the sun, have retained elements of all different atomic weights in their original proportion except as these ratios have been modified by thermonuclear

processes and radioactive decay. Thus deviations from uniformity in composition presumably arise from nuclear processes occurring within their own interiors. The spectra of the stars may be studied in much the same way as that of the sun, although usually in less detail, since spectroscopic observations of high dispersion can be made only with relatively bright stars. Insofar as they have been analyzed, the spectra of most stars show striking similarity to others of the same surface temperature and surface gravity. More specifically, the compositions of most of the stars seem to resemble that of the sun fairly closely. Exceptions must be made for stars that are presumably very much more ancient than the sun and for certain highly evolved stars which show in their atmospheres the evidences of nuclear transformations taking place within their interiors. Since the chemical analyses of the sun and stars will occupy the bulk of our discussions, let us first of all review some of their essential properties that will be required in later chapters.

1-4. Concerning the Luminosities, Color, and Spectra of Stars

The observable parameters most frequently available for stars are: (1) their positions in the sky, (2) their brightnesses as measured by a wide band-pass light-measuring device, usually a photographic plate or a photocell with a filter, and (3) their colors.

Unless the star is very faint, say a thousand times fainter than the faintest star visible to the unaided eye, we can also observe its spectrum and its motion in the line of sight. If measurements of position are obtained with many years separating the two epochs of observation, it is likewise possible to get the motion across the line of sight or the so-called *proper motion*. For nearby stars the direct trigonometric parallax can be measured, whereas for more remote stars one must employ statistical methods making use either of the motions of the stars or their association with objects of known intrinsic luminosities. The astronomical yardstick of stellar distances, the *parsec*, is 3.26 light years. As seen from a distance of 1 parsec, the maximum observed separation between the sun and the earth would amount to 1 second of arc.

The brightnesses and colors of stars are usually expressed in terms of quantities called magnitudes. The magnitude scale is logarithmic; a 5-magnitude difference corresponds to a hundredfold ratio in brightness while a 1-magnitude difference corresponds to about a 2.5 ratio

in brightness. Thus, a star of the 1st magnitude is two and a half times brighter than one of the 2nd magnitude, but is one hundred times as bright as a star of the 6th magnitude. The zero point of the magnitude system is arbitrarily defined. The brightest star in the sky, Sirius, has a visual magnitude of -1.4 , the full moon has an apparent magnitude of -12 , and the sun an apparent magnitude of -26 . The faintest star visible to the unaided eye is around 6, and the faintest star that can normally be photographed with a large telescope is around 21. The apparent magnitude, m , refers to the observed magnitude as the star actually appears in the sky, whereas the absolute magnitude is the magnitude the star would have if it could be observed at a distance of 10 parsecs.¹ On this scale, the absolute magnitude of the sun is 4.7, which means that it would be nicely visible on a clear moonless night. Sirius would be fainter than it appears at present, $M_v = 1.5$, while the bright blue star in Orion, Rigel, $M_v = -6$, would cast a distinct shadow, outshining every object in the night sky except the moon.

We want to emphasize that the absolute magnitude of a star expresses its intrinsic brightness as measured with a light-sensitive device which usually has a fairly broad band-pass. It does not refer to the total energy radiated, and if we wish to estimate the total radiation output of the star we must apply large corrections to the measured magnitudes both for cool stars, because of the large amount of their infrared radiation, and for hot stars because of the preponderance of radiation emitted in the inaccessible ultraviolet. The magnitudes when thus corrected are called *bolometric magnitudes*.

The colors of stars may be measured with the aid of a photographic plate or by a photocell equipped with appropriate filters. For many years, most astronomers used only two colors. They measured the so-called photographic magnitudes of stars with a blue-sensitive plate with no filter and the so-called photovisual magnitudes of stars with a yellow-sensitive plate and a yellow filter. The difference between the photographic and photovisual magnitude is called the *color index*. A red star which is bright visually and faint photographically has a positive color index. More recently, photoelectric color measurements have been made in three colors, usually a so-called

¹ The relation between absolute magnitude, apparent magnitude, and distance in parsecs is $M = m + 5 - 5 \log r$.

ultraviolet or U color, a blue or B color which corresponds roughly to the photographic magnitude system, and finally, the visual or V color. Magnitudes measured in the V system are very close to visual magnitudes.

Although the galaxy contains thousands of millions of stars, the spectra of nearly all of them can be classified into a relatively small number of spectral classes. A typical star like the sun shows a continuous spectrum upon which are impressed dark lines characteristic of familiar elements or compounds. The spectral classification now in use was devised at Harvard in the closing years of the past century. Since it was an empirical classification, carried out without regard to any theoretical interpretation and with observational techniques that were novel and in their day difficult, it is not surprising that the spectral sequence does not follow the alphabetical order.

In order of diminishing temperature or increasing redness, the spectral sequence is as follows: *O*, *B*, *A*, *F*, *G*, *K*, and *M*. The stars of spectral class *O* have surface temperatures ranging from around 30,000 to 50,000°K. They show the lines of hydrogen, helium, and other permanent gases in high stages of ionization. The stars of spectral class *B* range in surface temperature from about 12,000 to 28,000°K and are characterized by strong lines of hydrogen and helium. There are also lines of permanent gases usually in the first ionization stage. In spectral class *A* (7800 to 10,000°K), the hydrogen lines attain their greatest strength and in the later subdivisions of spectral class *A* the lines of the metals become increasingly prominent. In spectral class *F* (7700 to 6100°K) the hydrogen lines, although still the strongest features in the spectrum, are less impressive than in class *A*, and the metallic lines are stronger. In particular, the H and K lines of ionized calcium are very strong. The sun, whose temperature is 5780°K, belongs to spectral class *G* which is characterized by intense lines not only of ionized metals but also of neutral metals as well. The strongest feature in the spectrum are the H and K lines of ionized calcium. In spectral class *K* the lines of the metals become yet stronger; the star is cooler having a temperature between about 3700°K and about 5000°K if it is similar to the sun. There also appears bands characteristic of certain fragmentary molecules or radicals, particularly cyanogen, CN, OH, and CH. In spectral class *M*, in which the temperature is 3800°K or less, appear intense lines of titanium oxide. In addition to these regular spectral classes, there are

also side branches among the cooler stars, spectral classes *R*, *N*, and *S* whose significance will be discussed presently. Decimal subdivisions to spectral classes are also employed; thus the sun is classified as *G2* which means that it falls between *G0* and *K0* but much closer to *G0*.

As previously emphasized, spectral class is correlated with the color of a star and with its surface temperature. The entire spectral sequence from *O* to *M* corresponds to stars of very nearly the same chemical composition. The essential parameter that produces spectral differences from one star to another is the surface temperature (and, to a lesser extent, atmospheric pressure). At higher temperatures all gases become highly ionized. In particular, metallic lines disappear because all resonance transitions of highly ionized metals fall in the inaccessible ultraviolet. Those lines which do fall in observable ranges come from such high levels that few ions can be excited to them. Hence, only a few metallic lines appear in hotter stars. They are due to abundant elements such as magnesium, aluminum, and iron. At lower temperatures metal atoms are only singly ionized and their important lines fall in accessible spectral regions, while at the very lowest temperatures, conditions permit formation of molecules such as carbon monoxide and the hydroxyl radical OH.

The behavior of the hydrogen lines merits special attention. The Balmer lines arise from the second level, 10.6 volts above the ground level, whereas the resonance lines (the Lyman series) fall in the far ultraviolet which is totally inaccessible from earth's surface. In the hot *O* and *B* stars, hydrogen is predominantly ionized and only a small fraction of the neutral atoms are in the second level capable of absorbing the Balmer lines. At the low temperatures of the *K* and *M* stars, hydrogen is neutral but extremely few atoms are excited to the second level. In between, at spectral class *A*, the number of atoms excited to the second level has become appreciable while the ionization of hydrogen has not yet decimated the number of neutral atoms. Hence, the hydrogen lines show a pronounced maximum at spectral class *A* in the spectral sequence. The metallic lines also show maxima at temperatures corresponding to their optimum conditions of excitation. Resonance lines of the neutral atoms go on increasing in intensity to the very lowest temperatures until they are finally concealed by the formation of strong molecular bands. A stellar spectrum

indicates not only atmospheric chemical composition and temperature but also atmospheric pressure and hence surface gravity.

Let us now turn briefly to some fundamental correlations that exist between observable stellar properties. In particular, we must mention a correlation between absolute luminosity and spectral class. This spectrum-luminosity correlation, often referred to as the Russell diagram or the Hertzsprung-Russell diagram, is one of the most fundamental correlations that has been established in observational astronomy. In order to construct such a diagram we must know the distances, apparent magnitudes, and spectra of the stars. In some instances we plot stellar absolute magnitude against color index instead of absolute magnitude against spectral class. Since color index and spectral class are both closely connected with a star's surface temperature, it is possible to convert from one of these systems to the other, depending on the circumstances of the investigation. Since stellar colors can be measured for rather faint objects, whereas stellar spectra can be classified only for brighter objects, color-magnitude plots are emphasized in studies involving apparently very faint stars.¹

Essentially two procedures may be followed to construct a luminosity-color or luminosity-spectrum diagram. We may utilize stars of known apparent magnitude and distance in the neighborhood of the sun or we may construct a color-apparent magnitude diagram for a star cluster and then convert the apparent magnitudes to absolute magnitudes by fitting the so-obtained diagram with the similar diagram obtained for stars in the solar neighborhood. Consider, first of all, the construction of a Russell diagram for the stars in the solar neighborhood. Absolute magnitudes of faint, nearby stars can be determined with relatively high accuracy since their distances can be measured relatively easily. On the other hand, distances of more remote stars frequently cannot be established with a corresponding accuracy. Hence, high-luminosity stars in the diagram will tend to be more affected by errors than will low-luminosity stars. Further-

¹ For main-sequence stars of the spiral-arm or galactic-cluster population, the B - V colors and spectral types are related as follows:

-0.3	-0.2	-0.1	0.0	0.1	0.2	0.3	0.4
B0	B3	B8	A0	A3	A7	F0	F3
0.5	0.6	0.7	0.8	1.0	1.2	1.5	
F7	G0	G8	K0	K3	K5	M1	

more, observational selection tends to favor selection of stars of high luminosity. They can be seen at very great distances from the sun, whereas faint stars can be observed only in the immediate solar neighborhood. Hence, a Russell diagram compiled for all stars brighter than the 8th apparent magnitude, for example, would show a very strong effect of observational selection. On the other hand, if we seek to construct such a diagram using only those stars that fall within a pre-assigned distance, say within 10 parsecs or 33 light years of the sun, we will find that very few stars of intrinsically high luminosity are included, and that most of the objects are actually fainter than the sun.

Therefore, although the spectrum-luminosity diagram is not necessarily quantitatively correct in that it shows the relative numbers of stars of different luminosities in their correct proportions, it is useful in showing the types of stars that are found insofar as these two parameters, luminosity and surface temperature, are concerned. It is clear that if we could transform spectral class or color accurately to surface temperature, and if we could reduce observed visual absolute magnitude to actual intrinsic luminosity, we could convert the spectrum-luminosity diagram into a relation between stellar luminosities and radii. One difficulty is that we normally plot color against visual absolute magnitude. To go from visual absolute magnitude to intrinsic luminosities, one must apply certain correction factors which depend on the temperature of the star. These bolometric corrections, as they are called, allow for the amount of energy which is radiated in spectral regions that are not covered by the light-sensitive device used to measure the visual magnitude. The relation between intrinsic luminosity and radius is of fundamental interest in the theoretical interpretation of stellar structure and evolution.

A schematic spectrum-luminosity diagram for the solar neighborhood is shown in Fig. 1-1. Most of the stars fall along a relatively thin curve running diagonally from the upper left-hand, i.e., bright blue, to the lower right-hand, faint red, corner. This thin band is referred to as the *main sequence* or sometimes as the *dwarf sequence*. There is a continuous gradation of stars from the top to the bottom with respect to luminosity and surface temperature which decline, mass which also declines, and density which continuously increases. The sun falls at the point G2, 4.7. It is a typical dwarf star somewhat brighter than average, and we often express luminosities, radii, and

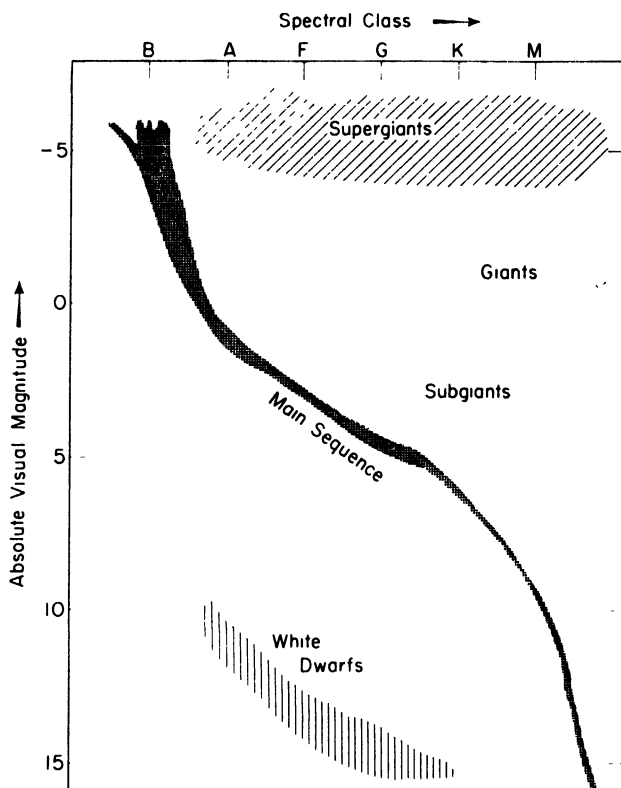


Fig. 1-1. Spectrum-luminosity diagram for the solar neighborhood. Spectral class (abscissa) is plotted against visual absolute magnitude (ordinate). The cross indicates the position of the sun.

masses of the other stars in terms of corresponding quantities for the sun.

Above and to the right of the main sequence fall a number of stars; one group is concentrated near absolute magnitude 0 and ranges in spectral class from around middle *G* to late *M*. These stars are referred to as *giants*. Between the giants and the main sequence there fall a few stragglers which are often referred to as *subgiants*. Many of these objects are found in eclipsing binary systems. Scattered across the top of the diagram is a thin sprinkling of objects ranging from absolute magnitudes around -2 to -7 or -8. These are the rare but

highly luminous *supergiants*. They include objects such as Antares and Betelgeuse, which if placed in the position of the sun would engulf the earth and the orbit of Mars as well. By contrast, the giant stars have diameters of 40 to 60 million km, while the stars of the main sequence range in diameter, for the most part, from 3 or 4 million miles to a few hundred thousand miles.

To the left of the main sequence, and far below, lies another group of stars, namely, the *white dwarfs*. These stars are very much smaller in size than the sun, although many of them have masses comparable with it. Their densities are correspondingly very high. Numerically, the main sequence contains more stars than all other groups put together, but the white dwarfs are more numerous than giants and supergiants or even all main-sequence stars more than a magnitude brighter than the sun.

We emphasize that the spectrum-luminosity diagram depicted in Fig. 1-1 applies to the solar neighborhood, i.e., to a part of the local spiral arm in our galaxy. In the central bulge of our own galaxy or in an elliptical nebula, such as the companions to the Andromeda spiral, M32 and NGC205, the Russell diagram is considerably different. Analogous diagrams may be constructed for galactic clusters (Fig. 1-2), such as objects like the Pleiades, the Hyades, Coma Berenices, and the globular clusters, although the latter objects are so remote that we must use magnitudes and colors rather than magnitudes and spectral types.

Color-luminosity diagrams for clusters offer a number of opportunities for studies of stellar evolution. First, all stars are at essentially the same distance from the observer so that their relative luminosities yield their absolute luminosities as soon as the intrinsic luminosity of any one star is found. This step is usually accomplished by comparing stars on the main sequence at about the same luminosity and color as the sun. Second, all stars have essentially the same chronological age. A possible exception may be made for very faint stars (much fainter than the sun) which may not yet have evolved by contraction to the main sequence. Third, all stars have the same chemical composition.

We must distinguish between galactic clusters, such as the Pleiades or the Hyades on the one hand, and globular clusters on the other (Fig. 1-3). The galactic clusters have ages ranging from a few million years to several thousand million years so that the effects of stellar

ceased, or occurs very infrequently, whereas in the spiral arms, as we shall see, stars appear to be yet in the process of formation.

It is possible to interpret the color-luminosity array (Russell diagram) in terms of evolutionary stages in the history of a star. The main sequence corresponds to stars that are relatively young. They are still burning hydrogen into helium in their cores; the hydrogen has not yet been exhausted from the central regions. The giants and supergiants are stars that were once on the main sequence but have since converted all the hydrogen in their cores into helium. The conversion of hydrogen into helium now occurs in a thin shell surrounding the inert core. Surrounding this energy-producing shell there is an extended, less dense envelope that accounts for the large physical dimensions of these stars. The white dwarfs represent the last stage in stellar evolution; presumably they follow more or less immediately the giant and supergiant phases, but the exact mechanism or path by which a star evolves into the white-dwarf stage is not now known.

Let us consider briefly the evolution of a star. A number of lines of evidence indicate that stars are being created continually from grains and gas of the interstellar medium in the spiral arms of our galaxy. Highly luminous main-sequence and supergiant stars always appear to be associated with dust and gas clouds in our own and other galaxies. These stars are absent in stellar systems where no dust or gas exists or where the gas simply forms a halo surrounding the system. Photographs of extended luminous dust and gas clouds in our own galaxy sometimes show compact dark clouds or globules superposed upon them. These globules may be the earliest stages in the formation of proto stars.

In some regions of the sky, such as near the stars ζ Lacertae, one finds a number of hot luminous stars moving away from a common point in space as though they had all been formed there and had sufficient kinetic energy to escape from their mutual gravitational attraction. A number of such expanding associations, as they are called, have been found. Some are characterized by highly luminous *O* and *B* stars, others by more modest stars near spectral classes *G* and *K*. One of the most striking examples is the pair of stars AE Aurigae and μ Columbae, which (although many degrees apart in the sky at the present time) have motions which show that they originated at a single point in the constellation of Orion less than two million years ago!

The color-magnitude arrays for some clusters, such as in Orion, Messier 8, and NGC2264, show evidence of star formation. If one plots the color-magnitude array in the usual way, he finds that a conventional main sequence is defined for stars brighter than about $M_v = 0$. Below this point the stars appear to fall above the main sequence, and furthermore they show abnormal spectra which often are characterized by bright lines. Their positions on the color-magnitude array correspond exactly to the contracting phase of a star evolving toward the main sequence.

The rate of radiation of a star and consequently its life span will depend upon its mass. The more massive a star, the more rapidly it will radiate energy, the energy output being proportional not simply to the mass but to its third or higher power. Hence a star twice as massive as the sun will be of the order of ten times as bright; correspondingly, a star less massive than the sun will be fainter. A star like the sun would have a life span of the order of 7000 million years, one twice as massive would be gone in 2000 million years, while a faint red-dwarf star like Krueger 60 could last for 50,000 or 100,000 million years. A star ten times as massive as the sun will consume its fuel thousands of times as rapidly, and hence the lifetimes of such massive and luminous objects, the bright blue stars of our own and other galaxies, will be measured not in thousands of millions but in tens of millions of years. Since the age of the solar system is of the order of 5000 million years and presumably the galaxy is much older, the main-sequence *O* and *B* stars must be relatively recent creations. They cannot be ordinary stars like the sun, built up to huge masses by the accretion of material obtained in passing through a dense cloud of interstellar material. On the contrary, they must be stars that are built from the beginning in the interstellar medium.

The exact process of star formation is not known, either theoretically or observationally, but it is believed that in the cold regions of the interstellar medium where solid grains and gas are collected, effects of radiation pressure, differential gas pressure, and perhaps magnetic fields may conspire to create large masses of material that become sufficiently dense to contract under the influence of their own gravitational fields. A large contracting mass presumably would have a considerable angular momentum and the only way this angular momentum could be dissipated would be for the mass to break up into a number of submasses. Then a whole group of stars may form in-

stead of only one. Some of these in turn evolve into binary stars or even into solar systems.

At the beginning of its life a star shines by Kelvin contraction as it pulls itself together gravitationally. During this period the temperature and density in the interior rise gradually. The star lies above the main sequence but moves toward it at a rate which depends upon its mass. Massive stars reach the main sequence fairly rapidly, whereas less massive stars may take a much longer time to contract. As a star contracts, all the deuterium, lithium, beryllium, and boron are destroyed at temperatures of a few million degrees, but because these substances are so rare they make a negligible contribution to its luminosity. Finally, the temperature in the core rises high enough for conversion of hydrogen into helium to take place either by the proton-proton reaction or by the carbon cycle.

If the star is much more massive than the sun, it will have a core in convective equilibrium wherein the material is thoroughly mixed. If it has the solar mass or less, the central regions will be in radiative equilibrium, and mixing cannot occur. The hydrogen at the very center is destroyed most rapidly and depletion in surrounding regions depends upon the temperature, density, and hydrogen concentration at any one time. As long as the hydrogen is being converted into helium in these cores, the stars change relatively little in size and temperature. Eventually, the star will exhaust the hydrogen at its center and form an "inert" core consisting of helium, carbon, and some heavier elements. When such an inert core develops, energy generation will continue to take place in a surrounding shell. From this point on, profound and extremely interesting changes occur in the star. The general features of the development are understood at least qualitatively and many of the details remain to be worked out. Certain definite trends, however, are indicated by the work of Schwarzschild, Hoyle, and their co-workers, and more recently by Biermann and his associates.

When the helium core at the center of the star contains about 12 per cent of the stellar mass, the star begins to depart more or less rapidly from the main sequence. Hydrogen is burned in a shell surrounding the core and the material in the inner envelope is gradually consumed. The ashes, however, are compressed into an inner core which increases in mass but does not increase substantially in size. As the star evolves, the outer portions gradually expand, while the

inner core not only becomes denser but gradually rises in temperature. In this way, the star moves to the right of the main sequence and becomes a red giant or perhaps a supergiant.

The history of the star depends very critically upon its mass. It has been suggested that the heavier elements are gradually built up by nuclear processes occurring in highly compressed cores of massive stars. As the core becomes denser and hotter as a consequence of its gravitational contraction, a situation eventually develops where helium can be burned into carbon at a temperature of the order of $140,000,000^{\circ}$. Up to this point the star had been brightening as it evolved into a redder and bigger giant, but when helium burning starts in the core, while hydrogen burning continues in an outer shell, a very complicated situation may develop. The outer envelope probably becomes unstable and detaches itself from the star entirely. The residue, including the central core, apparently settles down as a small, blue, intensely hot object which contracts into the white-dwarf stage.

No detailed evolutionary tracks have ever been computed for this phase of a star's life. One possibility is that the stellar core becomes unstable and the material of the core becomes mixed throughout the entire volume of the star which itself becomes so unstable that it explodes and scatters the material throughout the neighboring region of space. The debris from the defunct star is thus added to the interstellar medium, enriching it in helium and perhaps other, heavier, elements. Another possibility is that the mixing between the core and the surrounding regions may occur more quietly and the star may settle down to the white-dwarf stage without the violent cataclysmic outburst.

Whether the star explodes in the violent outburst of the supernova or whether the outer envelope is simply lost into space, much of the material is returned to the interstellar medium from which new stars are eventually formed. If there has been any substantial mixing between the outer layers and the core material, it follows that the interstellar medium will become enriched in helium and perhaps heavier elements as well so that we might expect that young stars formed out of the interstellar medium would have a higher proportion of helium and a higher ratio of metals to hydrogen than have older ones. The core of the star contracts finally into a white-dwarf stage unless its mass is greater than a certain critical mass, in which event

further nuclear reactions may take place. The material which is consigned to the white-dwarf residue is forever lost to the recycling process that occurs between the stars and the interstellar medium.

It is in the later stages of the stellar evolution that the processes of element building appear to occur, and it is precisely these stages which cannot yet be handled in theoretical investigations. Nevertheless, the hypothesis that elements are continuously being formed in stars is supported by an impressive array of evidence. Not all elements are manufactured in all stars nor are the proportions of the elements manufactured constant from one object to the next. All stars initially convert hydrogen into helium. Some may manufacture heavier elements but only a rather massive star can produce the heaviest elements in the periodic table. Certain heavy atoms appear to be produced only in catastrophic conditions, and we shall mention these in more detail subsequently.

1-5. Element Building in Stars

Earlier theories of element building favored the hypothesis that the elements were manufactured in a pre-stellar state of matter, either during the initial stages of an expanding universe or under some equilibrium situation in which the elemental distributions were "frozen." All these theories encountered severe if not actually fatal difficulties. For example, the hypothesis of Gamow and his co-workers suggested that the material of the original universe, called the *ylem*, was a neutron gas. The neutrons decayed into protons and electrons, and, as the gas expanded, heavy elements were built by successive neutron captures. This hypothesis ran into the serious difficulty that no stable nuclei of masses 5 or 8 exist. Hence three-body collisions, which are possible only at high densities, would have to be invoked. Nevertheless, if one could solve the problem of masses 5 and 8, perhaps by building the elements at a higher density than Gamow imagined, the mechanism might work. The neutron-capture hypothesis did explain a number of well-observed features of the elemental distributions.

The evidence for element building in stars is empirical and may be summarized very briefly as follows. Studies of spectra of stars in globular clusters and of the so-called subdwarfs (which appear to be associated with a globular-cluster type of population) indicate that these very ancient stars have a metal/hydrogen ratio smaller than

that of the sun. This effect is to be anticipated if these old stars were formed out of material which consisted almost entirely of hydrogen. The younger stars which are associated with galactic clusters and spiral arms have a higher metal/hydrogen ratio because they were formed out of the debris of previously existing stars in which helium and yet heavier elements have been manufactured from hydrogen.

Although most stars appear to have essentially identical chemical compositions, there exist some whose composition deviate markedly from the norm. One of these groups comprises the hydrogen-deficient stars in which hydrogen is either scarce compared to helium or does not appear at all. This category includes such objects as ν Sagittarii, Popper's helium star HD124448, and Bidelman's helium star HD160641. There also exist the so-called Wolf-Rayet stars in which helium predominates over hydrogen. In one group, intensely strong lines of nitrogen with very weak lines of carbon are present, and in the other strong lines of carbon and of oxygen appear but with very weak lines of nitrogen.

The most striking and exciting examples are provided by the coolest giant and supergiant stars of spectral classes *M*, *N*, *R*, and *S*. The *M* stars appear to have roughly the same compositions as the sun. The spectral differences are produced simply by a lower temperature and usually a lower density. Atomic lines of iron, titanium, nickel, etc., are prominent in their spectra, but the most conspicuous features are the strong molecular bands of titanium oxide. On the other hand, the *N* stars have strong bands of carbon and its compounds which cannot be reconciled with a "normal" stellar atmosphere in which oxygen is more plentiful than carbon.

The *S* stars present the most engaging problem. They contain bands of zirconium oxide which are often stronger than the bands of titanium oxide. Conceivably, one might explain the intensification of zirconium oxide with respect to titanium oxide by changes in pressure and temperature in the atmosphere and attempts have been made to do this. Such theories could not account for the fact that stars which show intensified oxide bands also show strong atomic lines of zirconium. Furthermore, atomic lines of neighboring elements in the second long period of the periodic table—for example, molybdenum, ruthenium, and niobium (columbium)—are also intensified. Most striking of all was Merrill's discovery of the lines of the synthetic

element number 43, technetium, which probably did not exist at all on the earth until it was manufactured by man. Its longest lived isotope has a half-life of the order of a million years, but the isotopes found in the *S* stars may have a much shorter lifetime.

Clearly, here appears irrefutable evidence that heavy elements are being manufactured in stars and that the compositions of these cool supergiants and giants may actually differ from that of the sun. A significant clue may be provided by the fact that every cool star of abnormal composition is a giant or a supergiant. They are often pulsating variable stars; i.e., they appear to border on instability, and somehow the effects of nuclear reactions occurring in their interiors have been felt in the atmospheric layers. Mixing has occurred without at the same time causing the star to become so unstable as actually to explode. These stars of abnormal composition are also known to be much more massive than the sun and presumably they have evolved at a much faster rate. Evidently, many of them have consumed all the hydrogen in their deep energy-producing interiors and are now experiencing nuclear transformations involving heavier elements.

The manufacture of elements in stars appears to be a many-staged process. All stars convert hydrogen into helium, some manufacture heavier elements, but only the most massive stars can produce elements in the upper part of the periodic table. Certain heavy nuclides appear to be produced only under catastrophic conditions, and no single mechanism of element manufacture will account for all existing elements. In fact, a number of discrete mechanisms have been proposed, as follows:

1. A star of normal composition and sufficient mass can build helium by the proton-proton reaction in the stellar core and subsequently in the shell-burning stage by the carbon nitrogen cycle. In the more massive stars the helium is built entirely by the carbon nitrogen cycle.

2. Carbon, oxygen, and neon can be produced by burning helium in the dense cores of highly evolved stars at temperatures in excess of $100,000,000^{\circ}$. If the temperature rises to something of the order of $400,000,000^{\circ}$, other elements may be produced by jamming carbon nuclei together with one another and with oxygen and other nuclei, etc.

3. If the temperature rises to something of the order of 5×10^9

degrees and the density to 10^6 g/cm³, nuclei will be broken up quite freely. An equilibrium situation will obtain in which elements in the neighborhood of iron in the periodic table can be formed.

4. Elements beyond the iron peak cannot be made in sufficient amounts by processes occurring under strict equilibrium conditions. Many of them appear to be formed only by the capture of neutrons by heavy atoms on a slow time scale.

5. Other nuclides (sometimes referred to as unshielded isobars) can be produced by neutron capture on a fast time scale, that is, one in which a nuclide that has captured a neutron will in most instances capture yet a second neutron before it has had a chance to undergo β -decay. Intense neutron fluxes are presumably produced only in catastrophic events such as a supernova explosion.

6. Proton-rich isobars are produced by photo-dissociation effects.

7. Lithium, beryllium, and boron are destroyed in stellar interiors. Presumably they and also deuterium are produced by spallation effects in flares in stellar atmospheres. In solar flares, particles are presumably accelerated to very high velocities, corresponding perhaps to cosmic-ray energies. Possibly such flarelike activity may be more frequent in magnetic stars and certain other objects than it is in the sun.

8. The anomalous abundances of the rare earths observed in the atmospheres of magnetic stars may be similarly produced by the acceleration of protons in local regions of their atmospheres.

We shall discuss the problem of element building and the characteristics of stars of abnormal composition in more detail in later chapters. Excluding those highly evolved stars whose atmospheres reflect the effects of element building actually going on within themselves at the present time (or very recently), we may distinguish among three broad types of stellar composition problems: (1) the sun whose composition presumably represents the original composition of the solar system, (2) the very ancient stars such as the members of globular clusters and the subdwarfs which show low metal/hydrogen ratios and (3) the present interstellar medium and the stars that are formed therefrom. These three compositions refer to epochs in the history of our galaxy separated by billions of years.

For a variety of reasons we shall emphasize the composition of the sun and that of the solar system, as well as some closely related stars believed to be of a somewhat similar composition. In this connection

we shall have to refer to the data obtained from studies of the composition of the earth's crust, from the atmospheres of planets, and particularly from the studies of meteorites. Our main emphasis will be on the composition results obtained from the spectroscopic analyses of stars and nebulae. The limitations of the available space do not permit us to discuss the chemistry of the earth's crust and of the meteorites in corresponding detail. These topics are handled adequately elsewhere.

Successive chapters will treat of studies of the compositions of the sun, stars, gaseous nebulae and the interstellar medium, the earth's crust, meteorites, and cosmic rays. After this we shall discuss general abundance compilations that have been suggested by Suess and Urey and by A. G. W. Cameron. Also, we shall propose our own guesses concerning the primordial composition of the solar system. A final chapter will deal with theories of the origin of elements in stars together with supporting observational data.

Selected References

For a fuller explanation of some of the astronomical concepts and terminology employed in this chapter, see, for example:

Schwarzschild, M., *Stellar Structure and Evolution*, Princeton University Press, Princeton, N. J., 1958.

Struve, O. H., Pillans, and B. Lynds, *Elementary Astronomy*, Oxford, New York, 1959.

The modern theories of element building in stars and the supporting astronomical evidence are given in

Burbidge, G. R., and E. M. Burbidge, in Flüggé (Ed.), *Handbuch der Physik*, vol. 51, Springer, Berlin, 1958.

Burbidge, G. R., E. M. Burbidge, W. A. Fowler, and F. Hoyle, *Revs. Modern Phys.*, 29, 547, 1957.

Cameron, A. G. W., "Stellar Evolution, Nuclear Astrophysics, and Nucleogenesis," *Atomic Energy of Canada, Ltd., Report CRL-41*, 2nd ed., Chalk River, Ontario, 1957.

Composition of the Earth and Its Crust

2-1. Introduction

One might suppose that the obvious first step toward establishing an abundance scale of the elements would be an analysis of the rocks of the earth's crust. Samples are readily obtainable, and the relative proportions of commoner rock types may be estimated. Insofar as the most plentiful elements are concerned, reasonably precise crustal abundances can be obtained.

Yet insofar as our goal is the establishment of abundance values for the solar system or even the over-all average for the earth itself, chemical studies of the earth's crust can be frustrating. A fundamental limitation is that one can analyze only samples found on or near the earth's surface. The most elementary arguments show that it is improbable that the interior and crust have the same quantitative chemical composition. Since less than 1 per cent of the earth's mass is contributed by its accessible crust, the average composition of the earth is determined entirely by that of the matter below the crust.

As suggested by Urey and others, the earth probably formed as a cold body, but its interior later became heated, partly perhaps as a result of gravitational contraction and partly because of radioactive decay. Superficially the earth's interior may have resembled certain properties of an ore-smelting furnace, although the mixture may never have become liquid enough for the material to flow freely. In a gravitational field certain elements tend to separate from others. Some sink to the bottom of the "crucible"; these are the siderophile elements which favor the metallic phase and include not only abundant Fe, Ni, and Co, but also noble rare metals such as gold, ruthenium, rhodium, and palladium. Other elements tend to rise in the "slag"; these include elements with a strong affinity for oxygen (lithophile elements) and those that have a strong affinity for sulfur (chalcophile elements). Some elements belong to more than one cate-

gory, while the behavior of yet others depends on whether or not certain specific elements (e.g., oxygen) are present in the mixture.

Thus the behavior of an element is to be understood, not in terms of its density or atomic weight, but rather in terms of its geochemical affinity, a term employed by Goldschmidt to describe the above-cited behavior of elements in a liquid melt. Certain elements will tend to concentrate in surface layers, others deep in the interior, whereas some may be more or less uniformly distributed. The concentration will depend on the past history of the particular rock under consideration.

The chemistry of the earth's crust is a subject of enormous complexity, and in this chapter we can only indicate some of the problems involved. In a few brief pages it would be presumptuous indeed to claim any more than a superficial presentation of the subject, sufficient perhaps to indicate some of the ways in which geochemical data can aid in an interpretation of solar and meteoritic data. Reference must be made to the treatises of Rankama and Sahama (1950), Rankama (1954), and Mason (1958).

In view of the complexities of the data, one may very well ask whether studies of the earth's crust can give much help in such problems as that of the primordial composition of the solar system. The over-all abundance distribution is certainly distorted, but in certain detailed problems studies of the earth's crust can be of great help.

First, consider isotope abundances. Although isotope ratios for some elements are distorted by geochemical or biological processes occurring on the earth's surface, reliable data can be obtained for most elements (Rankama 1954). Isotope ratios can be measured with high accuracy and probably represent very accurately the basic ratios for the solar system, at least for most elements.

Second, certain chemically similar elements can be expected to show their true abundance ratios in the earth's crust. The best examples are the lanthanide elements (classical rare earths) whose chemical separation is extremely difficult. The actinides (uranium series of rare earths) might be expected to behave similarly, but the instability of their nuclei complicates the picture.

Third, homologous elements, i.e., elements which have similar chemical properties because they fall in the same columns of the periodic table, offer the possibility of establishing certain abundance ratios (cf. Suess and Urey 1956). For example, the "cosmic" ratio of

krypton to xenon can be found only from the earth's atmosphere since the lines of these elements are never found in stellar spectra. Unfortunately, a similar determination of the argon/krypton ratio from the earth's atmosphere is not possible since much of the argon probably has originated from the β -decay of K^{40} .

Suess and Urey establish the cosmic abundance of bromine with the aid of the Cl/Br ratio obtained from sea water and the earth's crust. The iodine abundance cannot be obtained in this way as this element tends to be enriched in living organisms and therefore concentrated in sedimentary rocks rather than uniformly distributed. Other important abundance ratios used by Suess and Urey include titanium/zirconium, zirconium/hafnium, sulfur/selenium, and potassium/rubidium. It may be possible that in the future, abundances of many elements can be found more accurately from judicious use of samples of the earth's crust than from other sources. The geochemical influences are extremely important in all these discussions, however.

2-2. Concerning the Structure of the Earth

The total mass of the earth is 5.977×10^{27} g. Its surface density is 2.64 g/cm^3 , whereas the average density is 5.517 g/cm^3 . At the center the density must be of the order of ten times that of water. Astronomical data, such as the figure of the earth, the precession of the equinoxes, etc., combined with seismic data, yield some information on the earth's internal structure, namely, the increase of density and the variation of the elastic constants with depth.

An analysis of these and other geophysical data yields a reasonable, self-consistent picture of the earth's interior which we briefly summarize as follows. The crust of the earth has a thickness of about 30 km in the continental areas and about 5 km in oceanic areas. At its base the crust has a density about 2.87. The uppermost part of this crust is subject to all the usual geological phenomena—weathering, erosion, folding, uplift, sedimentation, and vulcanism. Seismic studies show that there is a distinct change in elastic properties at the above-mentioned base of the crust, the so-called Mohorovicic or Moho discontinuity. Below the M discontinuity there is a thick, rigid, shell extending to a depth of 2900 km. This mantle, as it is called, is solid in the sense that it transmits transverse elastic waves. Various subdivisions of the mantle have been proposed, and it is likely that the chemical properties, in addition to the physical proper-

ties, change with depth. Below the mantle there appears to be a sharp jump in density from 5 to about 10 g/cm^3 as the liquid core is reached. This core transmits compressional (longitudinal) waves but not transverse waves and accordingly is judged to be a liquid. Finally, there is some evidence from the seismic-wave studies that there is a solid core at the center of the earth.

Long ago it was suggested that the earth's core was predominantly iron. This abundant metal had about the requisite density. Furthermore, the iron meteorites which were interpreted as debris from a broken-up planet were cited as providing independent "evidence" for this earth model. A widely accepted modern view is that the core is predominantly iron and nickel, although it may contain other elements as well. Arguments have been given based on the elastic constants, the density, and the requirements of the dynamo theory of the earth's permanent magnetic field. To date, it has proved impossible to give any reliable quantitative estimates concerning its composition.

What can be said concerning the structure of the mantle? Its density and seismic properties show that it must be some kind of a silicate rock. Samples of the mantle are believed to be found in certain volcanic intrusions and suggest that the mantle is subsilicic rocks such as eclogite, dunite, and peridotite. Various investigators have suggested that the best approximation to the average composition of the mantle and perhaps that of the entire earth itself is provided by the chondritic meteorites (Chap. 3). The strongest argument is the similarity in chemical composition between these stony meteorites and the ultramafic rocks of the earth. Furthermore, the isotopic constitution of several elements is essentially the same in chondrites and in rocks of the mantle. There are some arguments that chondritic compositions may not agree with the earth in detail. Nevertheless, retaining the assumption that the mean composition of the earth is the same as that of the chondrites (or by making small adjustments in this hypothesis), it appears to be possible to construct a model for the earth that will fit all the astronomical, physical, and geochemical requirements.

To the earth's total mass the core contributes 31.4 per cent, the mantle 68.1 per cent, and the crust about 0.5 per cent. The total mass of the crust is about $2.4 \times 10^{25} \text{ g}$ of which $0.62 \times 10^{25} \text{ g}$ lie under the oceans and $1.76 \times 10^{25} \text{ g}$ are under the continents (including their

shelves). The oceans contain about 1.4×10^{24} g, the total mass of the atmosphere is about 5.3×10^{21} g.

2-3. Abundances of Elements in the Earth's Crust

Since the pioneering work of Frank Wigglesworth Clarke (1889), numerous quantitative analyses have been carried out for the continental rocks of the earth's crust. As representative examples of these investigations we mention the work of Clarke and Washington (1924), Goldschmidt (1933), Rankama and Sahama (1950), Wickman (1954), Poldervaart (1955), and Green and Poldervaart (1958). The crustal rocks consist almost entirely of oxygen compounds, particularly the silicates of aluminum, calcium, magnesium, sodium, potassium, and iron. Hence Goldschmidt spoke of the earth's crust as the "oxygenosphere."

Although the details of different abundance compilations differ, they show that about 98 per cent of the earth's crust is contributed by the eight elements: O, Si, Al, Fe, Ca, Mg, Na, and K, followed by Ti, P, H, and Mn. All other elements contribute less than 0.6 per cent.

The earth's crust includes everything above the Mohorovicic discontinuity, and to get the total composition we should include not only the continental rocks (including the shields, platforms, and mountain ranges) but also volcanic islands and the crust under the ocean.

We emphasize that the rocks that comprise the continental shield (granite and granodiorite) differ substantially in composition from the crust under the ocean (basalts). To get a rough idea of the mean composition of the earth's crust (excluding the oceans), we take a weighted average of the composition of the continental crust from Poldervaart (1955, p. 129) and that of the Pacific olivine basalt (Green and Poldervaart 1958).

Table 2-1 gives the logarithm of the abundances, on the scale $\log N = 6.00$ for silicon, for the six most abundant elements in the crust exclusive of oxygen. Notice that Na, Al, K, Ca, and Ti are enriched in the crust (with respect to the sun), whereas the opposite is true for Mg and Mn. The enrichment or deficiency factors are usually not very large and the elements that are abundant in the earth's crust are also abundant in the sun.

In a compilation of general abundance tables for the earth's crust

Table 2-1. Comparison of Logarithmic Abundances of Common Elements in the Earth's Crust

	Na	Mg	Al	Si	P	K	Ca	Ti	Mn	Fe
Suboceanic crust, 25%	5.05	5.40	5.58	6.00	3.61	4.42	5.54	4.68	3.36	5.31
Continental crust, 75%	5.00	5.02	5.49	6.00	3.51	4.71	5.06	4.17	3.26	5.00
Total crust	5.02	5.15	5.51	6.00	3.54	4.65	5.24	4.36	3.29	5.11
Solar abundances	4.80	5.90	4.70	6.00	3.84	3.20	4.65	3.18	3.40	5.07

the major elements present no problem insofar as chemical procedures are concerned. Analyses by conventional chemical methods usually are reliable enough. Clarke and Washington obtained the essential results and such revisions of their figures as have been made are due to differing opinions with regard to the importance of various rock types.

The less abundant elements present several problems:

1. The abundance of the elements must be found in various samples. For a rare element this step may entail difficult analytical techniques. Older determinations of rare-element concentrations often gave spurious results—abundances usually too high because of contamination of the samples with impurities in reagents, etc. Among the methods employed are amperometric titration, X-rays, spectrochemical, colorometric, and neutron activation. See, e.g., the discussions by Sandell (1959) and Ahrens and Taylor (1961). For many elements, particularly certain lanthanides, the most promising procedure is the neutron-activation method originally suggested by von Hevesy and Levi (1936) and now employed by many workers (see Meinke 1955).

2. The contribution of the sample to the total crust of the earth must be evaluated. This step is critically important for rare elements. For example, mercury appears in specific ores (e.g., cinnabar), whereas more abundant europium is scattered in small concentration in many types of rocks. The abundant elements, titanium and zirconium, appear in small crystals scattered in silicate rocks of the earth's crust. Gallium is more abundant than lead, and hafnium is more plentiful than antimony or bismuth, but it appears in concentrations of less than 1 per cent in minerals of zirconium. Some

stable elements such as rhenium and ruthenium are really very rare in the universe.

For a summary of the earlier abundance compilations, see M. Fleischer (1953). Among more recent compilations we note especially that by K. Rankama (1954) and revised by L. Ahrens and S. Taylor (1959) and that by B. Mason (1958). Mason's figures for the more abundant elements are based mostly on rock analyses and are therefore biased in favor of the continental crust against the less silicic suboceanic crust (see, however, Poldervaart 1955). Vinogradov (1956) has given data for ultramafic rocks (dunites, peridotites, peroxenites); mafic rocks (basalts, gabbro, diabases, etc.); intermediate rocks (diorites and andesites); silicic rocks (granites, liparites, rhyolites, etc.); sediments and sedimentary rocks (clays and shales).

Table 2-2 gives the atomic abundances of the elements in the earth's crust. For purposes of comparison with other sources we select Rankama's data recently revised by Ahrens and Taylor. We also give Vinogradov's data which refer to continental igneous rocks (two parts silicic plus one part subsilicic). An inspection of this table and a comparison with the corresponding data for the chondritic meteorites (Chap. 3) and the sun (Chap. 5) show that elements that are abundant in the earth's crust are cosmically abundant, but the converse is not necessarily true. Volatile substances have been lost from the earth and fractionation has occurred.

2-4. The Internal Structure of the Earth and Its Mean Composition

The crust forms less than 1 per cent of the earth's mass, and has experienced considerable fractionation and geochemical separation. Hence any estimate of the composition of the earth as a whole must depend on the assumed character of the mantle and the core.

Various types of data may be employed. First, we can obtain from the earth's moment of inertia, its figure, and from the rate of lunisolar precession some data on the variation of density with depth below the surface. Astronomical data, such as the amplitude of nutation, the variation of latitude, and Michelson's experiments with the artificial tides, show that the mantle of the earth, despite its high temperature, must have a rigidity comparable with that of steel.

Second, the speed of seismic waves depends on the ratios of the shear and bulk moduli to the density, i.e., κ/ρ and μ/ρ . Hence analyses

Table 2-2. Atomic Abundances of the Elements in the Earth's Crust: Igneous Rocks

Element	Z	Si = 10 ⁶	
		Vinogradov	Ahrens and Taylor
He			
Li	3	700	470
Be	4	45	22.4
B	5	115	28.1
C	6	1850	2710
N	7		108
O	8	2,970,000	2,960,000
F	9	3360	3750
Ne	10		0.00036
Na	11	105,000	125,000
Mg	12	68,000	87,300
Al	13	290,000	306,000
Si	14	1,000,000	1,000,000
P	15	2800	3860
S	16	2720	1640
Cl	17	626	430
Ar	18		0.100
K	19	62,000	67,100
Ca	20	80,000	91,700
Sc	21	28	45
Ti	22	8900	9310
V	23	172	240
Cr	24	217	195
Mn	25	1760	1850
Fe	26	81,000	91,000
Co	27	29.9	34.6
Ni	28	165	60.5
Cu	29	107	88.0
Zn	30	117	62.0
Ga	31	35.8	27.4
Ge	32	2.68	1.55
As	33	2.58	2.70
Se	34	(0.0123)	0.11
Br	35	2.16	3.94
Rb	37	316	137
Sr	38	385	520
Y	39	21.6	32.1
Zr	40	180	173
Nb	41	20.8	26.2
Mo	42	1.65	1.02
Ru	44	0.00010	0.0010
Rh	45	0.0010	0.0010

Table 2-2.—Continued

Element	Z	Si = 10 ⁶	
		Vinogradov	Ahrens and Taylor
Pd	46	0.0172	0.036
Ag	47	0.172	0.094
Cd	48	0.110	0.135
In	49	0.084	0.098
Sn	50	26	1.70
Sb	51	0.244	0.18
Te	52	0.0007	0.00144
I	53	0.31	0.238
Cs	55	7.2	3.8
Ba	56	450	73.5
La	57	28	13.0
Ce	58	27.4	33.2
Pr	59	4.8	4.0
Nd	60	20.1	17.0
Sm	62	2.6	4.4
Eu	63	~0.7	0.72
Gd	64	4.3	4.15
Tb	65	0.69	0.58
Dy	66	2.4	2.80
Ho	67		0.735
Er	68	1.15	1.52
Tm	69	0.58	0.119
Yb	70	1.10	1.59
Lu	71	0.55	0.43
Hf	72	1.62	1.70
Ta	73	1.44	1.22
W	74		1.15
Re	75	0.00051	0.027
Os	76	0.000034	0.00054
Ir	77	0.000052	0.00054
Pt	78	0.0024	0.0025
Au	79	0.00048	0.0010
Hg	80	0.029	0.040
Tl	81	0.80	0.64
Pb	82	7.5	7.35
Bi	83	0.046	0.097
Po	84	9.3×10^{-11}	1.45×10^{-10}
Rn	85	2.75×10^{-12}	
Ra	86	4.1×10^{-7}	5.8×10^{-7}
Ac	89	2.3×10^{-10}	1.33×10^{-10}
Th	90	5.4	4.3-7.2
Pa	91	3×10^{-7}	3.6×10^{-7}
U		1.07	1.3-1.7

of earthquake data tell how these quantities vary with depth below the surface. A judicious combination of astronomical and seismic data reveals how κ , μ , and ρ all vary in the earth's interior, and show that the only compounds of abundant elements that can predominate in the mantle are silicates such as dunite, peridotite, and eclogite. Volcanic rocks that come from great depths contain but little aluminum and alkali metals. See, for example, the discussions by Birch (1954), Ringwood (1958), and MacDonald (1959).

Third, limitations on the type and distribution of materials in the mantle are imposed by heat-flow data. Discussions by Birch (1958) and by MacDonald (1959), for example, show that radioactive elements such as U, K, and Th must be concentrated near the surface. Otherwise, since the thermal conductivity of rocks is so low, the temperature must rise so steeply that the rocks of the mantle would become liquefied! Other elements are likewise differentiated. Hence the mantle is probably not chemically homogeneous, but there are presumably no sharp demarcations in the mantle between zones of utterly different composition. The core of the earth is often assumed to be nickel-iron, but it may very well contain quantities of silicon and other metals as well.

All estimates of the mean composition of the earth must be based on direct hypotheses of its internal structure. Within the framework of the limitations imposed on speculations by the density distribution, variation of κ and μ , the electrical conductivity required for the dynamo theory of the earth's magnetism, etc., a considerable range of possibilities is embraced. Estimates of the mean composition of the earth were made by Washington (1925) and by Niggli (1928). B. Yu. Levin (1957) constructed a model of the earth in which he took the silicate phase of the meteorites as contributing 92 per cent and the metallic phase as supplying 8 per cent. Mason (1958) calculated the mean composition of the earth, assuming that it had a core of meteoritic nickel-iron, a mantle of the composition of peridotite and 8 per cent of iron sulfide (the average amount observed in meteorites) dispersed through mantle and core. More recently he has favored the idea that mantle plus core has evolved from material of the average composition of chondritic meteorites. Table 2-3 gives his adopted composition (per cent by weight).

Whatever model we adopt for the earth, there is no escape from the conclusion that such elements as Na, Al, K, Ca, Ti, and the

Table 2-3. Average Composition of the Earth^a (per cent by weight)

Fe	38.80	Mg	11.25	Al	1.07	Co	0.20	P	0.08
O	27.17	S	2.74	Ca	1.07	Cr	0.19	K	0.06
Si	13.84	Ni	2.70	Na	0.51	Mn	0.13	Ti	0.06

^a After Brian H. Mason.

halogens tend to concentrate toward the earth's surface, whereas Mg, S, Mn, Fe, Co, and Ni are enriched in the deeper layers.

These differences are to be understood in terms of geochemical affinities and the earth's thermal history. Presumably the earth was originally cold and its interior became heated by contraction and release of radioactive energy. Major geochemical changes may have occurred relatively early or they may have occupied long periods of time. Gradual changes occurred in the mantle, the siderophile elements sinking, the lithophile elements rising. The upper part of the mantle melted in places, causing plutonic and volcanic activity. A complete separation of elements did not occur. Some Fe and Ni were trapped in chemical combinations in the silicates. Metals more electropositive than iron tended to replace it and to concentrate in the mantle and the lithosphere.

Only the great abundance of iron permitted it to remain in appreciable quantities near the earth's surface. Profound changes were gradually produced in the surface rocks as compared with the original mean composition of the earth. The crust became concentrated with the lithophile elements, i.e., the alkali metals, the alkaline earth metals, the lanthanides and actinides, Ti, Zr, V, Nb, Ta, W, and Re. Eventually the uppermost part of the lithosphere, the crust, was markedly affected by erosion, weathering, and sedimentation. It was the only part of the earth in contact with the atmosphere and hydrosphere. Furthermore, sulfur and chalcophile elements tend to be concentrated in the earth's interior. The cosmic abundance of sulfur greatly exceeds that found in surface rocks.

Geochemical complications are enhanced by the fact that some elements appear in more than one category and their behavior may depend on whether or not oxygen is present. Chromium is a lithophile element in the earth's crust, but if oxygen is deficient it may also be chalcophile in behavior. Carbon and phosphorus are siderophile under reducing conditions.

The terrestrial abundances of the volatile elements and of the permanent gases differ most profoundly from their cosmic abundances. Hydrogen and helium are overwhelmingly the most abundant elements in the universe, but on the earth hydrogen is retained in water whereas the original helium (if it were ever present) has mostly escaped. Likewise, much of the earth's supply of carbon and nitrogen may have been lost in the form of volatile gases such as NH_3 or CH_4 if the earth were ever hot. On the other hand, a fair proportion of oxygen may have been trapped as non-volatile oxides. The earth's atmosphere exhibits effects of fractionation, action of living organisms, and perhaps photochemical reactions as well!

These illustrations point out some of the complexities of geochemistry and emphasize the great care necessary in the interpretation of abundance data.

2-5. The Structure and Composition of the Planets

Additional clues concerning the primordial composition of the solar system and its evolution are provided by some of the other planets. Information is necessarily very limited compared with what can be learned for the earth and consists of data such as the following:

1. The masses of the planets are found most accurately from their mutual perturbations.

2. The diameters can be measured and hence the mean densities can be found.

3. From the oblateness (which is measured with the telescope) and rotation period, and also from perturbations produced by the deformation of figure of a planet upon the orbit of a nearby satellite, some clues to the internal density distribution may be found.

4. Spectrographic observations reveal some (but not all) of the gases that compose the atmosphere.

5. Observations with a thermocouple and high-frequency radio waves yield the temperatures of the planets, although in some instances these temperatures refer to atmospheric layers rather than to solid surfaces.

Unfortunately, we cannot yet obtain samples of the surface rocks, measure the planetary magnetism, nor study seismic waves. The density and density-distribution data do permit, however, certain important conclusions to be drawn. See particularly the discussion by de Marcus (1959).

Some years ago, Ramsey (1948) proposed as a working hypothesis that the terrestrial planets—Mercury, Venus, the earth, and Mars—were composed of essentially identical material throughout. In particular, the chemical composition of the earth was supposed to be uniform. Both mantle and core were made of olivine which was reduced to a metallic phase in the core by great pressure. A phase change resulting in a sudden doubling of the density seems unlikely, and it appears that the pressures required are so great that they are not even achieved at the center of the earth.

If all the terrestrial planets had the same composition, the jump in density should occur in each planet at the depth where the pressure is equal to the core-mantle interface on the earth. Thus, Mercury, Mars, Venus, and the earth should show a steady progressing of increasing density. Actually, Mercury is denser than Mars or Venus, and the chemical identity of the planets is disproved.

A possible interpretation might be that the silicate/iron ratio varies from one planet to another; that is, in the formation of the inner planets, Mercury lost a much larger fraction of its silicates than did Mars or even the moon, Urey (1951). On the other hand, Ringwood (1959) has interpreted the different terrestrial planet densities in terms of oxidation-reduction reactions, in which varying fractions of the iron that is present are tied up in oxidized or reduced form.

The density distributions in the inner and outer planets show striking differences. We have no such information on the internal structure of Mercury, the moon, or Venus. Since their rotation periods are very long, they show no detectable oblateness. The oblateness and satellite perturbations for Mars indicate that this planet is nearly homogeneous. On the other hand, similar observations show that Jupiter and Saturn have high mass concentrations toward their centers.

Various investigators have attempted to construct models for the outer planets, particularly Jupiter and Saturn. The most detailed and careful study is that made by de Marcus (1958, 1959) who finds Jupiter and Saturn, respectively, to contain 78 per cent and 63 per cent of hydrogen by weight provided that they are cold bodies. By numbers of atoms the H/He ratio exceeds 14 and 7, correspondingly. He finds that the hydrogen abundance is insensitive to the relaxation of various assumptions made in the calculation, and concludes it is unlikely that models can be constructed in which hydrogen is not

predominant. The H abundance requires only slight alterations if the temperature in the interior is of the order of a few thousand degrees. Uranus and Neptune have larger densities in spite of their smaller masses; hence their hydrogen contents are lower. Ramsey suggested that metallic ammonium may exist in some of these planets.

These outer planets all possess extensive atmospheres in which the bands of CH_4 are strong. Bands due to H_2 under great pressure have been observed in the outer planets. Weak bands of ammonia are observed in the spectra of Jupiter and Saturn, but this substance is frozen out in Uranus and Neptune. More complex compounds exist in these atmospheres but have so far escaped detection. Probably helium exists in great quantities, but the evidence for its presence is indirect.

Mercury and the moon have no detectable atmospheres, whereas that of Venus contains great quantities of CO_2 and small amounts of water vapor, but no detectable oxygen. The bands of N_2 fall in the inaccessible ultraviolet, but the presence of this element may be decided eventually from observations of the Venusian aurora.

The Martian atmosphere contains somewhat more CO_2 than that of the earth, but the other constituents are unknown. Presumably, they are N_2 and Ar. Water is present but the vapor pressure is too low to permit detection in this form; it is observed as ice in the polar caps.

Selected References

- Ahrens, L. H. and S. R. Taylor, *Spectrochemical Analysis*, Addison-Wesley, Reading, Mass., 1961, Table 8.
- Birch, F., *Trans. Am. Geophys. Union*, **35**, 79-85, 1954; *Bull. Geol. Soc. Am.*, **69**, 483, 1958.
- Cameron, A. G. W., *Ap. J.*, 1959.
- Clarke, F. W., *Bull. Phil. Soc.*, *Washington* **11**, 131, 1889.
- Clarke, F. W. and H. S. Washington, "Composition of Earth's Crust," *U. S. Geol. Survey, Profess. Papers*, **127**, 1-117, 1924.
- de Marcus, W. C., *Astron. J.*, **63**, 25, 1958; *Handbuch der Physik*, vol. 52, p. 448, 1959.
- Fleischer, M., *U. S. Geol. Survey Circ.* **285**, 1953.
- Goldschmidt, V. M., *Fortschr. Mineral.*, **17**, 112, 1933.
- Green, J. and A. Poldervaart, *Geochim. et Cosmochim. Acta*, **13**, 89, 1958.
- Hevesy, G. V. and H. Levi, *Kgl. Danske Videnskab. Selskab. Mat.-fys. Medd.*, **14**, 5, 1936; **15**, 11, 1938.

- Levin, B. Yu., *Izvest. Akad. Nauk S.S.S.R., Ser., Geofiz.* **11**, 1323, 1957.
- MacDonald, G. J. F., in *Research in Geochemistry*, P. H. Abelson, ed., Wiley, New York, 1959; see also G. J. F. MacDonald and L. Knopoff, *Geophys. J.*, **1**, 284, 1958.
- Mason, B. *Geochemistry*, Wiley, New York, 1958.
- Meinke, W. W., *Science*, **121**, 177, 1955.
- Niggli, P., *Fennia*, **50**, no. 6, 3, 1928.
- Poldervaart, A., *Geol. Soc. Am., Spec. Papers*, **62**, 119, 129, Table 20, 133, 1955.
- Ramsey, H. W., *Monthly Notices Roy. Astron. Soc.*, **108**, 406, 1948.
- Rankama, K., *Isotope Geology*, McGraw-Hill, New York, 1954.
- Rankama, K. and S. Sahama, *Geochemistry*, University of Chicago Press, Chicago, 1950.
- Reed, G. W., H. Hamaguchi, and A. Turkevich, *Geochim. et Cosmochim. Acta*, **13**, 248, 1958.
- Ringwood, A. E., *Geochim. et Cosmochim. Acta*, **15**, 195, 1958.
- Sandell, E. B., *Colorimetric Determination of Traces of Metals*, Interscience, New York, 1959.
- Suess, H. and H. C. Urey, *Revs. Modern Phys.*, **28**, 74, 1956.
- Urey, H. C., *Geochim. et Cosmochim. Acta*, **1**, 209, 1951.
- Vinogradov, A. P., "Regularity of Distribution of Elements in Earth's Crusts," *Geokhimiya*, **44**, 1956.
- Washington, H. S., *Am. J. Sci.*, **9**, 351, 1925.
- Wickman, F. E., *Geochim. et Cosmochim. Acta*, **5**, 105, 1954.

Meteorites

3-1. Introduction

One of the basic beliefs in modern work on the cosmic abundances of the elements and on the origin of the solar system is that essential clues are contained in the meteorites—the rocks that fall from the sky. It was not until 1794 that the extra-terrestrial origin of meteorites was recognized, while only relatively recently has the true importance of these objects been established. With the development of highly sensitive techniques in analytical chemistry, accurate analyses of infinitesimal quantities of trace elements have become possible, thus opening broad vistas in cosmic chemistry. In order to assess these data we must discuss briefly:

1. the various types of meteorites,
2. the actual frequencies of the various types, not just for the recognized finds but rather for the actual bodies that strike the earth,
3. the mineralogical properties and compositions,
4. the ages and possible origins, and
5. the best mean composition for the average of meteorites in the neighborhood of the earth.

It is clear that topics 1, 3, and 5 are closely related. At the present time, only rough speculations concerning the origin of meteorites can be given. Analyses of meteorites may give us good data concerning the composition of the solar system. Even more important, however, these same meteorites may well unlock for us some essential features of its actual origin.

We must clearly distinguish between meteors and meteorites. The former appear as evanescent flashes of light across the sky, frequently followed by a luminous train. Since their substance is dissipated by resistance of the earth's atmosphere, they are never recovered except perhaps as meteoric dust. Extensive studies of their paths, particularly by photographic techniques (F. L. Whipple and associates at Har-

vard) and by radar (Lovell and his group at Manchester), and of their spectra (especially by Millman at Ottawa), have yielded important data on their orbits, sizes, tensile strengths, compositions, and in addition, on the structure of the earth's upper atmosphere. Briefly, they are mostly small objects varying from the size of peas or marbles to golf balls. They appear to have low internal strengths and to crumble rather easily upon impact with the earth's atmosphere. The shape of their orbits indicates that they have a cometary rather than a planetary origin (except possibly some sporadic meteors).

On the other hand, meteorites often appear as spectacular fire balls. Their size is sometimes sufficient to insure the recovery of at least a portion of the mass that struck the earth's atmosphere. The orbits of meteorites, which at best are only rather roughly determined, indicate that they may move in paths very similar to those of the minor planets. Most of these minor planets lie between Mars and Jupiter, but some are known whose orbits intersect that of the earth.

Hundreds of these minor planets are known and many thousands could be found with existing telescopic equipment. The known ones range in size from Ceres (770 km diameter) to rocks a few kilometers across. Many show short-period light variations indicating that they are irregular in shape, being splinters or even needles of rock. Hirayama, Kuiper, and others have presented strong arguments in favor of their having been produced by collisions between two or more original bodies perhaps the size of the moon or smaller. Once a pair of such small planets was shattered, collisions between the fragments would continue, grinding the remnants into smaller and smaller bits.

Small minor planets or large meteorites (the designation depends on our point of view) are believed to have collided with the earth in the past, producing such features as the Barringer "meteor" crater near Winslow, Arizona, and the new Quebec crater. Most of these impact craters unfortunately must have been obliterated. According to F. C. Leonard's and B. J. Finnegan's (1954) survey of the 1495 meteorites inventoried in the 'Prior-Hey catalogue, the integrated weight of the identified objects lies between 450 and 500 metric tons.

The notion that meteorites are remnants of a defunct planet or planets is one of the classical hypotheses of astronomy. More than a century ago, the French geologist, A. Boisse, suggested that the average composition of meteorites would give a good approximation

to that of the earth. Extended data, collected over the past half-century by many workers, have indicated that meteorites belong to a family of objects with a common origin, possibly bodies more nearly comparable with the moon than with the earth (Lovering 1957b).

From our point of view, meteorites are of interest in that they may represent a sample of the non-volatile, or even in some instances the volatile, components of the primordial material from which the solar system was formed.

3-2. Types of Meteorites

Three principal types of meteorites are recognized, the irons (siderites), the stony-irons (siderolites), and the stones (aerolites). These are divided into several classes. The standard classification is that by Prior (1920), although a more elaborate system was later proposed by Leonard (1948, 1951).

Siderites or iron meteorites are the best known and the most easily recognized type. They are composed mostly of nickel and iron—a rough average composition being Fe 90 per cent, Ni 8.5 per cent, Co 0.6 per cent, and Si <0.01 per cent by weight. The subclasses depend on the crystal structure and therefore on the alloys of Ni and Fe. In kamacite, the Ni/Fe ratio is about 0.06; in taenite it varies between 0.14 and 1.0. Mixtures of these two alloys are also known.

Nearly 80 per cent of known siderites are classed as octahedrites. When they are cut, polished, and etched with an appropriate acid, they display a particular type of octahedral structure called Widmanstätten figures, produced by a separation of the kamacite from the more brilliantly reflecting taenite.

About 8 per cent of the iron meteorites are hexahedrites and consist of crystals of kamacite. Polishing and etching reveals a cubic cleavage and the so-called Neumann lines.

Ataxites, which account for about 12 per cent of all siderites, show commonly neither the Widmanstätten figures nor the Neumann lines. They have a fine granular structure; some are nickel rich whereas others are poor in this metal.

Siderolites or stony-irons contain about equal amounts by volume of stony and nickel-iron constituents. They comprise the pallasites that contain nickel-iron and olivine and the mesosiderites that contain, in addition, hypersthene and anorthite.

The *aerolites* or stony meteorites are made up mostly of silicate

materials containing small amounts of sulfides, metallic nickel, and iron, and trace amounts of rare elements.

For our purposes, the most important meteorites are the chondrites. According to Ninninger (1952), 90 per cent of all meteorites that have hit the earth in historic times are of this kind. They are stony in appearance but contain characteristic spheroidal bodies or chondrules that may vary in size from less than a millimeter to about a centimeter. Chondrules are often grey or brown in color and show much the same range in composition as do igneous rocks. Mineralogically, chondrules are olivine, enstatite, bronzite, hypersthene, augite, plagioclase, and glass. Sometimes chondrules consist of a single rounded crystal of some mineral; in others they are conglomerates. The material in which the chondrules are imbedded consists of the same minerals of which they themselves are composed. The chondrules are best explained as molten droplets that have only partially crystallized even at the present time. Evidently the history of these objects is extremely complicated. Chondrites contain also bits of plessite, kamacite, and taenite that are always associated even in the smallest metallic flecks.

We may mention that there are several distinct classes of chondrites. The main classes are the carbonaceous chondrites, ordinary chondrites, and enstatite chondrites. These classes grade continuously into one another with respect to physical properties (e.g., hardness), mineralogical properties, free iron content, and content of certain trace elements. Carbonaceous chondrites are the most fundamental and primitive types of meteorites. They contain up to 5 per cent carbon and 20 per cent water, together with compounds of C with H, N, S, Cl, and other volatiles. Passing from these highly porous, fragile types to dense, hard, crystalline types we find a steady loss of C, O, and other volatile materials and formation of free metals. Apparently carbonaceous chondrites were never heated; other chondrites represent material that was heated under conditions such that carbon reacted with oxidized iron and nickel to form free metals, while volatile substances were lost. Chondrites with less than 6 per cent metals were porous, whereas metal-rich enstatite chondrites, which have undergone metamorphism and reduction, are mechanically strong. Mineralogical evidence indicates that chondrites were formed at a temperature below 1000°C, later cooling in about 10^8 years to about 300°C. Melting occurred under a high pressure of volatile substances

Table 3-1. Relative Numbers of Abundant Atoms in Stony Meteorites*

	Carbonaceous chondrites	Enstatite chondrites	Achondrite (Norton county)
Na	43,700	26,000	4500
Mg	1,030,000	760,000	1,100,000
Al	86,000	45,000	13,200
Si	1,000,000	1,000,000	1,000,000
P	9200	8600	200
K	3160	6150	860
Ca	74,200	33,200	8800
Ti	3000	1500	860
Cr	12,000	5500	1100
Mn	6200	4000	2200
Fe	845,000	1,180,000	9500
Co	2200	3100	
Ni	45,500	52,300	650

* The numbers are normalized to silicon = 10^6 . The data are taken from Wiik (1956) and from G. Edwards (*Geochim. et Cosmochim. Acta*, 8, 285, 1955) for Na and K. Note the scarcity of iron and the prominence of magnesium and silicon in the achondrite.

Recent data for rarer elements have been given as follows—P. W. Gast, *Geochim. et Cosmochim. Acta*, 19, 1, 1960—K, Rb, Cs. U. Schindewolf and M. Wahlgren, *Geochim. et Cosmochim. Acta*, 18, 36, 1960—Rh, Ag, In. U. Schindewolf, *Geochim. et Cosmochim. Acta*, 19, 134, 1960—Se, Te. H. Onishi and E. B. Sandell, *Geochim. et Cosmochim. Acta*, 12, 262, 1957—Sb, As; 9, 78, 1956—Ga. T. Hara and E. B. Sandell, *Geochim. et Cosmochim. Acta*, 21, 145, 1960—Ru. E. A. Vincent and J. H. Crockett, *Geochim. et Cosmochim. Acta*, 18, 143, 1960—Au. G. L. Bate, H. A. Potratz, and J. R. Huizenga, *Geochim. et Cosmochim. Acta*, 18, 101, 1960—Sc, Cr, Eu. W. D. Ehmann and J. R. Huizenga, *Geochim. et Cosmochim. Acta*, 17, 125, 1959—Bi, Tl, Hg. H. Hamaguchi, G. W. Reed, and A. Turkevich, *Geochim. et Cosmochim. Acta*, 12, 337, 1957—U. Ba. G. W. Reed, K. Kigoshi, and A. Turkevich, *Geochim. et Cosmochim. Acta*, 20, 122, 1960—Ba, Tl, Hg.

whose sudden loss caused rapid crystallization and chondrule formation.

Although achondrites lack chondrules, some resemble chondrites mineralogically while others more closely resemble terrestrial basalts and dolerites. Table 3-1 gives analyses for chondrites and one achondrite (Wiik 1956; Edwards 1955).

The chemical, mineralogical, and age relationships existing between major meteorite types suggest a co-genetic origin (Ringwood 1960,

1961). There are reasons not yet firmly established for believing siderites crystallized under substantial pressures and were derived from deep layers in their parent bodies.

3-3. The Relative Proportions of Different Types of Meteorites

If the abundances of many of the non-volatile elements in our part of the universe can be deduced most expeditiously from the average composition of the meteorites, we must know the relative proportions of stones, stony-irons, and irons, not just among those that are retrieved from the earth's surface, but among the objects in interplanetary space.

The first point to realize is that "observational selection" strongly favors the siderolites over the aerolites. The former can be recognized years after they have fallen, whereas the latter (especially the carbonaceous chondrites, which are very fragile) may be destroyed by weathering or may not be recognized. Also, because of the smaller density and lesser tensile strength of the aerolites, a larger fraction of a siderolite than of a stony meteorite will survive the passage through the earth's atmosphere.

Hence it is not difficult to understand why the earlier workers, e.g., Farrington (1915), argued in favor of the siderolites as being representative of the most frequent types. Nininger (1952, p. 79) described a program carried out during the second quarter of this century when a special effort was made to check up on all fireball reports and to get recoveries. The average composition of the meteorites obtained was vastly different from what had been found previously, and led him to regard present figures on compositions as "inconclusive." The stones vastly outnumbered the irons among recovered falls. Also, see, for example, the discussion in Max Hey's revision of Prior's *Catalogue of Meteorites*.

Analyses by Goldschmidt (1937) and by Harrison Brown (1949) attempted to derive the abundances of the elements by assigning weights to the silicate, metal, and sulfide "phases" in which the meteoritic material was found. Urey (1952a) proposed that the chondritic meteorites themselves represented an average sample, and we shall adopt this point of view here. Probably, the carbonaceous chondrites provide the best data since they have never been heated, as have other meteorites, and hence still retain many volatile con-

stituents. Unfortunately, they have not yet been adequately analyzed for most minor elements.

3-4. Qualitative Mineralogical and Chemical Features of Meteorite Compositions

Before we consider the quantitative aspects of meteorite compositions, let us examine some of the qualitative features. The minerals that occur possess definite patterns that may give important clues to the origin and development of meteorites.

The chondrites, which are the most common and significant type of meteorite, consist of olivine, orthopyroxene nickel-iron, troilite, oligoclase, and minor accessory minerals. Other meteorite types appear to have been formed by melting and differentiation of parent chondritic material. Their mineralogy resembles that of chondrites although the proportions of various minerals may differ greatly. An important exception to this statement is that plagioclase in mesosiderites and calcium-rich achondrites is closer to anorthite in composition.

Water is particularly scarce in most meteorites; it is not contained in minerals as water of crystallization. On the surface of the earth, weathering processes will cause olivine to take up water of crystallization and change to serpentine, a mineral which is not found in meteorites. Likewise, oxygen-free minerals are more prominent than in the crustal rocks of the earth. Quartz, one of the commonest of minerals on the earth's crust, is found very rarely in meteorites, although tridymite, which is a high-temperature modification of silicon dioxide, has been found in them. Free metals are found frequently in meteorites.

Certain types of minerals are peculiar to meteorites (Nininger 1952, p. 92). Among these are the oxygen-free minerals daubriéllite, FeSCr_2S_3 , oldhamite, $(\text{Ca}, \text{Mn})\text{S}$, and schriebersite $(\text{Fe}, \text{Ni}, \text{Co})_3\text{P}$. Others are known on the earth as relatively infrequently occurring minerals.

Gases are often released when meteorites are heated. These include N, He, Ar, H₂, as well as CO, CO₂, and CH₄ which may not exist in meteorites but could be formed by secondary chemical reactions when the meteorite was heated to a high temperature. The amount of gas is extremely variable. Some iron meteorites have very little

(i.e., a volume at NTP of less than 1 per cent of volume of meteorite) while others have a volume at NTP more than ten times the volume of the meteorite. The amount of gas in stone meteorites is also variable. Hydrogen, which exists in some in combined forms, varies a great deal in quantity.

3-5. The Ages and Origins of Meteorites

The ages of meteorites have been estimated by the following methods: (1) lead-isotope ratio $\text{Pb}^{206}/\text{Pb}^{207}$, (2) the β -decay of K^{40} to Ar^{40} , (3) the β -decay of Rb^{87} to Sr^{87} , (4) radiogenic helium, and (5) cosmic-ray helium.

The lead-isotope method was applied by Patterson (1956) to get the ages of stone meteorites, for which he finds a value $4.55 \pm 0.07 \times 10^9$ yr. A difficulty appears to arise from the fact that the Pb contents found by Patterson are inconsistent with the accurate uranium determinations for these same meteorites by Reed and Turkevich (1957), in the sense that Patterson's Pb values are too high. The Nuevo Laredo meteorite has an unusually high U content and only for this one meteorite can we say that a Pb age determination exists.

The K^{40} - Ar^{40} ages have been measured by Gerling and Pavlova (1951), Wasserburg and Hayden (1955), and by Thomson and Mayne (1955). As noted elsewhere, K^{40} decays to either Ar^{40} or Ca^{40} , but the branching ratio is known to only about 10 per cent. The method is considered to give a minimum age since some of the Ar may have been lost during a subsequent heating of the meteorite. The ages of stone meteorites estimated by this method range from 0.6×10^9 yr to 4.5×10^9 yr. Preliminary measurements by this method for iron meteorites indicate a somewhat greater age than for stone meteorites.

The half-life of Sr^{87} for β -decay to Rb^{87} is very long, (5.0×10^{10} yr); hence the method is useful only for very great ages. Schumacher (1955) employed this method for the Pasamonte achondrite.

The helium methods are of particular interest. Meteorites often have a large He^3 content and a high He^3/He^4 ratio. Only He^4 can be produced by radioactive decay, whereas cosmic-ray activity can create both He^3 and He^4 . Earlier estimates of the ages of meteorites by the helium method were based on the assumption that all helium came from the decay of U and Th. Carl Bauer noticed that the "ages" depended on the size of the sample in such a way that

the larger the meteorite, the "younger" it was. Presumably, much of the helium was produced by cosmic rays, and only careful isotopic measurements of the helium would distinguish between the two effects. Reed and Turkevich (1957) made a careful study of the radiogenic helium ages of stone meteorites. On the basis of their studies of the U content of stone meteorites, they assumed an average U content of 1.1×10^{-8} g/gr and that the Th/U and U^{238}/U^{235} ratios are the same on the earth and in meteorites. Then, making use of the published data on helium contents and isotope ratios, and assuming that the non-radiogenic helium consists of four He^4 atoms to each He^3 atom, they derived the radiogenic helium ages of stone meteorites.

The calculated radiogenic ages fell in the range 0.5×10^9 to 4.5×10^9 yr. In eight instances out of eleven, these ages agreed with those found by investigators who used other radiogenic methods, particularly the K^{40} - Ar^{40} method. Two stone meteorites, however, Nuevo Laredo and Holbrook, gave helium ages very much shorter than the Ar^{40} age or the lead age for Nuevo Laredo (Patterson). The radiogenic helium ages tend to fall in two groups, one with values up to about 1×10^9 yr and the other with ages 4 to 4.5×10^9 yr. Reed and Turkevich suggest that the larger age may represent the actual time of fractionation of the meteoritic materials and that some of the meteorites lost their helium and perhaps some argon about 10^9 yr ago, perhaps in the breaking apart of a parent planet.

The cosmic-ray ages deduced from the He^3 contents of aerolites, however, range from 5 to 300 million years. The discordances may be understood if we suppose that although the actual material of the meteorites solidified about 4.5×10^9 yr ago, the actual bodies have been flying about in space for only a few million years. Otherwise the cosmic-ray-induced activity would be much greater than is actually observed.

Although the age question is not finally settled, most major meteorite types seem to have the same age, i.e., about 4.5×10^9 years. At this time, the parent bodies of the present meteorites apparently underwent a major chemical differentiation into chondrites, achondrites, and irons or stony-irons. Although the overall composition of the parent body corresponded to that of a chondrite, a small proportion of chondritic material was melted at this time and differentiated to form achondrites, stony-irons, and irons in the small core.

Brown and Patterson (1948) remarked that "perhaps the most convincing evidence that fragments of meteoritic matter, now widely scattered, at one time existed in close contact with one another, is the evidence derived from the distribution of elements between the various meteoritic phases."

As previously mentioned, there are three main phases of the meteoritic matter: the silicate phase, composed primarily of silicates of Si, Mg, and Fe; the metal phase with Fe, Ni, Co; and the trolite phase composed mostly of FeS. Many years ago, W. A. Wahl pointed out that those major meteoritic constituents whose oxides have low heats of formation exist primarily in the metal phase, whereas those constituents whose oxides have high heats of formation appear primarily in the silicate phase. Prior also noticed that although the total amount of iron was nearly constant in a large number of chondritic meteorites, if the metallic iron phase was low, then the percentage of iron in the silicates was greater and the ratio of iron to nickel in the metal phase was lower than in the chondrites in which the amount of the metallic phase was large.

Urey and Craig (1953) found the chondrites to fall within two distinct groups with regard to both total iron content and oxidation state of iron. They found no simple mixing process by which one group could be derived from the other and concluded that the two groups of chondrites had been derived from different parent bodies. It requires oxidation and removal of the element iron to go from the high-iron group to the low-iron group. From an application of X-ray fluorescence to a study of the variations of Cr, Mn, Fe, Co, and Ni in meteorites, H. Brown and C. R. McKinney found four major families of chondrites. The concentrations of Fe, Co, and Ni with respect to Mn and Cr show a different specific ratio for each of these families.

Lovering, Nichiporuk, Chodos, and Brown (1957) found that iron meteorites could be grouped according to their gallium and germanium contents into four distinct classes. The chromium content also varied over a wide range, while concentrations of Co and Cu varied over relatively narrow ranges. E. W. Wardani (1957) found that the germanium in iron meteorites varied by more than a factor of 500, whereas the chondrites showed a fairly uniform Ge concentration. These examples illustrate some of the difficulties encountered in assessing the meteoritic data and setting up theories of their origin.

The parent bodies of the meteorites (minor planets—or perhaps objects comparable with the moon) are believed to have been formed at low temperatures. Subsequently, their interiors became heated. The concentrations of thorium and uranium are so low that radioactive heating cannot have played an important role. Short-lived radioactivity also seems unlikely. Urey and Donn (1956) proposed that chemical reactions between unstable compounds may have produced heat, although Urey concluded later that the amount would be insufficient. Gravitational contraction of largely gaseous primary objects of lunar size might produce the required heating.

B. Mason (1960) suggested that chondrites are not fragments of a disrupted planet but have always been independent individual objects, although he suggested that irons and stony-irons could be fragments of a body formed by aggregations of chondrites. Urey (1955) remarks that the production of the chondrites requires as a minimum:

1. The reduction of the oxidized iron to the metallic forms, the melting of the iron, its accumulation into massive chunks, and its slow cooling to form the nickel-iron alloys
2. The melting of the silicates and their crystallization to produce the minerals of the chondrites and achondrites
3. The violent smashing up of these materials
4. The accumulation of the fragments into the chondrites

In Urey's (1956) theory, primary objects formed by accretion are later broken up. Secondary objects formed from these fragments are smashed to form the actual meteorites. A new version of a classical theory of meteorite formation has been given by Ringwood (1961). The parent bodies of meteorites were of lunar dimensions or smaller and were formed by accretion from a cold dust cloud. They had a composition resembling the most primitive carbonaceous chondrites, e.g., Orgueil (cf. p. 43). In a typical planetoid melting occurred in the interior soon after accretion. When the molten region became extensive enough, convection set in. Molten chondritic material, containing water and carbon under a confining pressure rose to the planetoid surface where the pressure was released. Volatiles, chiefly H_2O , CO_2 , and also Pb, Tl, Bi, and Hg, rapidly escaped and the surface experienced marked vulcanism. The rapid escape of water caused immediate crystallization and resulted in the formation of the typical tuffaceous and chondritic structures. During the same heating process,

the free C and H reacted with oxidized iron and nickel to produce a metallic phase *in situ*, while the resulting CO₂ was lost with the volatiles. It is suggested that nearly all the material passed through this melting-convection-vulcanism stage, thus producing the familiar metal-containing chondritic meteoritic structure. Although the temperature at which melting occurred was near 900°C, and the main mass soon cooled to 300°C, temperatures above 1000°C were reached in the core, producing complete melting and differentiation of chondritic material. Some metamorphism and recrystallization occurred in the mantle. Irons and stony-irons came from the inner region, chondrites from the mantle when the planetoid was disrupted.

3-6. Loss of Elements by Fractionation

In order to make meaningful abundance comparisons between the compositions of the chondritic meteorites and other sources of data, e.g., the sun, we must consider possible preferential losses of certain elements in meteorites. Clearly, volatile elements were lost from meteorites in even greater proportions than they were from the earth. We must still ask to what extent the meteorites are representative of the non-volatile fraction of the cosmic material. This question can be answered only (if at all) by a detailed consideration of both the volatile and non-volatile compounds that may have been formed during the probable history of the meteorite. Urey (1952b) has examined this question in detail for Li, Be, B, F, Cl, Br, I, Na, K, Mg, Ca, Si, P, and S. He concluded that although P and S may have been removed to some extent, F, Cl, Br, and I probably have not been lost substantially by any volatilizational process. The other elements are essentially non-volatile and their losses must be small. Urey decided that all elements, except those that form stable compounds which are volatile at temperatures around 0°C, have been retained by the meteorites without serious loss. This conclusion implies that the asteroids and possibly some of the other planets were formed by an accumulation process at low temperature.

Urey suggested the possibility that in the formation of the parent bodies of the meteorites, or even of the planets themselves, a preferential loss of silicates may have occurred. He attempted to explain the density differences between the terrestrial planets in this way; e.g., Mercury lost much of its silicates, Mars relatively little. Ringwood (1959) has proposed an alternative interpretation in terms of oxida-

tion-reduction equilibria affecting the parental carbonaceous chondritic material. Thus Mars probably has no iron core because all its iron is tied up in oxides. In Mercury, on the other hand, probably most of the silicon, iron, etc., exists in a reduced form, while the Earth and Venus have metallic cores with thick mantles of oxidized rock.

It should be remarked that Suess and Urey (1956) regarded certain elements as depleted in the meteorites in addition to the usual volatile ones. For example, they assumed that Cl, S, Se, and Te have been depleted by substantial factors: selenium and sulfur by about a factor of 4, but Te by a somewhat smaller factor. The alkali metals may have been lost by a factor somewhat smaller than 2.

The carbonaceous chondrites retained many volatiles, particularly Cl, N, S, and the volatile metals, Pb, Ti, Bi, and Hg. Of particular interest are uranium, thorium, and lead. The carbonaceous chondrites give the primitive lead isotope ratios. Since they did not lose lead as did other meteorites, they have a high Pb/U ratio. Reed, Kigoshi, and Turkevich (1960) have determined amounts of Ba, Th, Hg, Pb, Bi, and U in these chondrites that are larger than those found in other meteorites.

No conceivable process occurring in meteorites can greatly alter the abundance ratios of elements of similar chemical properties, e.g., remove iron while leaving chromium behind.

3-7. Abundances in Meteorites

The determination of abundances in meteorites presents a host of problems which makes the subject one of the most exacting in analytical chemistry.

1. Some meteorites are fragile structures; others have high tensile strength like a chunk of basalt. All are subject to weathering so analyses, in order to be reliable, have to be carried out on freshly fallen, unweathered material.

2. One of the biggest difficulties is the scarcity of material. The average recovery from a fall is only a few kilograms and some are represented by only a few grams.

3. For most elements it is necessary to use microanalytical techniques of the highest sensitivity. In spite of the great care exercised by many workers, the older analyses often gave spurious results for the rarer elements. For example, the values obtained for Pb were too high by a factor of 10 or more as a consequence of impurities in reagents and material dissolved from the walls of glassware.

There still remains the question as to the proper average over the different types of meteorites. We adopt here the point of view of Urey and regard the best sample as that given by the chondritic meteorites themselves (Suess and Urey 1956, Table II). For comparison, however, we also give in Table 3-2 the average abundances for meteorites as computed by Levin, Koslovskaja, and Starkova (1958). They adopted a ratio of stones to metal in the meteoritic substance as 6/1, however. In general, there is a good agreement between the two results, particularly for the more abundant elements. In treating the rarer elements, it is, of course, necessary to be extremely critical in assessing the data. In the comparisons to be made in later chapters, we shall use Urey's results. We give abundances for scandium, chromium, and europium found by G. Bate and for Rh, Ag, In, Se, and Te by Schindewolf by the neutron-activation method. Note that the analyses for the rarer elements generally tend to be lower, particularly for indium which lies near the limit of detection.

Table 3-2¹ gives atomic abundances reduced to Urey's scale ($A(\text{Si})=10^6$). Certain elements such as oxygen, which form predominantly volatile compounds, have been omitted. Mercury, although included, appears to have too low an abundance because of its volatile characteristics even at low temperatures. The most reliable abundances are those for the elements forming the highly stable non-volatile oxides, i.e., Mg, Ca, Al, and Si for which good analytical data are available. It should be noted, however, that the ratios of even the more abundant elements in the chondrites, e.g., that of silicon to Fe, Mg, Na, or Al, vary by factors up to and even greater than 2 from one object to another. Among the rarer elements larger discordances are of course obtained.

A comparison of the composition of the meteorites with that of the earth's crust shows a number of significant differences. Considering for the moment only the most abundant elements in the earth's crust, we find the comparison with the chondritic meteorites to be as shown in Table 3-3. Sodium, aluminum, potassium, calcium, and titanium are much less abundant in the chondritic meteorites while the proportions of Mg, Mn, Fe, Co, and Ni are greatly enhanced.

The isotopic constitution of elements in meteorites as compared with terrestrial rocks is of the greatest interest. The most striking

¹ Older compilations of meteoritic abundances have been given by V. M. Goldschmidt (1937) and by Harrison Brown (1949).

Table 3-2. Atomic Abundances in Meteorites

(Si = 1×10^6)

		Suess and Urey (1956)	Other results (see p. 44)	L,K,S ^a (1958)
3	Li	100		73
4	Be	16		1.57
5	B	20		38
9	F	300		331
11	Na	43,800		48,000
12	Mg	912,000		902,000
13	Al	94,800		81,500
14	Si	1,000,000		1,000,000
15	P	5000		8150
16	S	98,000		98,200
17	Cl	2100		3570
19	K	3160		3640
20	Ca	49,000		63,000
21	Sc	28	32	17.5
22	Ti	2440		2300
23	V	220		249
24	Cr	7800	6400	7640
25	Mn	6850		5760
26	Fe	600,000		724,000
27	Co	1800		2420
28	Ni	27,400		37,600
29	Cu	212		100
30	Zn	180		48.3
31	Ga	11.4		18
32	Ge	65		87
33	As	4.0		14.7
34	Se	24	18.8	18
35	Br	49		43.3
37	Rb	6.5	6.0	14.5
38	Sr	18.9		39.4
39	Y	8.9		9.0
40	Zr	54.5		158
41	Nb	0.8		0.84
42	Mo	2.42		8.0
44	Ru	2.1	1.5	3.1
45	Rh	0.71	0.27	0.92
46	Pd	1.3		0.73
47	Ag	0.35	0.13	0.73
48	Cd	1.9		2.8

^a Levin, Koslovskaja, and Starkova, *Geochim. et Cosmochim. Acta*, 13, 76, 1958.

Table 3-2.—Continued

		Suess and Urey (1956)	Other results (see p. 44)	L, K, S ^a (1958)
49	In	0.26	0.0013	0.28
50	Sn	1.33		26.4
51	Sb	0.12	0.12	0.52
52	Te	0.16	0.73	0.12
53	I	1.5		0.12
55	Cs	1.3		0.95
56	Ba	8.8	10.0	8.0
57	La	2.1		2.35
58	Ce	2.3		2.35
59	Pr	0.96		0.90
60	Nd	3.3		0.34
62	Sm	1.1		1.05
63	Eu	0.28	0.078	0.31
64	Gd	1.6		1.63
65	Tb	0.52		0.51
66	Dy	2.0		1.9
67	Ho	0.57		0.56
68	Er	1.6		1.63
69	Tm	0.29		0.28
70	Yb	1.5		1.46
71	Lu	0.48		0.45
72	Hf	0.55		0.70
73	Ta	0.32		0.26
74	W	13.0		14.6
75	Re	0.05		0.0013
76	Os	0.97		0.90
77	Ir	0.31		0.19
78	Pt	1.5		2.4
79	Au	0.140	0.12	0.21
80	Hg	<0.006	4	0.007
81	Tl	0.11	0.13	0.107
82	Pb	0.122	3.5	1.5
83	Bi	0.21	0.16	0.12
90	Th	0.033		
92	U	0.0178	0.0078	

effects are observed for helium which is produced by radioactive decay or by cosmic rays. We have previously remarked that whereas the decay of uranium and thorium will produce He⁴ it can produce no He³. Cosmic rays produce both He⁴ and tritium that ultimately,

Table 3-3. Comparison of Abundances in the Earth's Crust and Meteorites

	Total crust (Table 2-1)	Chondritic meteorites (Urey, Table 3-2)
Na	104,000	43,800
Mg	141,000	912,000
Al	325,000	94,800
Si	1,000,000	1,000,000
P	3,430	5,000
S	(1,640)	98,000
K	45,000	3,160
Ca	174,000	49,000
Ti	23,000	2,440
Mn	1,950	6,850
Fe	126,000	600,000
Ni	(100)	27,400

decays into He^3 . In iron meteorites He^3/He^4 ratios up to 30 per cent are found, whereas in stone meteorites the ratios are much smaller, falling between 0.002 and 0.10 with an average value near 0.02.

Other cosmic-ray effects are noted in meteorites. For example, in the Sikhote-Alin iron meteorite, Vinogradov (1958) found certain neon isotope ratios differing from the terrestrial ratios and indicating spallation effects of cosmic rays on iron and other nuclei. Similarly, he found that certain isotope ratios in argon differ from those found on the earth, and that the total concentration of argon decreases with distance from the surface of the meteorite. The Ar^{40} in the earth's atmosphere comes largely from the decay of K^{40} , whereas Ar^{38} and Ar^{36} come from the spallation of iron and other nuclei in meteorites. The isotopic constitution of the Nuevo Laredo stone has been studied by Reynolds and Lipson (1937) for He, Ne, and Ar. It is to be noted, however, that the inert gases found in meteorites are probably entirely of radiogenic or cosmic-ray origin.

The natural isotopic constitution of elements in meteorites, i.e., those not influenced by radioactive decay nor by cosmic rays, appears to show a remarkably small dispersion about their mean values. Rankama (1954) has suggested that certain meteoritic values be adopted as standards to which the terrestrial values may be compared. In the rocks of the earth's crust, isotope abundance ratios are sometimes affected by melting, by subsequent fractionation, and for

lighter elements by biological processes as well, and only at great depths do the ratios approach the meteoritic values. Sulfur, studied by Thode, offers one example. Marine sulfates have a S^{32}/S^{34} ratio of 21.75, whereas ultramafic rocks (dunite) and stony meteorites both show a ratio of 22.20. For other examples see reviews by Rankama (1954) and Vinogradov (1958). Boato (1954) found that the deuterium/hydrogen ratio showed a substantial fluctuation in meteorites, but that this variation was well within the range appropriate to chemical fractionation processes. Hence, the deuterium/hydrogen ratio appears to be exactly the same in the carbonaceous chondrites as on the earth. Accordingly, we can take the terrestrial ratio as representative of the solar system as a whole.

3-8. The Composition of Meteors

The materials of which meteors are composed cannot be recovered for chemical analysis. Instead, we have to rely exclusively on studies of their spectra, excited as a consequence of the rapid dissipation of the energy of these objects as they pass through the upper atmosphere. Since the excitation conditions of their bright-line and continuous spectra are unusual, conventional astrophysical methods for quantitative spectrochemical analysis are not applicable, and it has not proved possible to obtain accurate abundances from the analysis of their spectra. The observed differences in meteoric spectra may arise from differences in physical processes as well as from chemical compositions. The earliest observations were necessarily visual, but photographic techniques were developed by P. M. Millman, J. A. Russell, A. F. Cook, and others. The observational techniques are difficult and the requirements for accurate spectrophotometric measurements likewise are stringent (Cook 1955).

Meteor spectra show the emission lines of abundant metals, NaI, MgI, MgII, AlI, SiI, SiII, CaI, CaII, CrI, MnI, FeI, FeII, and NiI. In addition, the emission lines of HI, NI, OI, and the continuous radiation of the N_2 molecule also have been observed. Millman (1953) regards it as likely that the hydrogen radiation comes from the hydrogen ices forming part of the meteor's fragile body, whereas G. S. Hawkins concludes that it is not obvious that the radiation from N, O, and H comes from beyond the earth's atmosphere.

If meteors represent fragments of defunct comets, their compositions should reflect that of these bodies. Comets are presumed to

originate from material which was "left over" when the solar system was formed, since it had such a low density that it could not form planets. This debris, which was scattered in the region of the solar system beyond the orbit of Pluto, eventually formed loose configurations of icy conglomerates. Perturbations by passing stars caused some of these condensations to move in orbits close to the sun where they appeared as comets. Some comets were perturbed by planets into short-period orbits and finally disintegrated. The volatile constituents gradually evaporated, while the remaining refractory particles moved sunward under the influence of the Poynting-Robertson effect. They produce the zodiacal cloud and meteors as they strike the earth's atmosphere.

Selected References

- Boato, G., *Geochim. et Cosmochim. Acta*, **6**, 209, 1954.
Brown, Harrison, *Revs. Modern Phys.*, **21**, 625, 1949.
Brown, H. and C. R. McKinney, *Trans. Am. Geophys. Union*, **38**, 383, 1957.
Brown, H. and C. Patterson, *J. Geol.*, **56**, 85, 1948.
Cook, A., In *Meteors: A Symposium in Meteor Physics*, Pergamon Press, London, 1955.
Farrington, O. C., *Meteorites, Their Structure, Composition and Terrestrial Relations*, Field Museum, Chicago, 1915.
Gerling, E. K. and T. G. Pavlova, *Doklady Akad. Nauk S.S.S.R.*, **77**, 85, 1951.
Goldschmidt, V. M., *Skrifter Norske Videnskaps-Akad. Oslo. I, Mat. Naturv. Kl. No. 4*, 1937.
Leonard, F. C., *Pop. Astron.*, **56**, 437, 1948; *Pop. Astron.*, **59**, 370, 1951; *Meteorites*, **1**, 150, 1954; *Meteorites*, **1**, 317, 1955.
Leonard, F. C. and B. J. Finnegan, *Meteorites*, **1**, 169, 1954.
Levin, B. Yu, S. V. Koslovskaya, and A. G. Starkova, *Meteoritika*, **14**, 38, 1958.
Lovering, J. F., *Geochim. et Cosmochim. Acta*, **12**, 238, 1957a; 253, 1957b.
Lovering, J. F., W. Nichiporuk, A. Chodos, and H. Brown, *Geochim. et Cosmochim. Acta*, **11**, 263, 1957.
Mason, B., *J. Geophys. Research*, **65**, 2965, 1960.
Millman, P. M., *Nature*, **172**, 853, 1953.
Nininger, H. H., *Out of the Sky*, University of Denver Press, Denver, Colo., 1952.
Patterson, Claire, *Geochim. et Cosmochim. Acta*, **10**, 230, 1956.
Prior, G. T., *Mineral Mag.*, **19**, 51, 1920; **18**, 26, 1916. *Catalogue of Meteorites*, British Museum, 1953.
Rankama, K., *Isotope Geology*, McGraw-Hill, New York, 1954.
Reed, G. W. and A. Turkevich, *Nature*, **180**, 594, 1957.
Reynolds, J. H. and J. I. Lipson, *Geochim. et Cosmochim. Acta*, **12**, 330, 1957.
Ringwood, A. E., *Geochim. et Cosmochim. Acta*, **15**, 257, 1959, in press 1961.
Schumacher, E., *Z. Naturforscher*, **11a**, 206, 1956.
Suess, H. and H. C. Urey, *Revs. Modern Phys.*, **28**, 53, 1956.

- Thomson, S. J. and K. I. Mayne, *Geochim. et Cosmochim. Acta*, **7**, 169, 1955.
- Urey, H. C., *Phys. Rev.*, **88**, 248, 1952a; *Geochim. et Cosmochim. Acta*, **2**, 269, 1952b; *Proc. Nat'l. Acad. Sci. U.S.*, **41**, 127, 1955; *Ap. J.*, **124**, 623, 1956; *J. Geophys. Research*, **64**, 1721, 1959.
- Urey, H. C. and H. Craig, *Geochim. et Cosmochim. Acta*, **4**, 36, 1953.
- Urey, H. C. and B. Donn, *Ap. J.*, **124**, 307, 1956.
- Vinogradov, A. P., *Geochim. et Cosmochim. Acta*, **15**, 91, 1958.
- Wardani, S. A., *Geochim. et Cosmochim. Acta*, **13**, 5, 1957.
- Wasserburg, G. J. and R. J. Hayden, *Phys. Rev.*, **97**, 86, 1955.
- Wiik, H. B., *Geochim. et Cosmochim. Acta*, **9**, 279, 1956.

Abundances Derived from Gaseous Nebulae

4-1. Advantages and Disadvantages

In preceding chapters we have seen that the difficulty in deriving "cosmic" abundances from analyses of the earth's crust and meteorites arises from the fact that these samples have undergone some kind of fractionation, severe for the earth's crust, less so, but still to a significant degree important, for the meteorites. Although accurate chemical analyses are possible, allowance for the loss of depleted elements is difficult.

Presumably the present "cosmic" composition in our part of the galaxy is best illustrated by the interstellar medium, out of which new stars are continually being formed. A quantitative analysis of this medium is difficult (if not downright impossible) for the vast bulk of this material. Only when a portion of it is subjected to radiation from a bright, intensely hot star, which causes it to fluoresce and emit a bright-line spectrum, can abundances of the most prominent gases be estimated. Examples are provided by the bright diffuse nebulae such as the Orion and Trifid nebulae.

In those regions of space where hydrogen is not ionized, the presence of interstellar gas is often revealed by the 21 cm radio-frequency line of neutral hydrogen and by the sharp, usually weak, lines of metals such as CaI, CaII, NaI, KI, and FeI. Invariably these lines arise from the lowest level and when molecules are present, the only lines observed are those likewise coming from the lowest level. It is difficult to obtain the total abundances of the corresponding elements from their resonance absorption lines because the gas is in a state far removed from thermodynamic equilibrium and we cannot be sure that the excitation conditions are uniform along the line of sight.

This chapter emphasizes the determination of abundances from the bright-line spectra of gaseous nebulae. The conditions of excitation of the spectrum differ profoundly from those existing in stellar

atmospheres or in the laboratory; yet the physical processes playing roles in the excitation of their somewhat exotic spectra appear to be reasonably well understood for most emission lines. For certain elements it is possible to obtain abundances more accurately than from stellar atmospheres; for the rarer elements no reliable estimates are possible.

Figure 4-1 illustrates spectral scans of the brightest part of the Orion nebula as obtained with a photoelectric scanner. The brightest lines in the spectral range from the "forbidden" [OII] doublet $\lambda 3726, 3729$ to the infrared HeI $\lambda 10830$ emission are depicted. Notice that, although the usual lines of helium and hydrogen are present, among the strongest of the radiations are the prominent forbidden lines of oxygen, neon, and sulfur in various stages of ionization, viz., [OII], [OIII], [NeIII], [SIII]. In this respect, the spectrum of a gaseous nebula differs profoundly from that of a mixture of similar chemical composition excited by a laboratory glow or spark discharge.

The inner bright portion of the Orion nebula represents a portion of the interstellar medium that is heated to incandescency. It includes not only the interstellar gas but also solid particles that are vaporized and raised to a gas kinetic temperature of 10,000 or 15,000° by illuminating stars. In the outer part of this nebula, the physical processes are rendered more complicated by the presence there of these solid particles. Hence it is advantageous to consider the ionized inner portions of objects like Orion or nebulae that are gaseous throughout, e.g., the planetaries.

To summarize, the gaseous nebulae offer certain distinct advantages for a study of cosmic abundances, viz.:

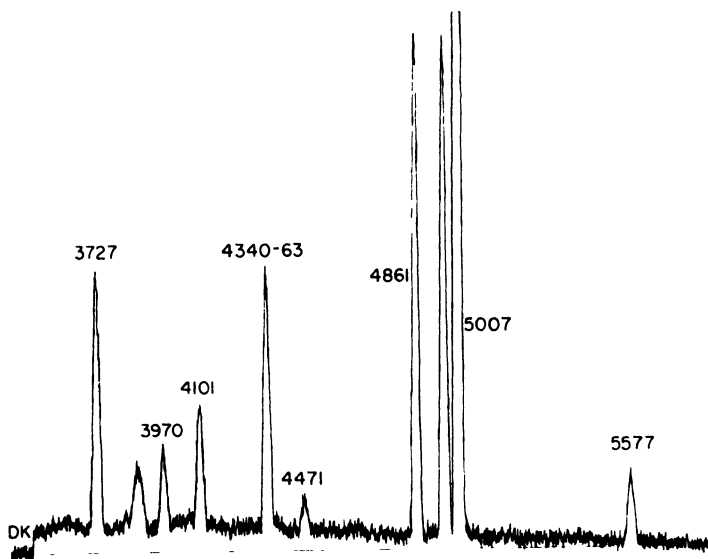
1. A diffuse nebula is likely to be uniform in composition as the interstellar medium tends to be churned up and mixed by radiation-pressure and gas-pressure differences produced by passing stars.

2. All portions of a nebula (as distinct from stars) are accessible to observation.

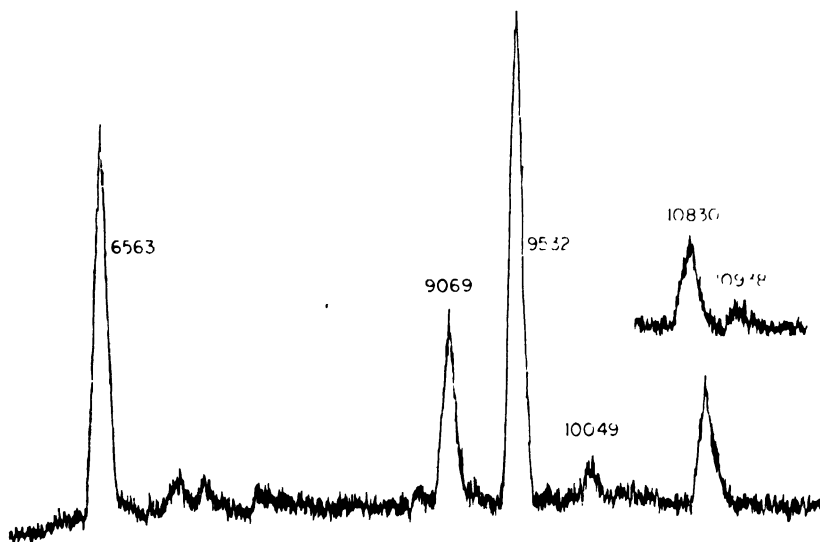
3. In spite of the fact that deviations from thermodynamic equilibrium are severe, the physical processes that produce the bright-line spectra are believed to be not only well understood, but amenable to precise theoretical treatment.

The disadvantages of the analysis are:

1. Usually the lines of only the most abundant elements are observed.



(a)



(b)

Fig. 4-1. (a) Orion nebula—blue cell; (b) Orion nebula—infrared cell.

2. A given element is often observed in only a few stages of ionization, although it may exist in the nebula in several different ionization stages. Hence it is necessary to allow for the distribution of atoms among the various possible ionization stages. This step has to be done empirically since the radiation field in the nebula is not at present amenable to theoretical calculation.

3. Most nebulae exhibit a filamentary structure, i.e., the density and temperature are not uniform from one point to another. Sometimes a stratification occurs, i.e., the inner part of the nebula is at a higher temperature and level of excitation than is the outer part.

For only a few nebulae are the observations sufficiently detailed to permit steps 2 and 3 to be carried out in detail.

4-2. Excitation of the Bright-Line Spectrum

With a few well-understood exceptions,¹ the bright lines of the spectrum of a gaseous nebulae are produced as follows.

Primary mechanism (Zanstra 1927; Menzel 1926): The photo-ionization from the ground term of an atom is often followed by the recapture of the electron in a high-energy level. The atom then cascades to lower-energy levels with a possible emission of lines in the observable region of the spectrum. The H and He lines are produced by this mechanism, as are certain much weaker lines of carbon, oxygen, neon, and a few other abundant elements. The capture of an electron by an ion also gives rise to a radiative continuum.

Collisional mechanism (Bowen 1928): The ions of elements such as N, O, Ne, and S have *metastable levels* that lie only a few electron volts above the ground term. These metastable levels belong to the same electronic configuration as the ground level, and hence no ordinary (electric dipole) radiative transitions can occur between them and the lower levels since these jumps would violate the Laporte parity rule. Inelastic collisions excite atoms from the ground level to these metastable levels. These atoms may then escape by either collisions of the second kind (events where passing electrons carry off excess energy), or by emission of forbidden radiation of the magnetic-dipole or electric-quadrupole type. Transitions of this type have

¹ Certain permitted lines of OIII and NIII are excited by a fluorescent mechanism, the energy for which is supplied by the resonance Lyman α transition $\lambda 303.780$ of ionized helium (Bowen 1935).

much lower probabilities than ordinary electric-dipole transitions. Let us now consider these mechanisms in more detail.

Atoms in a typical gaseous nebula are exposed to attenuated radiation from a very hot star. The spectral-energy distribution corresponds to temperatures between 20,000 and 200,000°K, whereas the radiation density corresponds to only a few degrees absolute. Almost all neutral hydrogen or helium atoms exist in the ground state; hence all photo-ionizations occur from the ground level. Recombinations, however, may occur on any level and as the atom cascades to a lower level it emits characteristic lines of the bright-line spectrum. Consider the $\lambda 4686$ line of HeII (Fig. 4-2). A singly ionized helium atom absorbs a quantum of energy shortward of (i.e., of higher frequency than) $\lambda 228$ and becomes doubly ionized. An electron is subsequently recaptured in the 4th level with the emission of a quantum shortward of $\lambda 3650$, or perhaps in a yet higher level with subsequent cascade to the 4th level. From the 4th level the atom jumps to the 3rd level with the emission of $\lambda 4686$, the first line of the Paschen series of ionized helium. From the 3rd level it may jump to the 2nd level or to the ground level, in either instance giving radiation in the unobservable part of the spectrum.

The recombination spectrum of hydrogen is similar except that corresponding transitions fall in different spectral regions; the Paschen

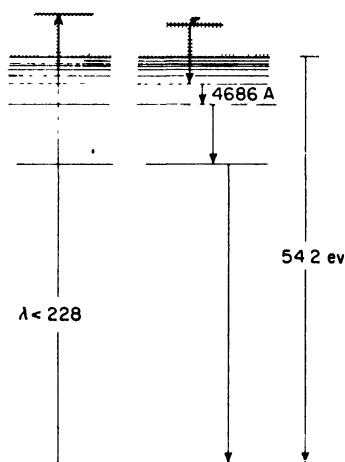


Fig. 4-2. Excitation of the recombination spectrum of ionized helium.

series of hydrogen falls in the infrared and the Balmer series in the visible range. The formal theories are equivalent, however. Recombination of singly ionized helium giving rise to the characteristic lines of neutral helium proceeds along somewhat the same pattern except that the physical situation may be complicated by the presence of the high metastable levels, 2^1S and 2^3S .

The emission per unit volume in a transition $n-n'$ in hydrogen or ionized helium may be written (Menzel 1937 or Aller 1956, p. 119) in the form

$$E_{nn'} = 1.42 \times 10^{-16} Z^6 (b_n(T_e) g/n'^3 n^3) N_i N_e T_e^{-3/2} \exp(157,000 Z^2/n^2 T_e) \quad (4-1)$$

Here n denotes the upper, n' the lower level. N_i is the number of ions of hydrogen (or doubly ionized helium)/cm³, N_e is the corresponding electronic concentration, Z is the charge on the nucleus, T_e is the electron temperature, $g_{nn'}$ is called the Gaunt correction factor to Kramers' formula—for most applications we can take it simply as unity.

The factor $b_n(T_e)$ is a measure of the deviation from thermodynamic equilibrium. That is, it gives the ratio of the actual population of the state n to the population it would have had in thermodynamic equilibrium in a gas of the same electron density and temperature. The numerical value of b_n will depend on the physical processes operative in the gas, whether the shell of gas is optically thin or thick, and whether collisions are important in exciting atoms to the level n . For numerical values see, for example, Baker and Menzel (1938) and Burgess (1958). In most planetaries, it appears that the b_n values computed for the thick-nebula approximation are valid.

Some values for hydrogen for the typical electron temperatures of 10,000 and 20,000°K are quoted from Baker and Menzel (see Table 4-1). See also Burgess (1958) and Seaton (1960).

Table 4-1. Values of b_n for Hydrogen for Optically Thick Nebula^a

$n =$	3	4	5	6	7	8	9	10
$T_e = 10,000$	0.089	0.166	0.233	0.296	0.341	0.379	0.417	0.448
20,000	0.330	0.404	0.460	0.512	0.550	0.577	0.600	0.620

^a Baker and Menzel (1938).

The electron temperature of the gas usually can be found from relative forbidden-line intensities. A measurement of the surface brightness in $H\beta$ (for example) of a homogeneous gaseous nebula of known distance then would give an estimate of the emission per unit volume and of the electron density or ion density. Usually, hydrogen is so much more abundant than helium that we can equate N_i (number of ions of hydrogen) to N_e without loss of accuracy.

A similar theory may be applied for neutral helium except that the calculation of the numerical values of the b factors is more difficult because of the less simple term structure of the helium levels. Estimates of the concentration of O^{++} ions from the OII recombination lines require rather involved calculations. A computation of the concentration of C^{++} from the CII $\lambda 4267$ line has been carried out for a number of nebulae, assuming that the b_n values are hydrogenic for the highest levels. It must be remarked that the b_n values for helium, carbon, oxygen, etc., involve not only the n but also the l value. Even in hydrogen, the b_n values depend on l but Burgess (1958) showed that for this simple atom the calculations carried out on the assumption that b_n is independent of l give very nearly the correct relative Balmer line intensities. Mathis (1957) and Seaton (1960) have given the theory for the helium lines. Seaton and Burgess have discussed the recombination of highly ionized oxygen ions and electrons.

Turning to the forbidden lines that dominate the spectra of most gaseous nebulae, we notice that they occur only for ions that have metastable levels lying just a few volts above the ground level. Typical transition schemes are illustrated for the ions of argon. Jumps from the middle metastable level (1D or 2D) to the ground (3P or 4S) terms are called *nebular-type* transitions, whereas jumps between the two higher terms are referred to as *auroral-type* transitions.

The number of collisional excitations/cm³/sec, \mathfrak{F}_{AB} , from a lower level A to an upper level B , will depend on the ion and electron density, the electron temperature, the excitation potential χ_{AB} of the higher level, the statistical weight of the lower level, g_A , and a parameter $\Omega(A,B)$ that will depend on the particular ion and transition involved (see Menzel, Aller, and Hebb 1941), viz.,

$$\mathfrak{F}_{AB} = 8.54 \times 10^{-6} [\Omega_{AB}/g_A] N_A N_e T_e^{-1/2} 10^{-\theta \epsilon \chi_{AB}} \quad (4-2)$$

Here $\theta_e = 5040/T_e$. For example, $g_A = 9$ for the 3P ground term in

OIII for which ion Seaton finds $\Omega(^3P - ^1D) = 1.59$, $\Omega(^3P - ^1S) = 0.22$ and $\Omega(^1D - ^1S) = 0.64$. The corresponding number of collisions of the second kind per cm^3 per second will be

$$\mathfrak{F}_{BA} = 8.54 \times 10^{-6} (N_B N_e / \sqrt{T_e}) / [\Omega(A, B) / (2J_B + 1)] \quad (4-3)$$

and under conditions of thermodynamic equilibrium, the two rates will naturally be equal to one another. Note $g = (2J + 1)$.

For simplicity, consider an ion with two nearby metastable levels A and B . We suppose that the third level is so high or that the electron temperature is so low that processes involving it may be neglected. The condition for a statistical steady-state will be

$$\begin{array}{ccccc} \text{No. of collisional} & = & \text{no. of collisional} & + & \text{no. of radiative} \\ \text{excitations} & & \text{de-excitations} & & \text{de-excitations} \\ \mathfrak{F}_{AB} & = & \mathfrak{F}_{BA} & + & N_B A_{BA} \end{array} \quad (4-4)$$

Here A_{BA} is the Einstein probability coefficient for the radiative transition BA . Hence $N_B A_{BA}$ will be the number of downward transitions/ $\text{cm}^3\text{-sec}$. The emission per unit volume of the forbidden line radiation will be

$$E_{BA} = N_B A_{BA} h \nu_{BA} \quad (4-5)$$

We may substitute Eqs (4-2), (4-3) and (4-4) into Eq. (4-5) in order to express E_{BA} in terms of N_A (essentially the concentration of the ions of type A in the gas). Then we will obtain an equation that

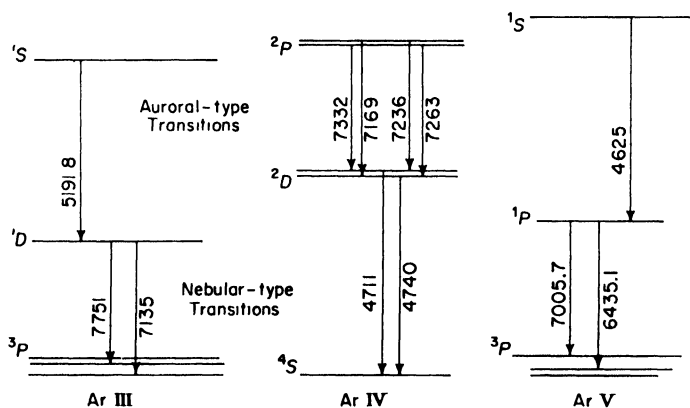


Fig. 4-3. Transition scheme for forbidden lines illustrated by the ions of argon. The configurations are respectively, $3p^4$, $3p^3$, and $3p^2$.

will involve not only the electron density and temperature, but also the atomic collision parameters, $\Omega(A,B)$ and transition probabilities A_{BA} .

When it is necessary to take three terms into account, the equations become a bit more involved as one must consider the number entering and leaving each level by all possible radiative and collisional processes. The solution of this problem is straightforward provided the relevant atomic parameters are known. In particular, it turns out that we can write down an expression for the relative intensities of the auroral and nebular transitions of a given ion, for example, O^{++} , in terms of the electron density, electron temperature, the Ω 's and the A 's. If we have another electron density/electron temperature relationship such as is provided by the emission per unit volume in one of the Balmer lines, it is possible to solve for the temperature and density. Furthermore, if we observe the auroral- and nebular-line intensities for another ion, e.g., $[NII]$, we obtain yet another relation between the electron density, electron temperature, and the inevitable atomic parameters. If the radiations of the two ions are produced in the same layers, an estimate of N_e and T_e can be found from the forbidden lines alone (Aller and White 1949; Seaton 1954; Aller 1954b). It is possible also to obtain the density of the gas from the forbidden lines of one ion, i.e., those of $[OII]$ or $[SII]$ by comparing the intensities of the two components of the nebular transitions e.g., $\lambda 3726$ and $\lambda 3729$ of $[OII]$. Uncertainties in the distance of the nebula, effects of interstellar absorption, and the assumption of a uniform density do not influence the result.

In order to interpret measured forbidden-line intensities, we must have both transition probabilities and target-area or cross-section parameters. The former are relatively easy to calculate; the latter are much more difficult to obtain although good values appear to have been calculated by M. J. Seaton (1953, 1955). When the electron densities and temperatures found by combining the forbidden-line data of $[OIII]$ and $[NII]$ are compared with those obtained, using the surface brightness data in $H\beta$, it turns out that the forbidden-line data often give a higher (sometimes a substantially higher) electron density. The interpretation of this result has been that the material is concentrated into distinct condensations or filaments, a prediction that seems to be confirmed by direct observation for those objects where a test is possible.

4-3. Determination of the Ionic Concentrations

The basic observational data for a gaseous nebula consist of measurements of the relative intensities of accessible emission lines and of the continuum, the average surface brightness of the nebula in one or more of the stronger monochromatic radiations in units of ergs/cm²-sec-steradian, and the angular size. It is desirable to have not only the average surface brightness but also the brightness distribution, i.e., the intensity contours for the monochromatic images. In practice this information can be obtained only for the stronger lines.

From the relative intensities of the Balmer and Paschen lines and the intensity decrement in the Balmer series it is possible to determine the amount of space absorption. Then one may correct the intensities for the influence of the interstellar reddening and the surface brightness for the total absorption suffered.

From the surface brightness of the nebula in H α or H β (or better from its surface brightness in the light of the Balmer recombination continuum¹), from the angular size of the nebula and its estimated distance,² and from the relative intensities of the auroral and nebular transitions in [OIII], one can make a preliminary estimate of N_e and T_e . If, in addition, auroral and nebular transitions are observed for other ions whose Ω 's and A 's are known, other solutions for N_e and T_e can be made. If several ion pairs are available it may turn out that no unique N_e and T_e will satisfy the observed intensity relationships. This situation occurs if the radiations are predominately produced in layers of different density, e.g., the [SII] lines tend to predominate in regions of high density, the [OII] lines in regions of relatively low density. When the nebula has a filamentary structure, it is appropriate to use the electron densities and temperature obtained from the forbidden lines in the subsequent analysis.

Once the electron densities and temperatures have been evaluated, and the line intensities corrected for the influence of space absorp-

¹ The advantage of the Balmer recombination continuum intensity is that no assumption concerning the value of b_n is needed; in the continuum the b factors are exactly 1.

² The uncertainty in the distances of the planetary nebulae imposes one of the greatest difficulties for their study. Various methods of distance determination have been proposed; none of them is satisfactory.

tion, the concentrations of all observed ions are found. In practice, reliable A -values are available for most ions represented by p^2, p^3 , or p^4 configurations, but only a few of the A -values for the metallic forbidden lines involving equivalent d -electrons have been computed. Unfortunately, target areas for collisional excitation of metastable levels are available only for a relatively small number of ions. For all ions in the second and third rows of the periodic table, except SII, it is necessary to extrapolate the target areas by comparing them with corresponding ions in the preceding row. Thus target areas for SIII have been estimated by comparison with OIII. New target-area computations are underway so that this unsatisfactory procedure can be eliminated.

The concentration of hydrogen relative to that of oxygen, neon, etc., is obtained by noting that N_e is essentially equal to the number of hydrogen ions. In the luminous region of the nebula, the concentration of neutral hydrogen is probably very small, while the number of electrons contributed by helium is probably an order of magnitude smaller than that contributed by hydrogen. The concentration of helium relative to that of hydrogen is found by comparison of the helium and hydrogen recombination lines and the theory of the helium recombination spectrum as developed by Mathis (1957).

In deriving relative ionic concentrations, one takes into account as far as possible the stratification within the nebula, i.e., the fact that radiations of [NeV], for example, tend to be concentrated in the inner portions, [OII] radiation in the outer portions. This means that one should obtain intensity measurements at several points within a nebula that shows pronounced effects of stratification. Alternately, one may measure isophotic contours to get the variation of surface brightness over the nebula. Then if one can assume some sort of symmetry in the nebula, the emission per unit volume $E(n \rightarrow n')$ can be found; for examples see Zanstra and Bradenburg (1951) and Aller (1956). Some nebulae, e.g., NGC7027, appear to show no stratification at all; in others, e.g., NGC2392, it is possible to observe single knots and filaments. In nebulae that show a pronounced filamentary structure, the assumption is often made that all ions are mixed more or less evenly from one filament to another. If [OIII] tends to be concentrated in one filament and [NII] in another, difficulties will arise in the analysis.

4-4. Estimates of the Ionization

Finally, in order to derive abundances, one has to allow for the fact that each element actually exists in several different stages of ionization but may be represented by observable ions in only one or two stages of ionization. Neon is often observed as [NeIII], [NeIV], and [NeV], but the only forbidden lines of nitrogen observed are usually those of [NII]. Hence, from the relative numbers of ions of O, O⁺, O⁺⁺, Ne⁺⁺, Ne⁺⁺⁺, and Ne⁺⁺⁺⁺ one has to infer the relative concentrations of ions of other elements as well. This step, which has to be carried out empirically, introduces greater uncertainties than any other step in the analysis. Theoretical calculations of the level of ionization are not possible since the far ultraviolet radiation field is unknown. It is further complicated by the fact that the degree of ionization in different filaments may differ from one another.

We compare first the numbers of ions in successive stages of ionization, e.g., HeI/HeII, NI/NII, OI/OII/OIII, NeIII/NeIV/NeV, etc., to find how the relative concentration of an ion depends on the ionization potential. It is then assumed that the same general curve for the distribution of atoms among different stages of ionization holds for all elements. Clearly, the abundance of neon, determined with the aid of concentrations of NeIII, NeIV, and NeV is estimated more securely than that of nitrogen which is not observed in ionization stages higher than NII. Actually, the [NII] lines show a capricious behavior from one planetary to another, and the high nitrogen concentrations found in objects such as NGC2440 may represent not an abnormal abundance of this element but rather an abnormal condition of excitation.

We illustrate the estimation of the ionic concentrations in a nebula with the data for NGC7009, a relatively high excitation object which has been rather extensively studied, both photoelectrically and photographically. Its internal motions have been studied by Wilson (1958). In particular, the flux radiated by the nebula in H β and the green nebular lines have been measured. If the nebula can be approximated as a spherical shell of thickness d and outer radius A , let us define

$$D \equiv 3d [1 - (d/A) + (d^2/3A^2)] \quad (4-6)$$

If $N_i = N_e$, the flux in H β in ergs/cm²/sec² is related to the electron

density (e.g., Aller 1954a, p. 208) by

$$S_{\beta} = 7.37 \times 10^{-20} (N_e N_{\epsilon} / T_{\epsilon}^{3/2}) b_1(T_{\epsilon}) D e^{X_n} \quad (4-7)$$

For such low densities as obtained in the planetary nebulae, we estimate the electron temperature from the ratio of the intensity of the auroral $\lambda 4363$ line to the nebular $\lambda 4959 + \lambda 5007$ N_1, N_2 lines of [OIII], by the formula (Seaton 1954; Aller 1954b, equation 14)

$$I(4363)/I(N_1 + N_2) \cong 0.113 \times 10^{-14, 300/T_{\epsilon}} \quad (4-8)$$

Observations give a value of 0.0063 for the left-hand side of Eq. (4-8), whence we compute $T_{\epsilon} = 11,300^\circ\text{K}$. Correspondingly, we find from $\log S_{\beta}$, the value of D (which depends on the assumed distance of the nebula) and $b_n(T_{\epsilon})e^{X_n}$ [which may be taken from the work of Seaton (1959)], $\log N_{\epsilon} = 3.80$. The electron density estimated from the observed intensity ratio of the 3729/3726 lines of [OII], viz., 0.7 may be obtained also from Seaton's (1954) formula

$$I(3729)/I(3726) \cong 1.5 [(1 + 3.3x)/(1.02 + 11x)]$$

$$\text{where } x = N_{\epsilon}/100 \sqrt{T_{\epsilon}} \quad (4-9)$$

appropriate for $T_{\epsilon} \cong 11,000^\circ\text{K}$. In this way we find $N_{\epsilon} = 3.1 \times 10^3$, a value about half that corresponding to the mean surface brightness. This result is not surprising in view of the fact that the [OII] radiations come from the outer, less dense parts of the nebula. A more accurate formula has been given by Seaton and Osterbrock (1957).

For the interpretation of the forbidden-line intensities we shall adopt $T_{\epsilon} = 11,300^\circ\text{K}$ and $N_{\epsilon} = 6.3 \times 10^3$ electrons/cm³. Then, making use of the target areas for collisional excitation and the transition probabilities we can calculate factors [cf., Aller 1954, Eq. (18)] $P_{\lambda, \text{ion}}(N_{\epsilon}, T_{\epsilon})$ for each forbidden-line multiplet that will give the ionic concentration, N_{ϵ} , thus

$$N_{\text{ion}}/N(\text{O}^{++}) = P_{\lambda, \text{ion}}(N_{\epsilon}, T_{\epsilon}) [I_{\lambda, \text{ion}}/I(N_1 + N_2)] \quad (4-10)$$

where $N(\text{O}^{++})$ is the number of O^{++} ions/cm³, $I(N_1 + N_2)$ is the intensity of the two green nebular lines, and $I_{\lambda, \text{ion}}$ is the total intensity of the forbidden-line multiplet in question. In Table 4-2, column 1 designates the ion, column 2 gives the type of transition as described in Fig. 4-3, column 3 gives the intensity, I , as corrected for the effects of space absorption, and column 4 gives $P(N_{\epsilon}, T_{\epsilon})$. The actual con-

Table 4-2. Forbidden Transitions in NGC7009

Line	Type of transition	<i>I</i>	$P(N_e, T_e)$	N_{ion}	Ionization correction	Adopted concentration, (atoms/cm ³)
NII	Neb	31	0.54	0.023	27	0.62
OI	Neb	2.4	13.7	0.045	1.06	2.35
OII	Neb	22.6	1.7	0.052		
OIII	Neb	1390		1.95		
	Aur	8.7				
NeIII	Neb	150	3.6	0.75	1.25	0.95
NeV	Neb	1.96	4.6	0.012		
SII	Trans A	2.7	2.7	0.010	6.2	0.33
	Neb	5.8		0.002		
SIII	Neb	90	0.44	0.05	5.6	0.014
ClIII	Neb	4.5	0.4	0.0026		
ArIII	Neb	28 <	1.0	0.04 <		
ArIV	Neb	10.7	0.9	0.013		0.04

centration $N(\text{O}^{++})$ is obtained by comparing intensities of the forbidden lines of [OIII] and the H_β recombination line. The relevant relation is

$$N(\text{O}^{++}) = 3.7 \times 10^{-6} [b_4(T_e) 10^{16, 780/T_e} / T_e^{3/2}]$$

$$N_e^2 [1 + 9380 (\sqrt{T_e}/N_e)] [I(N_1 + N_2)/I(\text{H}_\beta)]$$

Putting in numerical values for NGC7009, $b_4 = 0.24$ and $I(N_1 + N_2)/I(\text{H}_\beta) = 13.9$, we find $N(\text{O}^{++}) = 1.95$. Column 5 gives the concentration of the various ions in the nebula.

Next we estimate the distribution of atoms among various stages of ionization by comparing the ratios of different ions of the same element, e.g., OI/OII/OIII, NeIII/NeV, HeII/HeIII, SII/SIII, assuming that the degree of ionization is determined by the ionization potential. That is, we neglect the varying influence of the different frequency dependence of the continuous-absorption coefficient for each ion. The corresponding graph is shown in Fig. 4-4 where $\log N$ (relative) is plotted versus the ionization potential. Column 6 gives the factors by which the observed ionic abundance is to be multiplied to get the concentration of the element in question. The factor is large for nitrogen and small for oxygen and neon. We must emphasize that the target areas for sulfur, chlorine, and argon are crudely esti-

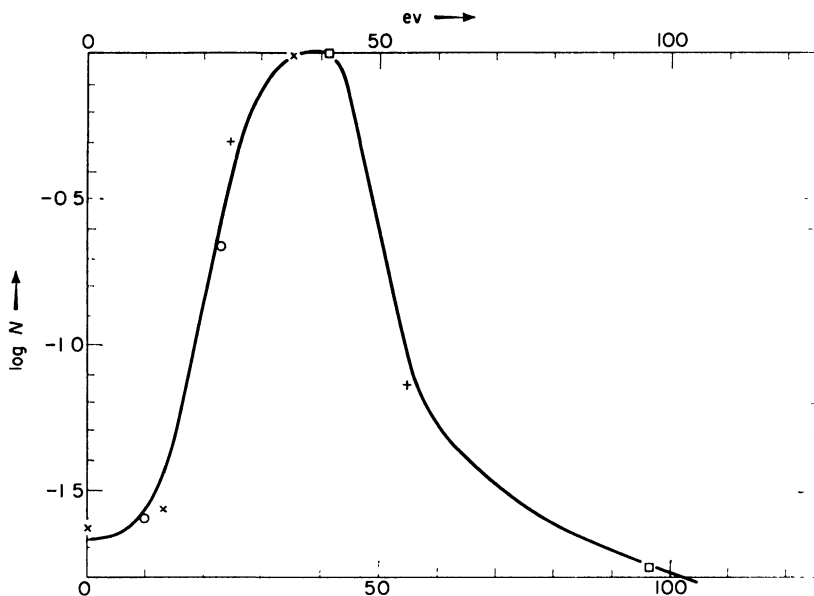


Fig. 4-4. Estimation of ionic concentrations in a nebula, NGC7009.

mated and final results must await exact calculations. The last column gives the adopted concentrations of the various elements as deduced from forbidden lines. The helium and carbon abundances may be estimated from their recombination lines. Thus the concentration of ionized helium is determined from the lines of neutral helium, that of doubly ionized helium from the lines of singly ionized helium. The carbon estimate rests on the single line, $\lambda 4267$, whose intensity is uncertain.

Analyses have also been carried out for the nebulae NGC1535, 2022, 2165, 2392, 2440, 6741, 7027, 7662, and IC5217, and Anon 21^h31^m +39°22'. Lines of fluorine, potassium, and calcium are observed only in NGC7027, whereas the other elements are observed in three or more nebulae. Table 4-3 compares the composition of NGC7009 with the mean composition as deduced from the several nebulae for which analyses have been carried out.

The last column entitled "range" gives the spread of the results in terms of the tabulated values as unit. Thus, with the abundance of oxygen held as 10,000, the nitrogen abundance ranges from 870 to

Table 4-3. Mean Abundances of Elements in Planetaryrics

	NGC7009	Mean composition	Range ^a
H	2.7×10^7	1.7×10^7	0.6 -1.35
He	5.0×10^6	3.2×10^6	0.66 -1.38
C		7,000	
N	2,600	4,000	0.22 3.0
O	10,000	10,000	Standard
F		4	
Ne	4,000	1,900	0.67 2.1
S	1,400	900	0.245-4.0
Cl	60	34	0.25 -4.4
Ar	160	130	0.52 1.8

^a Exclude NGC2440. Compare with Seaton (1960).

12,000. The behavior of the [NII] lines is such that we are inclined to attribute the great range in [NII] line intensities to excitation conditions, although it is possible that real abundance differences may play a role. The spread in S, Cl, and Ar is certainly partly due to our poor estimates of the collisional cross sections for these ions. Possibly the best estimates are found for those elements represented by several different ions. It would appear that the Ne/O ratio is definitely less than about +0.5. The H/He ratio is established as about 5, while that of carbon depends on an as yet incompletely worked out theory of recombination.

The results of all subsequent investigations have substantiated the pioneer work by Bowen and Wyse (1939) who concluded that when the excitation mechanisms are taken into account, the compositions of the planetaryrics do not differ markedly from those of normal stars. Composition differences in nebulae may be more difficult to establish than in stars and would have to be large in order to be detected at all. Since planetary nebulae belong to the type II population, we would not expect them to have exactly the same composition as nebulae connected with the type I population. Furthermore, it must be noted that planetary nebulae are associated with late stages in the evolution of type II stars. Accordingly, their compositions may reflect effects of nuclear transformations in stellar interiors and not be true indices of the composition of the material from which these stars were formed.

4-5. Composition of the Interstellar Medium

The conditions of ionization and excitation in the interstellar medium are so extreme that an adequate estimate of its composition is virtually impossible. Weak absorption lines of interstellar origin are often observed in the spectra of distant (particularly) hot stars. They are resonance lines of metals like sodium, potassium, or calcium, or occasionally molecular lines arising from the lowest level of the molecule. The alkalis and alkaline earth metals can lose one or two electrons, but no more; there will always be a few neutral-sodium or singly-ionized-calcium atoms along the line of sight passing through a cloud of interstellar matter. Estimates of the concentration of sodium and calcium in the interstellar medium must depend on appraisals of the radiation field and density fluctuations. The neutral-hydrogen concentration (under certain circumstances) may be found from the 21 cm radio-frequency radiation of hydrogen. The Na/H or Ca/H ratio found in the interstellar medium seems consistent with that found for the stars.

Emission lines of hydrogen and the forbidden lines of [OII] and [OIII] are observed in regions where the interstellar gas is ionized by radiation from hot stars. Only the strongest nebular lines are ever observed in these objects of low surface brightness.

Possibly the best analyses of the interstellar medium may be made from studies of such bright diffuse nebulae as Orion or Messier 8. In these objects, as in the planetaries, the gas is heated to incandescence by the presence of very hot stars. The recombination and forbidden lines and continua characteristic of gaseous nebulae are observed. The first attempt at an analysis of a diffuse nebula was made by Wyse (1942) who concluded that the composition of the Orion nebula was similar to that of the stars and planetary nebulae. A photoelectric spectrophotometric study (Liller and Aller 1959) of the brightest part of the nebula shows very good agreement with Wyse's eye estimates of line intensities. The density of this portion of the nebula is near 4×10^3 electrons/cm³. The electron temperature (estimated from the 4363/ $N_1 + N_2$ ratio) is 9000°K. In denser filaments the N_e approaches 2×10^4 cm³ while in the outer parts of the nebula Osterbrock (1955) gets much lower densities from the 3729/3726 ratio. If we calculate the abundances by the procedures previously described for the planetaries we find a comparison between the Orion nebula

Table 4-4. Abundances in the Orion Nebula and the Hot *B* Stars (given in Log *N*).

Element	H	He	C	N	O	Ne	S	Cl	Ar
Nebula	12.0	11.1	8.4	7.7	8.6	8.8	8.0	5.9	6.6
Star	12.0	11.2	8.2	7.9	8.8	8.9	7.7	6.2	6.9

and the hot *B* stars which are believed to have been formed from it (see Table 4-4).

The H/He ratio for the Orion nebula was determined by Mathis (1957). Carbon is based on the single weak recombination line $\lambda 4267$ and is uncertain. Oxygen is represented by OI, OII, and OIII. Neon is represented only by NeIII while the sulfur abundance depends largely on the lines of [SIII], which like those of [ClIII] [ArIII], and [ArIV] involve interpretations via uncertain cross sections. We must emphasize that the stellar data for chlorine and argon are likewise uncertain and the calculated abundances probably represent upper limits. Nevertheless, improvements in the observational data on the one hand, and in the theoretical interpretation on the other, will greatly improve our estimates.

Selected References

The physical theory and observational data are discussed in detail in:

- Aller, L. H., *Gaseous Nebulae*, Wiley, New York, 1956.
 Menzel, D. H., ed. *Physical Processes in Gaseous Nebulae*, Dover, New York, 1961.
 Minkowski, R., and O. C. Wilson, *Planetary Nebulae*, North-Holland Publishing Co, in press.
 Seaton, M. J., *Progr. Phys. (Physical Society, London)* **23**, 313, 1960. This concise, well-written exposition of the theory appeared after the present manuscript had gone to press. It contains a compilation of useful atomic parameters, equations, and tables.
 Wurm, K., *Die Planetarische Nebeln*, Akademischer Verlag, Berlin, 1951.
 Aller, L. H., *Nuclear Transformations, Stellar Interiors and Nebulae*, Ronald, New York, 1954a; *Ap.J.* **120**, 401, 1954b.
 Aller, L. A., and W. Liller, *Ap. J.*, **130**, 45, 1959.
 Baker, J. G., and D. H. Menzel, *Ap. J.*, **88**, 52, 1938.
 Bowen, I. S., *Ap. J.*, **67**, 1, 1928; **81**, 4, 1935.
 Bowen, I. S., and A. B. Wyse, *Lick Observatory Bull.*, **19**, 1939.
 Burgess, A., *Monthly Notices, Roy. Astron. Soc.*, **118**, 477, 1958.
 Mathis, J., *Ap. J.*, **125**, 328, 1957.
 Menzel, D. H., *Publ. Astron. Soc. Pacific*, **38**, 295, 1926; *Ap. J.*, **85**, 330, 1937.

- Menzel, D. H., L. H. Aller, and M. H. Hebb, *Ap. J.*, **93**, 230, 1941.
- Menzel, D. H., and L. H. Aller, *Ap. J.*, **102**, 239, 1945.
- Osterbrock, D. E., *Ap. J.*, **122**, 235, 1955.
- Seaton, M. H., *Proc. Roy. Soc. (London)*, **218**, 400, 1953. *Monthly Notices Roy. Astron. Soc.*, **114**, 154, 1954. *Ann. d'Ap.*, **17**, 74, 1954. *Proc. Roy. Soc.*, **231**, 37, 1955. *Revs. Modern Phys.*, **30**, 987, 1958. *Monthly Notices Roy. Astron. Soc.*, **119**, 81, 1959; 90, 1959.
- Seaton, M. J., and D. E. Osterbrock, *Ap. J.*, **125**, 66, 1957.
- White, M. L., and L. H. Aller, *Astron. J.*, **54**, 181, 1949.
- Wilson, O. C., *Revs. Modern Phys.*, **30**, 1025, 1958.
- Wyse, A. B., *Ap. J.*, **95**, 356, 1942.
- Zanstra, H., *Ap. J.*, **65**, 50, 1927; *Z. Astrophys.*, **2**, 1, 1931.
- Zanstra, H., and W. J. Brandenburg, *Bull. Astron. Inst. Netherlands*, **11**, 351, 1951.

Abundances of Elements from Normal Stellar Atmospheres

The astronomer's data differ so strikingly from the chemist's that stellar chemical analysis requires some elucidation. In a few respects the astrochemical analysis resembles a spectrochemical analysis, but in most respects it is fundamentally different. A stellar spectrum is produced in a medium wherein density and temperature vary continuously over a large range from the highest to the lowest of relevant layers. The physical conditions under which the spectrum is formed have to be inferred from essentially the same data as yield the chemical composition of the radiating strata. Sometimes an iterative procedure is necessary, e.g., when the ratio of hydrogen to helium or hydrogen to the metals differs markedly from what we had expected. In this chapter we confine our attention to the so-called "normal" stars, i.e., objects that appear to have compositions roughly similar to that of the sun, deferring a discussion of stars of abnormal composition to a later chapter.

5-1. The Observational Data

The spectroscopic information ideally available for an analysis of a stellar atmosphere consists of: (1) Measurements of relative energy distribution in the continuous spectrum, and also sometimes the actual flux of energy in a range λ to $\lambda + \Delta\lambda$ expressed in ergs/cm² sec; (2) the shapes or profiles of the stronger spectral lines; and (3) the integrated intensities of (or total absorptions produced by) the spectral lines, i.e., their equivalent widths. In place of energy-distribution curves, we sometimes have available only measurements of stellar colors which are essentially energy distributions observed with broad-band pass filters. If the star is a member of an eclipsing binary system, its mass and radius often can be found. Hence the surface gravity can be calculated directly. If it is a member of a cluster it may be possible to infer its age.

In Chap. 1 we mentioned that the radius and luminosity of a star of a given initial mass, angular momentum, and composition are determined by its evolutionary status. The mass, radius, luminosity, and chemical composition uniquely determine the color and spectrum of a star, at least during the stages of evolution when the star is near the main sequence. We shall attempt to show how the composition factors may be separated from other influences on the spectrum of a star.

Spectral-energy distributions are measured by comparing the program star with a standard star whose energy distribution is known. In fundamental work the star is compared with a standard energy source. Earlier workers used photographic photometry, but at the present time all basic work is done with photoelectric scanners. The main difficulties are those imposed by the transparency of the earth's atmosphere and by the scarcity of suitable energy sources for comparison with hot stars in the violet and ultraviolet. Nevertheless, energy-distribution measurements can now be made with such high accuracy as to provide a formidable challenge to the theorist. In addition to the usual energy-distribution measurements, observations of certain critical intensity ratios in the spectrum have proved very useful. For example, Strömgren has measured the ratio of intensities of two relatively narrow spectral regions, one taken above and the other taken below the Balmer limit. He also compared the $H\beta$ line with the adjacent continuous spectrum at $\lambda 5000$ and $\lambda 4700$. A combination of these pairs of data yielded extremely important information on stellar luminosities, ages, and compositions.

The profiles or actual shapes of stellar absorption lines provide a wealth of information concerning the physical state of the atmosphere and factors underlying the formation of the line. Solar line profiles can be measured at different points on the disk, but for the stars it is possible normally to observe the line shapes only in light integrated over the disk. Ordinarily, such profiles are measured by photographic photometry, but for the sun and brighter stars photoelectric traces are sometimes possible. For all except the very broadest lines, the instrumental profile, due to the lack of resolution of the spectrograph, causes the line to be broadened. Hence it is necessary to correct the observed profile for lack of resolution and scattered light (if any). With high-dispersion instruments such as the vacuum spectrograph at the McMath-Hulbert Observatory, true profiles of even rather

weak lines can be measured in the sun if the importance of the problem warrants it (Fig. 5-1). Resolving powers as high as 700,000 can be obtained with the aforementioned instrument.

Stellar spectroscopy is necessarily limited to lower resolutions than is solar work. Usually the resolving power is determined by the projected slit width. Hence it is advantageous to use spectrographs with long collimators and short-focus cameras. For most lines, it is possible

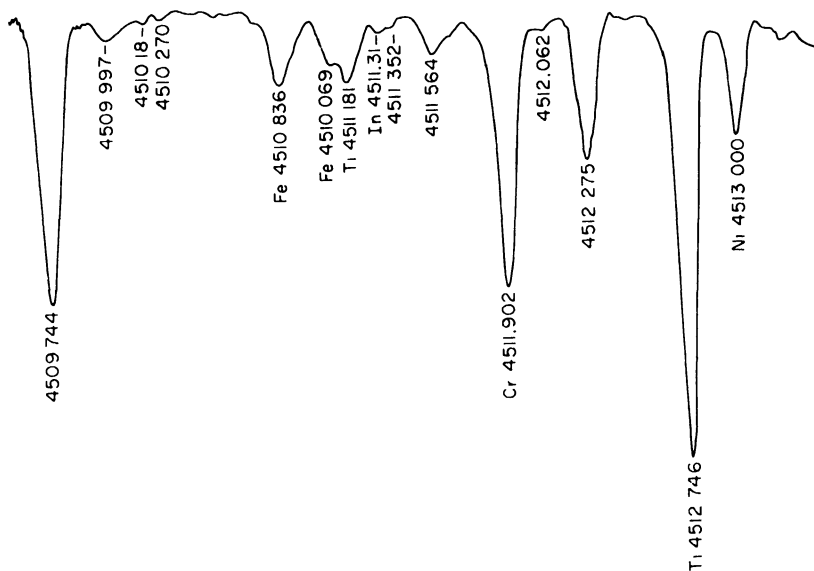


Fig. 5-1. Tracing of a small portion of the solar spectrum. This tracing shows a number of metallic lines between 4509 and 4513. The lines of the relatively abundant metals Cr, Ti, and Ni are relatively strong and capable of reliable measurement, but rare elements such as indium are represented (if at all) by weak lines that are difficult to measure. (McMath-Hulbert Observatory, University of Michigan.)

to obtain only the total absorption or amount of energy subtracted from the continuous spectrum. This quantity is ordinarily referred to as the *equivalent width* and is expressed in angstrom units. (E.g., a line of intensity 50 mA subtracts an amount of energy from the neighboring continuum equivalent to 0.05 Å.) Equivalent widths have been measured by many observers in many stars and in the sun. The work has been done mostly by photographic photometry. Great care is necessary to eliminate systematic errors. Errors range from around 10 per cent for strong lines to 50 per cent or more for weak lines. Accuracy is limited by blending with other lines, by uncertainties in the location of the continuum, and, for weak lines, by accidental errors (produced by plate grain, etc.).

Before modern photometric techniques were available, observers often made eye estimates of intensity on an arbitrary scale. Such estimates, when properly calibrated, proved valuable in the pioneering investigations on solar and stellar spectra, but they now have been almost entirely replaced by quantitative measurements. Nevertheless, for many purposes, particularly when suitably prepared comparison scales are used, eye estimates are valuable for a preliminary reconnaissance.

5-2. The Continuous Spectra of the Stars

In order to interpret the aforementioned observational material, it is necessary to know at the outset the values of the appropriate physical parameters, i.e., the physical source of the continuous absorption, the transition probabilities for the spectral lines, and their line-broadening coefficients. Some of these quantities can be computed adequately by theory; others must be determined experimentally or estimated.

Consider first the continuous spectrum. Temperature and pressure must increase monotonically with depth in the star. If the atmosphere is in hydrostatic equilibrium, the increment in pressure with depth is given by

$$dP = -g\rho dh \quad (5-1)$$

where h is measured positively outward from the center of the star.

We define an element of optical depth (a dimensionless number) as

$$d\tau_r = \kappa_r \rho dh \quad (5-2)$$

where κ_ν is the coefficient of continuous absorption at frequency ν per gram of stellar material. It depends on the temperature, T , electron pressure, P_e , and the exact nature of the absorption mechanism. Next divide Eq. (5-1) by Eq. (5-2) to obtain

$$dP/d\tau_\nu = -g/\kappa_\nu(P_e, T) \quad (5-3)$$

If T is known as a function of τ_ν , P can be found from Eq. (5-3) provided that P , here set equal to the gas pressure P_g , is known as a function of P_e and T , viz.,

$$P_g = P_g(P_e, T, \text{chemical composition}) \quad (5-4)$$

This numerical relationship depends only on the assumed chemical composition. See Aller, 1953, page 91, for an example. Specifically, at lower temperatures it depends critically on the abundance ratio of hydrogen to the metals. For high temperature stars one must add the contribution to the mechanical force exerted by radiation.

Now let us suppose that each volume element of the stellar atmosphere obeys Kirchhoff's law, i.e.,

$$j_\nu = \kappa_\nu 4\pi B_\nu(T) \quad (5-5)$$

$B_\nu(T)$ is Planck's function for specific intensity (e.g., Aller 1953, p. 101), j_ν is the total emission per gram in all directions per unit frequency interval and κ_ν is the mass coefficient of absorption. Let θ denote the angle between the ray to the observer and the outward draw normal. Then the intensity of the emergent ray will be

$$I_\nu(0, \theta) = \int_0^\infty B_\nu(T) \exp(-\tau_\nu \sec \theta) \sec \theta d\tau_\nu \quad (5-6)$$

Since τ_ν depends on κ_ν , the same numerical value (e.g., 0.7) will refer to different physical depths in the stellar atmosphere. It will be shallower in regions where κ_ν is large; deeper where it is small. Hence one may put

$$d\tau_\nu = (\kappa_\nu/\kappa_{\nu_0}) d\tau_{\nu_0} \quad (5-7)$$

where ν_0 refers to some particular frequency of the spectrum. $T(\nu_0)$ is presumed given while τ_ν may be expressed in terms of τ_{ν_0} and T given as a function of τ_ν . Unlike other stars, it is possible to measure the monochromatic surface brightness at various points upon the solar disk. In particular, observers measure $I_\nu(0, 0)$, i.e., the intensity

at the center of the solar disk, at different frequencies in the continuous spectrum. Also the limb darkening

$$\phi_\nu(\theta) = I_\nu(0, \theta)/I_\nu(0, 0) \quad (5-8)$$

can be measured at different frequencies for different positions on the disk. An analysis of these data with the aid of Eq. (5-6) permits a determination of $T(\tau_\nu)$ for each frequency of observation, and also the frequency dependence of κ_ν for various temperatures. In particular, one may obtain $T(\tau_0)$ as a function of optical depth at $\lambda 5000$.

From this empirical $T(\tau_\nu)$ relationship it is established that the flow of energy through the outer layers of the solar atmosphere is primarily by radiation rather than by convection currents, although the latter may exist in the deeper layers. It appears that the atmospheres of most stars are similarly in radiative equilibrium. If the continuous-absorption coefficient were independent of frequency, i.e., if the material were grey, the temperature would depend on the optical depth τ according to

$$T^4(\tau) = \frac{3}{4} T_{\text{eff}}^4 [\tau + q(\tau)] \quad (5-9)$$

where $q(\tau)$ is a function that varies smoothly from $q(0) = 1/\sqrt{3}$ to $q(\infty) = 0.71045$. For most purposes we may take $q = \frac{2}{3}$. The effective temperature T_{eff} is the temperature a black body would have if it radiated the same amount of energy as the sun.

The ν dependence of κ_ν shows that the principal source of continuous absorption in stars like the sun is the negative hydrogen ion. A hydrogen atom can attach an extra electron with a binding energy of 0.75 ev. The photo-detachment of this electron by radiation of all wavelengths shorter than $\lambda 16650$ Å produces a smoothly varying, continuous absorption that rises to a maximum near $\lambda 8500$ Å. In the far infrared, free-free absorptions produce the bulk of the opacity. In the observable region of yet cooler stars, molecular-band absorptions block much outgoing radiation. Continuous molecular absorption and Rayleigh scattering may become important in atmospheres at lower temperatures and pressures, respectively. Among stars hotter than the sun, the principal source of continuous absorption is atomic hydrogen.

Fortunately for the astrophysicist, hydrogen is overwhelmingly the most abundant element in the universe. Its line- and continuous-absorption coefficients can be calculated with an accuracy sufficient

for most purposes. In all except the very coolest of stars, blocking of outflowing stellar radiation is produced almost entirely by hydrogen, or by electrons liberated by hydrogen atoms.

Figure 5-2 displays a tracing of the spectrum of the star θ Crateris as photographed with the slitless spectrograph of the Crossley reflector of the Lick Observatory. The temperature of this star is about $12,000^\circ\text{K}$. The deep indentations in the continuous spectrum produced by the Balmer lines are clearly indicated. The most striking feature of the trace, however, is the abrupt fall of intensity as the Balmer limit is approached. On the high-frequency side of this point, the spectrum is continuous. Could we observe the spectrum of this star (freed from the influence of the earth's atmosphere), we would see a similar, although smaller, break at the Paschen limit and a much larger one at the Lyman limit. In this star the photoelectric ejection of electrons from successive energy levels of the hydrogen atom produces most of the absorption.

Per atom in the n th level, the absorption coefficient at the frequency ν (see, for example, Aller 1953, p. 146) is given by

$$\begin{aligned}\alpha_n(\nu) &= (64\pi^1\epsilon^{10}m/3\sqrt{3} ch^6) (1/n^5) (g_{11}/\nu^3) \\ &= 2.82 \times 10^{29} (g/n^5\nu^3)\end{aligned}\quad (5-10)$$

where ϵ and m are the electronic charge and mass, respectively, and

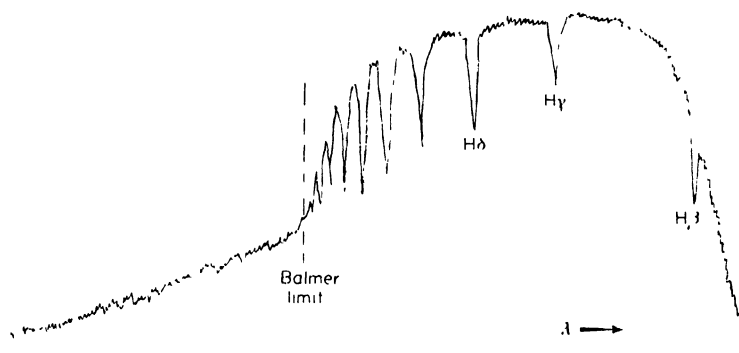


Fig. 5-2. A microphotometer tracing of the spectrum of θ Crateris. The ordinate is not proportional to the intensity but contains the effects of the density $\log I$ relationship and the wavelength dependence of the sensitivity of the photographic emulsion as well as the influence of atmospheric extinction, transparency of the optics, and non-linearity of dispersion. T_{eff} is about $12,000^\circ\text{K}$.

g_{II} is a correction factor of the order of unity that varies slowly with wavelength. At any one frequency, we must sum over the contributions of all levels that can participate at that frequency and add the effects of the free-free transitions. At $\lambda 3500$ we would include the $n = 2$ and all higher levels, whereas at $\lambda 5000$ we would sum over the levels beginning with $n = 3$. The sharp dependence of the absorption coefficient on frequency produces a marked departure of the stellar atmosphere from greyness. Consequently, the emergent energy distribution will be appreciably different from that of a grey body.

Two additional sources of opacity contribute in the hotter stars: helium absorption and electron scattering. Figure 5-3 shows the be-

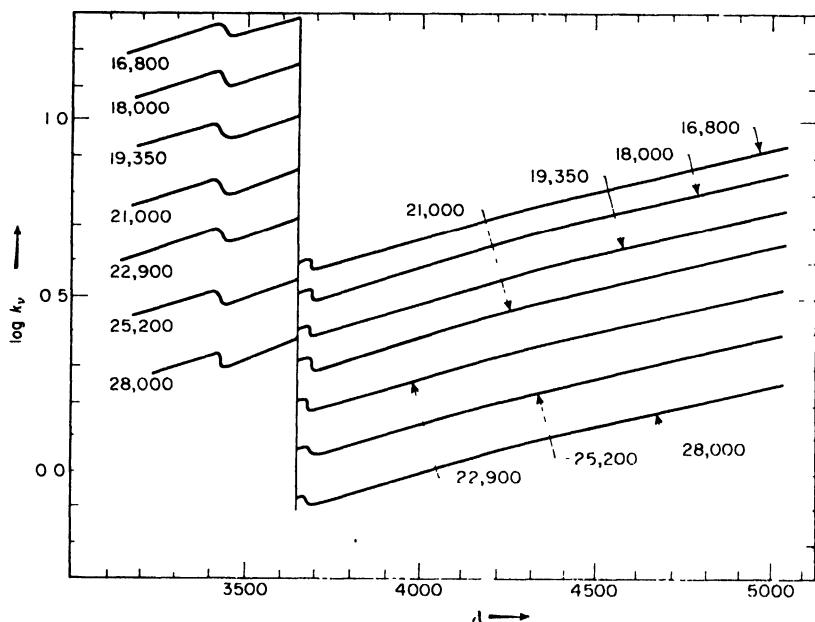


Fig. 5-3. The continuous absorption coefficient in hot stars. We plot $\log k'$ against the wavelength λ where k' is the coefficient of continuous absorption (corrected for the negative absorptions) computed per gram of stellar material and electron pressure of 1000 dynes/cm. It is assumed that H contributes 85 per cent and helium 15 per cent of the stellar atmosphere by weight. The electron scattering is not included. The total extinction coefficient for an electron pressure P_e is

$$k_v = k'_v(P_e/1000) + \sigma$$

where σ is the coefficient of electron scattering.

havior of the continuous-stellar-absorption coefficient at higher temperatures where both the hydrogen and helium absorptions are taken into account. The effects of discrete lines are not included; hence the abruptness of the discontinuity at the Balmer limit is exaggerated. Electron scattering, which is independent of wavelength, also has to be taken into account in computing the total actual extinction coefficient. Since electron scattering does not follow Kirchhoff's law, the problem of radiative transfer becomes more complicated in stellar atmospheres where electron scattering is important. The spectral-energy curves of stars show departures from those of black bodies for three reasons: (1) the existence of a temperature gradient in the atmosphere, (2) the nongreyness of the absorbing material, and (3) the influence of absorption lines. Nevertheless, it is often possible to deduce the effective temperature of a stellar atmosphere from its energy distribution by taking into account the $T(\tau_\nu)$ relationship and the dependence of κ_ν on temperature and electron pressure. The stellar-energy distributions provide essential data for the construction of model atmospheres (see Sec. 5-6).

5-3. The Coefficient of Line Absorption

The intensity at a point in a stellar-spectrum line depends essentially on the ratio of the line-absorption coefficient to the coefficient of continuous absorption and the variation of this ratio through the line-producing layers of the atmosphere. The absorption coefficient of a spectral line α_ν will depend on the mechanism of line broadening and also on its transition probability or its f -value.

If a spectrum line is broadened by natural damping only, α_ν will be given by

$$\alpha_\nu = (\pi e^2 / mc) f_{n'n} \{ (\Gamma_R / 4\pi^2) / [(\nu - \nu_0)^2 + (\Gamma_R / 4\pi)^2]^{-1} \} \quad (5-11)$$

where

$$\Gamma_R = 1/T_n + 1/T_{n'} \quad (5-12)$$

T_n and $T_{n'}$ being the lifetimes of the upper and lower levels n and n' , respectively. Under most circumstances likely to be encountered in a stellar atmosphere, negative absorptions may be neglected and we can write

$$1/T_n \cong \sum_i A_{ni} \quad (5-13)$$

where the summation is taken over all lower levels to which a transition can occur. Here ν_0 is the frequency of the center of the line, while $f_{n'n}$ denotes the Ladenburg f or *oscillator strength* which is related to the Einstein coefficient of spontaneous emission, $A_{nn'}$, by

$$A_{nn'} = (g_{n'}/g_n)(8\pi^2\epsilon^2\nu^2/mc^3) f_{n'n} = 6.67 \times 10^{15}(g_{n'}/g_n)(f/\lambda^2) \quad (5-14)$$

if λ is given in Å. Here g_n is the statistical weight of the upper level, $g_{n'}$ that of the lower level, and the other symbols have their usual meaning. The f -value is an atomic constant which is independent of the physical conditions under which the atom is radiating. One can show that the integral over the absorption coefficient is

$$\int_0^\infty \alpha_\nu d\nu = (\pi\epsilon^2/mc) f_{n'n} = 0.02654 f_{n'n} \quad (5-15)$$

In a typical stellar atmosphere, a line is also broadened by collisions of the radiating atom with its neighbors. If a line is broadened by the linear Stark effect (e.g., hydrogen and certain helium transitions), one must employ the statistical broadening theory (as given, for example, by Kolb and Griem 1958): The lines of the metals or those of most of the permanent gases are widened by collisions of a type (quadratic Stark effect or Vander Waal's interaction) for which the discrete-encounter (or phase-shift) theory is valid. Under these circumstances we may use Eq. (5-11) with $\Gamma_R/4\pi$ replaced by

$$\delta' = (\Gamma_R/4\pi) + (S/2\pi) = (\Gamma_R + \Gamma_{\text{coll}})/4\pi \quad (5-16)$$

where Γ_{coll} is the collisional damping constant, which is obtainable from S , the number of damping collisions per second. In order to compute S , we must know the target area for collisional broadening, $\pi\rho^2$. This target area depends on the level involved and the foreign gas present. Some estimates have been made by quantum mechanics but reliable experimental data on collisional damping are needed. Unfortunately, in stars like the sun, the principal broadening agent is atomic hydrogen, and it is difficult to perform laboratory experiments in which atomic rather than molecular hydrogen widens spectral lines.

All spectrum lines are broadened by Doppler motions of the atoms. For a strictly monochromatic line broadened only by the Doppler effect (see, for example, Aller 1953, p. 59), the absorption coefficient would be given by

$$\alpha_\nu = (\pi\epsilon^2/mc)f(1/\sqrt{\pi})(c/V\nu_0) \exp [-(\nu - \nu_0)^2 c^2/\nu_0^2 V^2] \quad (5-17)$$

where V is the most probable value of the velocity of the radiating atom. If these velocities are produced solely by gas thermal motion, $V = \sqrt{(2kT/M)}$ where M is the mass of the atom. If there are also large-scale mass motions in the stellar atmosphere such that the mean free path of a photon is larger than the dimensions of one of the turbulent elements,¹ then

$$V = \sqrt{(2kT/M) + \xi^2} \quad (5-18)$$

where ξ is the most probable value of the velocity of a turbulent element. We assume that the turbulent eddies are moving with random velocities (i.e., the velocity distribution is Maxwellian).

If both Doppler broadening and collisional plus radiation damping have to be taken into account, the expression for α_ν is no longer given by simple closed expressions such as Eqs. (5-11) or (5-17). One may write

$$\alpha_\nu = \alpha_0 H(a, v) \quad (5-19)$$

where α_0 , the absorption coefficient at the center of the line for zero damping, is given by

$$\alpha_0 = (\sqrt{\pi}\epsilon^2/mc) f_{n'n} \lambda/V \quad (5-20)$$

Also

$$H(a, v) = a/\pi \int_{-\infty}^{+\infty} \{e^{-s^2}/[a^2 + (v - s)^2]\} ds \quad (5-21)$$

where

$$v = \Delta\lambda/[(\lambda/c) V] \quad (5-22)$$

and

$$a = \delta'\lambda/V \quad (5-23)$$

Here V is the most probable velocity as defined by Eq. (5-18) and δ' is given by Eq. (5-16). The function $H(a, v)$ has been tabulated

¹ If the mean free path of the quantum is small compared with the size of the turbulent eddy, each portion of the star's disk will radiate a line profile shifted from ν_0 by a different amount and the resultant profile observed in the integrated light of the star will be broadened.

as a function of u and v by F. Hjerting (1938) and by Daniel Harris (1948). As an illustration, we give in Fig. 5-4 the absorption coefficient ratio α_r/α_0 for a resonance line of aluminum for different depths in the solar atmosphere.

If the number of atoms acting to produce a given line is so small that it is very weak (e.g., $W_\lambda \sim 20 \text{ m}\Lambda$), only the Doppler broadening will be of importance, and one need not know the damping constant in order to interpret the line intensities in terms of abundances. On the other hand if the line is strong, the absorption at distances from the line center—large compared with $\Delta\nu_0$ —will become important and the profile of the line will depend on the damping constant

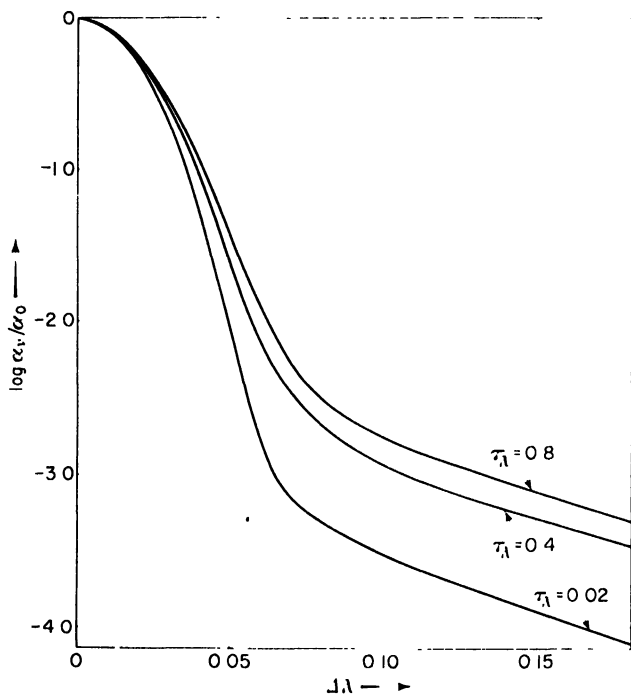


Fig. 5-4. Absorption coefficient for resonance lines of aluminum. The logarithm of the ratio α_r/α_0 is plotted against $\Delta\lambda$ for three different points in the solar atmosphere, $\tau_\lambda = 0.02$ which corresponds to layers where the part of the line near the center is found, $\tau_\lambda = 0.4$ where line wings are formed, and $\tau_\lambda = 0.8$ which contributes to the far wings of strong lines. The centers of strong lines are formed in the chromosphere.

Γ as well as on the f -value. Hence the interpretation of a strong line requires more physical parameters than does an analysis of a weak one.

To summarize, the equivalent width or profile of a spectral line not only depends on the transition probability and on the abundance of the element, but also will be strongly influenced by line-broadening agencies. All lines are broadened by Doppler effect and by radiation damping. In addition, some are also influenced by hyperfine structure. In the atmospheres of stars like the sun collisional broadening is also important, while in giant and supergiant stars random macroscopic motions of the gas, sometimes called "turbulence," produce pronounced broadening effects. The observed spectral lines are also often washed out by the rotation of the star, but such effects are to be regarded as extrinsic causes of line broadening.

5-4. Transition Probabilities and Damping Constants

The line absorption coefficient $l_\nu = N_\tau \alpha_\nu$ (where N_τ is the number of atoms per gram capable of absorbing the line in question) cannot be computed unless at least the f -value is known. In principle, if we know the variation of gas pressure, electron pressure, temperature, and coefficient of continuous absorption with depth in the star, we may assume different values of f , or the elements abundance N_E , and compute the line profile. Then, by fitting the computed to the observed profile we obtain the product $N_E f$. Only if f is known can N_E be found.

Now f -values may be determined experimentally or sometimes they may be computed or estimated by theory. In either circumstance it is usually easier to get relative f -values than absolute ones. Among experimental methods we mention the following: (1) anomalous dispersion method; (2) absorption lines produced in an electric furnace under known pressures and temperatures; (3) atomic beam method; (4) whirling water or stabilized arc; (5) lifetime of excited levels; (6) luminous shock tube; and (7) emission spectra from flames and ordinary arcs.

In the anomalous dispersion method, advantage is taken of the fact that in the neighborhood of a line the index of refraction of a gas is related to its absorption coefficient. A gas is introduced into the system of a Jamin interferometer used in conjunction with a spectrograph. Straight-line interference fringes are observed except in the

neighborhood of absorption lines where they become "hook shaped." This method is satisfactory for resonance and low-level lines.

The electric-furnace method has the advantage that it can be used for low-level lines of a large number of metals. Light from a continuous source passes through the metallic vapor before it enters the spectrograph. If the vapor pressure can be determined accurately, the number of atoms in the line of sight can be calculated and the absolute f -values determined from the equivalent widths of the absorption lines. This method has been used particularly by R. B. King and his associates (1954). H. Kopfermann and G. Wessel (1951) introduced the atomic beam method which was subsequently modified by R. B. King, P. Rötly, Bell, and Davis (1958). A small quantity of the metal to be studied is vaporized in a vacuum, the metallic atoms pass through a narrow slit through which a white-light beam is passed, and the atoms finally collect on a cool surface. The equivalent width of the absorption line produced by the beam of atoms is measured while the number of atoms in the line of sight is known from the rate of increase of the weight of the collecting surface. The experiments are difficult and tedious because the vapors of many metals tend to attack the walls of the container.

At Kiel, W. Lochte-Holtgreven (1952) and his associates developed the whirling-water arc as a tool for measuring the f -values of various gases. An arc is struck along the axis of a rapidly rotating tube along whose wall water is flowing. The vapor at the center of the tube becomes dissociated, excited, and ionized, producing a brilliant spectrum of hydrogen and of oxygen in various ionization stages. With this experimental set-up, the f -values of lines of oxygen and carbon have been measured and theories of line broadening have been tested. By introducing various salts into the fluid stream, the spectra of other elements may be observed. The whirling-fluid arcs tend to be unstable, and a more promising type for the study of absolute f -values in permanent gases appears to be thermal arcs operated at atmospheric pressure with currents of several hundred amperes. H. N. Olsen of the Linde Company has measured f -values in argon with an arc of this type.

One of the difficulties in the absolute measurement of f -values has been the necessity of knowing the exact number of absorbing or emitting atoms in the line of sight. The lifetime of an excited level in the absence of collisions is determined by the transition probab-

ities to all lower levels. Hence an experimental measurement of this quantity could give the sum of the A -values for the downward transitions without any knowledge of the actual population of the upper level whatever. The experimental difficulties are considerable. One method is to illuminate an atomic beam by monochromatic resonance radiation and then observe the decay of the excited energy state as the atoms travel in the beam. It is necessary to take into account the different possibilities for transitions to various lower levels.

The luminous shock tube has been developed as a tool for astrophysical research, particularly at the laboratory of O. Laporte at Michigan. A bright-line spectrum is produced when the kinetic energy of a shock wave is suddenly dissipated into heat. Since the thermodynamics of the shock-wave mechanism is known, the temperature and density in the heated gas can be computed from the initial densities, pressure ratios, and observed flow velocities. Then the f -values may be found from the measured emission line intensities. The shock-tube method promises to be the most accurate tool for f -value determinations.

Emission spectra from flames and arcs have been used principally to establish relative f -values. The precise determination of the temperature is difficult, and it is necessary to avoid self-absorption which tends to occur in the outer cooler parts of the heated gas and with strong lines. Measurements of arc-line intensities carried out under carefully controlled conditions at the Bureau of Standards should provide very useful data for estimates of f -values. C. W. Allen (1957) prepared bars of copper alloyed with very small but known amounts of other elements. Then when an arc was struck between two such electrodes it was assumed that the vapor contained the same proportions of standard elements. If the alloy contained metals whose absolute f -values were known, e.g., Fe, along with other "program" metals, the standard elements could be used to calibrate the intensities of all lines of all elements and determine their f -values. Unfortunately, the experiment seems to involve some unexpected difficulties, e.g., different metals may diffuse out of the arc at different rates.

Unfortunately, trustworthy f -values are known only for relatively few elements. For some atoms and ions it is possible to get f -values by theoretical calculations by quantum mechanics. For some transitions

in some atoms precise computations with exact wave functions have been made, but for most elements it is necessary to resort to approximations. One set of approximations which is useful for the high-level lines of light elements is provided by the Bates and Damgaard tables (1949), while for transitions involving the ground level, we often use the f -sum rule.

Exact quantum mechanical calculations have been carried out for a few elements by the Hartree-Fock method which takes into account electron exchange, configuration interaction, and the polarization of the core. The method is laborious and has been applied only to a few simple atomic structures such as the alkalis and alkaline earths. In the Bates-Damgaard method absolute f -values are computed by assuming that the wave functions are hydrogen-like except that n is replaced by $n^* = Z/\sqrt{E}$ where E is expressed in units of 13.54 volts and Z is the charge to which the electron is subject (1 for a neutral atom, 2 for a singly charged ion, etc.). Relative f -values within a transition array are found with the aid of appropriate tables published by White and Eliason (1931), and Goldberg (1935), or by formulae such as those obtained by Rohrlich (1959). (Examples of such calculations are given by Aller 1953, p. 131.)

In the absence of any information on the f -values, one sometimes uses the f -sum rule and approximations based thereon. In its rigorous form, the rule states that the sum of all f -values for all transitions both up and down (including X-ray transitions) is equal to the total number of electrons in the atom. In applications, the approximation is usually made that the sum of the f -values for all transitions arising from a given level, n , to all higher levels, n'' , including the continuum, κ , and to all lower levels, n' , equals the number of valence electrons, k .

$$\sum_{n''} f_{nn''} + \int_0^\infty f_{n\kappa} - \sum (g_{n'}/g_n) f_{n'n} = k \quad (5-24)$$

where the g 's are the statistical weights. The downward transitions are involved in the sum with a negative coefficient. For a complicated atom such as nickel or iron we make the following approximation. Let us define an f_T which is a sort of average for the entire transition array (i.e., all the possible transitions between all the levels of the lower configuration and those of the higher configuration). Then the f -value for a particular line, a , will be

$$f_a = (s/\sum s)(S/\sum S)(\lambda_T/\lambda_a)(g_T/g_a)f_T \quad (5-25)$$

where g_T is the statistical weight of the whole configuration, g_a is the statistical weight of the line in question, λ_T is an average wavelength for the whole transition array, s is a quantity called the strength of the line λ_a , and Σs_a is taken over the lines of a multiplet. Here S denotes the strength of the multiplet which contains the line λ_a and ΣS is taken over all multiplets of the configuration array.

In the application of the sum rule it is supposed that the f -sum rule is valid for the f_T 's. Most of the contribution to the sum comes from the first line of the series; the higher lines and the transitions to the continuum are relatively small. Hence one assumes that $f_T \sim \Sigma f$. In the single-electron alkali-type spectra, LiI, NaI, etc., the f -values of the first series members, $2s-2p$, $3s-3p$, $4s-4p$, etc., are about unity. Unsöld (1948) adopted $f_T = 1$ for the first members of transitions like $p^k n' p - p^k n d$, $d^k n' s - d^k n p$, etc. A comparison of the sum-rule predictions with the experimental data for those elements where a comparison is possible suggests that $f_T = 1$ for atoms with equivalent p -electron configurations when applications are made to the first members of the $s-p$ and $p-d$ series, but $f_T \sim 2$ for $d f$ configurations.

The f -sum rule may be badly in error for configurations of the equivalent d -electrons such as occur in the iron group. Consider, for example, lines arising from the low even FeI configuration, $3d^7 4s$. In the transition array $3d^7 4s-3d^7 n p$ only one electron is involved, whereas in the transition array $3d^7 4s-3d^6 4s n p$ seven equivalent d -electrons are involved. The experimental data by King, Routly, Bell, and Davis (1958) show that the sum for both transition arrays ($n = 4$) is about 1. Further, the f_T for the transition array $3d^7 4s-3d^7 4p$ is greater than the f_T for the array $3d^6 4s^2-3d^6 4s 4p$ which involves two electrons or the f_T for the $3d^7 4s-3d^6 4s 1p$ array which involves seven electrons. From his copper-arc studies, C. W. Allen concludes that for the metals from scandium to iron, $f_T = 0.7$ provides a good representation of the data. In the application of the f -sum rule, one must certainly exclude double electron jumps. For complex atoms experimental rather than theoretical f -values would appear to be required. The sum rule is actually no more than a rough guide. That astronomers are forced to use it as a device for "computing" f -values points up the necessity of fundamental work on f -value determinations.

The situation with respect to damping constants is even less satis-

factory than it is for the f -values. For many transitions, the practice has been to measure damping constants with helium as the foreign gas and then extrapolate to hydrogen by plausible formulae.

Some elements are represented in the sun and cooler stars only by their compounds. Examples are boron and the halogens. Dissociation potentials and f -values are needed for a number of compounds and corresponding molecular lines. Fortunately, many of these compounds can be produced and studied in the laboratory with electric-furnace techniques. Programs such as those initiated by J. G. Phillips and Leo Brewer at the University of California should contribute greatly to our knowledge of fundamental molecular parameters. Transition probabilities have been measured there for such astrophysically important molecules as C_2 , TiO , ZrO , CN , VO , YO , MgH , and CaH .

5-5. The Analysis of Stellar Atmospheres in the Isothermal Approximation

Although the temperature and density monotonically increase with depth in a normal stellar atmosphere, in the first approximation we can interpret the spectrum of a star as though all the lines were formed in a layer characterized by some average temperature T and electron pressure P_e . Since P_e and T both increase with depth, the increase in ionization brought about by a rise in temperature is to some extent compensated by a decrease in ionization caused by an increase in P_e . The compensation is not complete and ionization gradually increases with depth, but for many elements the isothermal approximation is not as poor as it might seem to be at first glance.

Another approximation which is sometimes made is to suppose that the continuous spectrum is formed entirely in the photosphere and that the line spectrum is formed in an overlying "reversing layer." In this model, which is called the Schuster-Schwarzschild (SS) approximation, we can speak of the "number of atoms above the photosphere" as the number required to produce the absorption lines with the observed intensity. The "optical depth of the photosphere" is the depth to which one must go in the real atmosphere to secure the number of atoms necessary to reproduce the lines with their observed intensities in the idealized atmosphere. Unfortunately this quantity is not precisely defined. It can be estimated by comparing the results of the precise model-atmosphere calculations with those obtained in

the approximate theory. As one might expect, it varies from neutral atoms to ions, and from resonance lines to those arising from high levels. For purposes of a first reconnaissance, a choice of optical depth τ_0 of about 0.3 or 0.4 seems appropriate for neutral metals in the sun.

In another type of approximation, called the Milne-Eddington (ME) approximation, it is assumed that both the line and continuous spectrum are formed in the same layers in such a way that the ratio of line-absorption coefficient to continuous-absorption coefficient is constant. In the sun and similar stars the SS approximation is best for molecules and perhaps for lines of neutral elements, whereas the ME approximation is better for lines of ionized metals. Both approximations have been used extensively in astrophysical studies.

For purposes of illustration let us suppose that the lines are formed according to the Schuster-Schwarzschild approximation. Then, with sufficient accuracy for our purposes,¹ we can write for the residual intensity in the line (Menzel 1936)

$$I_\nu/I_c = r(\nu) = 1/(1 + N\alpha_\nu) \quad (5-26)$$

Here I_ν is the intensity at the frequency ν in the line profile and I_c is the intensity in the continuum. N is the number of atoms above the photosphere capable of absorbing the line. The equivalent width of the line is defined as

$$\begin{aligned} W_\lambda &= (c/\nu_0^2)W_\nu = (c/\nu_0^2) \int_0^\infty [1 - r(\nu)]d\nu \\ &= (c/\nu_0^2) \int_0^\infty ([N\alpha_\nu/(1 + N\alpha_\nu)]d\nu \quad (5-27) \end{aligned}$$

If we substitute for α_ν from Eqs. (5-19) to (5-23) we can obtain a relation between W_λ and Nf . This relationship is complicated and cannot be expressed for all values of Nf in simple analytic terms, but it has been evaluated numerically. We may plot $\log [(W/\lambda)(c/\nu)]$ as ordinate against $\log N\alpha_0$ as the abscissa. Such a relationship is called

¹ A more sophisticated treatment of the problem would give a more complicated formula but would add little to physical insight. Precise curves of growth for the SS approximation have been given by Wrubel. Unsold proposed a formulation of the curve of growth very similar to that by Menzel except that he used an empirical-profile formula due to Minnaert.

a *curve of growth* and was first introduced by Minnaert and Slob. Improved forms have been proposed by Menzel (1936), Unsöld (1938), Wrubel (1949, 1950) and others. A different curve will be obtained for each different choice of the parameter a .

By way of illustration we shall describe Menzel's version of the curve of growth. Since the coefficient of continuous absorption varies with wavelength, the "depth of the photosphere" will likewise vary and one may take this variation into account by multiplying N by κ_0/κ_λ where κ_0 is the absorption coefficient at some standard wavelength λ_0 . Further, if the line is not totally black at the center but has a depth R_c , one takes $\log [(W/\lambda)(c/v)(1/R_c)]$ as the ordinate. Let us define

$$X_0 = N\alpha_0 \quad \text{and} \quad p_c = \kappa_\lambda/\kappa_0 \quad (5-28)$$

For small values of N or α_0 , i.e., $X_0 \ll 1$, the equivalent width is proportional to the number of absorbing atoms, i.e.,

$$(W/\lambda)(c/vR_c) \sim \sqrt{\pi}(X_0/p_c) \quad \text{or} \quad W/\lambda \sim Nf\lambda \quad (5-29)$$

As the product $N\alpha_0$ increases, the curve flattens off and the equivalent width grows slowly in a domain described approximately by the expression

$$Wc/\lambda v R_c \sim \sqrt{[\ln(X_0/p_c)]} \quad (5-30)$$

Intermediate values of $\log X_0$ have to be calculated by numerical integration. Finally, when the product $N\alpha_0$ is very large, the equivalent width increases as $\sqrt{(N\alpha_0\Gamma)}$, i.e., the intensity of the line depends not only on N and f but also on the damping constant Γ , viz.,

$$(W/\lambda)(c/vR_c) = (\sqrt[4]{\pi}/2) \sqrt{(X_0\Gamma_c/p_c v \tau)} \quad (5-31)$$

This dependence occurs because most of the equivalent width of the strong line is contributed by the damping "wings" whose depth depends on the collisional or natural damping. Different curves of growth will be obtained for different values of the damping constant.

The number of atoms capable of absorbing the line in question, N , will hereafter be denoted as $N_{r,s}$, the number of atoms in the s th state for the r th ionization stage of the element. If the populations in the various levels can be described by Boltzmann's formula for some local excitation temperature T_x , then

$$N_{r,s} = N_r [g_{r,s}/u_r(T)] \exp(-\chi_{r,s}/kT_x) \quad (5-32)$$

N_r is the total number of atoms above the photosphere in the r th stage of ionization, $g_{r,s}$ is the statistical weight of the s th level, $u_r(T)$ is the partition function, $\chi_{r,s}$ is the excitation potential of the s th level. The ratio of the number of the atoms of the particular element existing in the r th ionization stage to the number in the $(r-1)$ stage (see, for example, Aller 1953, p. 79) is given by the Saha formula

$$\log(n_r/n_{r-1})P_e$$

$$= -(5040/T)I + 2.5 \log T - 0.48 + \log(2u_r/u_{r-1}) \quad (5-33)$$

where I is the ionization potential measured in electron volts from the $(r-1)$ st to the r th ionization stage, P_e is the electron pressure in dynes/cm², n_r is the number of atoms in the r th ionization stage per unit mass of stellar material, and n_{r-1} the corresponding number for the next lower stage of ionization. At any one T and P_e we usually need to consider only the atoms in two successive stages of ionization.

If we now substitute Eqs. (5-20), (5-23), and (5-32) into equation (5-28) we find

$$\begin{aligned} \log X_0 = \log N_r + \log gf\lambda - (5040/T_x)\chi + \log(\sqrt{(\pi)\epsilon^2/mc}) \\ - \log V - \log u(T) \end{aligned} \quad (5-34)$$

In the practical use of the curve of growth we determine T_x by comparing empirical plots of $\log W/\lambda$ vs. $\log gf\lambda$ for lines of one excitation potential with similar plots for lines of another excitation potential. The T_x determined in this way will not necessarily be identical with the temperature indicated by the ionization equation or stellar-energy distribution. If there is no turbulence, one may calculate $\log [(W/\lambda)(c/v)(1/R_c)]$ by computing v as $\sqrt{(2kT)/M}$ and taking R_c from the observed depths of the lines. If turbulence occurs, the empirical curve of growth will lie above the theoretical curve and one must determine the mean square of the turbulent velocity ξ^2 such that $\sqrt{(v^2 + \xi^2)}$ instead of v gives the shift necessary to bring the two into coincidence. After T_x and V have been determined, one plots $\log [(W/\lambda)(c/V)]$ against $(\log X_0 - \log N_r)$ in order to determine N_r . One must then compute N_r/N_T by Eq. (5-33) where N_T is the total number of atoms of the element in question. Hence the actual abundance of the element in question can be found only after T and P_e

have been established by carrying this procedure out for several different elements, and by making use of other data such as the stellar colors, the broadening of the hydrogen lines, etc.

Let us elucidate the procedure by applying it to the curve of growth for aluminum lines in the sun. The relevant data are given in Table 5-1 where the first four columns give the transition array, the multiplet designation and its number (in Miss Moore's Revised Multiplet Table), the individual wavelengths and their J -values. Then we list the excitation potential of the lower level and the log gf -values calculated mostly by the Bates and Damgaard tables. The required value of p_c was calculated for $\lambda_0 = 5000$, $\log P_c = 1.0$, and $\theta = 5040/T = 0.9$ (values adopted on the basis of previous approximations for the solar atmosphere). The next to the last column gives the observed value of $\log W/\lambda$ for each of the lines. The quantity $\log C$ applies to model-atmosphere methods and will be described in Sec. 5-7. For AlI, $u(T) = 6$ at $T \sim 5700^\circ\text{K}$. The gas thermal velocity is obtained by assuming a solar temperature of 5800°K . The turbulent velocity could be found by fitting the empirical and theoretical curves of growth in the vertical direction. In practice, one does this by comparing the data for as many elements of different atomic weight as possible, giving particular emphasis to those (such as iron) that define an apparently reliable curve of growth. In this way one obtains an estimate of $\xi = 1.3$ km/sec as appropriate for small eddies at the center of the sun's disk. Thus

$$v_{th} = [(2 \times 1.38 \times 10^{-16} \times 5800)/(27 \times 1.66 \times 10^{-24})]^{1/2} \\ = 1.89 \times 10^5 \text{ cm/sec}$$

and by Eq. (5-18), $V_{total} = 2.30 \times 10^5$ cm/sec. Substituting the numerical values for $\log V$, $u(T)$, $\log \sqrt{(\pi)\epsilon^2/mc} = -1.826$, into Eq. (5-34), we obtain

$$\log (X/p_c) = [\log N_r - 7.97] + \log [gf\lambda/p_c] - \theta\chi$$

Let us now define for each line the quantity

$$\log Y = \log (X/p_c) - \log (gf\lambda/p_c)$$

For aluminum, we have

$$\log Y = \log (X/p_c) - \log [gf\lambda/p_c] = [\log N_r - 7.97] - \theta\chi$$

*f_l*Table 5-4. Data for Aluminum Lines in Solar Spectrum^a

Transition array	Multiplet	λ	ΔJ	χ	$\log gf$	$\log p_c$	$\log W/\lambda$	$\log C$
$3s^23p-3s^24p$	$^2P^{\circ}, ^2S$	3961.54	3/2-1/2	0.00	-0.27	-0.04	-3.64	
	(1)	3944.02	1/2-1/2	0.00	-0.57		-3.78	
$3s^24s-3s^25p$	$^2S, ^2P^{\circ}$	6696.03	1/2-3/2	3.13	-1.35	0.09	-5.31	0.61B
	(5)	6698.67	1/2-1/2	3.13	-1.65		-5.30	0.31A
$3s^24s-3s^24p$	$^2S, ^2P$	13123.32	1/2-3/2	3.13	0.24	-0.08	-4.56	2.29B
		13151.02	1/2-1/2		-0.06		-4.71	1.99C
$3s^24s-3s^26p$	$^2S, ^2P^{\circ}$	5557.07	1/2-3/2	3.13	-2.10	0.04	-6.05	-0.11C
$3s^23d-3s^25f$	(6)							
	$^2D, ^2F^{\circ}$	8773.91	5/2-5/2	4.00	0.01	0.12	-4.95	1.14
$3s^23d-3s^26f$	(9)	8772.88	3/2-5/2	4.00	-0.17		-5.04	0.96B
	$^2D, ^2F^{\circ}$	7836.13	5/2-5/2	4.00	-0.33	0.12	-5.09	0.81A
$3s^23d-3s^27f$	(10)	7835.32	3/2-5/2	4.00	-0.51		-5.27	0.63A
	$^2D, ^2F^{\circ}$	7362.29	5/2-5/2	4.00	-0.48	0.11	-5.23	0.67B
$3s^24p-3s^24d$	(11)	7361.55	3/2-5/2	4.00	-0.66		-5.38	0.49B
	$^2P^{\circ}, ^2D$	16719.12	1/2-3/2	4.08	0.31	-0.30	-4.66	1.57B
		16750.65	3/2-5/2	4.05	0.57		-4.56	1.86C
		16763.48	3/2-5/2	4.05	-0.39		-5.03	0.54C

^a Adapted partly from Goldberg, Müller, and Aller, *Ap. J. Suppl.*, 11, 1960, Table 9; courtesy of the University of Chicago Press.

The theoretical curve is given with $\log Wc/\lambda v R_c$ as ordinate, but since the quantity $c/v R_c$ is known, we can plot this relation with $\log W/\lambda$ and $\log X_0/p_c$ as ordinate and abscissa, respectively.

Let us now sort the lines in Table 5-1 according to their excitation potential into three groups: (1) $\chi = 0$ ev, (2) $\chi = 3.13$ ev, and (3) $\chi = 4.00$ ev. Then for each of these groups we plot $\log W/\lambda$ vs. $\log gf\lambda/p_c$ and by fitting the plots to the theoretical curve of growth ($\log W/\lambda$ vs. $\log X_0/p_c$), we obtain for each group the value of $\log Y$. See Table 5-2.

A plot of $\log Y$ against χ , gives therefore $\log N_0$ and T_{ex} as 16.09 and 5520°K, respectively. With this value of T_{ex} , the curve of growth

Table 5-2. Determination of Excitation Temperature

Group	χ	Log Y
1	0	8.12
2	3.13	5.28
3	4.00	4.48

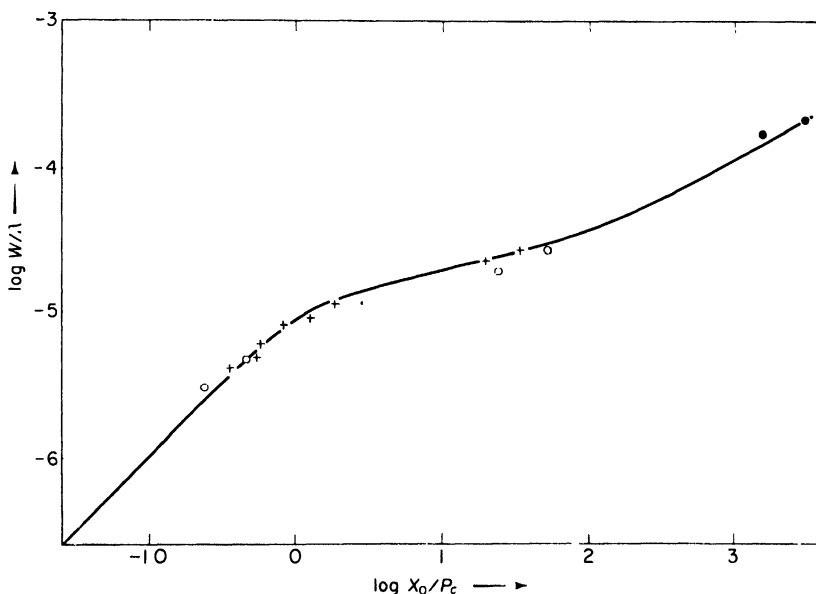


Fig. 5-5. Curve of growth.

shown in Fig. 5-5 is obtained. The strongest lines fall on the damping part of the curve of growth and serve to fix the value of $\log \Gamma/\nu$ in Eq. (5-31).

Notice that we obtain the number of neutral aluminum atoms "above the photosphere." In order to obtain the total amount of aluminum it is necessary to find the temperature and electron pressure appropriate for use in the ionization equation. This information cannot be obtained from data available for aluminum only. One must carry out this calculation for atoms represented by two stages of ionization, e.g., SrI and SrII, TiI and TiII, etc., and obtain the values of T and $\log P_e$ that will give the best representation of the data. T must be not far from the effective temperature of the sun. The analysis is complicated by the fact that f -values are poorly known for the ions of most elements, so we make the best estimates we can. A good representation is obtained for

$$\log P_e = 0.90 \quad \text{and} \quad T = 5600$$

(corresponding to an optical depth of 0.1 at $\lambda 4235$ or about 0.3 at $\lambda 5500$ on the basis of recent model atmosphere calculations). We now use these values of P_e and T in the ionization equation (5-33), with $I = 5.96$ eV, $\log (2u_{r-1}/u_r) = -0.50$ to obtain $\log N_1/N_0 = 2.13$ or $N_{\text{total}}/N_0 = 135$ and therefore $N(\text{Al}) = 1.66 \times 10^{18}$. Similar calculations carried out for other elements enable us to establish the relative abundances of the metals, to within the uncertainties of the f -values, and the inadequacies of the isothermal approximation.

What about the ratio of aluminum to hydrogen? If we take the optical depth of the line-forming region as 0.3 at $\lambda 5500$, we may compute the number of H atoms above this level by noting that

$$\tau_P = 0.3 = \alpha(\text{H}^-)P_e N_{\text{H}}$$

where $\alpha(\text{H}^-)$ is the absorption coefficient of the negative hydrogen ion as computed by Chandrasekhar (1946) per neutral hydrogen atom at unit electron pressure. At $T = 5600^\circ\text{K}$, $\alpha(\text{H}^-) = 5.81 \times 10^{-26}$, and we find $N_{\text{H}} = 6.5 \times 10^{23}$ hydrogen atoms "above the photosphere." The ratio of aluminum to hydrogen is then 2.6×10^{-6} , as compared with the value 1.6×10^{-6} obtained by the model-atmosphere method. Insofar as the metal/hydrogen ratio is involved, the Schuster-Schwarzschild approximation is clearly very crude since the assignment of the "depth of the photosphere" is dependent

on comparisons with analyses carried out with more elaborate methods.

A similar analysis could have been carried out in the Milne-Eddington approximation, where we no longer deal with number of atoms above the photosphere but rather with numbers of atoms per gram of stellar material. The continuous absorption coefficient then enters explicitly into the expressions. The Schuster-Schwarzschild model is probably as good as the Milne-Eddington model insofar as a determination of relative abundances of metals is concerned.

The curve-of-growth technique is used routinely in types of problems described in Chap. 9 where we compare a star suspected to be of abnormal composition with a supposedly normal star of as nearly as possible the same spectral and luminosity class. It is assumed that inherent errors due to approximations in the curve-of-growth technique will cancel out. For dwarf stars from *F*5 to *G*5 or *K*0 one often uses the sun as a reference standard.

If we compare the sun with a star of somewhat similar temperature and pressure, we have for each line of lower excitation potential χ

$$\begin{aligned} \log (X_*/p_i^*) - \log (X_\odot/p_i^\odot) &= \log N_{r,*} - \log N_{r,\odot} + \log p_{c,\odot}/p_{c,*} \\ &- 5040 \chi [(1/T_*) - (1/T_\odot)] + \log (V_\odot/V_*) \\ &+ \log [u(T_\odot)/u(T_*)] \end{aligned} \quad (5-35)$$

where the symbols \odot and $*$ refer to the sun and star, respectively. Of course N_r , the number of atoms above the photosphere in the r th stage of ionization, will depend on the coefficient of continuous absorption and hence we introduce the factors $p_{c,*}$ and $p_{c,\odot}$. From the spectrum and luminosity class a good enough estimate of T and P_c is obtainable to permit an estimate of the wavelength dependence of the depth of the photosphere.

With the aid of Eq. (5-35) it is possible to compare the relative number of ions of FeII, CrII, TiII, etc., in the sun and star. Likewise, the ratios of the numbers of many corresponding atoms can be determined, i.e., FeI, CrI, TiI, etc. If the level of ionization for the sun is known, we can find the level of ionization for the star, and hence the abundances of these elements in the star in question. Only one stage of ionization is observed for many elements, however.

The spectra of many stars have been analyzed by the curve-of-growth method. It is extremely valuable as a first reconnaissance

to give mean temperatures and densities for the line-producing layers. In giant and supergiant stars where realistic models of the atmospheres cannot be obtained, the curve of growth is probably the best procedure that has been devised. Sometimes referred to as *grobanalyse* or rough analysis, it provides a convenient starting point for more accurate and more sophisticated studies.

5-6. Method of Model Atmospheres

In the curve-of-growth procedure, it is supposed that all the essential properties of the spectrum can be represented by a single temperature and pressure. For example, Unsöld (1948) concluded that the level of ionization in the solar spectrum could be explained by $T = 5675^\circ\text{K}$ and $\log P_e = 1.51$. On the other hand, it is scarcely to be expected that the lines of potassium (ionization potential = 4.32 eV) and the observable oxygen lines (excitation potential = 9.1 eV) are formed in the same atmospheric layers.

In refined treatments of stellar atmospheres it is supposed that the distributions of temperature and pressure with depth are sufficiently well known for the calculation of the contribution of each stratum to the final line intensity to be evaluated.

In Sec. 5-2 we mentioned that $T(\tau_0)$ (where τ_0 is the optical depth at some specific wavelength, e.g., $\lambda 5000$) has been obtained for the sun from measurements of the energy distribution at the center of the sun's disk and the limb darkening $I_\nu(0, \theta)/I_\nu(0, 0)$. In the continuum the radiation $I_\nu(0, \theta)$ emerges from an average depth $\bar{\tau}_\nu = \cos \theta$. Hence limb-darkening measurements give little help concerning the deeper layers ($\tau > 1.5$). Likewise, since the continuum observations cannot be made very close to the limb, we cannot obtain from them the temperature distribution in the shallowest layers ($\tau < 0.02$). When the temperature distribution has been adopted, one can calculate the march of P_g and P_e with τ_0 from the condition of hydrostatic equilibrium. Various workers have constructed model solar atmospheres based on empirical and on theoretical considerations or both (see the summary by Minnaert 1953). These models differ from one another in that they assume different H/He ratios, and therefore they obtain different P_g/P_e ratios. More fundamentally, although they tend to agree with respect to $T(\tau_0)$ in intermediate layers $0.1 < \tau_0 < 1.0$, they show substantial departures in the deeper layers where convection apparently occurs and also in the upper-

most layers where deviations from local thermodynamic equilibrium become troublesome. Unfortunately, it is precisely in these upper layers that the stronger lines are formed. The very centers of the strong lines are formed in yet higher layers (i.e., the chromosphere), an outer envelope of the sun which marks the transition region between the photosphere and the corona. Weak lines, on the other hand, tend to be formed in the same layers as those producing the continuous spectrum where conditions are expected to approach thermodynamic equilibrium.

In the stars, sufficiently accurate data on limb darkening are not available to permit one to utilize the same technique as in the sun. The layers accessible to observation appear to be in radiative equilibrium, i.e., the temperature gradient is determined by the flow of radiation rather than by convection. In the cooler stars a convection zone underlies the visible atmosphere of the star.

In hotter stars we may postulate radiative equilibrium throughout, and therefore the flux of radiation must be constant. Model atmospheres intended for calculation of theoretical line intensities have been computed by a number of workers, e.g., M. Rudkjöbing, Miss A. Underhill, Miss J. K. McDonald, J. C. Pecker, A. Przybylski, J. Milligan, G. Traving, K. Hunger, R. Cayrel, S. Ueno, K. Osawa, S. Saito, and T. L. Swihart. In the following pages we shall give examples of the application of some of these models to particular stars.

The fundamental integral relation, Eq. (5-6), between the emergent intensity, the temperature, and optical depth, is valid for the continuum as long as Kirchhoff's law holds. If electron scattering is important, the emission per unit volume becomes independent of the temperature and $B_\nu(T)$ must be replaced by a more complicated expression. For most of the stars with which we shall be concerned we may assume that the influence of electron scattering can be neglected. The coefficient of continuous absorption is usually due to atomic hydrogen or the negative hydrogen ion, and its dependence on temperature and electron pressure is known.

If the line is formed under conditions approaching local thermodynamic equilibrium, (i.e., validity of Kirchhoff's law), we may use Eq. (5-6) to compute the intensity in the line, provided that κ_ν is replaced by $(l_\nu + \kappa_\nu)$ where l_ν is the coefficient of line absorption per gram of stellar material. The residual intensity in the line profile ac-

cordingly will be

$$\begin{aligned}
 r_\nu(\theta) &= I_\nu^L(0, \theta)/I_\nu^C(0, \theta) \\
 &= \int_0^\infty B_\nu(T) \exp(-l_\nu \sec \theta) \sec \theta \, dl_\nu / \\
 &\quad \int_0^\infty B_\nu(T) \exp(-\tau_\nu \sec \theta) \sec \theta \, d\tau_\nu,
 \end{aligned} \tag{5-36}$$

where $I_\nu^L(0, \theta)$ and $I_\nu^C(0, \theta)$ refer to the line and continuum, respectively, at a point on the solar disk where the ray to the observer makes an angle θ with respect to the outward normal. We define [compare Eq. (5-2)]

$$d\tau_\nu = \kappa_\nu \rho \, dh \quad dl_\nu = (\kappa_\nu + l_\nu) \rho \, dh \tag{5-37}$$

where both κ_ν and l_ν include the effects of negative absorptions.

Now $\kappa_\nu(P_e, T)$ is essentially fixed by the model atmosphere; in most instances it is due to processes involving hydrogen. On the other hand, l_ν depends on a number of factors; the line-broadening mechanism and the ratio of damping constant to Doppler width [cf. Sec. 5-3 and Eqs. (5-11) to (5-23)] the f -value for the transition (Sec. 5-4); the fraction of atoms in the relevant stage of excitation and ionization :cf. Eqs. (5-32 and (5-33); and finally the abundance itself. Line broadening depends on the velocities of the atoms and on gas pressure, while ionization depends on radiation temperature and electron pressure.

If thermodynamic equilibrium does not hold, the radiation emitted in a spectral line will no longer be fixed by the local temperature. On the contrary, the emission will be determined largely by the radiation field to which the atom is exposed. Boltzmann's formula and the Saha equations cannot be applied. This situation is difficult to handle because there are no clearcut theoretical procedures for handling deviations from thermodynamic equilibrium.

When the atmospheric structure is known, one may compute r_ν at each point in the profile and integrate to get

$$W_\lambda(\theta) = (c/\nu_0^2) \int_0^\infty [1 - r_\nu(\theta)] d\nu \tag{5-38}$$

the equivalent width at a point on the disk.

5-7. The Application of Model-Atmosphere Methods to the Interpretation of Stellar Atmosphere Compositions

The determination of the composition of a stellar atmosphere by model-atmosphere methods proceeds by successive approximations. First, a curve-of-growth analysis supplies an approximate composition, temperature, and surface gravity. Next, a calculation of a model atmosphere, or better yet a grid of model atmosphere, is carried out. Then theoretical total intensities of selected "model-sensitive" lines are computed. For example, for a star whose temperature is about 22,000°K, one may employ lines of SiII, SiIII, and SiIV which appear simultaneously in the spectrum. The model atmosphere should also predict correctly the hydrogen line profiles, the discontinuity at the Balmer limit, and the energy distribution in the continuous spectrum, i.e., the color temperature of the star. Once a suitable model has been identified or interpolated, a calculation of the theoretical equivalent widths is carried out. In practice we usually compute the individual curves of growth for the relevant elements and excitation stages and then derive the abundances from a comparison of observed and predicted W_λ 's. It is clear that each ionization stage must give the same abundance. Otherwise, clearly, something is wrong with the atmosphere model or the basic assumptions involved.

In stars we observe the integrated light of an entire hemisphere so that the expression (5-6) must be replaced by

$$F_\nu^c(0) = 2 \int_0^\infty B_\nu(T) E_2(\tau_\nu) d\tau_\nu \quad (5-39)$$

$$F_\nu^L(0) = 2 \int_0^\infty B_\nu(T) E_2(t_\nu) dt_\nu \quad (5-40)$$

where $F_\nu^L(0)$ and $F_\nu^c(0)$ refer to the line and continuum, respectively, and we have assumed that electron scattering can be neglected. Here $E_2(\tau_\nu)$ is the exponential integral function. Now

$$E_2(x) = \int_{y=1}^\infty (e^{-xy}/y^2) dy \quad (5-41)$$

Then the residual intensity in the line is

$$r_\nu = F_\nu^L(0)/F_\nu^c(0) \quad (5-42)$$

and the equivalent width is given by

$$W_{\lambda} = (c/\nu_0^2) \int_0^{\infty} [1 - r_{\nu}] d\nu \quad (5-43)$$

The calculation of W_{λ} is difficult because t_{ν} depends on ν in a complicated way; the relation depends steeply on $(\nu - \nu_0)$ across a line. With the advent of high-speed computers these particular difficulties can be surmounted. Eventually the relevant equations can be integrated directly once the basic model atmosphere is given.

An alternative procedure is to compute W_{λ} with the aid of Pecker's theory (1951). For any point on the solar disk, characterized by

$$\mu = \cos \theta \quad (5-44)$$

the equivalent width $W(\mu)$ is given by

$$W(\mu)/\lambda = \int_{-\infty}^{+\infty} (M/\mu) z(x) \Psi(Y/\mu, a) g_{\lambda}^{\mu}(x) e^x dx \quad (5-45)$$

Following G. Elste (1955), the variable of integration is taken as

$$x = \log \tau_{\lambda 0} \quad (5-46)$$

Also, μ is unity at the center of the solar disk. The other quantities appearing under the integral sign are discussed in detail elsewhere (Aller, Elste, and Jugaku 1957). We shall not reproduce these expressions here, but shall describe the physical significance of each factor.

For each line, M is a constant which includes the abundance with respect to hydrogen, certain physical constants, and the factor $gf\lambda$.

The factor

$$z(x) \sim e_{\lambda}/\kappa_{eff} \quad (5-47)$$

is proportional to the fraction e_{λ} of all atoms of the given element capable of absorbing the line in question and the total extinction coefficient at the point in question. Hence it involves the Boltzmann and Saha equation. It can be computed for each energy level of interest in each ion.

The function

$$\Psi((Y/\mu), a) = (2/\sqrt{\pi}) \int_0^{\infty} H(a v) \exp [-H(a v) Y/\mu] dv \quad (5-48)$$

is Pecker's saturation function. Here $H(a, v)$ is defined by Eq. (5.19). The function is so normalized that as

$$Y(x) = [Mc/\sqrt{(\pi)} V] \int_{-\infty}^x z(y) e^y dy \quad (5-49)$$

approaches zero, Ψ approaches 1. Now Ψ can be tabulated once and for all as a function of Y/μ and a . For a weak line Ψ will be near 1, but for a strong line Ψ will decrease rapidly with increasing depth. This behavior expresses the fact that a strong line is formed almost entirely in the upper part of the atmosphere, whereas a weak line of the same multiplet may originate primarily at a greater depth.

The function $g_{\lambda}^{\mu}(x)$ is the so-called weighting function. It falls off monotonically and eventually, steeply, with depth in the star. It depends only on the model atmosphere and on the wavelength and not at all on the element involved, as long as the material is in local thermodynamic equilibrium, (LTE), i.e., the excitation and ionization are given by the Boltzmann and Saha equations at the local temperature. In terms of τ_{λ} ,

$$g_{\lambda}^{\mu}(\tau_{\lambda}) = [1/I_{\lambda}^c(0, \theta)] \int_{\tau_{\lambda}}^{\infty} (dB_{\lambda}/d\lambda) \exp(-t_{\lambda}/\mu) dt_{\lambda} \quad (5-50)$$

Recently, Pecker has shown how the theory may be modified if the excitation temperature is not equivalent to the local temperature, i.e., if there are deviations from thermodynamic equilibrium.

In stellar atmospheres one must use the integrated flux, [see Eqs. (5-39), (5-40) and (5-42)] so that Eq. (5-45) is replaced by a more complicated expression, e.g.,

$$W_{\lambda}/\lambda = \int_{-\infty}^{+\infty} Mz(x)\Psi(Y', a) G_{\lambda}^{*}(x)[G''(x)/G'(x)] e^x dx \quad (5-51)$$

where the factor $G''(x)/G'(x)$ now allows for the integration over the disk of the star and $G_{\lambda}^{*}(x)$ is the weighting function for the flux taking into account the stimulated emissions. The integrand of Eq. (5-45) or (5-51) is called the *contribution function*. It depends on the transition in the element involved, its stage of ionization, excitation, and also on the abundance and line strength. Contribution functions are of interest in that they show precisely which layers are most important in the production of any particular spectral line.

The calculation procedure for a given star is as follows. With the

aid of the aforementioned criteria we first select the model atmosphere we wish to use. Then, we compute the weighting function $G_{\lambda}^*(x)$ and the correction factor $G''(x)/G'(x)$. The function $z(x)$ is computed for the lower term of every transition under consideration for each element. The quantities Y and a are evaluated. Since Ψ is known as a function of these parameters, the integrand of Eq. (5-51) can be computed at once. For all the lines arising from a given lower level, the ordinates $\log W$ are calculated by a numerical integration.

The abscissa of the curve of growth is

$$\log C = \log gf\lambda + \log kL^* + \Delta\chi\theta_m \quad (5-52)$$

Here $\theta_m = 5040/T_m$ refers to the "mean temperature" of the atmosphere. T_m may be the temperature found from the curve-of-growth analysis, although it is not necessary to choose precisely this value. For a level s in the r th stage of ionization, we choose

$$\Delta\chi = -\chi_{r,s}$$

whereas

$$\Delta\chi = (\chi_{r-1} - \chi_{r-1,s}) \quad (5-53)$$

for levels in the $(r-1)$ st stage of ionization. Then

$$L^*(\Delta\chi, \lambda) = \int_{-\infty}^{+\infty} z(x)G_{\lambda}^*(x)e^x dx \quad (5-54)$$

while k is a numerical constant that depends only on the mean molecular weight of the un-ionized material.

For each level of each element in each stage of ionization a particular curve of growth is obtained. The stratification effects, i.e., the dependence of the excitation and ionization on depth, are explicitly introduced both in the ordinates and in the abscissa. The integrands of the functions involved in both coordinates include $z(x)G_{\lambda}^*(x)$ while the ordinate includes also the saturation factor Ψ .

Figure 5-6 illustrates the contribution functions for SiII, SiIII, and SiIV in a model atmosphere computed by Miss J. K. McDonald and revised by J. Milligan. It corresponds to a temperature near 20,000°K (spectral class B3). The calculations are carried out for weak lines. Notice how the contributions from successive stages of ionization come from appreciably different optical depths. The SiII lines have a broad maximum at $\tau_0 \sim 0.09$, and the SiIII lines have a

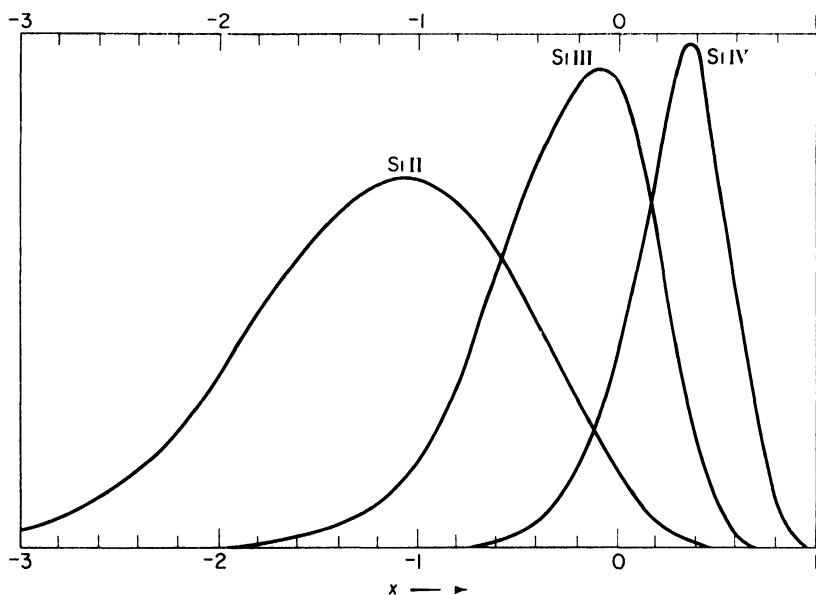


Fig. 5-6. Contribution function for silicon in the atmosphere of a hot star. The atmospheric model is that computed by Miss J. K. McDonald and revised by J. Milligan. The ordinates are arbitrary; abscissa is $x = \log \tau_{\lambda_0} (\lambda_0 = 5000 \text{ \AA})$.

maximum near 0.8, whereas the SiIV lines are formed mostly below an optical depth of unity.

Consequently, the differences between the curves of growth for silicon in various stages of ionization are not trivial (Fig. 5-7). Furthermore, as a consequence of the steep dependence of the coefficient of continuous absorption on wavelength, the curves may also differ from one wavelength region to another. The shapes of individual curves of growth as well as their horizontal shifts differ from one another, a fact which is not surprising in view of Miss Underhill's calculations of the theoretical profiles of silicon lines in the atmospheres of hot stars (1957). She found significant differences in the shapes of the SiII, SiIII, and SiIV lines in her model atmospheres. The silicon lines in the hot stars represent an extreme example. Lines of metals in the same stage of ionization, e.g., TiI, VI, and FeI in the sun, show rather similar curves of growth, but these in turn may differ from those of ions of the same element.

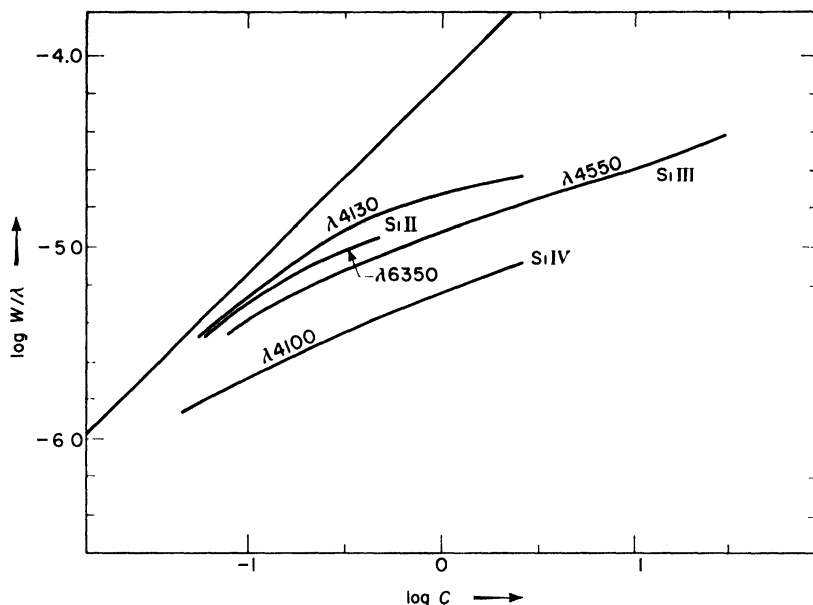


Fig. 5-7. Curves of growth for silicon in McDonald-Milligan model. Here $\log W/\lambda$ is plotted against $\log C$ for SiII, SiIII, and SiIV with values of the parameter $\log a = -1.4$ for SiII and SiIV, and $\log a = -1.0$ for SiIII. Notice that the curves for SiII $\lambda 4100$ and $\lambda 6350$ differ appreciably.

5-8. Stellar Applications of the Model-Atmosphere Techniques

In this chapter we shall discuss only results obtained by model-atmosphere methods, since for normal main-sequence stars they have rather generally replaced the earlier curve-of-growth studies. The latter technique is important for the comparison of stars for which model atmospheres are not available or where the accuracy of the data do not justify the extended calculations required.

The use of the model-atmosphere method to get abundances in the sun was initiated by Strömgren (1940). His techniques were applied (Aller 1949) to the B2 V star γ Pegasi with a model atmosphere very similar to that calculated by Miss McDonald (1953). Subsequently, much better model atmospheres and theoretical techniques have been developed.

The A0 V star, Vega, was studied by K. Hunger (1955) who cal-

culated a model atmosphere and took the stratification effects into account. He assumed that all lines except those of hydrogen and helium had essentially the same shape. Hence the form of the curve of growth (that given by Unsöld) was the same for all lines.

Table 5-3 summarizes Hunger's results for Vega; referred to $\log N = 12.00$ for H. The uncertainties for sodium and vanadium are large, while the large abundance of nickel is probably to be attributed to the selection of too large an f -value. Many of the differences between Hunger's values and those obtained for the sun are to be attributed to differences in the adopted f -values.

Among yet hotter stars we compare results by Traving, Cayrel, and Voigt, and by Elste, Jugaku, Boury, and Aller. See Table 5-4. The abundance determinations by Neven and de Jager were based on model atmospheres that appear to be in serious disaccord with those of other workers. The two "fine-analysis" determinations for τ Scorpii were based on different observational data as well as different theoretical analyses. For 10 Lacertae and 55 Cygni we compare the results of curve-of-growth analyses (Aller 1946; Voigt 1952) with model-atmosphere results (Traving 1957; Aller 1956). For most elements the differences are not large. R. Cayrel calculated the intensities of the lines in the supergiant ζ Persei by the methods of direct numerical integration. The stars τ Scorpii, γ Pegasi, 22 Orionis, and 114 Tauri were all analyzed by the Pecker theory. For τ Scorpii the model atmosphere calculated by Traving was modified for a lower surface gravity.

The analysis of γ Pegasi, 22 Orionis, and 114 Tauri was carried out in the following way. Instead of selecting a model atmosphere, calculating theoretical equivalent widths, and then deriving correc-

Table 5-3. Composition of Vega^a

Element	$\log N_i$	Element	$\log N_i$	Element	$\log N_i$
H	12.00	Si	7.24 ± 0.4	Mn	4.15 ± 0.5
He	11.14 ± 0.5	Ca	6.20 ± 0.3	Fe	7.05 ± 0.2
O	8.87 ± 0.5	Sc	3.78 ± 0.4	Ni	7.36 ± 0.5
Na	7.55 (3)	Ti	4.79 ± 0.4	Sr	3.12 ± 0.4
Mg	7.70 ± 0.3	V	4.32 ± 0.5	Y	2.09 ± 0.5
Al	5.71 ± 0.4	Cr	5.56 ± 0.4	Zr	2.84 ± 0.5

^a Adapted from K. Hunger, *Zeits. f. Ap.* 36, 42, 1955; 39, 273, 1956.

Table 5-4. Compositions of *B* Stars
(Relative Numbers of Atoms)

	10 Lacertae 09.5V		τ Scorpii BOV		ζ Persci B1(Ib)		γ Pegasi B2.5V		55 Cygni B3Ia		Adopted	
	<i>A</i> (1946) ^a		<i>T</i> (1955) ^a		<i>C</i> (1956) ^a		<i>A</i> / <i>J</i> (1959) ^a		<i>V</i> (1952) ^a		22 Ori 114 Tau	
	<i>T</i> (1957) ^a		<i>AE</i> / <i>J</i> (1956) ^a		<i>C</i> (1956) ^a		<i>A</i> / <i>J</i> (1959) ^a		<i>V</i> (1952) ^a		mean	
Hydrogen	9200	8500	8530	8900	8300	8700	8700	8000	8700	8700 ^b	8600	
Helium	800	1440	1450	1100	1700	1290	1970	1300			1380	
Carbon	0.9	2.0	2.0	0.45	1.5	3.3	1.1	2.2	1.9	1.1	1.7	
Nitrogen	1.0	2.0	3.1	1.6	1.7	0.9	2.8	3.7	0.54	0.59	1.3	
Oxygen	5.0	5.0	11.0	3.8	9.0	3.7	12.0	8.3	3.5	2.9	5.1	
Fluorine						0.028					0.03	
Neon	4.4	4.5	4.5	6.4	3.4	4.65					4.5	
Magnesium	0.25	1.4	0.46	1.8	0.49	0.76	0.38		1.0	0.38	0.75	
Aluminum		0.1	0.032	0.022	0.05	0.005	0.05		0.0048	0.0037	0.014	
Silicon	0.38	0.48	0.15	0.38	0.77	0.094	0.28	0.25	0.094	0.074	0.24	
Phosphorus						0.0028			0.0024		0.0026	
Sulphur				0.25		0.55			0.22	0.15	0.26	
Chlorine						0.014					0.014	
Argon						0.07					0.07	

^a A (Aller), C (Cayrel), E (Elste), J (Jugaku), T (Traving), V (Voigt).

^b In 22 Orionis and 114 Tauri the H abundance is taken as 8700.

tions to the model from discrepancies between theory and observation, an interpolation procedure was used. That is, for several model atmospheres that embrace the range in temperature and surface gravity exhibited by the program stars, the profiles and intensities of certain lines sensitive to these parameters are calculated. Then from a comparison of the observations with theoretical predictions, surface gravities and effective temperatures of the program stars are found.

It turns out that in the spectral range *B1* to *B5* ($T = 24,000$ to $18,000^\circ$ roughly), the intensity ratio of the SiII to the SiIV lines is very sensitive to the temperature, whereas the profiles of the hydrogen lines are sensitive to surface gravity and relatively insensitive to temperature. Thus temperature is fixed by the silicon lines and surface gravity by the profile of the $H\gamma$ line.

The hydrogen lines are broadened by the Stark effect produced by the electric fields of neighboring ions and electrons. The broadening coefficient is evaluated from the Kolb-Griem theory (1958). The ions behave according to the statistical Holtsmark theory while the electrons act according to the discrete-encounter theory, their influence being felt in the far wings of the line that are of particular astrophysical importance. The surface gravities calculated by fitting the theoretical to the observed profiles were always too large when only the Holtsmark theory was used; the application of the Kolb-Griem theory gives surface gravities in good accord with results obtained from eclipsing binaries.

One disquieting feature emerges from a comparison of these theoretical and observed silicon-line intensities. If we represent the intensities of the SiII and SiIV lines, the SiIII lines will be too strong; if we fit the intensities of the SiIII and SiII lines, the SiIV lines will be too strong. This discordance is not caused by the approximations of the Pecker theory; Miss Underhill (1957) had found the same results from precise calculations. Possibly the model atmospheres fail in the uppermost layers corresponding to the stellar chromosphere or deviations from thermodynamic equilibrium may be involved. Also, effects of stellar rotation may complicate the problem. In a rapidly rotating star, the polar regions are hotter than the equatorial regions. Preliminary estimates indicate that the effect would not be important until the star was rotating so rapidly as to approach instability in the equatorial regions. Further, the calculated energy

distributions do not fit the observed energy distributions as closely as one would like.

A detailed comparison of results obtained for γ Pegasi, 22 Orionis, and 114 Tauri with those found by various investigators for other stars shows that the abundance of silicon and aluminum are systematically lower in the Michigan results, although reasonably accordant values are found for other elements. Some elements, such as fluorine, chlorine, and argon, have been observed in only one star, γ Pegasi. Their abundances depend on very weak lines, some of which certainly must be blended with as yet unidentified lines of other elements. In addition, f -values are uncertain for most of the available lines.

One of the most troublesome problems is the ratio of helium to hydrogen. Unsöld and his co-workers found a H/He ratio by numbers of about 5. This value seems to be substantiated by the ratio of 7 found by Mathis for the Orion nebula, which presumably must have the same composition as the B stars which are formed from such objects. On the other hand, careful studies by Miss Anne Underhill tended to give a H/He ratio of the order of 1/20. The difficulty is the following. In B stars, most HeI lines are so strong that they must be formed largely in the stellar chromospheres. In these regions our model-atmosphere methods are of little help, so we have to use the observed profiles and the actual wings of the helium lines rather than their equivalent widths. In order to use the line wings, however, it is necessary to know not only conventional line-damping constants but also detailed shapes of the absorption coefficients, particularly at great distances from the line center. These parameters have not been experimentally established. The ionized helium lines, however, are formed in the "photospheric" layers where model-atmosphere methods may be employed, but the necessary line-broadening coefficients are not yet worked out. The intensities of the ionized helium lines, however, are extremely sensitive to the temperature; hence a small error in the assumed temperature can lead to a large error in the abundance. In the early B stars, the HeI line intensities are relatively insensitive to the temperature so that when adequate line-broadening data become available they should yield reliable abundances. The problem of the He/H ratio has been carefully discussed by Jugaku, who suggests that perhaps 1/6 or 1/7 is about the best estimate we can make until the necessary experimental parameters have been improved.

A considerable amount of attention has been paid to the compositions of the hot stars which presumably represent the present material of the interstellar medium. *B* stars, built very recently from the interstellar matter, might be expected to contain greater proportions by weight of the heavier elements than old stars like the sun. The work carried out so far indicates that abundances of elements in the first two rows of the periodic table are not substantially different in *B* stars and in the sun. This result suggests that the composition of the interstellar medium has not changed radically since the solar system was formed. If the interstellar medium has been repeatedly cycled through stars during the long history of the galaxy and elements have been built in the stars, the rate of element building must have proceeded much faster in the early history of our system than it has occurred in the last 4000 million years. We return to these questions in Chaps. 9 and 10.

Much more work needs to be done on model atmospheres and the detailed quantitative interpretation of stellar spectra. Our present model atmospheres cannot be regarded as fully satisfactory and the influence of stellar rotation and deviations from thermodynamic equilibrium must be taken into account. Improvements in the basic physical data are urgently needed.

5-9. The Composition of the Sun

Since the pioneer work of Russell (1929) who used eye estimates of line intensities, calibrated with the aid of approximate theoretical line strengths, to obtain a quantitative analysis of the sun, many investigations have concentrated on this problem, first by curve-of-growth techniques, and subsequently by model-atmosphere methods, using increasingly refined theoretical techniques and improved observational data.

We restrict our detailed comments to the results obtained by the method of model atmospheres. It was applied first by Strömgren, then by Minnaert and Claas, and subsequently by other workers. Abundance values obtained have differed from one another because of different choices of damping constants for strong lines, different *f*-values, and different atmospheric structures.

Strömgren had confined his attention to relatively strong lines of a few elements. Minnaert pointed out the value of using weak lines for which one need not know the values of the damping constants.

These quantities are often difficult to determine. Claas (1951) used the Barbier model which appears to have too high a boundary temperature and restricted himself to those elements with weak lines for which f -values were available. He used a single curve of growth for all elements.

Weidemann (1955) determined the abundances of Na, Mg, Al, Ca, and Fe using an improved model by K. H. Bohm (1954) for which the boundary temperature was 3400°K. He found that, compared with the results by previous workers, the abundances of the metals was cut down by a factor of about 2.

Some investigators have concentrated on particular elements, e.g., Bowen (1948) and also Cabannes and Dufay (1948) determined the abundance of oxygen, Hunaerts (1947) got the concentration of carbon, nitrogen, and oxygen from molecular spectra, while lithium was studied by Greenstein and Tandberg Hanssen (1954), Greenstein and Richardson (1951), and Dubov (1955).

The Michigan program of solar abundances (Goldberg, Müller, Aller 1960) involved a systematic study of all tractable elements in the solar atmosphere. First a solar atmospheric model was chosen. A model was selected for the intermediate layers that gave the best representation to the accurate photoelectric limb-darkening observations by A. K. Pierce and his associates. G. Elste extended this atmosphere both to deeper layers where convection occurs and to shallower layers where the limb-darkening data can be of no help. Then on the basis of this model atmosphere, Elste computed precise special curves of growth for medium strong lines with the aid of a high-speed electronic computer. New f -value data were employed wherever possible. New observations of solar-line intensities were secured in the infrared with the lead-sulfide cell detector attached to the Snow telescope at Mount Wilson, and also in the ordinary spectral regions with the new vacuum spectrograph at the McMath-Hulbert Observatory. The Utrecht Atlas of the solar spectrum (Minnaert et al., 1940) covers the spectral region $\lambda\lambda 3332$ to 8771 , while equivalent width measurements by C. W. Allen (1934, 1936, 1937, 1938) covered the solar spectrum from $\lambda\lambda 3924$ to 11830 . The Michigan Atlas, of which only the domain $\lambda\lambda 8465$ to 25242 has been published, covers the range $\lambda\lambda 2993$ to 25578 . O. C. Mohler (1955) has published the wavelengths and intensities for the range $\lambda\lambda 11984$ to 25578 , while the Utrecht astronomers have obtained equivalent

widths from $\lambda\lambda 3332$ to 8770 . The range $\lambda\lambda 6600$ to 8770 has been published (1951).

The observational data show a considerable range in accuracy depending on their intensity, the nature of the continuous background, and possible blends. The intensity of a line of equivalent width greater than 100 mÅ, falling in a region where the continuum is well defined, can be measured to an accuracy of the order of 10 per cent. The results are particularly uncertain for $\lambda < 4000$ Å, where the equivalent width may be in error by factors of 2 or even 5 . When the line of interest is blended with that of some other element, it may be possible to measure the equivalent width with considerable accuracy, but it may be impossible to obtain the relative contributions of the two components. These observational difficulties are particularly troublesome with the weak lines with which we usually deal. For abundant elements we choose weak lines because of difficulties with damping constants of strong lines. Among rarer elements we have no choice; their lines are always weak and few in number. We must always keep in mind the possibility of blending with unknown contributors—molecular or atomic lines not yet identified in the sun.

Of the elements found on the earth, the majority have been found in the sun, but there are a number which are rare, whose lines fall in an inaccessible part of the spectrum, or are masked (Moore 1953). Other elements are represented by lines produced under excitation conditions that make them unusable for abundance studies. This group includes the second most abundant element, helium, whose lines are produced in the chromosphere, and argon whose forbidden lines are observed in the solar corona. Eventually, as better observations are secured in the ultraviolet below $\lambda 2900$ we may be able to identify such elements as Cl and Br. Elements such as Kr, Xe, I, Hg, Te, Se, whose lines also fall in this region may be more difficult to recognize because their lines will certainly be weak because of their rarity.

Although their strongest lines fall in accessible spectral regions, Re, Tl, Bi, Ra, and U have not been observed in the sun partly because of their intrinsic rarity and partly because the f -values are low. B and F are found in the form of hydrides. While Cd, Th, and Au are represented by only one line apiece, Charlotte Moore (1953) regards the identifications as reasonably reliable.

Not found and not expected are the radioactively unstable elements Tc, Pm, At, Fa, and synthetic elements of the actinide "rare earth" group.

Some elements whose lines are found in the sun in plentiful supply, such as the lanthanide rare earths, are not suitable for abundance determinations because term analyses have not been worked out sufficiently in detail to permit the calculation of partition functions. For many elements, as we shall see, the f -values are so poorly known that good estimates of the abundances cannot be made.

Table 5-5 summarizes the recent abundance determinations for the sun together with more detailed information concerning the analysis made at Michigan. The first column gives the atomic number and the designation of the element. The second column gives the number of lines used in the Michigan work and the spectral regions involved. In some instances, data from different spectral regions (column 3) arise from widely different excitation potentials and yield different abundances. In some elements, such as lithium or beryllium, only a few lines are involved and the explicit λ is given. Column 4 denotes the type of curve of growth used. The very weak lines fall on the linear part of the curve of growth, denoted as L. For a number of elements, curves of growth were computed by Elste. Unfortunately, for many elements only segments of the curves of growth were provided, but for most neutral metals, the iron curve of growth calculated for a turbulent velocity of 1.8 km/sec gives a satisfactory representation of the observations.

The fifth column gives the excitation potential of the lower level (when only one multiplet is involved) or the range in excitation potentials of the lower levels expressed in volts. The sixth column gives the source of the observational data. The most frequently used data are those given by the Utrecht observers (U), by Allen (A), or by Mohler and his associates at the McMath-Hulbert Observatory (M). In the seventh column we indicate whether empirical or theoretical f -values are used or a combination of both. The next column gives the references to the f -values actually used. Occasionally other f -value determinations are listed in parentheses, but no attempt is made to provide a complete list, such as is given in the original reference (Goldberg, Müller, and Aller 1960).

The column headed Q gives an assessment of the quality of the f -values, based on consultations with C. W. Allen and A. S. King.

Table 5-5. Summary of Recent Abundance Determinations for the Sun

At. no.	Ele- ment	No. of lines	Spectral region	Curve of growth	Range of λ	Sources of obser- vations	Kind of f -value	Ref. to f -values	Q	Log N	Results of other observers	Re- marks
(1)	(2)	(3)	(4)	(5)	(6)	(7)	(8)	(9)	(10)	(11)	(12)	
3	Li	1	6708	L	0	M, U	exp	41, 11	S	0.96	1.08C, 1.26GTH, 0.93D	1, 2
4	Be	3	3321	L	2.71	M	th	4	F	2.36	2.18GTH	
6	C	24	4770-20,000	T, E	7.5-8.5	M	th	4 (28, 36)	S	8.72	8.29U, 7.56M, 9.06H	
7	N	10	7400-9000	T, E	10.3-10.6	M, U	th	4 (1)	S	7.98	8.61U, 8.09M, 9.02H	
8	O	4	5400-6500	L	10.69	M, U	exp	19	S		8.65C, 8.73U, 8.56M	
		5	7774-8496	T, E	9.1-9.5		th	4 (25)	S	8.96	9.23H, 8.20B, 8.73C-D	
		3	5700-6363		0-2		th	13	S			
11	Na	13	4500-22,000	T	2.1-3.2	M, U	th	4	S	6.30	6.33C, 6.28U, 6.56M 6.13W, 5.96S, 60R	
12	Mg	4-6	4571	T, E	0	M, U	exp	2 (7, 35)	F	7.40	7.57C, 7.51U, 8.39M	
		14	4500-16,000		4-6		th	4 (40)			7.28W, 7.60S, 7.25R	
13	Al	14	5500-16,800	T, E	3-4	M, U	th	4, 6, 43	S	6.20	6.17C, 6.33U, 6.39M 6.13W	
14	Si	56	4103	T, E	1.9	M, U	exp	4, 2	F	7.50	7.12C, 7.29U, 7.87M	
			4100-22,000		4.9-6.7	A, W	exp, th	4				
15	P	7	9790-10,700	L	7	M		4, 1	F	5.34		
16	S	22	4690-10,500	T, E	6.5-7.8	M, U, A	th	4	D	7.30	6.92U, 7.57M	
19	K	4	4040-12,500	T, Fe	0-1.6	M, U	th	6, 44 (12, 38, 15)	F	4.70	5.01C, 5.20U, 5.09M 5.32S	
20	Ca	42	4000-6800 6572	T, E	1.9-2.6	M, U	exp	31, 2	S	6.15	6.46C, 6.23U, 6.57M	
							exp	2 (ABS)	F		6.17W, 6.42GTH, 6.23S	
21	Sc	23	3900-5800	T, Fe	0-2.3	M, U, A	th	4	D	2.82	3.33U	
22	Ti	80	3900-6800	T, E	0-1.9	U, C, A	exp, rel	20, 1	S	4.68	7.56C, 4.96U, 4.57M	
23	V	85	4000-6600	T, E	0-2.4	U, C, A	exp, rel	21, 1 (32)	F	3.70	4.05U, 4.09M	
24	Cr	36	4000-5500	T, E	0.94-2.9	U, A	exp	17, 33	D	5.02	5.58U, 4.87M	p. 128
								17, 3	D	5.36*		

25	Mn	18	4000-4900	T, E	2.1-2.9	U, A, M	exp	18, 33, 3	F	4.90	5.46U
26	Fe	43	4200-5500	T, E	0-3.5	U, A, M	exp	20, 8, 5	S	6.57	7.16C, 7.26U, 6.99M 6.55W
27	Co	38	3900-5700	T, Fe	0-3.24	U, A, M	exp	23, 32, 2, 3	F	4.64	5.03U, 4.69M
28	Ni	30	5000-5900	T, E	3.6-3.9	U, A, W	exp	16, 3	S	6.15	5.95U, 6.39M
		33	4500 5700		3.5-4.1	U, A, W	th, exp	1, 3	F	6.05	
			3000-4000		0-0.4	M	exp	22, 3	S	5.49	p. 127
29	Cu	7	5100-8100	T, Fe	1.3-3.8	C, U, M	exp	5, 42 (rel), 32	S	5.04	adopted value 4.80C, 4.23U, 4.39M
30	Zn	5	4600-6400	T, Fe	4-5.8	U, M	exp	37	S	4.40	4.52C, 4.78U, 5.57M
31	Ga	2	4033-4172	T, Fe	0	M	exp	3 (4, 34)	F	2.36	
32	Ge	1	4226.6	T, Fe	0	M	th	4	D	3.29	
37	Rb	2	7800-7948	L	0	U	exp	39 (14, 4, 1)	S	2.48	
38	Sr	11	4600-7100	T, Fe	1.8-2.3	M, U	th, exp	4, 9 (34)	F	2.60*	2.88C, 3.35U
	SrII	1	4162		2.93	C, A, W	th	4		2.66	
39	Y	15	3600-6600		0-1.4	M, U, A	th	4, 1	P	2.25	3.21U
40	Zr	11	4000-4900	L	6.2-6.3	M, U, A	th	1 (4)	D	2.23	2.37U
41	Nb	6	3700-4200	L	0	M	th	1 (4)	D	1.95	
	(Cb)										
42	Mo	3	5500-5600	L	1.33	M, U	th	4 (1)	D	1.90	1.78U
44	Ru	10	3300-4000	L	0-0.4	M	th	1 (4)	D	1.43	
45	Rh	7	3400-3700	L	0-0.43	M	th	1 (4)	D	0.78	
46	Pd	8	3200-3600	L	<1.45	M	th	1 (4)	D	1.21	
47	Ag	2	3383-3281	L	0	M, U	th	4 (2)	D	0.14	
48	Cd	1	3261	L	0	M	th	30, 24	S	1.46	
49	In	1	4511	L	0	M	th, exp	34 (4, 45)	S	1.16	
50	Sn	2	3360-3801	L	0	M	exp	3	F	1.54	
51	Sb	3	3000-3300	L	0	M	th	4	D	1.94	
56	Ba	8	3800-6500	T, E	0	M	th, rel	4 (29, 27)	F	2.10	2.38C, 2.95U
70	Yb	1	3988	L	0	M, U, A	th	4	D	1.53	
82	Pb	4	3500-4100	L	1.0-2.7	M	exp	unpubl. (Allen)	S	1.33	2.55U, 1.25K

(Continued)

Table 5-5. Summary of Recent Abundance Determinations for the Sun—Continued

Col. 4:		6. L. Biermann and K. Lubeck, <i>Z. Physik</i> , 25 , 325, 1948.
L = line falls on linear part of curve of growth		7. G. Boldt, <i>Z. Physik</i> , 150 , 205, 1958.
T, E = theoretical curve calculated by Elste		8. W. W. Carter, <i>Phys. Rev.</i> , 76 , 962, 1949.
T, Fe = theoretical curve calculated by Elste for iron is fitted to the data		9. A. Eberhagen, <i>Z. Physik</i> , 143 , 392, 1955.
		10. F. B. Estabrook, <i>Ap. J.</i> , 113 , 684, 1951.
Col. 6:		11. A. Filippov, <i>Z. Physik</i> , 69 , 526, 1931.
A = C. W. Allen (1934, 1936, 1937, 1938)		12. A. H. Filippov, <i>J. Exp. Theoret. Phys. (U.S.S.R.)</i> , 3 , 520, 1933.
M = McMath-Hulbert Observatory		13. R. Garstang, <i>Monthly Notices Roy. Astron. Soc.</i> , 111 , 113, 1951.
U = Utrecht (1951)		14. G. I. Goldberg, <i>Izv. Glavn. Astr. Obs. Pulkovo</i> , 20 , no. 156, 126, 1956.
W = K. O. Wright		15. J. F. Heard, <i>Monthly Notices Roy. Astron. Soc.</i> , 94 , 458, 1934.
C = Class (1951)		16. R. L. Heid and G. H. Dieke, <i>J. Opt. Soc. Am.</i> , 44 , 402, 1954.
Col. 7:		17. A. Hill and R. B. King, <i>J. Opt. Soc. Am.</i> , 41 , 402, 1951.
exp = experimental <i>f</i> -value		18. L. Huldt and A. Lagerquist, <i>J. Opt. Soc. Am.</i> , 42 , 142, 1952.
th = theoretical <i>f</i> -value		19. G. Jurgens, <i>Z. Physik</i> , 138 , 613, 1954.
rel = relative <i>f</i> -value		20a. R. B. King (unpublished).
Col. 8: (The bracketed values were not used in the abundance determination)		20. R. B. King and A. S. King, <i>Ap. J.</i> , 87 , 24, 1938.
1. <i>f</i> -sum rule with <i>f</i> = 1		21. R. B. King, <i>Ap. J.</i> , 105 , 376, 1947.
2. C. W. Allen, <i>Monthly Notices Roy. Astron. Soc.</i> , 117 , 622, 1957.		22. R. B. King, <i>Ap. J.</i> , 108 , 87, 1948.
3. C. W. Allen and A. S. Asaad, <i>Monthly Notices Roy. Astron. Soc.</i> , 117 , 36, 1957.		23. R. B. King, B. Parnes, M. Davis, and K. Olsen, <i>J. Opt. Soc. Am.</i> , 45 , 350, 1955.
4. D. R. Bates and A. Dangaard, <i>Phil. Trans. Roy. Soc. London</i> , A242 , 101, 1949.		
5. G. D. Bell, M. N. Davis, R. B. King, and P. M. Routly, <i>Ap. J.</i> , 127 , 775, 1958.		

24. R. B. King and D. L. Stockbarger, *Ap. J.* **91**, 488, 1940.
 25. R. F. Kingsbury, *Phys. Rev.* **99**, 1846, 1955.
 26. M. Z. Khokhlov, *Izvest. Crimean Ap. Observatory*, **21**, 84 and 103, 1959.
 27. A. M. Kruithof, *Physica*, **10**, 493, 1943.
 28. H. Maecker, *Z. Physik*, **135**, 13, 1953.
 29. R. C. Mason, *Physica* **5**, 777, 1938.
 30. C. G. Matland, *Phys. Rev.* **91**, 436, 1953.
 31. K. H. Olsen, P. M. Routly, and R. B. King, *Ap. J.* **130**, 688, 1959.
 32. Yu I. Ostrovsky, 1958, thesis Leningrad. See also Yu I. Ostrovsky and N. P. Penkin, *Optika i Spektroskopiya* **5**, 345, 1958.
 33. Yu I. Ostrovsky and N. P. Penkin, *Optika i Spektroskopiya* **3**, 193, 1957.
 34. Yu I. Ostrovsky, N. P. Penkin, and L. N. Shabanova, *Izvest. Akad. Nauk S.S.S.R., Ser. 22*, No. 6, 725, 1958.
 35. W. K. Prokofjew, *Z. Physik*, **50**, 701, 1928.
 36. J. Richter, *Z. Physik*, **151**, 114, 1958.
 37. J. W. Schuttevaer and J. A. Smit, *Physica* **10**, 502, 1943.
 38. K. H. Schwarzschild, *Physica* **7**, 361, 1940.
 39. G. Stephenson, *Proc. Phys. Soc. (London)* **A64**, 458, 1951.
 40. E. Treffitz, *Z. Physik*, **26**, 240, 1949; **28**, 67, 1950.
 41. B. Trumpy, *Z. Physik*, **61**, 54, **66**, 720, 1930; *Z. Physik*, **71**, 720, 1931.
 42. H. J. van den Bold, thesis Utrecht, 1945.
 43. C. M. Varsavsky, thesis Harvard, 1958.
 44. D. Villars, *J. Opt. Soc. Am.*, **42**, 552, 1952.
 45. L. A. Weinstein, *Izv. Akad. Nauk S.S.S.R., Ser. Fiz.*, **22**, No. 6, 671, 1958.
- Col. 9. (Quality of f -value)
- S = satisfactory
- F = fair
- D = doubtful but nothing better is available
- P = poor
- Col. 11.
- C = Claas (1951)
- GTH = Greenstein and Tandberg-Hanssen (1954)
- D = E. E. Dubov (1955)
- B = I. S. Bowen (1948)
- C-D = J. Cabannes and J. Dufay
- H = J. Humaerts (1950)
- M = Menzel quoted by Goldberg and Aller (1943)
- S = B. Stromgren (1940)
- W = V. Weidemann (1955)
- U = A. Unsöld (1948)
- K = M. A. Kikhlov (1955)
- R = M. Rudkjobing (1945)

S denotes satisfactory, F = fair (not yet adequate), D = dubious and P = poor. Column 10 gives the adopted value of $\log N$ based on the scale $\log N(\text{H}) = 12.00$. We make no attempt to assign uncertainty factors to this number as in many instances we have no basis for so doing. Column 11 lists results by other observers and the last column contains some general remarks. In addition, we list for each element particular remarks pertaining to its abundance determination.

By way of illustration, let us first discuss the curve of growth for aluminum as analyzed by the model-atmosphere technique (Fig. 5-8). With the exception of the strong $\lambda 3961$ and $\lambda 3944$ resonance lines, the same lines and f -values are used as were employed in our curve-of-growth example. Elste calculated two small sections of the theoretical curve of growth which closely fitted the mean iron curve of growth. The resultant aluminum abundance of 6.20 is to be compared with our results obtained with the Schuster-Schwarzschild model.

A few general comments may be made:

1. For lines falling below about $\lambda 4000$, the effects of line blending become so serious that it is doubtful we ever see the true continuum. The line intensities have to be compared with an approximate continuum drawn through peaks of the tracings. Frequently, the lines

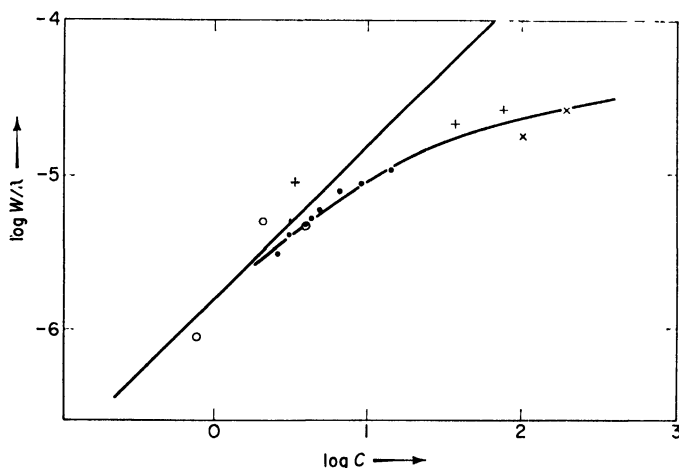


Fig. 5-8. Precise curve of growth for aluminum in the sun. (Adapted from Goldberg, Müller, and Aller, *Ap. J. Suppl.*, 45; courtesy of the University of Chicago Press, 1960.)

fall on the wings of strong lines of abundant metals and are often themselves blended with lines of comparable intensity. Furthermore, the weighting functions are difficult to determine for this region. Accordingly, a new approximation will be necessary in which the circumstances of the formation of the individual lines will have to be given.

2. With few exceptions the abundances have been derived from the lines of the neutral element. Many metals, e.g., Be, Ca, Ba, Sr, and elements such as silicon, are represented by enhanced lines for which f -values are known or could be calculated.

3. In a number of instances, particularly among metals of the iron group, only relative gf -values are known and absolute gf -values have to be found by establishing the f -value for some particular line. We may illustrate most of the difficulties encountered by taking nickel as one example, chromium as another.

There are three groups of lines for nickel: (a) low excitation lines $0 < \chi_1 < 0.4$ ev, (b) lines of intermediate excitation $3.5 < \chi_1 < 4.1$ ev, and (c) lines measured in emission by Heid and Dieke $3.6 < \chi_1 < 3.9$ ev. The lines of group *a* all fall in the ultraviolet region, $\lambda < 4000^\circ\text{K}$. Hence their intensities and theoretical interpretation are uncertain for reasons noted in paragraph 1. The relative f -values measured by King from absorption spectra are in good agreement with Allen and Asaad's f -values measured in emission and reduced to an absolute scale. For the lines of group *b*, the f -values were calculated for LS coupling with $f_T = 1.0$. Then the reduction factor was obtained by comparing these f -values with Allen and Asaad's results. The relative gf -values for the group *c* lines were obtained from measurements by Heid and Dieke (1954) of relative intensities of emission lines arising from upper levels of nearly the same excitation potential. For both groups, *b* and *c*, it was assumed that the same reduction factor held for both the $4s-4p$ and $4p-4d$ transition arrays. The equivalent widths for lines of groups *b* and *c* were reliable since they fell above $\lambda 4000$ but the group *b* lines showed a considerable scatter because LS coupling is a poor approximation, whereas the lines of groups *a* and *c* defined a good curve of growth. We obtain the abundance from each group separately. For groups *b* and *c* it is convenient to get the abundance in two steps. First we assume $f_T = 1.0$, and then we choose one or another of the absolute f -value determinations by Estabrook, or by Allen and Asaad.

Table 5-6 illustrates the process. The first two columns are self-explanatory. The third column gives the source of relative f -values and the fourth column the value of $\log n(N_1)/N(H)$ obtained by fitting the empirical curve of growth computed with $\log gf_{\text{rel}}$ to the theoretical curve. Columns 5, 6, and 7 give the reduction factors obtained by assuming the absolute f -values of Allen and Asaad, those of Estabrook, or $f_T = 1.0$. The last three columns give the absolute nickel abundances for each choice of line group and f_{absolute} .

The difficulty with nickel clearly comes from the fact that the f -values are not as accurate as we would like. For some metals the f -values appear to depend on excitation potential in such a way that we get different abundances depending on whether we reduce relative f -values to absolute f -values with the resonance lines or with lines arising from levels at 1 or 2 volts excitation potential. A particularly bad example of such a dependence is found for chromium. One possible procedure is to derive a reduction factor by assuming $f_T = 1$, and calculating by LS coupling the $\log gf$ -values for the lines of the $3d^5 4s-3d^5 4p$ transition array for which Hill and King measured relative f -values. A large discrepancy is then found to exist between the reduction factors obtained from the ground level lines, the lines arising from the levels at 1 eV, and the highly excited lines. The lines arising from the ground level are too strong to use in abundance work; yet most workers have measured absolute f -values for these lines only and one must relate the f -values for the observed lines to those for these resonance lines! Different experimenters obtain different results for the resonance lines! Thus King et al. (1958) got $\log R = -3.41$, Allen and Asaad obtained -3.67 , Ostrovsky and Penkin got -3.00 ; the sum rule $f_T = 1.0$ gives -2.53 . The lines of chromium actually used arose from levels with an excitation potential of about 1 eV; hence it would seem most reasonable to use the factors for low excited lines. Data from Ostrovsky and Penkin give $\log R = -3.42$, those from Allen and Asaad give $\log R = -3.76$!

Some comments on the individual elements are given herewith.

Hydrogen: We take $\log N = 12.00$ for this element. The continuous absorption in the sun is produced by the negative hydrogen ion whose absorption coefficient is adequately known. Since the residual intensity at any point in the wing of the line of any element depends on the ratio $l_r/\kappa(H^-)$ and $l_r \sim Nf$, we may fix the ratio element/hydrogen from the equivalent width of the line.

Table 5-6. Determination of the Abundance of Nickel

Group	χ_e	Relative f -values	$\frac{\log [N(\text{Ni})/N(\text{H})] + \text{const.}}{}$	Logarithm of reductive factor		Log $N(\text{Ni})$ (abs.)	
				Allen & Asaad ^a	Estabrook ^a $f_T = 1.0$	Allen & Asaad ^a	Estabrook ^a $f_T = 1.0$
<i>a</i>	0.0-0.4	King (1948) absorption spectra	1.50	3.99	4.66	3.35	5.49
<i>b</i>	3.5-4.1	LS coupling $f_T = 1.0$	5.50	0.55	1.22	0.00	6.05
<i>c</i>	3.6-3.9	Heid & Dieke (1954) emission	3.10	3.05	3.72	2.50	6.15
							6.82
							4.85
							5.50
							5.60

^a Adapted from Goldberg, Muller, and Aller, *Ap. J. Suppl.*, No. 45; courtesy of the University of Chicago Press.

References

Allen, C. W., and A. S. Asaad, *Monthly Notices Roy. Astron. Soc.*, 117, 36, 1957.
Estabrook, F. B., *Ap. J.* 113, 684, 1951.
Heid, R. L. and G. H. Dieke, *J. Opt. Soc. Am.*, 44, 402, 1954.
King, R. B., *Ap. J.* 108, 87, 1948.

Helium: The $\lambda 10830$ line which is of chromospheric origin appears occasionally in absorption on the disk. Unsöld attempted to establish the H/He ratio from the spectra of prominences, but the physical state of the chromosphere and of prominences is not yet sufficiently well understood to permit abundance determinations. Deviations from thermodynamic equilibrium are severe. Eventually, it should be possible to determine the helium abundance in the sun.

Lithium and beryllium: Improved observational data for these elements have been obtained at the McMath-Hulbert Observatory and are being analyzed by more elaborate methods (see page 138). Urgently needed are measurements of f -values for both BeI and BeII lines. Both of these elements are extremely important for assessing the structure of the hydrogen convection zone in the sun.

Boron: As previously mentioned this element is observed only in the compound BII and should be reinvestigated. The old estimate by Russell is much too high, and no new analyses are available. This element also is of interest in connection with the problem of the structure of the solar hydrogen convection zone.

Carbon: Note that only lines coming from high levels are involved. The experimental f -values measured by Maecker (1953) are in good agreement with those obtained recently by Foster in London, but are not in good accord with the measurements by Richter.

Nitrogen: No experimental f -values are available. For this element Mugglestone compared the predictions of methods based on weighting functions with a method he calls the Planckian-gradient method, which he considers the more reliable. Actually, differences between the two methods tend to be masked by uncertainties in f -values. With three different model atmospheres he got nitrogen abundances of 7.71, 7.81, and 7.93 (by his method) as compared with 7.94, 8.04, and 8.23 from the weighting-function method.

Oxygen: Jurgens (1954) at Kiel obtained f -values in good agreement with theoretical values computed by the Bates-Damgaard tables. Kingsbury (1955), who used self-consistent field wave functions and configuration interactions, got strengths larger than those computed by the Bates-Damgaard tables. The $\lambda\lambda 5577, 6300, 6363$ lines represent forbidden transitions. Notice the wide range of excitation potentials.

Sodium: The resonance lines are too strong so transitions arising from higher levels are employed. A number of Russian workers have

calculated A -values for some of these high-level transitions; the resultant f -values do not agree with those found by the Bates-Damgaard tables.

Magnesium: Except for the low-level intercombination line $\lambda 4571$, all of the lines arise from high levels. Relative f -values have been measured for a few lines. The f -value for the intercombination line is uncertain. Boldt's (1958) result is 2.5 times larger than Allen's result, Prokofjew's result is about the same as Allen's, whereas the relative value by Kersten and Ornstein reduced to Treffitz's absolute scale is smaller than Allen's by a factor of 1.6.

Aluminum: (See page 126 and Fig. 5.8.)

Silicon: Equivalent widths by C. W. Allen, K. O. Wright, and the Utrecht and Michigan groups are in good agreement. The experimental f -values were measured by Allen and Asaad and by Lochte-Holtgreven, and the results are not in good accord with the theoretical predictions. The curve of growth shows a considerable scatter indicating that the f -values are unreliable. Unfortunately, the strategic $\lambda 3905$ and $\lambda 4103$ lines are difficult to observe in King's method because the lines fall at 1.90 ev. Silicon is too active to use in an atomic beam; the resonance lines fall in the far ultraviolet where a suitably bright continuum is hard to produce. The lines of SiI and SiII follow different curves of growth. The SiII lines were not used in the Michigan work. An improvement in the f -values is necessary.

Phosphorus and sulfur: All lines arise from high-energy levels; their f -values have to be calculated by the Bates-Damgaard tables.

Potassium: Since the resonance lines are too strong it is necessary to use faint subordinate lines. Unfortunately, experimental f -value determinations are in disaccord with the theoretical f -values and with one another. Possibly the best values are those obtained by Villars and by Biermann and Lubeck. The lines of K, Rb, and several other elements tend to be formed in the uppermost part of the solar atmospheres, where all atmospheric models become uncertain.

Calcium: The relative gf -values measured by Olsen et al., provide a well-defined curve of growth. These relative values are reduced to an absolute scale, first by adopting an experimental value of the ratio f_{4226}/f_{8572} where $\lambda 6572$ is an intercombination line, $\lambda 4226$ is the resonance line, and then taking $f_{4226} = 1.66$ (Allen 1957). Unfortunately, the theoretical and experimental f -values for $\lambda 4226$ dis-

agree with one another, ranging from 1.12 from one spectrum of copper alloy bars to 2.31 from determinations of the lifetime of the upper level. (See Goldberg, Müller, Aller 1960, Table 49.)

Scandium: The relative f -values measured by Ostrovsky (1958) did not define a curve of growth; new f -value measurements are needed, but this element is difficult to obtain in a pure form. It could be measured in a copper alloy arc.

Titanium: Relative f -values have been given by the Kings and by Ostrovsky, who appears to get f -values for high excitation lines that are too large. Probably this is a temperature effect. The reduction factor is obtained by invoking the sum rule $f_T = 1.0$ to derive the factor 6.6×10^{-4} by which King's relative f -values are to be multiplied to get absolute f -values. (Allen has suggested a conversion factor of 6×10^{-4} .) The determination of absolute f -values for titanium is difficult because the ground level is complex and the individual f -values are small.

Vanadium: No absolute f -values have been given, although Ostrovsky's and King's experimental relative f -values are in good agreement. These relative f -values were reduced to absolute values on the assumption $f_T = 1.0$ for the $3d^4 4s-3d^4 4p$ transition array by the same method as has been described for Cr. A plot of the theoretical $\log gf$ -values vs. the $\log gf_{ie1}$ by King shows marked breakdown of LS coupling; the $a^6D-z^6P^0$ transitions give a reduction factor $\log R = +3.20$, whereas the $a^6D-y^6F^0$ and $a^6D-y^6D^0$ give a log reduction factor $+3.70$. A mean log reduction factor $+3.45$ was adopted, although Allen suggests $+3.70$ as a better value, in which event an abundance of $\log N = 3.95$ is obtained. Absolute f -values are urgently needed for vanadium, which should be a more tractable metal than titanium. The observed points define a good curve of growth that follows the mean iron curve of growth with little scatter.

Chromium: (See page 128.) The abundance is extremely uncertain because of the poor f -values. One obtains $\log N = 5.02$ with Ostrovsky and Penkin's data, 5.36 from the Allen-Asaad data.

Manganese: The $\log gf_{abs}$ values measured by several teams for the lines of the resonance a^6S-z^6P multiplet are in good agreement. Only those lines whose f -values were measured by Allen and Asaad were utilized. The lines arising from the higher excitation potential give a well-defined curve of growth, which yields the tabulated abundance. One suspects that the f -values for the lower lines may be in error by a factor of 2.

Iron: The theoretical curve of growth was calculated for several excitation potentials and wavelength regions. Reliable relative and absolute f -values have been determined, the results for the 3720 and 3737 resonance lines as measured by different investigators are in excellent agreement. Hence the abundance of iron should be fixed within about 20 per cent, within the framework of our model-atmosphere and theoretical assumptions.

Cobalt: The relative f -values by King's group are in good agreement with those obtained by Ostrovsky, while absolute f -values have been obtained by Allen and Asaad. This element is far from LS coupling. Recently, King and his associates have obtained a lower limit to the f -value for $\lambda 3527$, whence an upper limit to the abundance of cobalt is obtained.

Nickel: (See page 127.)

Copper: The relative f -values by van den Bold are reduced to the absolute scale by measurements by Bell et al., (1958). The absolute f -values appear to be reliable, the uncertainty lying in the available relative f -values. The use of Ostrovsky's f -values would reduce the copper abundance to 4.67.

Zinc: The f -values appear reliable, the lines appear to fit the standard iron curve of growth very well. The resonance lines fall in the ultraviolet.

Gallium: The abundance of this element depends essentially on only one line, $\lambda 4172$, for which the f -value is not accurately known, although it could be measured in the atomic beam. If Ostrovsky's f -values are used instead of Allen's, the abundance is 2.54, while the f -values computed from the Bates and Damgaard tables would give 2.89.

Germanium: Only the one line, $\lambda 4226.57$, which falls near the center of the strong CaI $\lambda 4226.74$ line was used in the abundance determination. The f -value is uncertain, although improved calculations are possible.

Rubidium: The different f -value determinations are all in excellent agreement, but the solar lines are very weak and are affected by blends.

Strontium: The f -values have been measured by a number of observers, among which the results of Ostrovsky who got $f(\lambda 4607) = 1.5$ are probably as good as any. There is a large discordance between abundances obtained for the high-level lines and those found from the resonance $\lambda 4607$ line. Hence the final abundance rests on the

$\lambda 4607$ line for which the Bates-Damgaard approximation gives 2.53 and Ostrovsky's values give 2.61. The SrII line gives 2.66 with the Bates-Damgaard approximation.

Yttrium: If the f -values are computed from the Bates and Damgaard tables the abundances derived from the 0 and 1.40 ev lines are $\log N = 1.40$ and 3.10, respectively. These f -values could be measured by some experimental technique such as the atomic beam; the calculated values are worthless.

Zirconium: The spectrum of this refractory metal is difficult to produce in the furnace and absolute f -values cannot be measured in the atomic beam method. Transition probabilities by LS coupling and the Bates and Damgaard tables are unreliable.

Columbium (niobium), ruthenium, rhodium, and palladium: The lines of these elements are faint, frequently blended with lines of other elements, and usually fall on the linear part of the curve of growth. The f -values were all calculated by the f -sum rule and only lines involving single electron jumps were used. The Bates-Damgaard tables give f -values about 10 to 30 per cent smaller for Ru, Rh, and Pd than the f -sum rule.

Molybdenum: The f -values calculated from the f -sum rule are about 20 per cent larger than those from the Bates-Damgaard tables. The result is uncertain.

Silver: The two blended resonance lines fall in the far ultraviolet; their intensities are uncertain. The f -values are taken from the Bates-Damgaard tables; the values measured by Allen are too high.

Cadmium: The only line observed in the solar spectrum is the faint resonance intercombination line $\lambda 3261.05$. The f -values are accurately known; the uncertainty here lies in the basic solar data.

Indium: The resonance $\lambda 4511$ appears as a faint but essentially unblended line whose intensity as measured at Michigan is about three times greater than the value measured at Utrecht. The adopted f -value due to Ostrovsky appears to be reliable.

Tin: The two faint lines observed in the solar spectrum fall in a heavily blended ultraviolet region. The Allen f -values may be too high, but it might be possible to compute the f -values for these intercombination lines by theory.

Antimony: The ultraviolet lines fall in a crowded region and both intensities and f -values are uncertain.

Barium: Barium is observed only as BaII. Relative f -values have

been measured by several experimenters but no absolute f -values have been determined. Several faint lines are observed in the solar spectrum.

Ytterbium: The resonance $\lambda 3988$ line is unblended and forms the basis for the abundance determination wherein the validity of the Bates-Damgaard tables is assumed. Actually, this metal probably shows strong deviations from LS coupling so that the derived abundance is very uncertain.

Lead: The intensities of some of the lines are uncertain but $\lambda 3683$ is virtually unblended. Transition probabilities by Allen and by M. Z. Khokhlov are in good agreement. The f -sum rule and the Bates and Damgaard tables give uncertain results since this element departs so far from LS coupling. Nevertheless, quantum mechanical calculations may be carried out for these lead lines. The results obtained so far indicate a closer agreement with the approximate theoretical calculations, i.e., lower f -values and hence a higher lead abundance!

5-10. Deviations from Thermodynamic Equilibrium and Other Complications

In the preceding analyses it has been assumed that one can calculate the populations in various levels and stages of ionization by the Boltzmann and Saha equations, using the local temperature at each point. Pecker (1957) has suggested that there may exist large differences between the gas kinetic temperature on the one hand, and the excitation temperature on the other. Consequently, the method of abundance determinations has to be revised by using a different weighting function. He employs an iteration procedure based on the central intensities of the lines. The deviations from local thermodynamic equilibrium are most severe for the lower levels. Upon applying these methods to titanium, Kandel concluded that the abundance of titanium had to be revised upward by an order of magnitude. On the other hand, Miss Müller, using the Michigan model solar atmosphere rather than the Claas atmosphere employed by Pecker's group, found no significant differences between the abundances derived from low and high excitation lines. She concluded that Pecker's results depended largely on the atmospheric model and that, "Within the accuracy of our knowledge of the equivalent widths, atmospheric models, and f -values, the procedure used in the Michi-

gan analysis is adequate to yield a mean abundance for each element in the solar and stellar atmosphere."

Deviations from local thermodynamic equilibrium are closely related to the problem of "interlocking." That is, a given energy level (c) may be fed by excitation from the ground level (a) to a higher level (b) with subsequent cascade ($b \rightarrow c$) in such a way that the number of transitions ($b \rightarrow c$) greatly exceeds the number of transitions ($c \rightarrow b$). Hence there is no longer any detailed balancing and thermodynamic equilibrium does not exist. (See Woolley and Stibbs 1953, p. 152.) Such effects certainly occur in the extended atmospheres of stars; their importance in the sun is not clearly established.

Strong resonance lines in the solar spectrum may be formed predominantly by the mechanism of "scattering," i.e., each quantum that is absorbed is forthwith re-emitted and the temperature plays no role other than in the establishment of the level of ionization. The problem of line formation could be handled for this situation were it not for the additional complication that the scattering is not strictly coherent. That is, a quantum taken up at one point in the line profile is re-emitted in another. In practice, quanta absorbed in line wings may be re-emitted near the line center. (See Woolley and Stibbs 1953; Unsöld 1955.) Scattering can play no important role for lines involving highly excited levels, for which any deviations from thermodynamic equilibrium are likely to be much smaller.

Deviations from thermodynamic equilibrium must certainly exist in the upper atmosphere of the sun. Studies of center-limb variations of certain solar lines by K. H. Böhm and by Miss Bretz show that such deviations can affect intensities of moderately strong lines. Whether large revisions in the abundances derived from weak lines will be required is open to question. Nevertheless, the question of deviations from thermodynamic equilibrium will have to be taken into account in refined work, but the subject cannot be adequately pursued until accurate f -values have been obtained, and accurate model atmospheres established.

5-11. Diffusion

Another complication lies not in the determination of solar abundances but in their interpretation. We observe the composition of the outermost layers of the sun and we tacitly assume that this composition is that of the primordial solar system, except, of course, for

such elements as boron, beryllium, and lithium that have been affected by nuclear reactions occurring at temperatures of the order of 100,000 or 1,000,000°K. The outer part of the sun is in convective equilibrium, i.e., the material is constantly being recirculated and churned up in this region, so that it is kept chemically homogeneous. The inner region, whose radius is about 80 per cent of that of the sun, is in radiative equilibrium. Under the influence of the temperature gradient and density gradients in the sun, heavy atoms tend to diffuse across the boundary of the convection zone into the interior, never to reappear at the surface of the sun. The rate of diffusion depends on the mass and charge of the ion. It is greater for iron than for silicon and greater for lead than for iron. The exact calculation of the rate of loss by thermal and gravitational diffusion is difficult partly because the appropriate coefficients for different mixtures of gases are not well established. A much more serious source of uncertainty is that the extent and structure of the solar convection zone throughout the last 4.5×10^9 yr is not known. Preliminary calculations (Chapman and Aller 1960) indicate that this effect has to be taken into account in the most exact work. The problem is important since we must know if the seemingly small abundance of lead in the solar surface layers is characteristic of primordial solar material or partly an effect of diffusion. An empirical test would be found by comparing the lead/gold ratio in the sun, since these two elements would diffuse downward at nearly the same rate. Let D denote the factor by which the derived abundance ratio Fe/Si or Pb/Si has to be multiplied in order to allow for the effects of depletion by diffusion from the solar convection zone. If the time interval is 4.5×10^9 years since the sun was formed, D depends on the depth, H , of the convection zone as shown in Table 5-7.

If the zone is as shallow as is indicated in Weymann's solar model

Table 5-7. Correction Factors for Diffusion*

Relative depth of convection zone	H/R	0.30	0.20	0.14
Element ratios by number	Fe/Si	1.07	1.05	1.19
of atoms	Pb/Si	1.19	1.27	1.54

* Reproduced from *Ap. J.*, 132, 469, 1960; courtesy of the University of Chicago Press.

(1957), the corrections for diffusion can become significant. On the other hand, if the depth of the zone is greater as would be suggested by the depletion of lithium due to thermonuclear destruction, the effect of diffusion is masked by the observational errors.

5-12. Improvements in the Basic Data and Their Interpretation

Because of the magnitude of the task involved, the Michigan abundance program necessarily entailed the systematic treatment of large quantities of data in a uniform manner. It was not possible to handle lines of particular elements on an individual basis. Substantial improvements in the basic solar data may be obtained from a consideration of the circumstances peculiar to the formation of each line, particularly the blending. In the ultraviolet where so many important lines of strategic elements are found, the blending and over-all lowering of the continuous background is produced largely by far wings of strong metallic lines. One must therefore include the "continuous" absorption produced by wings of strong lines in calculating theoretical intensities of weak ones, as well as allowing for the obvious blends. Furthermore, instead of measuring the equivalent width only at the center of the sun, observations are made as close as possible to the limb and at several other points on the disk. In this way a valuable check is obtained on the assumed atmospheric stratification.

Accordingly, a new program has been undertaken at Michigan for studies of elements such as lithium and beryllium, gallium, germanium, zirconium, palladium, rhodium, ruthenium, silver, indium, gold, ytterbium, and lead. Lithium and beryllium solar abundances will give important clues to the structure of the convection zone of the sun. Gallium, germanium, zirconium, palladium, rhodium, ruthenium, and silver are of geochemical interest. The lead/gold ratio is a datum of considerable interest in theories of nucleogenesis since it is virtually independent of any possible diffusion effects that might lower the lead/iron ratio.

Another improvement in the picture can be obtained by using the lines of ions, e.g., ScII, TiII, CrII, and FeII, which appear with great strength in the spectra of the sun and similar stars. Here the difficulty lies in securing adequate data on the f -values which are extremely difficult to measure for ions. Possibly shock tubes or cer-

tain stabilized arcs can be used for problems of this type, and f -values for some ions can be done by theory.

An extension of the solar spectrum to the far ultraviolet by observations secured above the earth's atmosphere may provide data for some of the elements whose lines are missing from the ordinary spectral regions, e.g., neon. Furthermore, such studies are likely to lead to a much better understanding of the upper part of the photosphere and of the chromosphere. The pioneering researches so far carried out have indicated the general nature of the solar spectrum in this region, but it has not been possible so far to employ adequate spectral resolution. It is certain that beyond $\lambda 3000$ we never see the true continuous spectrum of the sun. The lines overlap so closely upon one another that only their cores are observed, the wings being lost in general confusion. Hence, it will become very difficult to study the necessarily weak lines of rare elements. Molecular absorption also appears to add to the general background of absorption. Some elements will be represented by chromospheric emission lines, whose intensities can be interpreted in terms of abundances when the detailed structure of the chromosphere is understood.

To date, the opportunities offered by the already observable solar spectrum have not been fully exploited. Band spectra of molecules have been inadequately studied from the point of view of abundance problems. Hunaert's investigations have been mentioned. Newkirk's (1957) study of CO has shown the extreme sensitivity of the results to the structure of the uppermost layers of the solar atmosphere and to the dissociation potential of the molecule. As improved data become available for the dissociation potentials and f -values of molecules, an increasingly greater use can be made of band spectra for abundance determinations. Fluorine and boron are two elements whose abundances can be deduced from their hydrides. The latter is particularly important in connection with the problem of the solar convection zone.

Finally, the use of sunspot spectra can yield some extremely important information. Because sunspots are cooler than the photosphere, lines of easily ionized rare elements, such as rubidium and indium, appear in their spectra with higher intensities. Hence more reliable abundance determinations may be made from sunspots than from disk data. Many more molecular bands appear in the spectra of spots than in those of the photosphere and numerous weak

lines have not yet been identified. There are a number of technical difficulties to be overcome. Because of the sunspot magnetic fields, the lines suffer a Zeeman broadening which differs from line to line in a known but sometimes complicated way. Much more troublesome is the problem of observing a spectrum of a spot freed from the scattered light of the nearby photosphere.

In conclusion, one may expect that solar abundances will be greatly refined during the course of the next few years as the basic observational data are improved, the fundamental physical parameters, such as f -values and damping constants, are accurately determined, and the fundamental theoretical aspects of the problem are better understood.

Eventually, our knowledge of the primordial composition of the solar system may be established most securely from data secured by space probes sent to the outer parts of the solar system where the temperature is so low that the principal volatile constituents have not all been lost. Perhaps even the nearer members of the solar system, such as the moon, may yield information on the non-volatile constituents (Urey 1958).

Selected References

- Allen, C. W., *Mem. Com. Sol. Obs. Canberra*, No. 5, 1934. *Ap. J.* **85**, 165, 1937.
Mem. Com. Sol. Obs. Canberra, No. 6, 1938a; *Ap. J.*, **88**, 125, 1938b; *Monthly Notices Roy. Astron. Soc.*, **117**, 622, 1957.
- Aller, L. H., *Ap. J.*, **104**, 347, 1946; *Ap. J.*, **109**, 244, 1949; *Atmospheres of the Sun and Stars*, Ronald, New York, 1953; *Ap. J.*, **123**, 133, 1956.
- Aller, L. H., G. Elste, and J. Jugaku, *Ap. J. Suppl.*, **3**, No. 25, 1, 1957.
- Aller, L. H., and J. Jugaku, *Ap. J. Suppl.*, **4**, No. 38, 109, 1939.
- Bates, D., and A. Damgaard, *Phil. Trans. Roy. Soc. London*, **A242**, 101, 1949.
- Böhm, K. H., *Z. Astrophys.*, **11**, 182, 1954.
- Bowen, I. S., *Publ. Astron. Soc. Pacific*, **60**, 16, 1948.
- Cabannes, J., and J. Dufay, *Compt. rend.*, **226**, 1569, 1948.
- Cayrel, R., Unpublished thesis, University of Paris, 1956.
- Chandrasekhar, S., *Ap. J.*, **104**, 444, 1946.
- Chapman, S., and L. H. Aller, *Ap. J.*, **132**, 461, 1959.
- Claas, W. J., *Utrecht Researches* **12**, Part 1, 1951.
- Dubov, D. E., *Astron. Zhur.*, **159**, 11, 1955.
- Elste, G., *Z. Astrophys.*, **37**, 201, 1955.
- Goldberg, L., E. Müller, and L. H. Aller, *Ap. J. Suppl.*, **5**, No. 45, 1960.
- Goldberg, L. G., *Ap. J.*, **82**, 1, 1935; *Ap. J.*, **84**, 12, 1936.
- Greenstein, J. L., and Richardson, *Ap. J.*, **113**, 536, 1951.
- Greenstein, J. L., and E. Tandberg Hanssen, *Ap. J.*, **119**, 113, 1954.

- Harris, D., *Ap. J.*, **108**, 114, 1948.
- Hjerting, F., *Ap. J.*, **88**, 508, 1938.
- Hunaerts, J., *Trans. Int. Astron. Union*, **7**, 462, 1950.
- Hunger, K., *Z. Astrophys.* **36**, 42, 1955.
- King, R. B., *Indiana Conference on Stellar Atmospheres*, M. Wrubel, ed., 1954.
- King, R. B., P. Routly, G. Bell, and Davis, *Ap. J.*, **127**, 775, 1958.
- Kolb, A. C., and H. Griem, *Phys. Rev.*, **111**, 514, 1958.
- Kopfermann, H., and G. Wessel, *Z. Physik*, **130**, 100, 1951.
- Lochte-Holtgreven, W., *Observatory*, **72**, 142, 1952.
- McDonald, J. K., *Publ. Dominion Astrophys. Observatory, Victoria, B. C.*, **9**, 269, 1953.
- Menzel, D. H., *Ap. J.*, **84**, 462, 1936.
- Minnaert, H., *The Sun*, G. P. Kuiper, ed., University of Chicago Press, Chicago, 1953.
- Mohler, O. C., *A Table of Solar Spectrum Wavelengths*, University of Michigan Press, Ann Arbor, 1955.
- Moore, C. E., *The Sun*, G. P. Kuiper, ed., University of Chicago Press, Chicago, 1953, p. 186.
- Mugglestone, D., *Monthly Notices Roy. Astron. Soc.*, **118**, 432, 1958.
- Newkirk, G., *Ap. J.*, **125**, 571, 1957.
- Pecker, J. C., *Ann. d'Ap.*, **14**, 383, 1951. *Compt. rend.*, **245**, 639, 1957.
- "Photometric Catalogue of Fraunhofer Lines $\lambda\lambda 6600-8770$," *Utrecht Observatory Researches*, **12**, part 2, 1951.
- Rohrlich, F., *Ap. J.*, **129**, 441, 1959.
- Rudkjöbing, M., *Publ. Copenhagen Observatory*, No. 140.
- Russell, H. N., *Ap. J.*, **70**, 11, 1929.
- Stromgren, B., *Festschr. Eli, Stromgren*, Munksgaard, Copenhagen, 1940.
- Traving, G., *Z. Astrophys.* **36**, 1, 1955; *Z. Astrophys.* **41**, 215, 1957.
- Underhill, A. B., *Publ. Dominion Astrophys. Observatory, Victoria, B. C.*, **8**, 357, 1957.
- Unsold, A., *Physik der Sternatmosphären*, Springer, Berlin, 1938, 1955; *Z. Astrophys.*, **24**, 306, 1948.
- Urey, H. C., *Z. Physik. Chem.*, **16**, 346, 1958.
- Voigt, H. H., *Z. Astrophys.*, **31**, 48, 1952.
- Weidemann, V., *Z. Astrophys.*, **36**, 101, 1955.
- Weymann, R., *Ap. J.*, **126**, 208, 1957.
- White, H. E., *Introduction to Atomic Spectra*, McGraw-Hill, New York, 1934, p. 439.
- Woolley, R. v., and D. W. N. Stibbs, *The Outer Layers of a Star*, Oxford, New York, 1953.
- Wrubel, M., *Ap. J.*, **109**, 66, 1949; *Ap. J.*, **111**, 157, 1950.

Abundances from Cosmic Rays

6-1. Introduction

The origin and nature of cosmic rays is one of the most fascinating problems in astrophysics. Extensive research programs have been devoted to studies of the charge distribution, i.e. the relative proportions of nuclei of different Z , and to a determination of the energy spectrum (i.e., the number as a function of energy) of the primaries. Cosmic-ray particles observed at the surface of the earth, protons, neutrons, mesons, and high-energy electrons are secondaries produced by the impact of high-energy particles on air molecules. To observe the primaries themselves it is necessary to go to very high altitudes. Reliable determinations of relative primary abundances would appear to require measurements at points where the mass of the overlying atmosphere amounted to less than 10 g/cm^2 .

Early balloon work (Schein, Jesse, and Wollan 1941) indicated most primaries were protons. As early as 1939 Alfvén had suggested primaries might also contain heavier ions, but it was not until 1948 that the Minnesota and Rochester groups (Freier, Lofgren, and Oppenheimer; Bradt and Peters) detected massive high-energy particles. Since then, many investigations by numerous experimenters have been devoted to a study of these particles.

Primary cosmic rays are studied experimentally by special nuclear emulsions, Geiger counters, Cerenkov radiation detectors, proportional counters, scintillation counters, ion chambers, and cloud chambers. The resulting counts and particle tracks have to be analyzed to determine the energies, masses, and charges of the impinging particles. Cosmic-ray studies have been greatly aided by the development of balloons capable of lifting adequate amounts of experimental equipment to great heights in the atmosphere, and by the development of chemical techniques for the isolation and detection of minute traces of radioactive isotopes produced by cosmic rays. We shall not

attempt to describe any of these specialized, sensitive, and delicate techniques here; reference must be made to the particular literature.

The experimental techniques and interpretation of results obtained are extremely difficult. Even at the greatest heights reached by the balloons, there still remain several grams of air above each square centimeter. The correction of the counts to what they would have been above the atmosphere entails a tricky extrapolation and in the past this step has produced some marked discordances among results of different observers. One must recognize and eliminate from the analysis effects of showers, i.e. spallation effects produced in the atmosphere and the apparatus itself. In both emulsion and counter techniques it is difficult to identify uniquely the charges on all incoming particles. Further one must allow for the effects of events that occur during the ascent and descent of the apparatus. Finally, temporal fluctuations and such things as solar activity must be taken into account.

One great difficulty is the inability to measure proton fluxes well, in spite of the fact that protons are more numerous than any other cosmic-ray primary particle. Part of the trouble is that protons are often produced as secondaries in spallation processes and in order to separate primaries from secondaries one must measure penetration power, ionization, direction of motion, and velocity. Various workers have attempted to measure the upward flux of scattered and secondary protons. Eventually the proton flux may be measured at great distances from the earth with the aid of appropriate counters carried in satellites.

6-2. The Energy Spectrum

Before turning to the results obtained for the distribution of primaries with Z , let us briefly consider the energy spectrum. Except following the great February 23, 1956 flare, the primary flux does not change with time. This flux is probably isotropic, although Engler, Kaplon, and Klarmann (1958) concluded that it might be unsafe to infer the spatial and angular distribution of cosmic rays in the galaxy from measurements within the solar system. In other words, we cannot necessarily infer from our measurements the galactic cosmic-ray field.

Thus, certain difficulties stem from the fact that cosmic rays are charged particles and therefore are deflected by magnetic fields in the galaxy, in the solar system, and in the neighborhood of the earth itself.

The terrestrial magnetic field acts as a charge and momentum analyzer—it deflects charged ions, allowing only those to hit the atmosphere whose momentum is in excess of a certain critical value. A particle's cut-off energy (below which it cannot reach the earth) depends on its charge and the magnetic latitude at which it approaches the earth. The energy required for penetration increases from around 3 Bev for protons at high magnetic latitudes to about 15 Bev near the equator.

At the lowest energies (< 0.5 Bev/nucleon) one may infer the energy from the range, or from measurements of multiple scattering in a nuclear emulsion ($0.5 < E < 3$ Bev/nucleon). Above 15 Bev, the primary energies are evaluated from nuclear interactions, notably cosmic-ray *showers*. Primaries of the very highest energy (above 10,000 Bev/nucleon) are extremely rare but produce showers that can be detected over a large area of the earth's surface—primaries with energies up to a billion Bev have been observed in this way. Such particles are of special interest; they provide difficulties in any mechanism for cosmic-ray origin.

Electrons also may exist in the primary cosmic rays but so far they have not been detected. For a given energy they must be less than 1 per cent of the proton flux. Their presence in the primaries is confidently predicted by some on the basis of theories of cosmic rays.

The total flux of primary cosmic rays with energies greater than 0.5 Bev/nucleon is 4000 nucleons $\text{m}^2\text{-sec-sr.}$ and their average energy is 3.6 Bev/nucleon. Excluding rest mass, the cosmic-ray energy density is about 10^{-12} ergs/ cm^3 as compared with 8×10^{-13} ergs/ cm^3 for stellar radiation (Peters, 1959). Further, the energy spectrum which extends from 0.5 Bev to about 10^9 Bev, appears to be the same for nuclei of different elements. It is given by a power law with an exponent -1.5 .

6-3. The Charge Distribution Spectrum

A great effort has been expended in establishing the flux of primary cosmic rays above the earth's atmosphere. The proton flux entails a number of difficulties but that of helium is much more easily measured. For nuclei, $Z \geq 3$, especially lithium, beryllium, and boron, marked disagreements existed. The discordances arose, not so much from the measurements themselves as from the method of extrapolation to the top of the earth's atmosphere. Thus, the Bombay group (Appo Rao et al., 1958), on the basis of their method of extrapolation, concluded

that Li, Be, and B represent but a small fraction of the flux of heavy primaries. The Rochester (Noon and Kaplon 1955; Engler, Kaplon, and Klarmann 1958) and Bristol (Waddington 1957; 1958) groups arrived at a different interpretation. Results of a very high-altitude balloon flight (Freier, Ney, and Waddington 1959) justified the Bristol type of extrapolation and seemed to establish a relatively high abundance of Li, Be, and B. In addition to these results, we must mention the papers presented at the Varenna conference (1958) and studies by the groups at Chicago (Schein et al., 1958; Lohrmann and Teucher 1959), Turin (Cester et al., 1958), and Bristol (McDonald and Webber 1959). Lohrmann and Teucher (1959), for example, show that the extrapolation parameters are insensitive to the energies of the incoming particles.

Most investigators have simply grouped the elements as follows:

$$p, \alpha, L(3 \leq Z \leq 5), M(6 < Z < 9), H(10 \leq Z)$$

and sometimes the heavy group is further divided into

$$H(10 \leq Z \leq 19) \text{ and } HV(20 < Z)$$

Yates regards any additional subdivision as probably premature. Among larger values of Z , the results are often quoted as ± 2 . Measurements of heavy-element flux with high-charge resolution have also been reported by K. Kristiansson, O. Mathiesen, and B. Waldegskog. An investigator may more easily distinguish between B and C, than between Ti and V.

Table 6-1 shows the ratios of L 's and H 's to M as determined recently by different observers. Most of the results are in good accord; the Bombay results differ essentially because of the different method

Table 6-1. Ratios of L , M , and H Groups of Cosmic Rays

Observers	L/M	H/M
Freier, Ney, Waddington (1958)	0.37 \pm 0.06	0.33 \pm 0.06
Cester et al. (1958)	0.30 \pm 0.09	0.31 \pm 0.11
Schein, Schultz, Koshiba (1958)	0.32 \pm 0.07	0.48 \pm 0.10
Shapiro, Stiller, Obell (1958)	0.37 \pm 0.07	0.41 \pm 0.06
Waddington (1958)		0.37 \pm 0.10
Engler, Kaplon, Klarmann (1959)	0.30 \pm 0.06	0.39 \pm 0.07
Appo Rao et al. (1958)	0.073 \pm 0.08	0.29 \pm 0.05

Table 6-2. Relative Abundances of C, N, and O in Cosmic Rays

Observer	C	N	O
Schein et al., (1958)	1.6	1.1	1.0
Aizu et al., (1959)	2.4	1.3	1.0
Peters (1959)	1.0	0.63	1.0
Singer (1958)	1.5	1.0	1.0
Solar system (Chap. 8)	0.45	0.12	1.0

of extrapolation employed. Some observers have measured the relative proportions of carbon nitrogen and oxygen. Thus we quote the following comparisons (see Table 6-2). Aizu et al., (1960) have tabulated abundances for heavier elements in cosmic rays.

6-4. Suggested Abundances in Cosmic Rays

Table 6-3 gives our suggested abundances as based on results by different observers. The H/He ratio is essentially that proposed by

Table 6-3. Suggested Nuclear Abundances of Cosmic-Ray Groups Relative to Oxygen

Element	CR abundance	Solar system abundance
H	500	1100
He	40	180
Li	0.5	0.0000035
Be	0.3	0.0000007
B	0.5	0.0000008
C	1.5	0.45
N	1.2	0.12
O	1.0	1.0
F	0.06	10^{-3}
Ne	0.16	0.55
Na	0.02	0.0022
Mg	0.32	0.028
Al	0.08	0.0018
Si	0.16	0.035
15 < Z < 20	0.34	
21 < Z < 28	0.22	

Peters (1959). For all other elements, we have used the *L*, *M*, and *H* groups. The relative proportions of the *L* elements are uncertain, but we have adopted for purposes of illustration essentially the ratios proposed by Waddington (1957). The relative proportions of C, N, and O are adopted from Table 6-2 while the proportions of the "heavy" elements are taken from compilations of Aizu et al., (1960). The relative fractions of the *L*, *M*, and *H* groups are adapted from the data of Table 6-1 and are certainly much more reliable than the individual tabulated values. Peters (1959) has proposed the ratios given in Table 6-4. The chief difference between Peters' compilation and our own is in the Li, Be, B contributions. The last row of our Table 6-3 gives the solar-system abundances for elements prominent in cosmic rays. A number of comparisons are to be noted.

Table 6-4. Relative Abundances of the Most Common Constituents of Cosmic Rays^a

H	He	Li, Be, B	C	N	O	$10 < Z < 30$	$Z > 30$
530	37	0.18	1.0	0.63	1.0	0.63	0.001

^a Adapted from B. Peters, 1959.

1. Most medium and heavy nuclei ($7 > 6$) are an order of magnitude more abundant in the cosmic rays than in the sun and similar stars. A few elements such as neon may be more abundant in the stars than in cosmic rays, but the charges of the heavier particles cannot be established accurately enough to assert this unequivocally.

2. The ratio C/N/O is almost certainly different in cosmic rays than in the sun and similar stars. Fluorine is much more abundant in cosmic rays than in stars.

3. Lithium, beryllium, and boron are intrinsically rare in the universe, but are prominent in cosmic rays.

In summary, there exist substantial differences between the compositions of primaries and typical stars such as the sun. From these differences it should be possible to draw certain conclusions concerning the origin of cosmic rays.

6-5. Interpretation of Cosmic-Ray Abundances

The composition of the primaries above the earth's atmosphere does not correspond exactly to the original charge distribution of the

particles. The substantial amount of Li, Be, and B indicates that some spallation has occurred en route, since these elements are rare cosmically and cannot be produced by other means. Koshiba, Schultz, and Schein (1958) argue for a fair correlation between the primary abundances and the cosmic-ray abundances, pointing out that although the ratio of heavy to medium nuclei is different in cosmic rays and stars, the relative abundances of Mg, Si, and Fe are parallel in the two sets of data, and that pronounced peaks occur at elements of even- Z in both. The relatively high abundances of nuclides of odd- Z in the cosmic-ray data are readily explained as a consequence of spallation effects involving heavier elements.

If we take the L/M ratio as 0.35 at the top of the earth's atmosphere, we must conclude that the particles have encountered about 4 g/cm^2 of H on their way from the source to the earth and the lifetime of the primaries must exceed 10^6 yr. In that event the composition of cosmic rays should bear little resemblance to that of the original source, all fine structure should have been obliterated during the passage of the particles from the point of origin to the earth. On the other hand, Peters (1959) concludes that if the amount of matter encountered by the particles is less than 1 g/cm^2 , the age of the cosmic-ray primaries is probably less than a million years. Presumably there cannot have been too many encounters. Otherwise the abundances of elements of even- Z would not show such pronounced maxima! Singer has contended that there is no actual relation between the cosmic-ray-charge spectrum and the abundance of the elements. He asserts that it is possible to reproduce the observed primary-charge distribution by assuming an artificial model in which the original radiation consisted only of iron. The iron nuclei are assumed to collide with protons and after a passage through about 6 g/cm^2 a charge distribution of particles would result that would more closely resemble the observed distribution than do the cosmic abundances.

The cosmic rays appear to originate in some source where the density is not too high. Low-energy cosmic rays are known to originate in the sun, since enhancements of these particles have been noted at times of certain unusual flares, but high-energy particles do not come from the sun. They show no time variation. Probably, cosmic rays are produced in supernova explosions such as the one that caused the Crab nebula. This object emits a strong non-thermal radio emission, while the continuous optical radiation is polarized. The observational

data can be understood in terms of a mechanism in which the emission is produced by synchrotron radiation, i.e., the radiation from high-energy particles accelerated in a magnetic field. Certain of these particles escape and eventually acquire high energies by encounters with moving magnetic fields in accordance with the Fermi mechanism.

Some of these wandering fields are associated with clouds of ionized gas in the spiral arms of the galaxy, but material confined to the galactic plane apparently cannot account for the isotropy of the cosmic rays. It is generally believed that much of the scattering is produced in a spherical halo of attenuated gas surrounding the galaxy. It is believed to consist of turbulent magnetized gas clouds (density of about 0.01 atoms/cm^3) moving with speeds of the order of 100 km/sec . The gas is so rare as to emit virtually no optical radiation and is detected by its non-thermal radio-frequency emission. Presumably this radio frequency emission is produced by electrons accelerated in magnetic fields, which also serve to entrap the cosmic-ray particles and inhibit their escape from the galaxy. Furthermore, encounters between high-energy particles and randomly moving clouds of ionized gas carrying magnetic fields not only serve to diffuse the particles but may also accelerate them to high energies. Similar halos with radii of ten to twenty thousand parsecs are found in other galaxies. Possibly the cosmic rays of highest energy come from other galaxies.

In summary, cosmic rays are believed to originate in disturbed areas on stars or in supernovae, and to undergo interactions with other particles and with magnetic fields in the galaxy before they reach the detector. The charge distribution reflects the history of a sample of high accelerated matter and has no bearing on the cosmic abundance distribution.

Selected References

See especially the review article: Peters, B., *J. Geophys. Research*, **64**, 155, 1959, and report of the Varenna conference: *Nuovo cimento Suppl.*, **8**, part 2, 492-559, 1958.

An account of the important nuclear emulsion technique is given in: Powell, C. F., P. H. Fowler, and D. H. Perkins, *Study of Elementary Particles by Photographic Methods*, Pergamon, London, 1959.

Aizu, H., Y. Fujimoto, S. Hasegawa, M. Koshiba, I. Mito, J. Nishimura, and K. Yokoi, *Phys. Rev.*, **116**, 436, 1959.

Aizu, H., Y. Fujimoto, S. Hasegawa, M. Koshiba, I. Mito, and M. Schein, *Proc. Moscow Conference on Cosmic Rays*, 1960.

Alfvén, H., *Nature*, **143**, 435, 1939.

- Appo Rao, M. V. K., S. Biswas, R. R. Daniel, K. A. Neelakatan, and B. Peters, *Phys. Rev.*, **110**, 751, 1958.
- Cester, R., A. Debenedetti, C. M. Garelli, B. Quassiat, L. Tallone, and M. Vigone, *Nuovo cimento*, **7**, 371; **8**, *Suppl.* 523, 1958.
- Engler, M. F. Kaplon, and J. Klarmann, *Nuovo cimento*, **12**, 310, 1950; *Phys. Rev.*, **74**, 213, 1948.
- Freier, P., E. J. Lofgren, F. Oppenheimer, H. L. Brandt, and B. Peters, *Phys. Rev.*, **74**, 213, 1948.
- Freier, P., Ney, and C. J. Waddington, *Phys. Rev.*, **113**, 921, 1959.
- Koshiha, Schultz, and M. Schein, *Nuovo cimento*, **9**, 1, 1958.
- Lohrman, E., P. L. Jain, and M. W. Teucher, *Phys. Rev.*, **115**, 654, 1959.
- McDonald, F. B., and W. R. Webber, *Phys. Rev.*, **115**, 194, 1959.
- Noon, J. H., and M. F. Kaplon, *Phys. Rev.*, **97**, 769, 1955.
- Peters, B., Chapter on cosmic rays in *Handbook of Physics*, E. U. Condon and H. Odishaw, eds., McGraw-Hill, New York, 1958.
- Schein, M., W. P. Jesse, and E. O. Wollan, *Phys. Rev.*, **59**, 615, 1941.
- Waddington, C. J., *Phil. Mag.*, **2**, 1059, 1957; *Nuovo cimento*, **6**, 748, 1957.
- Waddington, C. J., and Rajopadhye, *Phil. Mag.*, **3**, 19, 1958.

Isotope Abundances

7-1. Introduction

A given nuclide may be characterized by giving any two of the three numbers: Z , N , or A . From the point of view of the nucleus, N is just as fundamental as Z , and a priori it would be just as reasonable to group nuclear species according to their N values (isotones) as to their Z values. Of course, this is not convenient in practice since Z determines the total number of electrons and therefore the chemical properties, outer structure, and optical spectrum of the atom. Hence we usually compare nuclides for a fixed value of Z , i.e., for a specified element, with different values of A and N . On the other hand, when we compare different elements we must take astronomical data, or a sample of the earth's crust, or of a meteorite and decide how to make a mixture valid for our corner of the universe. We can get terrestrial isotopic abundances, i.e., the relative abundances of atomic isotopes of the same Z , (but different N) with the aid of the mass spectrograph. It is a difficult, however, to establish the relative abundances of isotones or isobars. Then reliable relative abundances are necessary.

Highly refined experimental techniques have provided a wealth of information on the abundances of isotopes on the earth, and to some extent in meteorites as well (cf. Sec. 3-7). Isotopic constitution varies slightly from one type of terrestrial sample to another depending on its chemical composition and history and the possible role of biological processes. As previously noted, Rankama (1954) has suggested that the meteoritic values be accepted as standard for the solar system.

In this chapter we shall emphasize the astronomical data, summarizing the terrestrial results rather briefly. They are treated *in*

extenso in Rankama's comprehensive treatise (1954). We examine first the sources of astronomical data on isotopes.

Some information on the abundances of the very lightest isotopes, e.g., He^3/He^4 , D/H , etc., in the outermost envelopes of the sun may be obtainable from the direct observation of particles observed at times of high solar activity. The technique involves the direct counting of tracks in emulsions and is practicable only for light elements. The observations are difficult and likely to be complicated by the Van Allen belts if done in the neighborhood of the earth.

Otherwise, isotope effects have to be deduced from atomic and molecular spectra. Among heavier atoms, nuclides of the same Z but different N exhibit different hyperfine structures because of the differing nuclear spins involved. In astronomical sources, Doppler motions (and often the other sources of line broadening as well) are almost always so large that effects produced by hyperfine structure are unobservable. Hyperfine structure may act to broaden lines of certain metals in stellar spectra.

An isotope shift of 1.8 Å between $\text{H}\alpha$ and $\text{D}\alpha$ arises from the fact that the Rydberg constants differ slightly for hydrogen and deuterium. Unfortunately, if the ratio of the abundant to the rare isotope is very great, it is difficult to detect the latter. For elements heavier than helium, the isotope shifts are so small as to be undetectable.

Fortunately, band spectra reveal the isotopic constitution of the molecules involved. For example, the interatomic forces holding together a diatomic molecule $\text{C}^{12}\text{N}^{14}$ are quite nearly the same as those holding together a $\text{C}^{13}\text{N}^{14}$ molecule, but since the atomic masses are different the frequencies of vibration will differ. Consequently, the lines of the $\text{C}^{12}\text{N}^{14}$ band will be shifted with respect to those of the $\text{C}^{13}\text{N}^{14}$ band. In practice, the difference between the positions of the two lines is very small. For example, the close pair of lines ($K = 58$) $\lambda\lambda 3874.328, 3874.393$, $\text{C}^{13}\text{N}^{14}$, studied by Righini, is to be compared with the $\text{C}^{12}\text{N}^{14}$ line pair $\lambda\lambda 3874.194, 3874.129$.

Thus, in the stars the isotopic abundances are found from the appropriate molecular bands and many of the uncertainties that plague the determination of absolute abundances disappear. The dissociation constants are equal for the "normal" and "isotopic" molecules. Furthermore, for the pairs of lines considered, the f -values are all the same. The principal difficulty that occurs lies in the relation between the equivalent width and the number of molecules.

7-2. Empirical Rules for the Stability of Nuclei

Every stable nuclear species has been found on the earth and many others appear as well. Some naturally occurring unstable nuclides are decay products of longer-lived heavy elements; others, such as Rb^{87} , are themselves long lived. A discussion of the stability of nuclear species must underlie any appraisal of atomic abundances and isotope ratios. The stability of a nucleus depends on a number of factors; we shall attempt to assess a few of them. Among the lighter elements, β -decay sometimes occurs. For example, the decay of K^{40} to Ar^{40} is believed to have supplied most of the present argon in the earth's atmosphere. In heavy elements, such as thorium, α -decay limits the lifetime, while U^{235} may decay not only by α -emission but also by fission. Spontaneous fission occurs in heavy synthetic elements such as californium.

Supposedly, the elements were formed in the remote past by processes involving extremely high temperatures and densities. The resulting nuclides were collected in the primordial solar system, the unstable species decayed, and the present distribution represents the combined effects of the formation mechanism and the decay schemes.

If one plots the atomic number Z as ordinate against the number of neutrons as abscissae, the points representing stable nuclei cluster near a curve. Initially this curve has nearly a 45° slope but gradually it departs therefrom. Only hydrogen and He^3 have more protons than neutrons; up to chlorine most nuclei tend to have equal numbers of neutrons and protons, although isotopes such as C^{13} , O^{17} , and Ne^{21} exist. Beyond argon, nuclei with more neutrons than protons prevail until at Pb^{208} the neutron excess is 44. This fact can be understood in terms of the binding energies of the nucleons. The strictly nuclear shortrange attractive forces between protons and protons, neutrons and neutrons, and neutrons and protons are opposed by the coulombic repulsions between the protons. As heavier nuclei are built, more and more neutrons have to be added in proportion to the protons. Stable nuclei cease to exist when the repulsive forces are so great that a nucleus is unstable against the emission of heavy particles.

The *binding energy* of an atom Z, N of mass ${}_ZM_N^A$ (nucleus plus electrons) is simply

$$W(A, Z) = ZM_H + NM_N - {}_ZM_N^A \quad (7-1)$$

where M_H is the atomic mass of the hydrogen atom and M_N is the

atomic mass of the neutron. All masses are expressed in the physical system of atomic weights. Obviously the quantity W must be positive for a nucleus to exist, but this condition is only a necessary one, not a sufficient one.

Another quantity which is frequently used is the *mass defect* i.e., the difference between the atomic mass of the atom ${}_ZM_N^A$ and the integer A .

$${}_ZD_N^A = {}_ZM_N^A - A \quad (7-2)$$

As an example, consider the isotope ${}_8\text{O}_{10}^{18}$ for which ${}_ZM_N^A$ is 18.0049. The mass defect ${}_8D_{10}^{18} = 0.00485$ atomic mass units. In energy units, 1 atomic mass unit (amu) is $0.0014918 \text{ ergs} = 931.141 \text{ Mev}$.

Another quantity frequently used is the *packing fraction*

$$f = 10,000 ({}_ZD_N^A/A) \quad (7-3)$$

which is positive for elements lighter than O, decreases rapidly with A until it reaches a minimum of about -8 near iron and then slowly rises with increasing A .

Now the binding energy, W , may be expressed by an empirical formula of the type

$$W(A, Z) = a_1A - a_2A^{2/3} - (a_3/A)(N-Z)^2 - (a_4/A)Z(Z-1) - \delta \quad (7-4)$$

Here the first term a_1A expresses the fact that the specific nuclear short-range forces suggest a total binding energy that is proportional to the total number of particles. The second term is proportional to the surface area of the nucleus. It arises from the fact that only the protons and neutrons that lie "inside" the nucleus, i.e., are surrounded by their neighbors, will contribute their full share to W . Those that lie in or near the surface of the nucleus will not. The situation is somewhat analogous to that of surface-tension forces in a liquid drop.

Were it not for the coulombic repulsions between the positively charged protons in the nucleus, there would be a strong tendency for the number of neutrons to be equal to the number of protons. Hence there appears in the equation the $(a_3/A)(N-Z)^2$ term. The a_4 term arises from the coulomb repulsions between the Z charges that try to break up the nucleus. The total number of combinations of the Z charges taken two at a time is $Z(Z-1)/2$. The greater the mass, the

more important will this term become until it finally causes an intrinsic instability in the nucleus, leading to α -emission or spontaneous fission.

The last term, δ , arises from what is called *pairing energy*. It expresses the fact that nuclei with odd numbers of protons and neutrons are energetically less favored than those with even numbers of neutrons and protons. Consider an O-O nucleus (odd numbers of protons and neutrons). If one of the protons is changed to a neutron by the emission of a positron by the nucleus, the nucleus is now of the even-even E-E type and is more stable. Likewise, by a β -ejection, a neutron becomes a proton and the nucleus becomes one of the E-E type. The pairing energy for the formation of a proton differs from that for the formation of a neutron depending on the type of nucleus.

If we consider isobars of a given atomic weight, we may have two situations depending on whether A is even or odd. If A is odd, the nucleus must be of the E-O or O-E types. Protons and neutrons prefer to comprise pairs in the nucleus. If an extra proton or neutron is added to a nucleus of E-E type (even- A), the resulting nucleus of the E-O or O-E type will tend to be less stable than the previous nucleus of the E-E type. Of the stable nuclides found in nature, most are of the E-E type.

If the binding energy W is plotted against the neutron excess ($N-Z$) for odd- A nuclei, a single parabolic curve is obtained. Isobars tend to decay by β -emission to the lowest stable nuclei. With only two exceptions, nuclei with odd- A have only one stable isobar.

On the other hand, the binding energies of even- A isobars may be represented by parabolas representing O-O and E-E combinations of Z and N , separated by the effect of the pairing energy differences. In Fig. 7-1 the two stable isobars are C and E . All others can decay to them by β^+ or β^- decay. In Fig. 7-2 the effect of the pairing energy is such that the E-E isotopes A, C , and E , would be stable. Thus, even- A nuclei may have two or three isobars. Furthermore, even- A nuclides are more numerous than odd- A nuclides. Odd-odd nuclei tend to be unstable, although H^2 , Li^6 , and B^{10} , (while rare isotopes) are definitely stable. Nitrogen is of particular interest for it is a very abundant element and the odd-odd isotope is most abundant! Some O-O nuclei, such as K^{40} which decays to Ca^{40} and Ar^{40} are long-lived.

Although the simple empirical nuclear model we have described explains the general stability rules, there are important perturba-

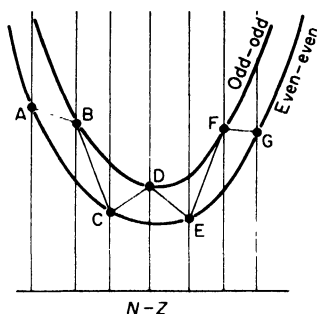


Fig. 7-1. Even- A nuclei with small values of the pairing energies δ .

tions. The binding energies of the nuclides do not fall on smooth parabolae. Most of these deviations can be explained in terms of the shell model which supplies a good picture of many nuclear properties.

Elsasser in 1933 called attention to the fact that nuclides containing specific numbers of neutrons or protons are particularly abundant. These so-called magic numbers are:

$$2 \quad 8 \quad 20 \quad 28 \quad 50 \quad 82 \quad 126$$

Subsequently, V. M. Goldschmidt and H. Suess noted that these magic-number nuclei included elements of high cosmic abundance.

The magic numbers are correlated with certain striking nuclear properties. For example, if we consider a sequence of even- Z elements we would expect that as Z was increased by two, the number

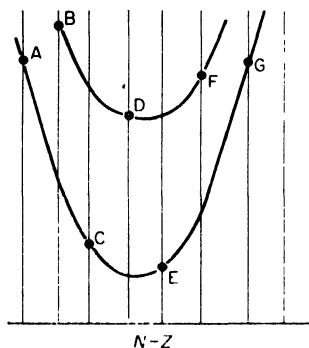


Fig. 7-2. Even- A isobars with large values of the pairing energy δ .

of neutrons would also go up by two, or perhaps by four or even six. This is usually true, but in going from Xe to Ba the number of neutrons ($N = 82$) in the heaviest isotope does not increase! The same is true for the heaviest isotopes of krypton and strontium ($N = 50$) and of calcium and titanium ($N = 28$). The binding energies of light nuclei show the influence of the magic numbers 2, 8, 20. Other evidence is provided by the pairing energies of light nuclei, the β -decay energies for the atoms in the intermediate mass range, also the great stability for the magic numbers $Z = 82$ and $N = 126$, and the thresholds for the ejection of the most lightly bound neutrons by γ -rays.

Additional data are provided by nuclear-capture cross sections for neutrons. It has been known for a long time that the behavior of thermal neutrons is extremely capricious, depending as it does on the chance positions of nuclear-energy levels. If the energy of the neutron is in the neighborhood of 1 Mev, D. J. Hughes and D. Sherman showed that the capture cross section increases fairly uniformly with Z except that there are pronounced minima at nuclei with neutron numbers near, or slightly above, the magic numbers $N = 50, 82$, and 126. Furthermore, all isotopes of Pb and Sn have small capture cross sections for neutrons. If the same picture holds in the 50 to 500 Kev region, which is likely to be of importance for element-building processes in stars, we can understand how magic-number nuclides build up to high abundances if neutron capture plays an important role.

The magic numbers are well explained by the nuclear-shell model (Mayer and Jensen 1955). This model is the nuclear analogue of the vector model for atomic spectra. The spin-orbit coupling, however, is much more important than in optical spectra so that the nucleus approaches "jj" rather than LS coupling.

Magic numbers are the analogues of the closed shells in the electronic structure of the atom. That is, whenever another nucleon is added after a magic number has been reached, its binding energy is unusually small. This situation is comparable to that exhibited in the alkali metals where the binding energy of the optical electron is much less than that of the last electron in the preceding noble gas in the periodic table. The effects, however, are not as marked as in the optical spectra and the analogue of the phenomenon of the heavy binding of the optical electrons in the noble gases is not exhibited.

The large number of stable isotopes of certain elements, such as calcium ($Z = 20$) and of tin ($Z = 50$) are to be understood in terms of the magic numbers. Likewise, although heavy O-O nuclei tend to be energetically unstable, a system with a closed neutron shell minus one neutron may be stable, e.g., V_{27}^{50} ($N = 28 - 1$).

7-3. Terrestrial Isotope Abundances

Rankama (1954) has discussed comprehensively the problem of terrestrial isotope abundances. Several aspects are involved. Most of the stable elements are represented by more than one isotope, the number being influenced by the value of Z and whether it is odd or even. Thus, stable odd- Z elements have only one or two stable isotopes, whereas even- Z elements often have two or more. Light elements ($Z < 20$) and very heavy elements ($Z \geq 81$) have fewer isotopes than those in the range ($28 < Z < 81$). Among elements with a particularly large number of isotopes, one may mention especially tin and xenon, each of which has seven even- A isotopes. Tin and xenon have three odd- A and two odd- A isotopes, respectively. Among the heaviest elements, stability against α -particle ejection decreases and the number of stable isotopes decreases rapidly. Bismuth ($Z = 83$) is the last stable element.

Among the elements up to nickel, one isotope is usually by far the most abundant, e.g., C, O, and Fe. Furthermore, among even- Z elements up to $Z = 20$ (calcium), the lightest isotope tends to be the most abundant and the heavy isotope is rare. Argon is an exception, but atmospheric argon may have been enriched heavily by the decay of K^{40} . Beyond $A = 60$, the relative proportions of isotopes are more nearly the same, those in the middle of the range tend to be the most abundant. For most of these elements, isotopes of even- A and N contribute most of the atoms. The lighter isotope is often the most plentiful for elements of odd- Z . Among heavier elements ($A > 70$), the most abundant isotope is the heaviest. As we might expect, on the basis of qualitative stability arguments, a given element of even- Z has more even- A isotopes (which show a greater mass-range) than do the odd- A isotopes. Also, the even- A isotopes make up the majority of the atoms of that element. If a given element has two stable isotopes of odd- A , these isotopes do not differ in abundance by more than a factor of about 3, whereas if there are several isotopes of even- A , the abundances may differ by several powers of 10!

When the isotope abundances are plotted against A , the odd mass-number species fall below the curve of the even-number species. The curves are irregular and the patterns differ from one element to the next.

We would not expect the abundances of nuclides to depend more closely on the number of protons than on the number of neutrons. Accordingly, it would be of interest to select nuclides of same N but different Z . This step is difficult to carry out (except perhaps for the rare earths) since one must know the abundances of the elements exactly.

All stable nuclear species are the remnants of some ancient nuclear processes and their abundances must depend on the property of the nucleus and on the initial condition of element formation. Hence, an adequate interpretation of the isotope abundances requires a knowledge of abundances of the elements, so we can discuss not only isotopes but also isotones and isobars. The abundances of nuclides should be a smoothly varying function of nuclear properties (e.g., the cross sections for neutron capture at high energies) after due allowance has been made for the separate β -decay schemes. This concept influences the abundance compilation of Suess and Urey (1956) and lies behind the abundance table suggested by A. G. W. Cameron (1959).

7-4. The Missing Elements

One of the most fascinating aspects of the problem of nuclear stability is that of the so-called "missing" elements which were sought so assiduously in early years of the present century.

After the brilliant work of Moseley on the X-ray spectra of the elements, the idea persisted that there must exist ninety-two elements. Certain of these elements corresponding to $Z = 43, 61, 85$, and 87 remained undetected, although the "discovery" of elements 43 "masurium" and 61 "illinium" was reported. These findings were never confirmed, but eventually all missing elements were synthesized in the laboratory. All isotopes of technetium ($Z = 43$) are unstable. Its longest-lived isotope has a half-life of 2,600,000 yr. The longest-lived promethium isotope P_m^{145} has a half-life of 30 yr while those of astatine ($Z = 85$) and francium ($Z = 87$) are even more ephemeral with half-lives of 8.3 hr and 21 min, respectively. For each odd- A only one stable nuclear species of odd- Z is permitted, but these

isotopes are already occupied by stable nuclei of other elements in the neighborhood of $Z = 43, 61, 83$, or 85 .

We would not expect to find any of these four elements in nature. The initial terrestrial supply of the longest-lived T_e isotope would have been attenuated by a factor of the order of $\exp(-2000)$! Nevertheless, T_e has been detected in the spectra of certain cool giant and supergiant stars. We return to this topic in Chap. 9 where we shall see that it has an important bearing on our concepts concerning the origin of elements.

Table 7-1. Summary of Isotope Ratio Results for Astronomical Objects

Isotope or isotope ratio	Objects in which studied	Abundance anomalies if any
D	Sun	No evidence, except perhaps in flares
	Interstellar medium	$H/D > 4500$
He^3	Sun	No evidence
	Magnetic star	He^3 possibly comparable with He^4
	21 Aquilae	
Li^6/Li^7	Sun	$< 1/4$, probably same as on earth
C^{12}/C^{13}	Planets	Probably same as on earth
	Sun	Probably same as on earth
	Hydrogen-deficient stars	Probably same as on earth or greater
	Carbon R stars	Ratio varies from 4 or 5 to terrestrial value (see text)
	Carbon N stars	Uncertain, but probably comparable with R stars
	G8-K5 giant stars	Probably normal
	Interstellar medium	Probably normal
O^{17}, O^{18}	M stars	Probably normal
Ti	K, M stars	Probably normal

7-5. Astrophysical Studies of Isotope Ratios

The tables of relative isotope abundances (e.g., Condon and Odishaw 1958) are based on terrestrial samples (See Table 1-1). Except for small alterations caused, for example, by biochemical processes or by melting and fractionation, these abundances are probably representative of the solar system as a whole. One exception may be noted for deuterium which may have been enriched on the earth as a consequence of the preferential escape of the lighter isotope

from the earth's gravitational field. Further, we would expect deuterium to be depleted in the solar atmosphere as a consequence of thermonuclear reactions occurring at temperatures less than a million degrees in the solar convection zone. Likewise, lithium, beryllium, and boron might be systematically destroyed in the solar convection zone. It is believed that there is no mixing between the surface layers of the sun and the deep interior where hydrogen is burned into helium. Hence we would expect the same abundance ratios for He^3/He^4 and $\text{C}^{12}/\text{C}^{13}$ as are found in the earth.

In other stars, there is no a priori reason why mixing with the interior cannot occur so that the influence of thermal nuclear processes can be manifest in these outer layers. Hence the aforementioned He and C ratios may be considerably different from the corresponding solar system values.

The abundances of only hydrogen and helium isotopes may be assessed from their atomic isotope shifts, whereas isotopes of other elements can be found only if these elements occur in compounds.

We shall now discuss isotope effects, element by element, in various astronomical sources (excluding meteorites which were treated in Chap. 3).

Hydrogen: The deuterium α -line is displaced from the $\text{H}\alpha$ -line, the deuterium β from the $\text{H}\beta$ line, etc., by small amounts, and theoretically it should be possible to disentangle the profiles of the two hydrogen isotope lines from one another. Unfortunately, the profile of $\text{H}\alpha$ in the sun is affected by blends with water vapor and the wings of other hydrogen lines are confused to some extent with metallic lines. There is also the intricate fine structure of the hydrogen line profiles due to the line-of-sight motions of the radiating gases. These Doppler displacements give rise to a "whiskery" appearance of the lines so well exhibited, for example, in the McMath-Hulbert Observatory spectrograms. Hence the interpretation of small asymmetries or modifications of the profile of the hydrogen lines is difficult. Likewise, even with the application of cosmic-ray techniques in satellite experiments it would be difficult to detect a small amount of deuterium. In this connection we mention the work of T. D. Kinman (1956), who used interferometric techniques and took advantage of the solar rotation to eliminate the effects of the water vapor. He found no evidence for any deuterium in the sun, although he suggested that a weak line with an equivalent width of about a milliangstrom corre-

sponding to a deuterium abundance of 1×10^{-5} that of hydrogen might remain undetected.

On the other hand, Goldberg, Mohler, and Miss Müller (1956) noted that the profile of the $H\alpha$ line in a bright-loop prominence connected with the great flare of February 10, 1956, was asymmetrical. It did not seem plausible to account for this asymmetry by gas-cloud velocities. The violet wing was elevated with respect to the red wing; the effect could be accounted for by supposing that an additional line component, displaced between 1.5 and 2.0 Å to the violet was superposed on the normal line. On the assumption that the additional line component was displaced 1.78 Å and was due to deuterium, they found that a D/H ratio of at least 4 per cent would be required. Such a high D/H ratio is surprising and the Michigan observers do not regard this result as in any way conclusive. Additional observations are needed. In particular, it is desirable to have simultaneous observations of lines of different elements so as to be able to disentangle velocity and isotope effects. Severny (1957) claims to have found D/H ratios as high as 10^{-4} in active regions in the sun.

Possibly the D/H ratio can be measured directly from counts obtained with detectors flown above the earth's atmosphere during the times of enhanced solar activity.

Since deuterium is always destroyed in thermonuclear reactions, the only plausible mode of its production involves the breaking up of complex nuclei by encounters with fast particles. The most likely mechanism according to Fowler and the Burbidges (1955) is neutron capture by ordinary protons. Presumably, protons become accelerated in flares and produce neutrons upon encounters with abundant light nuclei of C, N, O, and Ne. The neutrons produced are readily captured by protons to form deuterium. Deuterium has never been found in other stars nor in comets, nor has it been found in the interstellar medium. From an unsuccessful search for the deuterium rf line, Adgie (1958) at Cambridge obtained a lower limit of 4500 for the H/D abundance in the interstellar medium. The accuracy of the measurements are being improved, and it will be possible to detect interstellar deuterium if it is as abundant as on the earth. Deuterium might be expected in the outer planets, where its influence would be felt (if at all) in the band spectra of hydrogen compounds. The D/H ratio is so small, however, as to make a spectroscopic determination very difficult.

Recently, Bashkin and Peaslee (1961) have considered the production of light isotopes H^2 , He^3 , Li, Be, and B by cosmic ray particles accelerated in flares in stellar atmospheres. The (Li, Be, B) isotopes are produced by spallation reactions of fast protons on nuclei of the (C, N, O, Ne) group and if we suppose that the average star is a hundred times as active as the sun we can account for all the above isotopes except deuterium. Probably the high D/H ratio was produced by special processes during the formation of the solar system so that the general cosmic ratio may be about 3 orders of magnitude smaller.

Helium: The light isotope of helium, He^3 , is produced in the proton-proton reaction and we might suppose that if mixing occurred in the sun (or more likely in the ancestral stars from whose material the sun was formed), there would occur a small amount of this isotope. The concentration is small and will depend on the temperature at which hydrogen burning takes place. The lower the temperature, the greater the concentration of He^3 . Greenstein (1951) examined the wavelength of the helium lines in the spectrum of the sun and compared the results with the isotope shifts measured at the Argonne National Laboratory. He found no evidence for the existence of He^3 although if this isotope had been formed in small quantities, say less than around 1 or 2 per cent. it might have escaped detection. In the near future it will be possible to set an upper limit to the He^3/He^4 ratio by means of counters that measure the solar flare particles impinging upon the earth's atmosphere.

The Burbidges (1956) called attention to a possible presence of He^3 in the magnetic star 21 Aquilae. Measurements of helium lines in this star show a wavelength shift between singlet and triplet lines, part of which may be due to the Stark effect. A comparison of the results with laboratory measurements of isotope shifts between lines of He^3 and He^4 suggest that the major part of the displacement might be due to an isotope effect. The abundance of He^3 in this star may be comparable with that of He^4 . They suggest that the acceleration of protons in the stellar atmosphere leads to the production of neutrons and deuterons. The deuterons are then captured by other protons to form He^3 . On the earth He^3 occurs as the end product of the decay of tritium, and its concentration is about 1.3 parts in a million of ordinary hydrogen.

Lithium: Greenstein and Richardson (1951) concluded that if Li^6 exists in the solar atmosphere the ratio Li^6/Li^7 is less than 1/4, probably about the same as on the earth.

Beryllium: Beryllium is represented by only one stable nuclear species, i.e., it is monobaric.

Boron: Boron has two isotopes, B^{10} which contributes about 19 per cent and B^{11} which supplies about 81 per cent. The BH and BO bands occur in the sun and stars and could be used for a study of the isotope ratios.

Carbon: The important C^{12}/C^{13} ratio may be studied in the CN bands or in the C_2 swan bands in the carbon stars. Let us consider first the C^{12}/C^{13} ratio in the solar system.

From a study of the CO bands in the atmosphere of Venus, Kuiper concluded that the C^{12}/C^{13} ratio was the same as on the earth. Likewise, studies by N. T. Bobrovnikoff and by P. Swings suggest that the terrestrial ratio probably holds in comets, although the quantitative interpretation of cometary spectra is so difficult as not to preclude the possibility that actual differences may occur. The major planets show strong CH_4 bands, but no studies of carbon isotope ratios have been carried out for them.

The CN isotopic bands have been studied by King in the arc spectrum but the wavelengths are difficult to measure because the line shifts are very small. The most careful study of the C^{12}/C^{13} ratio in the sun is an investigation by Righini (1956) who observed the normal and isotopic 3874 CN lines with the vacuum spectrograph at the McMath-Hulbert Observatory. The $C^{13}N^{14}$ line was observable but very weak, although the corresponding $C^{12}N^{14}$ line had an equivalent width of about 30 mÅ. Righini concluded that the C^{12}/C^{13} ratio was about 10,000. The result is unconvincing since these lines fall in a region where the continuum is depressed by a host of overlapping lines and one cannot estimate the amount by which the intensity of any given line is falsified. These effects are particularly serious for very weak lines, such as those of the $C^{13}N^{14}$ isotope. There is no real evidence that the C^{12}/C^{13} ratio is different in the sun than in the earth.

The unstable isotope C^{14} has never been found in the sun or stars, nor is it likely to be found in view of its rather short lifetime.

Since it shows striking variations from one type of star to another, the determination of the stellar C^{12}/C^{13} ratio in stars has been an object of many investigations. Bidelman (1953) called attention to certain hydrogen-deficient stars (see Chap. 9) with strong bands of C_2 . He suggested that in these objects the C^{12}/C^{13} ratio may be equal to or even greater than on the earth. Stars in which no mixing occurred

between the surface and internal energy-generating regions might be expected to show the "normal" C^{12}/C^{13} ratio. This group includes the *R* Coronae Borealis variables—giant stars with an excess of carbon over oxygen. The *R* stars, which are slightly cooler carbon stars, show some interesting differences among themselves. In one group the C^{12}/C^{13} ratio appeared to be normal, but in the other group, McKellar found indications of a ratio of the order of 3 or 4, which is comparable with the ratio that would be produced by the carbon cycle.

Analyses were more difficult for the *N* stars, but these often indicated also excesses of C^{13} . Shajn and Miss Hase (1954) studied the $C^{12}C^{13}$ and $C^{13}N^{14}$ bands in *N*-type stars and found variations in the C^{12}/C^{13} ratios (i.e., $2 \rightarrow 20$) similar to those obtained for *R*-type stars. A. A. Wyller (1957) estimated the C^{12}/C^{13} ratio for five carbon stars. Using both a thin-layer hypothesis and a simplified radiative-transfer treatment, he concluded that the results of both methods confirmed previous estimates. Evidence from curve-of-growth effects, however, suggest caution in going from observed isotopic-band intensities to estimates of relative abundances.

The curve-of-growth effects for a band are different from those for a single line. If the number of atoms acting to produce a line is increased sufficiently, the profile will develop prominent wings and the equivalent width will rise as $\sqrt{Nf\tau}$. In a band, however, the lines are closely spaced so that the wings would overlap as the number of absorbing molecules increased until saturation occurred and the band would become almost totally "black."

In this connection we may describe the work of Climenhaga (1960) who determined the curve of growth for a section of the C_2 swan bands of carbon in the spectra of the cool carbon stars in order to obtain improved values of the C^{12}/C^{13} ratio. A novel feature of this study was the measurement of the C_2 bands near $\lambda 4740$ in the variable star RU Camelopardis at different phases of its light cycle. The spectrum of this Cepheid variable ($P = 22^d.123$) oscillates between *R0* and *K0*; the strength of the C_2 bands are variable with phase, being strongest at minimum light. Climenhaga determined the C^{12}/C^{13} abundance ratio, first neglecting curve-of-growth effects on the simple assumption that W depended on the number of molecules. A plot of the derived ratio against total band strength showed that curve-of-growth effects, although present, were small.

In low dispersion necessarily employed for observation of faint objects, the bands are not resolved into their individual lines and one often must work with the total equivalent width of the region of the band heads. Climenhaga calculated the profiles for the head-forming region of the $\lambda 4737$ $C^{12}C^{12}$ and $\lambda 4745$ $C^{12}C^{13}$ swan bands for different numbers of carbon molecules and different values of the C^{12}/C^{13} ratio. He found that the spectra of stars showing C^{13} bands gave a best fit with the theoretical profiles for an abundance ratio in excess of 4/1.

A plot of the equivalent width of a band head against relative numbers of absorbing molecules demonstrated that all observed bands showed curve-of-growth effects (See Table 7-2). From the moderate dispersion spectrograms, Climenhaga obtained results which show that the mean ratio is 5.8. On the other hand, from the five high dispersion spectra of two *R*-type stars, RU Cam and HD156074, he obtained 4.7. In any event, the ratio is 50 per cent or more higher than the value of 3.5 obtained without curve-of-growth effects. The two *R*-type stars that showed no C^{13} bands, HD182040 and HD201626 have a C^{12}/C^{13} ratio in excess of 100. The C^{12}/C^{13} ratios determined for the two *N*-type carbon stars, 19 Piscium and DS Pegasi which show much stronger bands than do the *R*-type stars, were 8.1 and 16.1, respectively, but those values are uncertain.

The interpretation of the C^{12}/C^{13} ratios in these late-type stars in terms of nucleogenesis arguments has been discussed by Cameron (1957), and by the Burbidges, Fowler, and Hoyle (1957). The high

Table 7-2. Curve-of-Growth Effects

Star	Spectral class		C^{12}/C^{13}
	Draper	Keenan-Morgan	
HD156074	<i>R0</i>	<i>C1</i>	4.2
209621	<i>R3</i>	<i>C3p</i>	4.0
5223	<i>R3</i>	<i>C2p</i>	5.3
223392	<i>R3</i>	<i>C3</i>	4.7
76846	<i>R1</i>		5.3
197604	<i>R4</i>		8.8
36972	<i>R8</i>		8.5
RU Cam	<i>K0-R0</i> <i>C0-C3</i>		5.7

C^{12}/C^{13} ratios are invariably found in stars in an advanced stage of their evolution, i.e., red giants and supergiants. Such stars have deep convection zones and in addition compact, dense cores where it is possible that helium is burned into the carbon isotope C^{12} . The resulting C^{12} is mixed into the surface layers. If it passes en route through a sufficiently thick zone where hydrogen is being consumed to helium, it acts as a catalyst in the carbon cycle, and some of it is changed into C^{13} and nitrogen. When the carbon reaches the surface it may then have an abundance ratio appropriate to the carbon cycle equilibrium value, viz., about 4.6. On the other hand, if the C^{12} passes outward without encountering H-burning region, the C^{12}/C^{13} ratio might be as high or higher than that found on the earth. In this connection, we may mention the paradox suggested by the variable WZ Cass, where McKellar found a strong lithium line indicative of a large concentration of this vulnerable element. At the same time, the star shows a strong C^{13} band. At the temperatures of the carbon cycle required to produce C^{13} in the quantity observed, lithium would certainly be destroyed.

John D. Schopp (1954) attempted to determine the lower limits to the abundance ratio of C^{12} to C^{13} in the atmospheres of G8 to K5 giant stars from the CN band near $\lambda 3883$. For all the stars with sufficiently strong lines to yield meaningful results, he found a lower limit greater than 6.5 which is in excess of the equilibrium ratio of 4 or 5 predicted for matter involved in the carbon cycle. Unfortunately, the data are beset by such large uncertainties that one cannot assert that the C^{12}/C^{13} ratio is really different from the terrestrial ratio. Schopp suggests that it is likely that the normal red giants do not undergo a mixing process which would bring the products of the carbon-cycle operation to the surface. Hence they must differ from the typical *R* and *N* stars which show abundant C^{13} .

Bidelman pointed out that those *R* stars which McKellar found to show no C^{13} bands were peculiar. Two were high-velocity carbon stars with strong CH bands, while HD182040 showed strong C_2 and CN bands and atomic C, but was apparently deficient in hydrogen. Thus these particular carbon stars all appear to be abnormal in some respect.

From the interstellar lines of the CH^+ molecule, $\lambda 4232.58$ and $\lambda 3957.72$, O. C. Wilson (1948) obtained a lower limit of 5 for the C^{12}/C^{13} ratio, but the lines were so weak that we cannot be sure that

the ratio is different from the terrestrial value. Nothing is known concerning the isotopic constitution of carbon-isotope ratios in external galaxies.

Ordinary nitrogen has two stable isotopes, N^{14} (99.635 per cent) and N^{15} (0.354 per cent), and several unstable ones, but N^{15} has never been observed in the stars. The carbon/nitrogen cycle would produce an N^{14}/N^{15} ratio greater than 100,000. Large ratios in isotope abundances are extremely difficult to establish spectroscopically.

Oxygen has three stable isotopes, O^{16} (99.759 per cent), O^{17} (0.0374 per cent) and O^{18} (0.2039 per cent). Were the less abundant isotopes relatively more plentiful in the M stars, the effects would appear in the TiO bands. McKellar (1949) finds no evidence for any such enhancement in the M stars. Probably the M stars represent something approaching the "normal", i.e., solar composition, and a more likely place to find abundance anomalies would be in the S stars whose spectra show evidence of recent nuclear transformations. Meteorites and the deeper rocks of the earth's crust show about the same O^{16}/O^{18} ratios.

The magnesium hydride bands are observed in the M stars and isotope effects should be investigated for this metal.

Titanium has five stable isotopes. The terrestrial relative abundances of these isotopes are:

46	47	48	49	50
7.93%	7.28%	73.94%	5.51%	5.34%

Herbig (1948) made a careful study of the TiO bands in nine bright-giant and supergiant stars of spectral classes $K0$ to $M6$, the variable O Ceti, an M dwarf, and an S star. The separation of the band heads produced by TiO molecules differing in titanium mass by one unit is 0.45 Å at the $\lambda 4951$ (1, 0) head of the alpha system, increasing to 1.6 Å at the $\lambda 4421$ (4, 0) head. The $Ti^{46}O$, $Ti^{47}O$ heads are free from interference by the $Ti^{48}O$ heads, but the situation for $Ti^{49}O$, and $Ti^{50}O$ was less favorable because of the heavy band and line absorption at the most promising heads. An increase of the relative abundance of one of the less prominent isotopes by a factor of 4 or 5 could have been detected and Herbig concluded that it is probable that the titanium isotope ratio is the same on the earth and in the stars.

Zirconium would be a most interesting element to study, because of the nuclear reactions in the interior that might have caused fluc-

tuations in the isotope ratios. Four of the five isotopes are of comparable abundances and marked changes in their relative proportions should be detectable from the band spectrum of ZrO . Other elements show molecular bands in cool stars, for example, aluminum oxide and lanthanum oxide. They pose, however, incredibly difficult problems, requiring observations obtained with very high dispersion.

The isotope-ratio problem is closely connected with that of abundance differences between stars to which we turn our attention in Chap. 9.

Selected References

- Adgie, R. L., *Paris Symposium on Radio Astronomy*, R. Bracewell, ed., Stanford University Press, Stanford, Calif., 1958, p. 352.
- Bashkin, S., and D. C. Peaslee, *Ap. J.*, in press, 1961.
- Bidelman, W. P., *Ap. J.*, **117**, 25, 1953.
- Burbidge, E. M., and G. R. Burbidge, *Ap. J.*, **124**, 655, 1956.
- Burbidge, E. M., G. R. Burbidge, W. Fowler, and F. Hoyle, *Revs. Modern Phys.* **29**, 547-650, 1957.
- Cameron, A. G. W., *Chalk River Report CRL-44*, 1957; *Ap. J.*, **129**, 685, 1959.
- Climenhaga, J., Unpublished thesis, University of Michigan, Ann Arbor, Mich., 1960.
- Condon, E. U., and H. Odishaw, eds., *Handbook of Physics*, McGraw-Hill, New York, 1958.
- Goldberg, L., O. C. Mohler, and E. Müller, *Ap. J.*, **127**, 302, 1958.
- Greenstein, J. L., *Ap. J.*, **113**, 531, 1951.
- Greenstein, J. L., and R. S. Richardson, *Ap. J.*, **113**, 536, 1951.
- Herbig, G., *Publ. Astron. Soc. Pacific*, **60**, 378, 1948.
- Kinman, T. D., *Monthly Notices Roy. Astron. Soc.*, **116**, 77, 1956.
- Mayer, M. G., and H. Jensen, *Shell Model of the Nucleus*, Wiley, New York, 1955.
- McKellar, A., *Publ. Astron. Soc. Pacific*, **61**, 1999, 1949.
- Rankama, K., *Isotope Geology*, McGraw-Hill, New York, 1954.
- Righini, G., *Liege Symposium*, "Les Molecules dans les Astres," 1956.
- Schopp, J. D., *Ap. J.*, **120**, 305, 1954.
- Severny, A. B., *Publ. Crimean Ap. Obs.* **16**, 12, 1956; *Russian Astronomical J.*, 1957.
- Shajn, G. A., and V. Hase, *Liege Symposium*, "Processus Nucleaires dans les Astres," 1954.
- Suess, H., and H. C. Urey, *Revs. Modern Phys.* **28**, 53, 1956.
- Wilson, O. C., *Publ. Astron. Soc. Pacific*, **60**, 198, 1948.
- Wyller, A. A., *Ap. J.*, **125**, 177, 1957.

General Abundance Compilations

8-1. Introduction

In this chapter we shall discuss several of the attempts that have been made to obtain "cosmic abundance distributions." Such compilations do not refer to the chemical composition of the universe as a whole. Rather they apply only to the solar system or to objects that are relatively close to the sun as galactic distances go.

Except for those nuclides, such as H^2 , Li, Be, and B that are destroyed at relatively low temperatures, the solar composition represents the so-defined "cosmic abundance" of the elements. As we saw in Ch. 5, however, the determination of abundances from solar data is beset by many difficulties. Hence it is necessary to make a critical compilation of data from all available sources. A number of such attempts have been made, some of the more recent and comprehensive of these, by Suess and Urey (1956) and by Cameron (1959), will be examined in some detail.

The earliest investigations were naturally confined to analyses of the earth's crust. Later the importance of meteorites was recognized and only recently has it been possible to add data from the sun, stars, and gaseous nebulae (Fig. 8-1). Present abundance compilations make use of all three of these principal different sources of data and other information as well, e.g., factors suggested by theories of nucleogenesis.

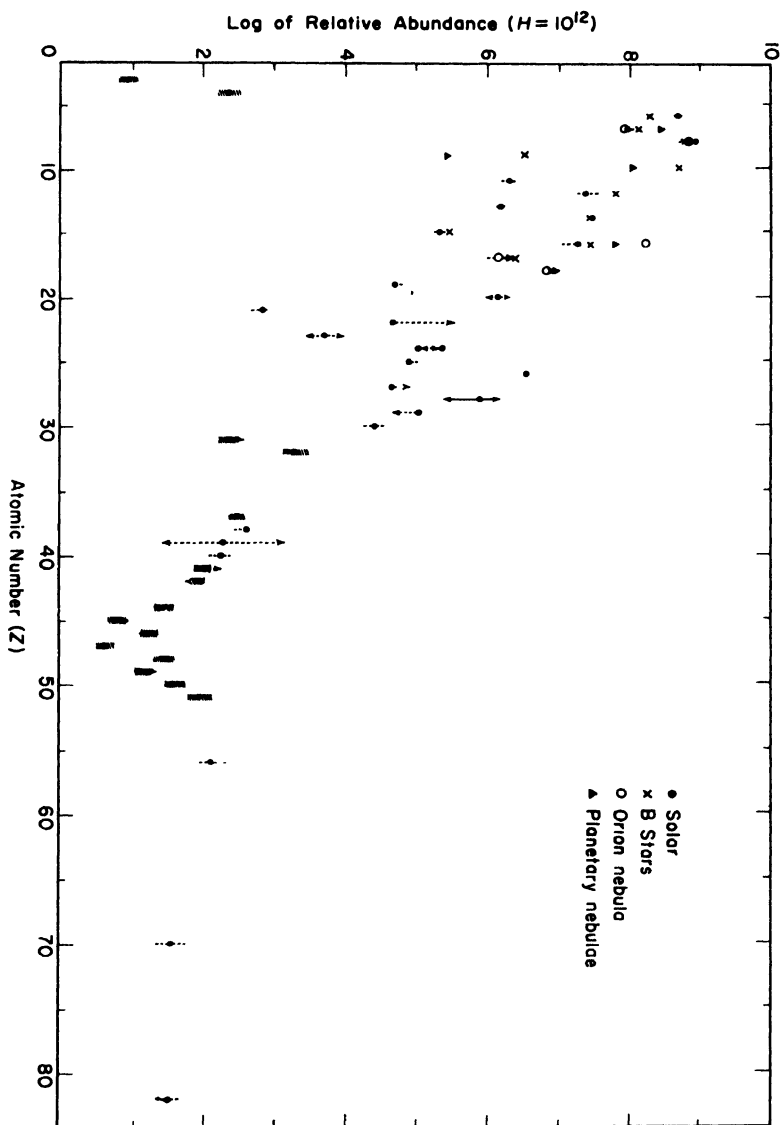
Apparently Frank Wigglesworth Clarke (1889) was the first to consider the problem of the relative abundance of the elements. From analyses of rocks of the earth's crust he showed that all abundant elements were of relatively low atomic weight. Iron was the heaviest of the abundant elements. The noble metals and familiar heavy elements such as mercury, lead, and bismuth were rare. When he plotted observed abundance against atomic weight, Clarke found no correlation between an element's abundance and its position in the periodic table. Of course, we now know that no such correlation is to be expected since the abundance of a particular atomic nucleus depends on its inherent stability and binding energy and also on the

effectiveness of the nuclear process by which it is believed to have been formed.

As the accuracy of analyses improved it was possible to refine the estimates, until shortly after the beginning of the present century some of the principal qualitative features of the abundance picture became rather well established. An important step forward was made by V. M. Goldschmidt (1937) who compiled the first modern table of cosmic abundances. He realized that chondritic meteorites probably represented the best available sample of the non-volatile constituents of the solar system.

One of the first regularities noted was that pointed out by Oddo in 1914, namely, that elements whose atomic weights when rounded off to the closest integer are divisible by four make up most of the lithosphere. The rule of Oddo is even more impressive if we consider the solar and stellar abundances of the elements He, C, O, Ne, Mg, Si, S, Ar, Ca, and Fe (see Table 5-4). A somewhat more fundamental relationship, however, is that known as "Harkins' rule." In 1917 Harkins observed that the seven most abundant elements found in some four hundred odd meteorites, viz., O, Si, Mg, S, Ca, Ni, and Fe, have even- Z 's. They make up more than 98 per cent of the meteoritic matter. The same rule holds for the lithosphere, although less impressively, and the deviations have been cited as proof that the lithosphere was produced by selective geochemical processes acting to concentrate the lithophile elements (cf. Chap. 3). Furthermore, nuclides of even- N are more abundant than those of odd- N . Subsequently, Suess (1947) noted that isobars of even- A tend to be more abundant than isobars of odd- A , and that the sum of the abundances of consecutive even- A isobars always exceeds the sum of the "cosmic" abundances of consecutive odd- A isobars.

The foregoing abundance rules are not accidental; they are what might be expected from the shell model of the nucleus. The abundances may be plotted against atomic weight, (mass number) A , atomic number, Z , or the number of neutrons, N . Each type of plot has its own advantages, e.g., a plot of abundance against A shows the relative proportions of various isotopes of a given element. A plot of elemental abundances is usually prepared first, since relative abundances of elements are normally open for adjustment, the terrestrial isotope abundances being well known from the mass spectrometric studies.



If one examines a plot of relative abundance of various nuclear species (nuclides) against the mass number, several general characteristics become evident. Details differ a little, of course, depending on the source of data employed, for example, that of Brown (1949), that of Suess and Urey (1956), or that of Cameron (1959). Hydrogen and helium are by far the most abundant elements in the universe; then follow in number the elements of the latter half of the first row of the periodic table, C, N, O, and Ne. The abundance declines as mass number increases, but not uniformly. Immediately following hydrogen and helium there is a deep minimum corresponding to the light nuclei of deuterium, lithium, beryllium, and boron. Then there is the strong maximum of the oxygen group of elements followed by an irregular decline to about $A = 45$ (near scandium). Thereafter follows a conspicuous peak at iron followed again by a steep decline to gallium and germanium. Then, in a rough way, up to about $A = 105$, the abundance falls off exponentially with A . Thereafter, the decline of abundances is very much slower and extremely irregular.

In addition to these general behavioral characteristics of the nuclides, there are details in the plot that are of considerable interest. Harrison Brown's results, for example, show maxima at arsenic, zirconium, tin, tungsten, platinum, and lead. Certain of these abundance peaks are connected with magic numbers. In the solar data some of the peaks are less conspicuous or are replaced by others. In the compilation by Suess and Urey, tellurium is more prominent than tin, barium and xenon are important, and lead is less abundant than osmium, iridium, or platinum. Cameron postulates a high lead abundance. Some of the differences between various abundance compilations must be attributed to errors in the methods of analysis; others simply arise from differing opinions of compilers. A basic task in a compilation of a fundamental cosmic abundance table is to disentangle natural regularities from results of poor analyses.

Fig. 8-1. Abundances of elements in the sun, gaseous nebulae, and stars. The dots represent solar values; crosses represent *B* stars; triangles, planetary nebulae; open circles, Orion nebula. Shaded areas around dots indicate roughly uncertainties due to measured line intensities, dotted lines those due to *f*-values for elements observed in the sun. The "error flags" are intended to convey the order of magnitude of uncertainties, not their actual values. Hydrogen and helium are not plotted on this graph.

Compilations of tables of nuclide abundances are difficult because chemical actions tend to separate neighboring elements of differing properties. Hence analyses of meteorites, rocks of the earth's crust, etc., all suffer from unknown influences of these agencies. The astrophysical situation is not impressively better because of errors introduced by uncertainties in f -values, blending, and inaccuracies in stellar model atmospheres.

8-2. The Suess-Urey Semi-Empirical Abundance Tabulation

That definite regularities must exist in the primordial abundances of the elements is strikingly illustrated by the behavior of the so-called rare earths. See Fig. 8-2 and Table 8-1. These lanthanides have chemical affinities that are so alike that their separation by conventional chemical methods is exceedingly difficult. In fact they are almost as difficult to separate from one another as are isotopes of the same element. The lanthanides show a rhythmic alternation of abundances between even and odd atomic numbers and, furthermore, the abundance changes with Z in a systematic manner. Suess recognized that this smooth pattern meant that this type of behavior of nuclides ought to hold in general, and that variations of abundances of isotopes of each successive element could throw light on the over-all abundance pattern of elements. Suess and Urey base their compilation of abundances ultimately upon the regularities suggested by the lanthanide nuclides. They remark:

Accordingly, it is assumed that the relative abundances of all isotopic species are meaningful and not the result of "chance" variations. This assumption is shown to be valid in nearly all cases, and of course, we believe that it is true in all cases even though quite frankly we do not always see that this must be true. We do not pretend to understand fully the regularities and irregularities which we present. It might well be that the abundances of the nuclides of odd mass, for example, follow a rough curve with the individual nuclides falling above or below this curve in an irregular way. For the most part we believe that this is not the case but that the isotopic abundances of the elements determined the slope of the curves surprisingly closely and especially the slope of the odd mass curve. Also the curves for the logarithms of the abundances of the even and odd mass elements follow curves which are displaced over most of the mass range by nearly a constant amount relative to each other when properly interpreted.

As sources of their empirical data of abundances, Suess and Urey relied on astrophysical determinations for many light elements, and primarily information from chondritic meteorites for heavier ele-

ments. Their data on lead, for example, are taken exclusively from meteoritic data where E. Goldberg and H. Brown (1950) found that this element was fifty times less abundant than had previously been assumed. Suess and Urey carefully described the sources from which their data are compiled; we summarize here some of the main points of their discussion. The abundances are normalized with respect to silicon as 10^6 . On this scale, the ratio of hydrogen to silicon is about 4×10^4 . The atomic abundances of lithium, 100, and beryllium, 20, are adopted from silicate meteorites; that of boron, 24, is taken from terrestrial data.

Suess and Urey selected the abundances of carbon, nitrogen, oxygen, and neon from astrophysical sources. They took the atomic abundance of fluorine from terrestrial and meteoritic data as 1600, a value somewhat smaller than that derived from the gaseous nebulae. Very extensive and good analyses are available for the elements from sodium to iron, both for the earth's crust and for meteorites. Suess and Urey adopted the abundances of Na, Mg, Al, and Si from Wiik's (1956) results for meteorites. Since his analyses were carried out by the best modern techniques of analytical chemistry, they are probably the best available data for meteorites. These elements are observed not only in the sun but also in the hot stars where their abundances have been derived by several investigators (Chap. 5). Suess and Urey noticed that astrophysically derived abundances of phosphorus, sulfur, and chlorine were considerably higher than the meteoritic values, so they chose an approximate astronomical abundance for phosphorus and an abundance intermediate between the astrophysical and meteoritic value for sulfur. For chlorine, they selected a value as high as they could and yet retain "a reasonable separation of the odd and even mass curves." Suess and Urey interpolated Ar^{36} and Ar^{40} between S and Ca, since the Ar^{40} in the earth's atmosphere has been enriched by the decay of K^{40} . The atmospheric krypton/xenon ratio, however, may be the same as the original solar system value.

They used Wiik's results to establish the abundances of Ca, Ti, Cr, and Mn, and the compilations by Urey and Craig for chondritic meteorites for Fe, Co, and Ni.

Certain important abundance ratios are supplied by chemically similar elements that go along together in successive fractionation processes e.g., the halogens, K and Rb, S and Se. For example, the

well-established titanium/zirconium/hafnium ratios appear to be nearly the same in meteorites and the earth's crust. Thus the atomic abundance Ti/Zr ratio is about 45, whereas the similar Zr/Hf ratio is about 110. The S/Se ratio similarly should be useful, but sulfur

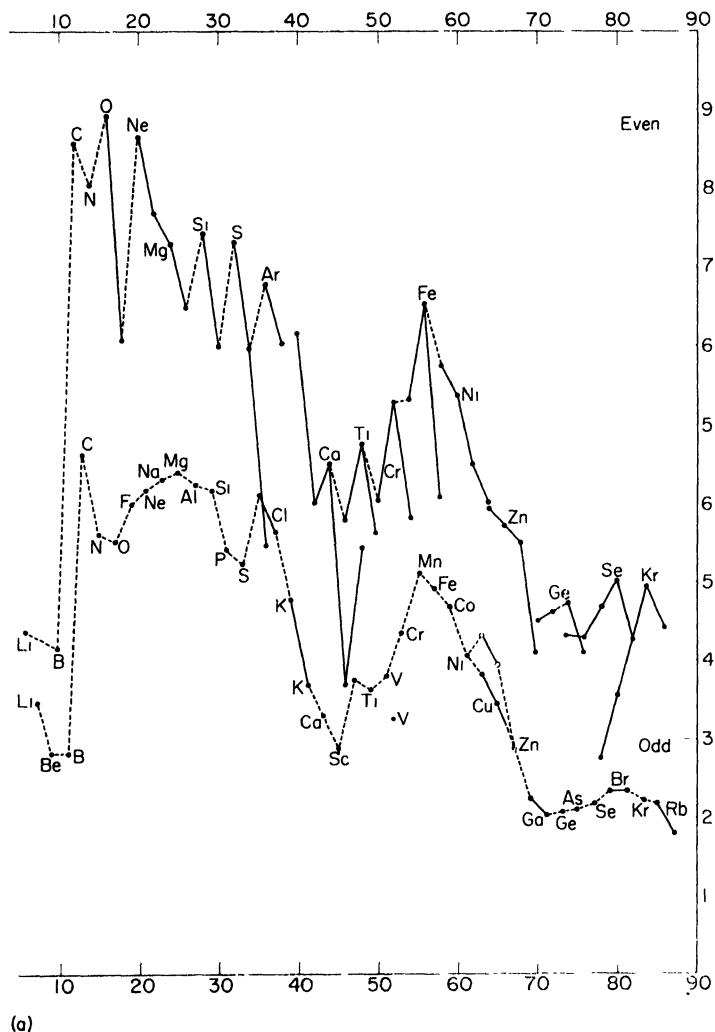


Fig. 8-2. (a) Lighter elements abundance plotted vs. log A.

may have been lost from the meteorites preferentially. Suess and Urey took 67.6 as the atomic abundance of selenium and simply interpolated the tellurium abundance. They used the ratio of chlorine to bromine derived from an analysis of sea water to secure the atomic

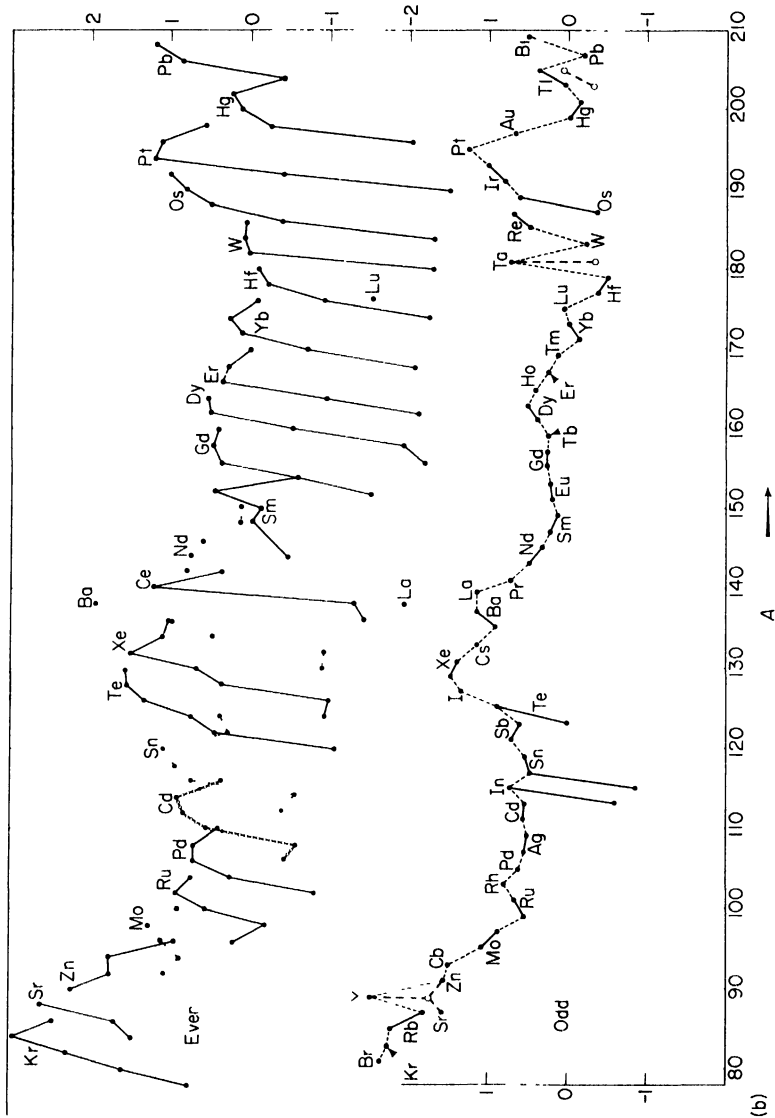


Fig. 8-2. (b) Heavier elements. The odd and even nuclides are plotted separately.

bundance of bromine. The Br/I ratio, however, is affected by the sage of iodine by marine organisms. The K/Rb ratio was employed get Rb. Also the nickel/gold and nickel/palladium ratios derived rom siderites were useful for fixing the abundances of the heavier metals in the high-mass range.

For many elements, abundances were chosen on the basis of the analytical results from chondritic meteorites, e.g., Cu, Ga, As, Sr Mo Sb, Nb, Th, and Bi. Abundances of certain other elements, e.g., Ag, In, I, Cs, Ta, W, and Hg, were essentially interpolated between neighboring elements to provide smooth abundance curves.

The lanthanide rare earths should stay close to one another in the rocks of the earth's crust and hence it should be possible to obtain reliable relative abundances for them. Unfortunately, there are large discordances, possibly due to analytical errors, between the results obtained by Ida Noddack (1935) from meteorites and those found by E. Minami (1935) on sedimentary rocks which should give a good average for the earth's crust. Suess and Urey selected Minami's values with a few slight adjustments, and then adjusted the abundance of the group as a whole to secure "a reasonable interpolation to the abundances of the lower and higher mass elements." They adopted the abundance of hafnium from the Zr/Hf ratio (as mentioned above) and estimated the abundances of rhenium, osmium, indium, and platinum on the basis of the meteoritic data, assuming that the latter three elements were concentrated in the iron phase.

Lead, uranium, and thorium present a special problem since the lead found associated with U and Th represents a mixture of original lead "urblei" and radiogenic lead. Hence the isotopic structure of the lead must be studied and the separation of the two components obtained. Metallic lead will not dissolve in iron but may go along with the silicates or sulfides. In iron meteorites the lead is concentrated in the sulfide phase. Suess and Urey assumed that the isotopic composition of original lead corresponded to this sulfide phase. The U and Th were separated from the lead at the time the meteorites were formed. If we took a sample of a chondrite and determined the amount of U and Th present and the isotopic composition of the lead, it would be possible to estimate the age of the sample and the amount of original lead present when the meteorite was formed. In this way Suess and Urey obtained an atomic abundance for lead of about 0.1.

Table 8-1. Abundances of Nuclides^a

Element	<i>A</i>	<i>N</i>	<i>I</i>	log <i>A</i>	log <i>N</i>
H	1	0	-1	12.00	12.00
	2	1	0		12.00
He	3				8.15
	4				11.21
Li	6	3	0	3.50	2.37
	7	4	1		3.47
Be	9	5	1	2.80	
B				2.88	
	10	5	0		2.15
C	11	6	1		2.79
	12	6	0	8.60	8.58
N	13	7	1		6.63
	14	7	0	8.05	8.05
O	15	8	1		5.61
	16	8	0	8.95	8.95
F	17	9	1		5.52
	18	10	2		6.06
Ne	19	10	1	6.0	6.0
	20	10	0	8.70	8.66
Na	21	11	1		6.18
	22	12	2		7.69
Mg	23	12	1	6.30	
	24	12	0	7.40	7.30
Al	25	13	1		6.40
	26	14	2		6.44
Si	27	14	1	6.22	
	28	14	0	7.50	7.46
P	29	15	1		6.17
	30	16	2		5.99
S	31	16	1	5.40	
	32	16	0	7.35	7.33
	33	17	1		5.22
	34	18	2		5.97
	36	20	4		3.49

(Continued)

Table 8-1.—Continued

Element	<i>A</i>	<i>N</i>	<i>I</i>	log <i>A</i>	log <i>N</i>
Cl				6.25	
	35	18	1		6.12
	37	20	3		5.64
Ar				6.88	
	36	18	0		6.80
	38	20	2		6.08
	40	22	4		
K				4.82	
	39	20	1		4.79
	40	21	2		0.90
	41	22	3		3.66
Ca				6.19	
	40	20	0		6.18
	42	22	2		4.00
	43	23	3		3.30
	44	24	4		4.52
	46	26	6		1.70
	48	28	8		3.44
Sc	45	24	3	2.85	
Ti				4.89	
	46	24	2		3.79
	47	25	3		3.78
	48	26	4		4.75
	49	27	5		3.63
	50	28	6		3.61
V				3.82	
	50	27	4		1.22
	51	28	5		3.82
Cr				5.38	
	50	26	2		4.03
	52	28	4		5.30
	53	29	5		4.36
	54	30	6		3.80
Mn	55	30	5	5.12	
Fe				6.57	
	54	28	2		5.34
	56	30	4		6.56
	57	31	5		4.92
	58	32	6		4.09
Co	59	32	5	4.75	
Ni				5.95	
	58	30	2		5.78
	60	32	4		5.37

Table 8-1.—Continued

Element	<i>A</i>	<i>N</i>	<i>I</i>	log <i>A</i>	log <i>N</i>
	61	33	5		4.04
	62	34	6		4.51
	64	36	8		4.01
Cu				4.50	
	63	34	5		4.33
	65	36	7		3.99
Zn				4.28	
	64	34	4		3.97
	66	36	6		3.72
	67	37	7		2.89
	68	38	8		3.55
	70	40	10		2.11
Ga				2.45	
	69	38	7		2.23
	71	40	9		2.05
Ge				3.20	
	70	38	6		2.52
	72	40	8		2.64
	73	41	9		2.08
	74	42	10		2.77
	76	44	12		2.09
As				2.11	
Se				3.33	
	74	40	6		2.31
	76	42	8		2.30
	77	43	9		2.20
	78	44	10		2.70
	80	46	12		3.03
	82	48	14		2.28
Br				2.65	
	79				2.35
	81				2.34
Kr				2.21	
	78	42	6		0.76
	80	44	8		1.56
	82	46	10		2.27
	83	47	11		2.26
	84	48	12		2.97
	86	50	14		2.45
Rb				2.35	
	85	48	11		2.21
	87	50	13		1.79

(Continued)

Table 8-1.—Continued

Element	<i>A</i>	<i>N</i>	<i>I</i>	log <i>A</i>	log <i>N</i>
Sr				2.70	
	84	46	8		1.45
	86	48	10		1.68
	87	49	11		1.54
	88	50	12		2.61
Y	89	50	11	2.45	
Zr				2.50	
	90	50	10		2.21
	91	51	11		1.55
	92	52	12		1.73
	94	54	14		1.74
	96	56	16		0.94
Cb	93	52	11	1.50	
Mo				1.88	
	92	50	8		1.06
	94	52	10		0.85
	95	53	11		1.08
	96	54	12		1.10
	97	55	13		0.87
	98	56	14		1.26
	100	58	16		0.87
Ru				1.44	
	96	52	8		0.20
	98	54	10		-0.21
	99	55	11		0.55
	100	56	12		0.55
	101	57	13		0.67
	102	58	14		0.94
	104	60	16		0.70
Rh	103	58	15	0.80	
Pd				1.26	
	102	56	10		-0.84
	104	58	12		0.23
	105	59	13		0.61
	106	60	14		0.69
	108	62	16		0.69
	110	64	18		0.39
Ag				0.82	
	107	60	13		0.54
	109	62	15		0.51
Cd				1.45	
	106	58	10		-0.46
	108	60	12		-0.60
	110	62	14		0.54

Table 8-1.—Continued

Element	<i>A</i>	<i>N</i>	<i>I</i>	log <i>A</i>	log <i>N</i>
In	111	63	15	0.75	0.56
	112	64	16		0.83
	113	65	17		0.54
	114	66	18		0.91
	116	68	19		0.33
Sn	113	64	15	1.57	−0.63
	115	66	17		0.73
	112	62	12		−0.42
	114	64	14		−0.59
	115	65	15		−0.88
Sb	116	66	16	0.95	0.73
	117	67	17		0.46
	118	68	18		0.95
	119	69	19		0.51
	120	70	20		1.09
Te	122	72	22	2.05	0.25
	124	74	24		0.35
	121	70	19		0.71
	123	72	21		0.58
	120	68	16		−1.06
I	122	70	18	1.35	0.44
	123	71	19		−0.00
	124	72	20		0.72
	125	73	21		0.90
	126	74	22		1.32
Xe	128	76	24	2.06	1.59
	130	78	26		1.58
	127	74	21		
	124	70	16		−0.96
	126	72	18		−0.99
Cs	128	74	20	1.16	0.34
	129	75	21		1.48
	130	76	22		0.67
	131	77	23		1.39
	132	78	24		1.49
	134	80	26		1.08
	136	82	28		1.01
	133	78	23		

(Continued)

Table 8-1.—Continued

Element	<i>A</i>	<i>N</i>	<i>I</i>	log <i>A</i>	log <i>N</i>
Ba				2.08	
	130	74	18		−0.91
	132	76	20		−0.93
	134	78	22		0.47
	135	79	23		0.90
	136	80	24		0.97
	137	81	25		1.14
La	138	82	26		1.94
				1.10	
	138	81	24		−1.95
Ce	139	82	25		1.10
				1.29	
	136	78	20		−1.42
	138	80	22		−1.31
	140	82	24		1.24
Pr	142	84	26		0.34
	141	82	23	0.66	
Nd				1.36	
	142	82	22		0.79
	143	83	23		0.44
	144	84	24		0.74
	145	85	25		0.28
	146	86	26		0.59
	148	88	28		0.11
Sm	150	90	30		0.11
				0.89	
	144	82	20		−0.51
	147	85	23		0.17
	148	86	24		−0.04
	149	87	25		0.09
	150	88	26		−0.14
	152	90	28		0.42
Eu	154	92	30		−0.66
				0.48	
	151	88	25		0.16
Gd	153	90	27		0.20
				1.05	
	152	88	24		−1.54
	154	90	26		−0.61
	155	91	27		0.22
	156	92	28		0.37
	157	93	29		0.25
	158	94	30		0.45
	160	96	32		0.39

Table 8-1.—Continued

Element	<i>A</i>	<i>N</i>	<i>I</i>	log <i>A</i>	log <i>N</i>
Th	159	94	29	0.25	
Dy				1.08	
	156	90	24		-2.20
	158	92	26		1.96
	160	94	28		-0.56
	161	95	29		0.36
	162	96	30		0.49
	163	97	31		0.48
	164	98	32		0.53
Ho	165	98	33	0.39	
Er				0.84	
	162	94	26		-2.16
	164	96	28		-0.99
	166	98	30		0.36
	167	99	31		0.22
	168	100	32		0.27
	170	102	34		-0.01
Tm	169	100	31	0.08	
Yb				0.78	
	168	98	28		-2.08
	170	100	30		-0.74
	171	101	31		-0.06
	172	102	32		0.12
	173	103	33		-0.01
	174	104	34		0.28
	176	106	36		-0.10
Lu				0.06	
	175	104	33		0.05
	176	105	34		-1.53
Hf				0.40	
	174	102	30		-2.38
	176	104	32		-0.93
	177	105	33		-0.37
	178	106	34		-0.21
	179	107	35		-0.50
	180	108	36		-0.09
Ta	181	108	35	0.75	
W				0.60	
	180	106	32		-2.31
	182	108	34		0.02
	183	109	35		-0.25
	184	110	36		0.08
	186	112	38		0.05

(Continued)

Table 8-1.—Continued

Element	<i>A</i>	<i>N</i>	<i>I</i>	log <i>A</i>	log <i>N</i>
Re				0.90	
	185	110	35		0.47
	187	112	37		0.70
Os				1.40	
	184	108	32		-2.34
	186	110	34		-0.40
	187	111	35		-0.38
	188	112	36		0.52
	189	113	37		0.61
	190	114	38		0.82
	192	116	40		1.01
Ir				1.20	
	191	114	37		0.79
	193	116	39		0.99
Pt				1.70	
	190	112	34		-2.51
	192	114	36		-0.41
	194	116	38		1.22
	195	117	39		1.23
	196	118	40		1.11
	198	120	42		0.56
Au	197	118	39	0.66	
Hg				0.75	
	196	116	36		-2.05
	198	118	38		-0.25
	199	119	39		-0.02
	200	120	40		0.12
	201	121	41		-0.13
	202	122	42		0.23
	204	124	44		-0.41
Tl				0.55	
	203	122	41		0.02
	205	124	43		0.40
Pb				1.50	
	204	122	40		-0.37
	206	124	42		0.89
	207	125	43		-0.17
	208	126	44		1.22
Bi	209	126	43	0.50	
Th	232	142	52	0.00	
U				-0.30	
	235	143	51		
	238	146	54		

* The second column gives the atomic weight, A , the third column the number of neutrons, N , the fourth column the neutron excess, I , the fifth column the logarithm of the abundance $\log A$, and the last column $\log N$, the logs of the abundance of the individual nuclides. The entries are adopted from the compilation by Suess and Urey (1956) but with the revised abundances.

The finally derived abundances show the influences of the magic numbers. Suess and Urey found a minimum in the curve in the region on the low-mass side of the neutron number 50 and a similar minimum below neutron number 82. The curves indicate a maximum at bromine and a minimum at germanium. Broad maxima in the abundance curves near mass numbers 130 and 194 are attributed to magic-number effects of shell closures at $N = 82$ and $N = 126$ from a neutron buildup. Several features of the distribution cannot be explained in terms of the simple shell model, e.g., the maximum at 58, the break at $A = 120$ and 121, and the sharp minima around mass numbers 135 and 206 immediately preceding the $N = 82$ and $N = 126$ shell closures.

There is a marked qualitative difference in the behavior of nuclides beyond zirconium. In lighter atoms the sum of the isobaric abundances of the even- A nuclides fluctuates irregularly from one A -value to the next, and the abundances are strongly dependent on the neutron excess. Nuclides with a smaller neutron excess tend to be favored. Beyond zirconium, the heavier isotopes of a given element (nuclides with greatest neutron excess) are the more abundant. The abundance of the isobar with lower neutron excess (the so-called shielded isobar) is appreciable only if this isobar has a considerably greater binding energy than has the unshielded one.

The general impression that one obtains is that the heaviest elements were formed by processes that tended to favor nuclides with an excess of neutrons, the lighter nuclides by processes that formed the neutron-deficient nuclei. A process of neutron capture followed by β -decay would account for the neutron-rich nuclei but not the shielded isobars. In the intermediate range between iron and strontium, the odd- A nuclides fall on a smooth curve, whereas the even- A nuclides show an irregular behavior. On the other hand, if one draws lines connecting nuclei with the same neutron excess a smooth dependence will be found. That is, in regions between nucleon numbers where shells are closed, the binding energy will be a smooth

function of mass number for nuclides with the same neutron excess. Suess and Urey regard the smoothness of this pattern as indicative of an essential connection between binding energy and cosmic abundance. The odd- A abundance curve shows no correlation of abundances with neutron excess.

8-3. Cameron's Abundance Compilation and Nucleogenesis

The Suess-Urey abundance compilation is semi-empirical. It is based partly on measured abundances and where these are deemed unreliable, the abundances are based upon considerations of nuclear stability. A yet more theoretical point of view is that taken by Cameron whose abundance table has been constructed with attention to theories of nucleogenesis.

He chose the Suess-Urey abundance for many elements, viz., Li, Be, B, F, Na, Mg, Al, Si, P, S, K, Ca, Sc, Ti, V, Cr, Mn, Co, Ni, Cu, Rb, Y, Mo, Pd, Ag, Cd, In, Sn, Cs, Ba, and Au. The abundances of other elements were adjusted for a variety of reasons. Those whose adopted abundances were reduced with respect to the Suess-Urey results are Ne, Cl, Fe, Se, Ru, Te, I, Ga, Ge, As, Br, Kr, Zr, Nb, La, Ce, Eu, Sm, Pr, Nd, Lu, Hf, Ta, W, Re, Os, and Ir. On the other hand, the adopted abundances of Tb, Dy, Ho, Yb, Hg, Er, Tm, Sr, Tl, and especially Pb were enhanced. He chose a selenium abundance about 28 per cent that of Suess and Urey on the basis of new analyses. The abundance of zinc was reduced to make Zn^{67} fall on a smooth odd mass-number curve. Abundances of As, Br, Ru, Re, Yb, Lu, Ir, Pt, and Tl were fixed by interpolation between their neighbors on the basis of capture cross section for neutrons. Strontium and zirconium abundances 3 and 0.25 times the Suess-Urey values were chosen on the basis of nucleogenesis arguments. Element building on the fast time scale leads to a peak corresponding to the closed shell at 82 neutrons. The group Xe, I, Te, and Cs may be fitted together relatively easily but the main difficulty is to fit this group with the other elements. Cameron concluded that no accurate way of interpolating the Kr abundance existed so he used the "by passed" isotopes to interpolate the abundances.

Selenium, barium, and hafnium were chosen as "fixed points" for the abundance curve and the rare earth abundances were tied in by a consideration of the relative neutron-capture cross sections for Ba^{138} and La^{139} . Cameron chose Noddack's abundances for the rare

earths rather than those of Minami, but he concluded that ytterbium and lutecium were too high relative to the trend of anticipated results so Yb and Lu were interpolated between Er and Hf. The abundance of uranium was taken from the analysis by Hamagouchi, Reed, and Turkevich (1957), that of thorium from the analyses by Bate, Huizenga, and Potratz (1957) for chondrites. The abundance of mercury was fixed by nuclear-physics arguments, while Cameron concluded that the meteoritic abundance of bismuth is too low to accord with nucleogenesis arguments so its abundance is estimated on the basis of theories of element building. On the basis of his theory of element building Cameron adopted a lead abundance which is somewhat larger than the amount of lead found in meteorites and apparently in the sun also.

Cameron's abundance scale gives a peak at 165 that is more prominent and more symmetrical than in the Suess-Urey adjustment. He believes that this peak results from the fission of very heavy nuclei on the fast time scale after nuclear capture stopped.

The abundance table proposed by Cameron is of interest in that it represents a systematic attempt to construct a scale on the basis of theories of nucleogenesis. Unfortunately, the relevant physical parameters, neutron capture, and photodisintegration cross sections, etc., as well as the conditions in the element-building crucible are insufficiently known to permit a calculation of reliable theoretical abundances. The treatment is not fully satisfactory from another point of view. Several of the abundances adopted by Cameron are in disaccord with astronomical data. For example, compare the concentrations of Ne, S, Cl, and Ar ($O = 10,000$) given in Table 8-2. See also the discussions by Burbidge (1960) and Cameron (1960). Results for lead are still in doubt. The most reliable lead abundance is probably that derived from carbonaceous chondrites (Reed

Table 8-2. Comparison of Abundances

	Planetary nebulae	Orion nebula	γ Pegasi	Cameron compilation
Ne	1,500	12,000	12,600	32
S	900	2,500	1,500	150
Cl	34	20	42	1.05
Ar	130	100	190	60

Kigoshi, and Turkevich 1960) which is around five times smaller than that suggested by Cameron and somewhat greater than the adopted solar value. If the experimental f -values of lead are as much in error as recent (unpublished) theoretical calculations indicate, the solar abundance of Pb may be higher and closer to Cameron's result.

8-4. An Abundance Compilation Based Primarily on Astrophysical Data

We now attempt to compile a table of atomic abundances for the primordial solar system. We pay special regard to the astronomical data, particularly for establishment of certain fixed points, e.g., the elements of the first two rows of the periodic table, iron and its associated elements, the strontium group, barium, and lead. The general run of abundances is then established in a rough way and proportions of other elements are allocated from a comparison of astrophysical, meteoritic, and other data.

For heavier elements the astronomical record is inevitably incomplete, and any attempt to draw up a composition table for the solar system must necessarily depend on data obtained from meteorites and the earth's crust. In the present compilation I have been strongly influenced by the method of Suess and Urey. For elements for which solar or stellar data were missing or questionable, I have tended to accept their proposed abundances as the basis for further adjustments. The rare earths provide one exception; for them I have adopted the relative abundances in the chondritic meteorites Allegan and Richardson as given by Schmitt et al. (1960) (see Fig. 8-3 and Table 8-3).

The general procedure has been to make a "best" initial estimate. Then the abundances of the isotopes of odd and even atomic numbers are plotted separately and the trends of the curve noted. Since, in most instances, the adopted abundances agree closely with those of Suess and Urey, the same general features are retained, but there are a few exceptions and irregularities. For several elements, revisions in the initial estimates are suggested. The extremely tentative nature of this compilation must be emphasized; it still depends on highly uncertain data, particularly for heavier elements.

For elements lighter than potassium I have relied almost entirely on the astronomical data described in Chap. 5. Lithium, beryllium, and boron are excepted since the solar concentration of these elements is affected by thermonuclear processes at the bottom of the solar

convection zone. Hence the Suess-Urey values are accepted for them. The carbon and nitrogen data are adopted from the results for the sun and *B* stars. The sun and *B* stars are in fairly good agreement for oxygen, but here I have accepted the solar data.

The abundance of fluorine is highly uncertain. It is not observed in the Orion nebula and has been found only in NGC7027 among

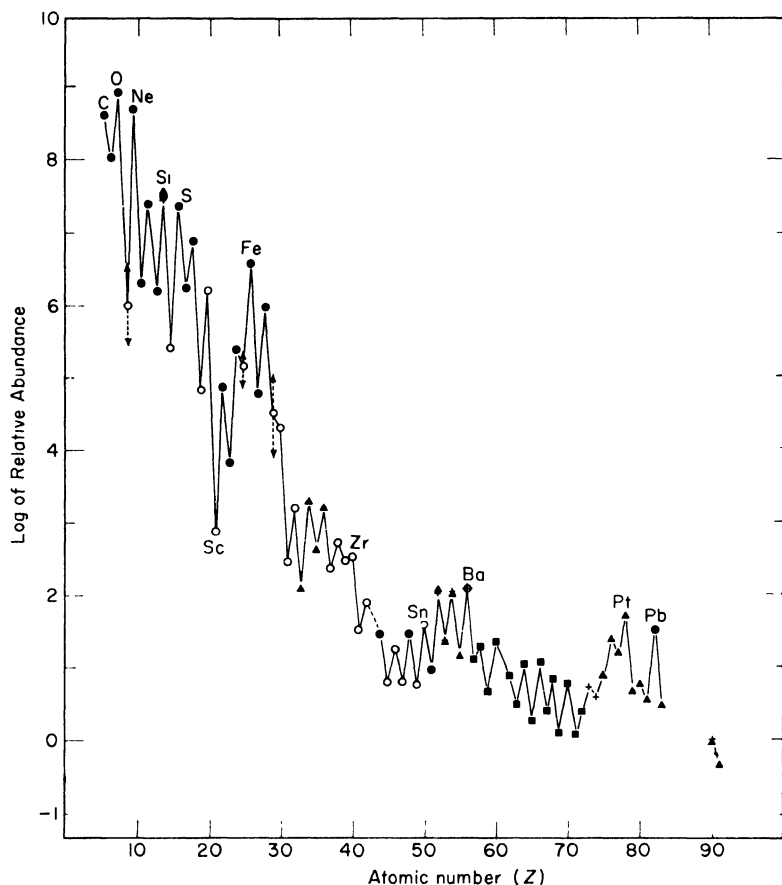


Fig. 8-3. Abundance scale for the solar system. The closed circles represent numbers based primarily on solar (or stellar) data; open circles represent data from Suess and Urey (or in a few instances from Cameron) and the sun; triangles represent Suess and Urey or Cameron data; and squares data from chondritic meteorites according to Schmitt et al.

Table 8-3. Abundance Scale for Solar System

Element	log N	Source	Δ
H	12.00	S, B, O	
He	11.21	O, B	
Li	3.50	U	
Be	2.80	U	
B	2.88	U	
C	8.60	S, B	
N	8.05	S	
O	8.95	S	
F	6.0	B, U	1.8
Ne	8.70	B	0.25
Na	6.30	S	0.16
Mg	7.40	S	-0.06
Al	6.22	S, B	-0.28
Si	7.50		
P	5.40	S, U	0.00
S	7.35	S, B	0.33
Cl*	6.25	O, B	0.76
Ar	6.88	O, B	0.24
K	4.82	S, U	-0.30
Ca	6.19	S, U	-0.04
Sc	2.85	S, U	-0.13
Ti	4.89	U	-0.21
V	3.82	U, S	-0.14
Cr	5.38	U, S	-0.03
Mn	5.12	U, S	0.43
Fe	6.57	S	-0.71
Co	4.75	U, S	-0.11
Ni	5.95	U, S	0.11
Cu*	4.50	U, S	1.22
Zn	4.28	S, U	0.20
Ga	2.45	U, S	-0.14
Ge	3.20	U, S	0.09
As	2.11	U	
Se	3.33	U	
Br	2.65	U	
Kr	3.21	U	
Rb	2.35	S, U	0.17
Sr	2.70	U, S	-0.18
Y*	2.45	U	
Zr	2.50	S, C	-1.0
Cb	1.50	U	.45
Mo	1.88	U, S	0.02
Ru	1.44	C, S	
Rh	0.80	U, S	
Pd	1.26	U, S	
Ag	0.82	U, S	-0.28

Table 8-3.—Continued

Element	$\log N$	Source	Δ
Cd	1.45	U, S	0.01
In	0.75	U, S	0.62
Sn	1.57	U, S	
Sb	0.95	U, S	1.05
Te	2.05	C, U	
I	1.35	C, U	
Xe	2.06	C, U	
Cs	1.16	C, U	
Ba	2.08	S, U	
La	1.10	Sc	
Ce	1.29	Sc	
Pr	0.66	Sc	
Nd	1.36	Sc	
Sm	0.89	Sc	
Eu	0.48	Sc	
Gd	1.05	Sc	
Tb	0.24	Sc	
Dy	1.08	Sc	
Ho	0.39	Sc	
Er	0.84	Sc	
Tm	0.08	Sc	
Yb	0.78	Sc	
Lu	0.06	Sc	
Hf	0.40	C	
Ta*	0.75	C, U	
W	0.60	C	
Re	0.90	C, U	
Os	1.40	C, U	
Ir	1.20	C	
Pt	1.70	C	
Au	0.66		
Hg	0.75		
Tl	0.55		
Pb	1.50	S	
Bi	0.50		
Th	0.00		
U	-0.30		

Source of data:

B = B star data (Chap. 5).

C = Cameron (1959).

O = Orion nebula (Liller-Aller 1959 Chap. 4).

S = Sun (Goldberg-Müller-Aller 1960 see Chap. 5).

Sc = Schmitt et al. (1960).

U = Suess-Urey (1956).

 Δ = Solar or stellar (Suess-Urey).

* = Tabulated values are revised; see text.

planetaries. In this compilation I have generally avoided data from the planetaries. These nebulae are believed to be objects of population type II whose evolutionary history is obscure. Hence their chemical compositions might represent effects of nuclear processes occurring within the stars (cf. Chaps. 9 and 10). Weak fluorine lines are observed in the spectrum of γ Pegasi. The tabulated value is a sort of compromise between the γ Pegasi result (cf. Chap. 5) on the one hand, and the Suess-Urey and planetary-nebula result on the other. The data for neon are taken from *B* stars, which indicate that this element is nearly as abundant as oxygen. For Na, Mg, P, and Al, solar and stellar data are used. The abundance of sulfur is based primarily on the solar value since its curves of growth for *B* stars show a deplorable scatter. The abundances of sulfur, chlorine, and argon may also be deduced from their forbidden lines in the gaseous nebulae, but the trouble here is that their cross sections for collisional excitation are not known. Calculations undertaken by Stanley Czyzak at the University of Michigan should soon remove this limitation and enable us to fix the astronomical abundances of these elements more accurately.

The chlorine abundance originally obtained in γ Pegasi seems much too high. A re-examination of the data suggests that a still highly uncertain value, $\log N = 6.2$, is a better guess. Nevertheless, the chlorine abundance adopted from this estimate and the Orion-nebula analysis (cf. Chap. 4) may still be too high by a factor of about 5. Yet the nebular data do not suggest a chlorine abundance as low as that of phosphorus. Strong forbidden chlorine lines are observed in a number of gaseous nebulae, but those of phosphorus have never been observed.

Forbidden argon lines are observed in the solar corona, but these are useless for abundance determinations. Hence it has been necessary to rely on results for the Orion nebula and *B* stars which seem to be in good accord. From potassium to nickel the solar and Suess-Urey abundances are in as good agreement as the uncertainties in the *f*-values would permit. A striking exception is iron for which various measurements of *f*-values are in good accord with one another. Iron appears to be relatively less abundant in the sun than in the chondritic meteorites, a result which poses a number of puzzling problems as has been emphasized by Urey. I have adopted the solar iron

abundance, but not without serious misgivings.¹ The solar abundance seems to agree with nucleogenesis arguments (Chap. 10, Fig. 2). Cameron has also adopted a low iron abundance.

The solar copper abundance is considerably higher than in the meteorites and Suess-Urey compilation; a further investigation of the f -values for this element is indicated. For zinc, gallium, and germanium there appears to be reasonably good accord between the Suess-Urey and solar abundances. No solar data are available for arsenic, selenium, bromine, and krypton, and I have adopted the Suess-Urey numbers. If the chlorine/bromine ratio from sea water is accepted as "cosmically" valid, then the above-suggested chlorine abundance is too high. On the other hand, if the astrophysical abundance of chlorine is correct, this ratio would imply that some of the primordial chlorine was preferentially lost from the earth. At the moment, the sea water ratio does not seem sufficiently reliable.

Rubidium and strontium are in fair agreement with the Suess-Urey results, but I cannot reconcile the solar strontium result with the value suggested by Cameron. The solar Sr value is obtained from two stages of ionization of this element, which give results in excellent accord with one another. The f -value situation for yttrium is one of complete chaos and lines arising from different levels yield results in discord with one another. For zirconium I have adopted a compromise between the solar and Cameron values. This number may be too small since our adopted f -values may be too large. The solar values for columbium (niobium), molybdenum, ruthenium, rhodium, palladium, silver, and cadmium are uncertain but are in as good agreement with the Suess-Urey values as could be expected. Silver is too low (which is hard to explain unless the adopted f -values are much too large), while indium and antimony are too high. Tellurium, iodine, and xenon are not observed in the sun, while cesium is observed only in sunspots and no data on line intensities are available.

The solar and Suess-Urey barium abundances are in good agreement, and I have used it as a "fixed" point in the abundance compilation for this reason. Recent work by Reed et al. suggests that

¹ The higher chondritic iron abundance may still be correct for the sun as well, if there are large deviations from thermodynamic equilibrium, errors in the f -values actually used, etc. Any process depleting iron in meteorites should also deplete other metals which, however, show no such effects as compared with the sun.

the barium abundance may have to be increased by a factor of two, however.

The rare earths present a perplexing problem. Their relative abundances can be established with some degree of reliability, but there seem to be some differences between the meteorite and terrestrial crustal-rock results. Some of the discordance may be real; but some of it may represent bad analyses of the meteorite material, or fractionation processes in the earth's crust. Minami (1935) obtained systematically different relative abundances for the rare earths in terrestrial shales than Noddack (1937) had found for stony meteorites. Both used X ray spectroscopic techniques. More recently, Schmitt, Mosen, Suffredini, Lasch, Sharp and Olchy (1960) determined the relative abundances of all rare earth elements (lanthanum to lutetium) in two chondritic meteorites by the neutron activation method. This powerful technique of analysis should give extremely accurate results. Actually it is possible to determine only the abundances of certain isotopes of each element. The final abundances of all elements are then derived by assuming that the terrestrial and meteoritic isotope ratios are the same. This conclusion seems substantiated by such checks as are available. Unfortunately, no solar-abundance determinations for these elements are available. The term analyses are incomplete and the f -values are unknown. Hence the solar lines cannot as yet be utilized.

An attempt was made at Michigan to estimate the solar abundance of ytterbium, but it now appears that the uncertainties are much greater than had been anticipated. Our solar abundance was obtained from only one line which appears to be unblended, but the derived abundance is ten times larger than the value adopted herein. The hafnium abundance is fixed from the Zr/Hf ratio. Tantalum, tungsten, rhenium, osmium, iridium, platinum, mercury, and thallium are not observed in the sun, while the f -value of the observed gold line has not been measured. Hence the abundances of these elements have to be estimated from the terrestrial and meteoritic data or by nucleogenesis hypotheses. Similarly, bismuth, thorium, and uranium are not observed in the sun. The platinum peak may be too high, or the rare earths may have been placed too low.

Fortunately, several lines of the strategically important element, lead, are observed in the sun, and we can draw some conclusions

concerning its abundance. The f -values of these lines have been measured by C. W. Allen and in the Soviet Union with results that are in good accord, but recent theoretical work suggests somewhat different values. A new investigation of solar lead lines by Paul Mutschlechner, who has taken into account the problem of blending in a stratified atmosphere, substantiates the low lead abundance found in the Michigan program. The chief uncertainty appears to lie in the f -value determination.

When the plots of the individual nuclides are examined, a number of irregularities are noted. As previously remarked, the stellar abundance of chlorine may be too high. If it is reduced by a factor of 5 to obtain a smoother curve, it is more nearly in accord with the Suess-Urey result. Likewise, a reduction of the copper abundance by a factor of about 3 would yield a smoother curve. Unless our adopted abundances for strontium and zirconium are much too low, the yttrium abundance ought to be reduced by about a factor of 5. Finally, a reduction of the tantalum abundance by a factor of 10 would appear reasonable.

The chief value of this particular compilation may lie in pointing out domains in which analyses should be improved. Of the solar and stellar data, which supply most of the information on light, volatile elements, we particularly need information on such elements as fluorine, chlorine, sulfur, and argon—elements whose lines are weak or for which the relevant atomic parameters are not yet known. We may add to the oft-repeated pleas for accurate f -values of abundant elements, a request for similar measurements of rarer, strategic metals, such as germanium, yttrium, zirconium, niobium, molybdenum, ruthenium, rhodium, palladium, silver, indium, tin, antimony, ytterbium, and gold. The faint solar lines of these rare elements have been measured at the McMath-Hulbert Observatory in an intensive program aimed at improving basic observational data, but such programs can be of little help unless reliable f -value measurements are supplied.

Abundance data for most elements will be greatly improved when modern analytical techniques, such as neutron activation methods, are applied to carbonaceous chondrites which, of all meteorites, have been least affected by heating and fractionation.

It seems very likely that the question of the primordial compo-

sition of the solar system will not be cleared up until actual samples of material from remote parts of the solar system (e.g., satellites of distant planets) are analyzed with space probes.

Theories of nucleogenesis (Cameron 1957; the Burbidges, Fowler, and Hoyle 1957) as well as of the origin and development of the solar system depend on a precise formulation of the original composition of the material of which the sun and earth were formed (cf. Chap. 10).

Note added in proof, April 12, 1961: Rare earth abundances in shales and granites appear to be affected by fractionation effects, although basalts appear to give results in good accord with meteorites.

Selected References

- Ahrens, G. L., and S. R. Taylor, *Spectrochemical Analysis*, Addison-Wesley, Reading, Mass., 1960.
- Bate, G. L., J. R. Huizenga, and H. A. Potratz, *Science*, **126**, 612, 1957.
- Brown, H., *Revs. Modern Phys.*, **21**, 625, 1949.
- Burbidge, E. M., G. R. Burbidge, F. Hoyle, and W. Fowler, *Revs. Modern Phys.*, **29**, 547, 1957.
- Burbidge, G., *Ap. J.*, **131**, 519, 1960.
- Cameron, A. G. W., *Chalk River Report CRL-41*, 1957; *Ap. J.*, **129**, 676, 1959; *Ap. J.*, **131**, 521, 1960.
- Clarke, F. W., *Bull. Phil. Soc. Washington*, **11**, 131, 1889.
- Goldberg, E., and H. Brown, *Anal. Chem.*, **22**, 308, 1950.
- Goldschmidt, V. M., *Geochemische Verteilungs Gesetze der Elemente*, IX Skrifter Norske Videnskaps-Akad. Oslo. I. Mat. Naturu. Kl., No. 4, 1937; *Geochemistry*, Oxford New York, 1954.
- Hamagouchi, H., G. W. Reed, and A. Turkevich, 1957, *Geochim. et Cosmochim. Acta*, **12**, 337.
- Harkins, W. D., *J. Am. Chem. Soc.*, **39**, 856, 1917.
- Minami, E., *Nachr. Ges. Wiss. Göttingen*, *IV*, NF 1, No. 14, 155, 1935.
- Noddack, I., *Z. anorg. u. allgem. Chem.*, **225**, 337, 1935.
- Rankama, K., and G. Sahama, *Geochemistry*, University of Chicago Press, Chicago, 1950.
- Reed, G. W., K. Kigoshi, and A. Turkevich, *Geochim. et Cosmochim. Acta*, **2**, 122, 1960.
- Schmitt, R. A., A. W. Mosen, C. S. Suffredini, J. E. Lasch, R. A. Sharp, and D. A. Olehy, *Nature*, **186**, 863, 1960.
- Suess, H., *Z. Naturforsch.*, **22**, 311, 604, 1947.
- Suess, H., and H. C. Urey, *Revs. Modern Phys.*, **28**, 53, 1956.
- Wiik, H. B., *Geochim. et Cosmochim. Acta*, **9**, 279, 1956.

Composition Differences between Stars

9-1. Introduction

Although we have accepted the composition of the solar system as the "standard" we must recognize that it actually refers only to a small sample of the observable universe or even of our own galaxy. Within the neighborhood of the sun (i.e., in a domain small compared with the dimensions of the galaxy) are found objects showing a very considerable range in chemical composition. That such a diversity in composition existed has been fully recognized only relatively recently, although indications of abundance fluctuations among cool stars have been known for some time.

Striking differences in the appearance of stellar spectra can be brought about by variations in electron pressure, gas pressure, and temperature (cf. the spectral sequence), by the existence of an extended tenuous envelope around a star in which marked deviations from thermodynamic equilibrium can occur, and by the presence of magnetic fields which tend to intensify certain spectral lines. For a long time, explanations of stellar spectral differences were sought in terms of these effects. In any interpretation of spectral differences great care must be exercised to exhaust effects of differences in physical conditions before implications of abundance differences are invoked.

There are two broad aspects of abundance differences to be examined. The initial composition of each star is believed to represent that of the interstellar medium at the place and time the star was formed. Generally, it is supposed as a working hypothesis that the medium is fairly well mixed but becomes gradually enriched in heavier elements as time goes on. Hence the fraction (by weight), Z , of heavy elements in the galaxy gradually increases with time. Younger stars therefore have a greater proportion of heavy elements than do the older ones.

The other aspect of stellar-abundance differences is exhibited by the stars that show in their atmospheres the products of nuclear transformation in their interiors. To this group belong the hydrogen-deficient stars, the carbon stars, and the "heavy metal stars" that exhibit excess quantities of elements such as zirconium, barium, technetium, etc., in their atmospheres. These objects are of particular interest in connection with theories of element building in stars such as have been emphasized by the Burbidges, Fowler, and Hoyle, and by Cameron. They present most perplexing theoretical problems; how can products of nuclear transformations in the interior be mixed with the surface without invoking catastrophic results?

9-2. Observable Parameters Influenced by Composition Differences in Stars

The spectrum of a normal, non-variable star whose atmosphere is in hydrostatic equilibrium is determined by its surface gravity, temperature, and chemical composition. Two stars of the same surface gravity and temperature but different atmospheric chemical compositions will display differing line intensities and possibly differing continuous spectra as well.

Abundance differences between stars are often studied by comparing the spectrum of a suspected star with that of a normal star of very nearly the same temperature and surface gravity. This procedure entails construction of a curve of growth for each star, from which the abscissae are read for each observed $\log W/\lambda$ (cf. Sec. 5-5). For such a comparison it is not even necessary to know the f -values for the transitions involved, since one is interested only in abundance ratios between the two stars. On the other hand, abundance-difference determinations are beset by the usual troubles with blending, line-intensity errors, and in magnetic stars by the influence of the magnetic field on the line-absorption coefficient. For some elements, partition functions or even ionization potentials are not known. In more sophisticated treatments, model atmospheres are sometimes used, although for most stars of abnormal composition the surface gravities are unknown so that the model-atmosphere technique is not applicable, at least in a first reconnaissance.

Curve-of-growth or model-atmosphere techniques require high-dispersion spectra secured with very large telescopes. On the other hand, stars of abnormal composition sometimes exhibit peculiarities

of such a nature (e.g., weak metallic lines, absence of hydrogen lines where they should be strong, etc.) that they can be detected even with modest equipment. Composition abnormalities, particularly low metal/hydrogen ratios, sometimes affect the continuous spectra as well. An example in point is provided by the subdwarf stars which have an extremely low metal/hydrogen ratio. In a normal star with a temperature of about 6000°K , the spectral region shortward of about 4000 \AA is depressed by many overlapping strong metallic lines. On the other hand, in a star whose metal abundance is fifty or one hundred times lower, all metallic lines are much weaker and the ultraviolet spectrum is consequently much less depressed. Hence measurements of the colors of these stars on the Johnson Morgan UBV system give $U-B$ colors that indicate subdwarf stars to be abnormally blue compared with normal dwarfs.

Normally, stellar colors are measured with broad band-pass filters, but Strömgren (1958) demonstrated that with the aid of narrow band-pass filters at judiciously selected wavelengths one could accurately establish the relative abundance of hydrogen and helium on the one hand with respect to all other elements denoted as the "heavy elements" on the other. He employed six filters. One of them was a UV glass filter centered at $\lambda 3600$ and the other five were interference filters centered at $\lambda 5000$, $\lambda 4861$, $\lambda 4700$, $\lambda 4500$, and $\lambda 4030$. The six measured brightnesses $b(\lambda)$ could then be combined in various ways. One combination or "index" called " c " gives the jump in intensity at the head of the Balmer series, the other index called " l " gives the strength of the absorption line $H\beta$. The wavelength regions were so chosen that the c and l indices were insensitive to effects of interstellar reddening. Strömgren found that for stars of the same composition, these c and l indices could be used not only to derive luminosity and spectral classes but also to follow the evolutionary track of a star and to derive its age. He also devised an index " m " from the six brightness measurements, viz.,

$$m = \text{const} - 2.5[\log b(\lambda 5000) + \log b(\lambda 4030) - 2 \log b(\lambda 4500)]$$

which is particularly useful for F stars. This index, m , increases with increasing metal/hydrogen ratio but is insensitive to variations in T_e , g , and the interstellar reddening. Thus it is possible to pick out quickly from the F stars those objects that have abnormal metal/hydrogen ratios.

Finally, we must emphasize that the chemical composition affects not only the stellar spectrum but also the structure of the star, through influence on the opacity, energy generation, etc.

9-3. Population Types and Associated Characteristics

It is often suggested that our galactic system started out as a spherically symmetrical mass of gas that gradually contracted to a flat disk. During this process stars were formed by condensation. The oldest stars have a nearly spherically symmetrical distribution, the younger ones belong to systems that exhibit an increasing degree of flattening, while the very youngest objects move in the galactic plane in nearly circular orbits.

The oldest stars are the extreme population II members of what is called the "halo" population. This group includes the RR Lyrae stars with periods greater than 0.4 days, certain globular clusters that have high velocities in the direction perpendicular to the galactic plane, and the subdwarfs.

The youngest stars are those associated with the grains and gas of the interstellar medium. They include supergiant stars, young galactic clusters with bright *O* and *B* stars, Cepheids, and T Tauri stars. The latter are believed to be stars in the process of formation from the interstellar medium.

The vast majority of stars fall between these two extremes and their exact assignments have not been completely worked out. As a matter of convenience, we shall adopt the classification proposed at the Rome conference on stellar populations (see Table 9-1). Intermediate population II includes those high-velocity stars with velocities in the *z* direction (i.e., perpendicular to the galactic plane) greater than 30 km/sec and long-period variables with periods less than 250 days, and spectral classes earlier than *M*5. The disk population includes (1) the stars of the galactic nucleus, planetary nuclei, novae, RR Lyrae stars with periods less than 0.4 days, and (2) weak-line stars.

Actually, the different types gradually merge into one another. The sun is probably an "old population I" (i.e., spiral-arm stars), although some workers call it a disk-population star.

Table 9-1, compiled by the conference on stellar populations in Rome, lists in successive rows the average distance of the object from the galactic plane, the average velocity in the direction per-

Table 9-1. Stellar Populations.^a

	Halo population II	Intermediate population II	Disk population		Old population I	Young population I
			(a)	(b)		
z , parsecs	2000	700	450	300	160	120
v_z , km/sec	75	25	18	15	10	8
Axial ratio	2	5	~25			100
Concentration toward center	Strong	Strong	Strong	?	Small	Negligible
Distribution	Smooth	Smooth	Smooth	?	Patchy	Very patchy
Fraction of heavy elements by weight (Schwarzschild)	0.003	0.01		0.02	spiral arms	spiral arms
Age, 10^9 yr	6	6.0-5.0	5	1.5-5	0.03	0.04
Total mass, 10^9	16	47			0.1-1.5	< 0.1
					5	2

^a Adapted from O'Connell, D. J. K., ed., "Symposium on Stellar Populations," p. 419.

pendicular to the galactic plane, and the ratio of axes of spatial distribution represented as an ellipsoid of revolution. The disk and population II stars show a strong preference for the center of the galaxy and a smooth distribution. The spiral-arm population is concentrated to the arms and is somewhat patchy. The fraction of heavy elements by weight (as estimated by M. Schwarzschild) steadily increases from the halo to the spiral-arm stars. The estimated ages in units of 10^9 yr are given in the next to the last row. They are probably underestimated for the oldest population I stars and for the halo stars as well. The most recent work (Baum, Hiltner, Johnson, and Sandage 1959) indicates an age of the order of 10^{10} years for the globular cluster in Hercules M13! Ages as great as 2×10^{10} yr have been suggested recently for some clusters. The total masses of the various groups (as estimated by Oort) are given in the last row. Note that the vast bulk of the stars belong to the intermediate groups; the population I stars contribute only 10 per cent of the total in this compilation.

The Rome conference's nomenclature represents only a working scheme. Many investigators prefer to use only three groups, halo, disk, and arm, and for most purposes this simple classification seems adequate. Note that the grouping is essentially one according to age. The halo stars were formed before the gas contracted into the disk (their ages may actually be as great as 10^{10} yr), the intermediate type II stars were formed presumably during and immediately after the contraction into the disk, whereas the younger disk stars were formed slowly over a long period of time. One of the objectives of abundance studies is to establish as accurately as possible the dependence of the abundance of heavy elements on the epoch of star formation.

9-4. Remarks on the Composition of the Spiral-Arm Population

It is of great interest (cf. Chap. 5) to compare the younger stars of the spiral arms and galactic clusters with the sun to see if the composition of the interstellar medium from which these stars were formed has been enriched in heavier elements during the 5×10^9 yr that have elapsed since the sun was formed. That no substantial enrichment of the elements of the second and third rows of the periodic table has occurred during this time seems to have been established

by the Michigan work on the comparative composition of the sun and the *B* stars, as well as by the results of other workers on early type stars (cf. Chap. 5). Wallerstein and Helfer (1959) used curve-of-growth techniques and found the abundance of Na, Mg, Si, Ca, Sc, Ti, Cr, Mn, Fe, and Ni to be the same in the two stars of the Hyades as in the sun to within 25 per cent. Barium seemed to be overabundant by a factor of 2. If this result is substantiated it means that the rate of star formation is now drastically less than it was in pre-solar days.

On the other hand, Santirocco and Savedoff (1959) assumed that HD2154 and the two components of γ Virginis have approximately the same composition as the sun as far as the metals are concerned, then in 20 CVn the metals are overabundant by a factor of 4 to 7. This means that the giant star actually had this enhanced metal abundance when it was formed and has had time nearly to complete its hydrogen-burning phase on the main sequence. This problem needs further investigation. The possibility cannot yet be excluded that certain regions of the interstellar medium have different compositions than others so that stars formed at the same epoch but in different regions may have different amounts of heavy elements.

9-5. The Composition of the Halo Stars

At the other extreme, let us now consider compositions of the pronounced population type II (i.e., halo stars). Santirocco and Savedoff found that in RR Lyrae iron appeared to be depleted by a factor of 4.5 and the other metals by a factor of 5.5 with respect to the sun. The results depended essentially upon an hypothetical star possessing the same average spectrum as that recorded on their plates.

Particularly significant are the globular clusters which comprise a group of stars of different masses and luminosities but all of about the same very great age. Unlike galactic clusters whose color-luminosity plots were described in Chap. 1, globular clusters all have ages of 5 or 6×10^9 yr or greater. The galactic clusters show color-magnitude diagrams that differ from one another primarily because of their differing ages. On the other hand, although the color-magnitude diagrams of globular clusters resemble one another more closely, there are significant differences between them which apparently can be interpreted largely in terms of chemical-composition differences.

In comparing the color-magnitude array for a globular cluster

with that for a galactic cluster, one must remember that the color of a star depends not only on its surface temperature and gravity but also on its chemical composition. A color-magnitude diagram for a cluster of stars of "normal" chemical composition is not the same as that for a metal-deficient system, because the depression of the continuum by the spectral lines is different.

The UBV three-color photometry of individual stars in various clusters by Johnson, Arp, Sandage, and Walker show ultraviolet excesses for *F* stars, similar to those found for subdwarfs. For example, the stars in the globular cluster M3 show a violet excess in color $\Delta(B - V) = 0.3$ compared with the stars in the old galactic cluster, M67. This effect arises from the blanketing effect produced by the stronger metallic lines in the latter. Popper (1947) studied the spectra of red giants in the globular clusters, M3 and M13, and found the CN absorption to be peculiarly weak. Spectrograms of the brightest stars in M92 (Baum 1952; Keenan and Keller 1953) showed the CN bands and the metallic lines to be much weaker than in population I stars.

H. L. Helfer, G. Wallerstein, and J. L. Greenstein (1959), have constructed curves of growth for four *K* giant stars, two in the globular clusters, M13 and M92, the high velocity star, HDE232078 and a star in the galactic cluster, M41. The three population II stars show metal deficiencies, i.e., metal/hydrogen ratios, at least twenty to one hundred times smaller than that of the sun. The galactic-cluster star has the same hydrogen/metal ratio as has the sun.

W. W. Morgan (1956), studied integrated spectra of globular clusters on the Yerkes system of classification. He found that the spectra of M92, M15, M53, match very closely those of subdwarfs, the metallic lines being unobserved or very faint with most of the light arising from *F* stars, like IID140283 (cf. page 209). Hence the metal/hydrogen ratio is low, comparable with that in the subdwarfs. Furthermore, spectra of the clusters M5, M13, M3, ω Cen, NGC6229, also have weak lines, although their intensities are greater than in M92, M15, and M53. The clusters NGC6356, 6637, 6440, appear to have more nearly normal compositions with spectra characterized by strong metallic lines. Similarly, the spectrum of the nucleus of the Andromeda spiral galaxy, M31, does not show an excessive weakness of the metallic-line intensities. Hence, the stars in the central

bulge of M31 are not as ancient as are the oldest globular-cluster stars. Evidently the globular clusters display a range in composition suggesting that between the time of formation of the first and last of these objects, a considerable amount of material had been processed by nuclear reactions in stars into heavy elements. In fact, clusters such as NGC6356 may have compositions closely similar to that of the oldest galactic cluster, M67.

The best examples of the extreme type II population are provided by subdwarfs. Ordinary color-versus-magnitude plots place them below the main sequence. Adams and Joy suggested that such stars fall between the white dwarfs and the main sequence and called them intermediate white dwarfs. Spectra and color classifications in conventional systems based on normal compositions were difficult to make because of the weakness of the metallic lines. This line weakness also makes these stars brighter in the ultraviolet than ordinary stars. Miss Roman (1954) considered a typical group whose colors indicated a late *F* but which were too bright in the ultraviolet as compared with normal stars. Their visual absolute magnitudes were comparable with that of the sun. Their orbits about the galactic center are eccentric. Most of these stars must pass through the central bulge and their concentration to the galactic plane is comparable with that of globular clusters and RR Lyrae stars. Swihart has computed model atmospheres for these stars and finds that the energy distribution in the continuous spectrum is insensitive to the hydrogen/metal ratio in the range considered. It is of interest that Melbourne (1960) and also the Burbidges, Sandage, and Wildey (1960) find that if one corrects for the influence of the absorption lines upon the color, the subdwarfs and main-sequence stars would fall along the same curve on the color-magnitude plot.

Studies by Chamberlain and the present writer (1951) of the composition of the two subdwarfs HD19445 and HD140283 from plates secured by R. Sanford indicated that iron and calcium were an order of magnitude less abundant in these stars than in the sun; presumably the same results hold for other elements. The Burbidges (1956) found that λ Bootis had a composition fairly similar to that of HD19445 and HD140283, while in some of the other stars they studied, notably HD106223, HD161817 and 29 Cygni, the underabundance ratios were between these extreme subdwarfs and the

sun. In HD106223 and λ Bootis underabundance ratios of about 30 and greater than 20 have been found for barium, and these may be representative of ratios for very heavy elements.

More recent studies of subdwarfs have been made by Baschek (1959), who carried out an analysis of HD140283 on plates secured at Mt. Wilson by Unsöld, and by Greenstein and the present writer (1960) who investigated HD19445, HD140283, and HD219617. Baschek carried out a "rough analysis" and also a model-atmosphere treatment based on Unsöld's curve of growth. The methods of analysis differ in that whereas Greenstein and the writer used a differential method (cf. Chap. 5, p. 104) based on solar $\log N_{gf}\lambda$'s, Baschek used laboratory gf 's and attempted to reduce them to absolute values. Some of the advantages of the model-atmosphere method are incorporated in the differential method since the stars so closely resemble the sun in temperature and apparently also in surface gravity.

A metallic abundance deficiency, $\log N^{\circ}/N^{*} = +2.32$ which was obtained by Baschek by the model-atmosphere method, is to be compared with +2.00 from the more extensive data secured by Greenstein. Part of the discordance is due to differences in the measured intensities (Baschek had access to plates of smaller dispersion), part is due to the method of analysis, and part is due to the different temperatures assumed. Baschek chose $T = 5910^{\circ} \pm 250^{\circ}$ for HD140283, whereas Melbourne's spectral scans gave $T = 5450^{\circ}\text{K}$ for this star and $T = 5800^{\circ}\text{K}$ for HD19445. Thus these subdwarf stars are in fact G stars with very weak metallic lines. The profiles of the strong hydrogen lines were represented by the Kolb-Griem theory and Swihart's model atmosphere to a fair degree of approximation.

With temperatures derived from the photoelectric color measurements and spectral scans, Greenstein and the writer found deficiencies of the metals as compared with the sun of a factor of 40 in HD19445, 100 in HD140283, and 20 in HD219617. Another high-velocity star, HD161817, showed only small and uncertain metallic deficiencies. The detailed results are not in very good accord compared with those found by the Burbidges. The carbon abundance appears to be very low in these subdwarfs. See Table 9-2.

The subdwarfs represent the most nearly pure hydrogen stars that have ever been found. If the galaxy started as a gas cloud of pure hydrogen we would expect some pure hydrogen stars to exist.

Table 9-2. Abundance of Elements in Three Typical Subdwarfs

Element	Abundances ^a		
	HD140283 log N°/N^*	HD19445 log N°/N^*	HD219617 log N°/N^*
C	3.40 ^b	2.25 ^b	1.95 ^b
MgI	1.87	0.58	0.58
ArI	2.73	1.54	1.40
SiI	2.23	1.2	0.49
CaI	2.02	1.37	1.01
CaII	2.03		
ScII	2.34	1.84	1.92
TiI	1.72	1.20	1.17
TiII	1.85	1.52	1.08
VII	1.76	1.93	
CrI	1.94	1.86	1.50
CrII	1.23	1.51	
MnI	1.99	1.54	1.22
FeI	2.06	1.75	1.39
FeII	1.91	1.75	1.44
CoI	1.45	0.55	0.23
NiI	1.42 ^b	1.53 ^b	1.38 ^b
SrI	2.03	1.92	2.04
YII	2.59		
ZrII	2.30		
BaII	2.59	2.15	1.40

^a The logarithm of the ratio of the numbers of atoms in the sun to the numbers of atoms in the subdwarf as determined from the data for each type of atom and ion is tabulated.

^b The carbon abundances were found from the CH molecular data; the nickel abundances from direct curves of growth without comparison with the sun.

On the other hand, the original mass out of which the galaxy condensed may have been "seeded" with a few heavy nuclei, in which event the subdwarfs may actually be the original stars (*ursterne*).

9-6. Composition Differences in Intermediate and Disk Stars

The high velocity and "disk" stars are intermediate between the extreme populations represented by the subdwarfs and the type I stars (Keenan and Keller 1953). That is, high-velocity stars in the solar neighborhood show deviations from the chemical composi-

tions of the type I stars in the same sense as do type II stars, but to a less extreme degree. The most striking spectroscopic phenomenon is a weakening of the cyanogen bands in giants and subgiants in spectral classes G6 to K4. Miss Roman (1950) classified nearby stars in the spectral range *F*5 to *G*5 according to a three-dimensional scheme that grouped them as "weak-" or "strong-lined" objects in addition to the usual spectral class and luminosity assignments. The effects in the weak-lined stars are much less pronounced than in the extreme population II. M. and B. Schwarzschild (1950) studied two high-velocity stars in which they and Spitzer and Wildt (1951) found that the oxygen group is deficient by a factor of 2, while iron is deficient by a factor of 2 or 3 compared with normal type I stars. Subsequent investigations by numerous workers have indicated that composition differences are usually small.

L. Gratton, Liege 1953 Conference, p. 419, analyzed five stars, α U Ma, β Ser, ϵ Cyg, γ Leo A, and Arcturus. He found that as far as the metals were concerned the compositions of the stars were amazingly uniform. The two high-velocity stars, Arcturus and γ Leo A, have a greater hydrogen/metal ratio than do the normal stars, α U Ma and α Ser. Large fluctuations, however, are indicated within each group and Gratton concluded that high-velocity and low-velocity *K* giants are by no means two homogeneous groups of stars insofar as chemical composition is concerned. The fluctuations within each group are of the same order as the differences between them. In practice it seems very difficult to tell which high-velocity giants are members of Baade's population group II. Since the CH lines were fainter in the high-velocity group than in normal stars, it appears that the abundance of carbon is smaller than in the type I population.¹ Gratton reached similar conclusions for oxygen and nitrogen although these results were less securely established, since changes in the adopted atmospheric model may influence the results profoundly.

A spectroscopic comparison between high-velocity and low-velocity *K* giants was carried out by the Schwarzschilds, L. Searle, and A. Meltzer (1956). They studied the high-dispersion spectra of six high-velocity and ten low-velocity *K* giant stars. The spectrum of

¹ Curiously, there also exist high-velocity stars characterized by strong CH bands. (Cf. Bidelman 1956; Keenan 1958.) They appear to have about the same luminosities as other population type II giants. (See p. 227.)

the high-velocity giant, ϕ^2 Orionis, deviated from that of the low-velocity giants in that it showed an appreciable strengthening of CH relative to iron, a slight weakening of CN relative to iron, and a weakening of the neutral iron lines, all in agreement with previous results. The amount of the deviations were explained by a metal deficiency in ϕ^2 Orionis by a factor of 4 and a deficiency of carbon, nitrogen, and oxygen by a similar amount. Similar deviations, although to a smaller extent, were found for the high-velocity giants 14 And and Arcturus, while no significant deviations were found for HD39853, HD154733 and α Sct. With respect to the abundance of barium and the rare earths relative to iron, the Princeton workers found no significant difference among any of the high- and low-velocity giants. The conclusion to be drawn is that differences in composition between the high-velocity and low-velocity stars of the disk population are not very conspicuous. In the high latitude supergiants 89 Herculis and HD161796 Abt (1960) found that elements formed in equilibrium reactions (see Chap. 10) had roughly normal abundances, whereas those formed by slow neutron capture were underabundant. The stars were so far from the galactic plane that it is hard to see how they could have originated there.

To summarize, it appears that the enrichment of the interstellar medium in heavy elements took place very rapidly at first and then much more slowly. Much work remains to be done to establish the time dependence of the enrichment by the heavy elements.

9-7. Stars with Abundance Modifications Produced in Their Interiors

Up to now we have considered only those stars whose atmospheric compositions represented the composition of the interstellar medium at the time the star was formed. Throughout the rest of this chapter, we consider primarily stars whose atmospheric layers reflect the effect of nuclear transformations occurring in their interiors. For example, there appear to be stable stars in which hydrogen has been replaced by helium even in the surface layers! The following possibilities suggest themselves: (a) The stars may have exhausted the hydrogen out to the outermost layers which may have been blown off; subsequently the star may run on the helium-burning reactions; (b) There appear to exist stars in close binary systems whose outer layers were stripped off during the course of the evolution of the

system, possibly ν Sagittarii and HD30353 are examples of this sort; (c) There are stars in which outer and inner layers have become mixed.

Examples of stars in which helium has replaced hydrogen are: HD124448, HD160641, and HD168476. The star HD168476 was studied by A. D. Thackeray (1954). In this star no lines of hydrogen or oxygen are found, whereas the lines of HeI, ionized carbon, and neutral neon are prominent. There is a large range of excitation and ionization potentials. Ionized titanium (which has the same ionization potential as hydrogen and neutral oxygen) is definitely present. Except for hydrogen and oxygen a fair match can be made with a spectrum of the *B5* supergiant 67 Ophiuchi, but the equivalent widths of the lines in HD168476 are about twice those in 67 Ophiuchi. Such an intensification corresponds roughly to increasing the number of atoms above the photosphere by a factor of 10. Presumably the deficiency of hydrogen causes increased transparency in the atmosphere and produces the spectral characteristics of a supergiant star. Thackeray concludes that this star and also HD160641 are high-velocity objects. From the proper motion he suggests an absolute magnitude of -2 for HD168476.

A helium star corresponding to a spectral class of about *B0* is HD124448 which has been discussed by Popper (1942, 1947). Bidelman (1952) has described a helium star of a somewhat higher temperature, HD160641. A preliminary quantitative analysis of the spectrum of this star yields the following results by relative numbers of atoms: He 500; C 0.56; N 0.72; O 1.0; Ne 3.2; Si 0.05, and Mg 0.05 (Aller 1954). Within the accuracy of the analysis, the atmospheric composition of HD160641 resembles that of a normal *O* or *B* star in which hydrogen has been replaced by helium, and probably carbon, nitrogen, and neon are all more abundant with respect to oxygen than in population type I stars. The high temperature subdwarf, HZ44, analyzed by Münch, has considerably more helium than hydrogen, a marked deficiency of carbon, and a striking enhancement of nitrogen, all elements involved in the carbon cycle. Münch suggested that HZ44 may be a population type I star with absolute magnitude between $+3$ and $+5$ and a mass somewhat greater than that of the sun. It has a low space velocity.

To this group of hydrogen-deficient stars one might also assign the sharp-lined, dwarf, peculiar *B* star, HD135485, studied by John C. Stewart (1956). He analyzed the spectrum with the aid of a simple

model atmosphere, using the Balmer line widths, the SiII/SiIII intensity ratio and the helium line strengths to get the surface gravity, boundary temperature, and helium abundance. The star appeared to fall about 1 magnitude below the main sequence at *B6* with a helium abundance about ten times the normal. Except for a tenfold deficiency for magnesium, the abundances of the prominent elements in the first two rows of the periodic table, viz., C, N, O, Si, and S, are about normal.

The brightest known hydrogen-deficient star is the binary ν Sagittarii which was studied extensively by Greenstein (1940, 1947). The lines of helium and the ionized metals are strong, whereas the lines of hydrogen are amazingly weak. No Balmer continuous absorption can be detected. The star appears to be a supergiant with an effective temperature near 10,000°K. The increased intensity of the ionic lines is to be attributed to the fact that an atmosphere in which hydrogen is replaced by helium has a much higher transparency. This effect is even more strikingly exhibited in another somewhat cooler binary, HD30353 (Bidelman 1950). The problem of intrinsic blending is so severe in this star that it has not been possible to carry out a detailed analysis by conventional methods. Another, yet cooler star which is apparently rich in metals and possibly deficient in iron, HD101065, has been discussed by Przybylski.

The evolution of a close binary system differs fundamentally from that of a single star. When a component leaves the main sequence and evolves into the giant stage it expands in size and the outer envelope may be stripped off by the gravitational attraction of the other star. Perhaps most helium stars have evolved from normal stars in this way; the companion may have already reached the white-dwarf or some sub-luminous stage and no longer contributes to the light of the system. The carbon-rich hydrogen-poor stars are discussed in Sec. 9-8. These include the remarkable R Coronae Borealis variables.

The white-dwarf stars constitute a special group of hydrogen-deficient objects. All have reached virtually the end of their evolutionary careers. They are intrinsically faint, extremely dense, with enormously high surface gravities, and exhibit a considerable range in surface temperature. Greenstein (1958) has given a comprehensive description of the spectra of these objects. They cannot be classified by line ratios in the usual manner since stars of the same color may

have spectra that differ greatly in appearance. The objects classified by Greenstein as *DA* show only broad hydrogen lines that are greatly widened by the interatomic Stark effect, indicating an electron pressure of the order of 10^5 dynes/cm². They do not show helium or metallic lines; the atmospheres are extremely opaque. Greenstein's *DB* class show helium but no hydrogen lines, and the stars that show only a continuous spectrum may very well be helium stars since the other lines would be washed out by pressure effects. Some of the cooler stars show strong metallic lines. Ross 640, although it has a color corresponding to an *A* star, shows strong *K* lines and MgI $\lambda 3835$.

Of particular interest is V. Weidemann's analysis of the atmosphere of the white dwarf van Maanen No. 2, which Greenstein had observed to have color and spectral characteristics resembling a *G* star. The lines of iron are washed out by the high-density line broadening. From the ionization equilibrium Weidemann concluded that the temperature of this star was 5800° and that the upper limits of the hydrogen and metallic abundances were $\log N(\text{H})/N(T) = -1.1 \pm 0.6$ and $\log N(\text{metal})/N(\text{total}) = -3.9 \pm 0.3$.

Among the evolutionary precursors of the white-dwarf stars are the nuclei of the planetary nebulae. Although the nebulae themselves have compositions that apparently do not differ greatly from those of normal type I stars, the central stars show a wide variety of spectral features. They may be grouped roughly into four categories: (1) objects with broad emission lines of the Wolf-Rayet type, (2) stars with absorption lines and relatively narrow emission lines, (3) stars with absorption lines but with no emission, and (4) stars that show only a continuous spectrum. Chemical compositions are extremely difficult to establish for these objects. In the absorption-line stars very few lines of elements other than H and He are observed, while the H/He ratios in most of them seem to be "normal." One absorption-line planetary nucleus that seems to be a helium star is that connected with NGC246. It shows strong lines of HeII, CIII, and CIV but no trace of hydrogen.

Abundance studies in the stars showing emission-line spectra are more difficult, but the appearance of the spectra and general level of excitation suggest variations in the proportions of H, He, C, N, and O (Aller 1956). One difficulty in the interpretation of the data is illustrated by the small planetary BD + $30^\circ 3639$, Campbell's

Hydrogen-Envelope Star. The spectrum of the central star contains numerous strong emission lines of C, O, He, Si, etc., in various stages of ionization, but it shows no lines of nitrogen. Yet the lines of nitrogen are strong in the surrounding nebula!

Probably the planetary nebulae themselves and stars of the absorption-line type display the composition characteristic of disk-population stars, not that of extreme subdwarfs. On the other hand, the stars whose spectra resemble those of the Wolf-Rayet type may be unstable so that the results of nuclear reactions in the interior are mixed into the surface layers. The planetary nuclei whose spectra are known at present probably represent a variety of chemical compositions.

Among the least understood of stellar spectra in terms of atmospheric models, etc., are those of the Wolf-Rayet type. These stars, which are frequently found to exist in binary systems, show a strong clustering tendency, and belong to the extreme population I high-luminosity objects (see Aller 1954). Their most characteristic features are broad emission lines, sometimes 50 or 100 Å wide and ten times as intense as the continuous spectrum upon which they are superposed. Studies by Edlén, Beals, and Miss Payne showed that the Wolf-Rayet stars fall in two sequences, one characterized by prominent lines of carbon and oxygen and the other containing nitrogen. Helium is common to both sequences and the nitrogen sequence contains small quantities of carbon, and only a little nitrogen appears in the carbon stars. As noted above, some planetary nuclei show bright lines of the Wolf-Rayet type. In some instances the lines are relatively narrow; in others they are very broad as in the classical (i.e., population type I) stars. The planetary nuclei are often of the intermediate type, i.e., they show lines of O, C, and N as well as of helium.

The spectra of classical Wolf-Rayet stars often show a huge range in excitation, indicating that these stars have extended, stratified atmospheres. It is generally assumed that the atmospheres are expanding and certainly the lines must be produced under conditions departing rather substantially from thermodynamic equilibrium. Some attempts have been made to estimate the compositions of Wolf-Rayet envelopes. On the basis of a stratified model of the atmosphere, the present writer suggested (1943) that the observed features of the carbon sequence could be explained with a He/O

ratio of about 50 and a He/C ratio of about 17, whereas those of the nitrogen sequence could be interpreted with a nitrogen abundance about one-twentieth that of helium with carbon one-tenth or one-fifteenth as abundant as nitrogen. Hydrogen seems to be less abundant than helium in these stars, although the confusion of the Balmer series of hydrogen and the Pickering series of ionized helium makes any detailed comparison difficult. S. G. Sliusarev (1955) computed relative intensities of the bright-hydrogen and ionized-helium lines in the spectra of Wolf-Rayet stars from a theory of luminescence of moving stellar envelopes. By comparing this theory with observations, he established the relative content of hydrogen and helium in the atmospheres of HD192163 and BD+35°4013. By numbers, the helium/hydrogen ratio fell between 5 and 12 showing that the composition of these stars is anomalous. On the other hand, Miss Underhill (1959) has argued that the differences between the nitrogen and carbon sequences may be at least partly due to differences in the radiation field as a consequence of the differing temperatures of the stars. While effects of the type mentioned by Miss Underhill are certainly very important, it does not seem probable that all spectroscopic differences can be accounted for in this way, particularly since not just one stage of ionization but several stages of ionization of a given element are markedly weakened.

The classical Wolf-Rayet stars presumably represent very late stages in stellar evolution. The nitrogen stars may be objects wherein material processed in the carbon cycle is brought to the surface, the nitrogen/carbon ratio being a function of the temperature (Gamow 1943; Burbidge, Fowler, and Hoyle 1957). Presumably the material was processed at a very high temperature (of the order of 40,000,000°K). The carbon stars apparently contain very little nitrogen but much C and O and a little Ne, suggesting that these elements were built by the triple-alpha process $3\alpha \rightarrow \text{C}^{12}$ and subsequent α -particle captures, and the material reached the surface without modification in a hydrogen-rich zone (Salpeter 1953; Greenstein 1954). We would expect, therefore, the carbon Wolf-Rayet stars to contain little hydrogen. On the other hand, Sahade suggested Wolf-Rayet stars may be objects still in their premain-sequence gravitational contraction.

Novae, or "temporary" stars, are normally rather faint with visual absolute magnitudes about +4 or +5. They have very high surface

temperatures and many are members of binary systems. When an outburst occurs they rise abruptly to absolute magnitudes -6 or -7 and then decline more slowly. The light curve and accompanying spectroscopic features can easily be understood in terms of an expanding shell. Near maximum light novae show an absorption spectrum resembling that of a supergiant star. Figure 9-1 compares the tracing of a small region of Nova Scuti 1949 with that of ϵ Aurigae. Notice the general similarity of the metallic spectrum, except that the lines are stronger in the nova. Notice the great strength of the CI $\lambda 4762$ and $\lambda 4771$ lines and the emission features in the nova spectrum. As the star's brightness declines, the continuous spectrum fades and bright lines appear. At first the emission spectrum is characterized by strong lines of hydrogen and ionized metals. Later,

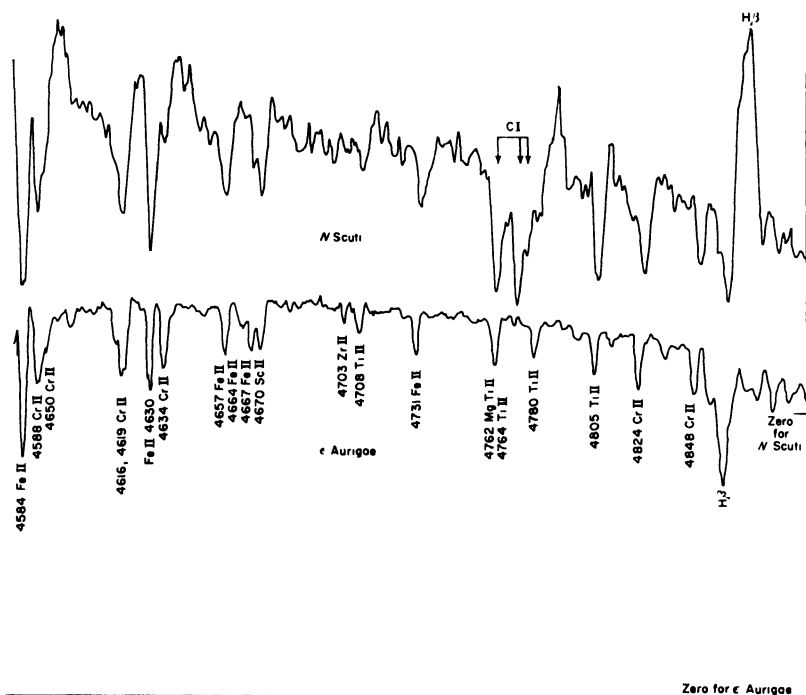


Fig. 9-1. Tracings of a portion of the spectra of the normal supergiant ϵ Aurigae (lower) and Nova Scuti 1949 (upper). Note the great strength of the metallic and carbon lines in the nova and the appearance of the emission lines.

the metallic spectrum fades and is gradually replaced by high excitation lines of permanent gases. Forbidden lines characteristic of gaseous nebulae appear, and still later the spectrum of the old nova resembles that of a planetary nebula. Abundance studies are difficult to carry out in spectra of envelopes that show such marked effects of time-dependent stratification, filamentary structure, and deviations from thermodynamic equilibrium.

S. R. Pottasch (1958) has determined the compositions of shells of novae from an analysis of lines of the emission spectrum, using methods developed for gaseous nebulae. In the nova one usually observes only one stage of ionization at a time, e.g., the radiation of [OI] will be observed at one epoch, that of [OIII] at a later time. Pottasch evaluated the population of each stage of ionization as a function of time and noted the epoch at which each stage of ionization reached its maximum prominence. The maximum value reached by the population of a single ionization stage was considered to give the total abundance of that element. In the table 9-3, we compare his mean abundances with those adopted for the solar system.

Table 9-3. Abundance Comparison between Novae and Solar System

Element	H	He	C	N	O	Ne	S	Ca
Log <i>N</i> (novae)	12.00	11.19	8.52	9.70	9.64	8.44	8.09	7.17
Log <i>N</i> (solar system)	12.00	11.21	8.60	8.05	8.95	8.70	7.35	6.19

The H/He ratio is about the same as that of carbon and neon, but the abundances of N, O, S, and Ca are greatly enhanced. The increased abundance of nitrogen is somewhat similar to what is observed in HZ44. It should be noted, however, that there appear to be marked differences in composition from one nova to another. Nova Pictoris had strong forbidden sulfur lines, whereas Nova Persei showed strong neon lines. It is likely that when novae are investigated in more detail they will show differences as marked as those exhibited by other type II stars in advanced stages of their evolution.

As for the supernovae, which probably represent actual explosions of entire stars, little is known concerning compositions, although Woltjer (1958) has studied the Crab nebula which is the remnant of a supernova observed in the year 1054 (Fig. 9-2). It attained a maximum luminosity about 200 million times that of the sun. It is a

strong emitter of radio-frequency radiation. The central amorphous mass of this object emits a continuous spectrum of partially polarized light. Presumably, this is synchrotron radiation. Surrounding the

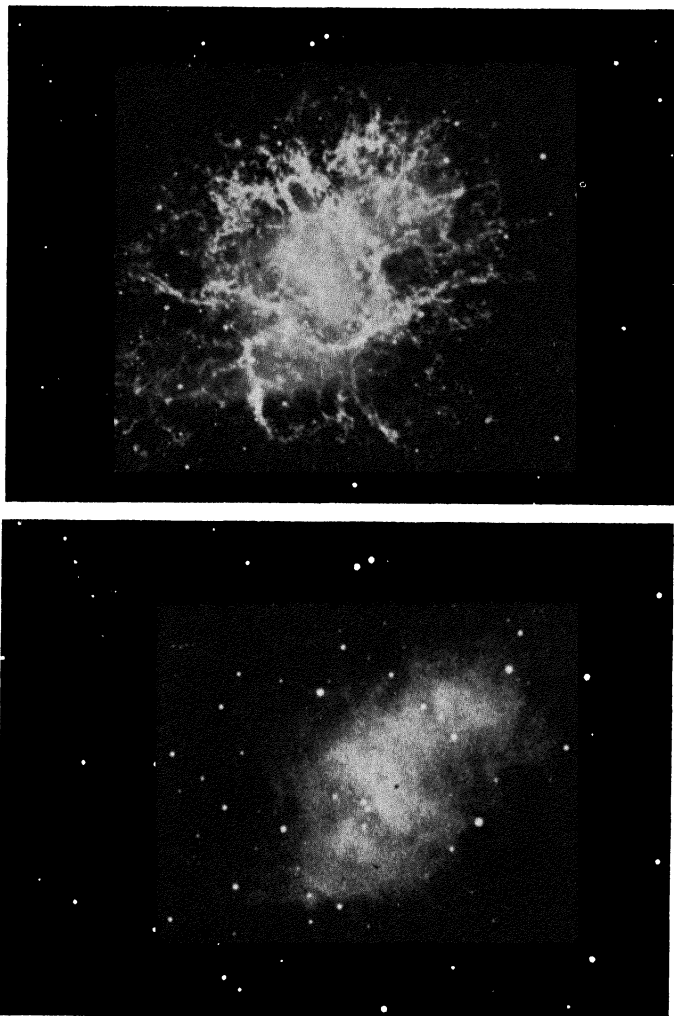


Fig. 9-2. The Crab nebula. The upper block shows the filaments as photographed in $H\alpha$; the lower block, the amorphous mass responsible for polarised, continuous radiation which is probably produced by a synchrotron mechanism. (Photographed by Walter Baade, Mt. Wilson and Palomar Observatories.)

central amorphous mass is a network of filaments which emit a bright-line spectrum resembling that of a planetary nebula. Woltjer has determined the abundances of the ions in this filament for different assumptions concerning the electron temperature and has attempted to deduce the composition of the gas. He finds the relative number of atoms (oxygen = 100) as shown in Table 9-4.

The H/He ratio is smaller in the Crab nebula than in the planetaries or in an ordinary star. The abundances of neon and sulfur are higher, but the high S abundance may be to some extent spurious because of the peculiar behavior of this ion in filaments and condensations.

Table 9-4. Relative Number of Atoms in Gas around Crab Nebula

Element	H	He	N	O	Ne	S
$T = 17,000^{\circ}\text{K}$	320,000	200,000	109	100	39	27
$T = 10,000^{\circ}\text{K}$	89,000	40,000	54	100	55	31
$T = 8,000^{\circ}\text{K}$	37,000	15,000	26	100	76	32

9-8. Carbon Stars and Related Objects

The effects of abundance differences are particularly striking in the cool giant and supergiant stars. Relatively small variations in the C/O ratio can produce striking effects in the appearance of the spectra of these cool stars. Several different, seemingly independent, variations are involved, e.g., C/O, metals/H, and total hydrogen content.

We illustrate some of the complexities involved by comparing the relative amounts of different compounds of C, N, O, and H and of TiO for different values of the carbon abundance in atmospheric models of late-type supergiant stars. Carbon and heavy-metal stars are found only among giants and supergiants. We calculate the numbers of molecules of the different types above the photospheres of supergiant stars with surface temperatures between 2500° and 6000°K . The gas pressures, electron pressures, and mass above the photosphere are calculated by conventional methods (see e.g., Aller 1953, p. 222). We assume the abundance of oxygen to be $\log N(\text{O})/N(\text{H}) = -3.1$ and investigate the following three situations:

Oxygen-rich (O=C) Carbon-rich

$$\log N(\text{C})/N(\text{H}) = -3.6 \qquad -3.1 \qquad -2.8$$

That is, there is a six-fold increase in the carbon abundance from the oxygen-rich to the carbon-rich; the concentrations of O and H are kept fixed. Our point of view is somewhat similar to that of Russell (1934) except that his calculations were carried out before the negative hydrogen ion was identified as a source of opacity in atmospheres of cool stars. Further improved values of the dissociation potentials of many molecules are now available. Extensive calculations of the dissociative equilibria of molecules have also been carried out recently by Neven and de Jager (1957).

The results of our calculations are exhibited in Figs. 9-3, 9-4, and 9-5. In the oxygen-rich model (Fig. 9-3) notice that most of the carbon is tied to CO which is the most abundant molecule next to H_2 . The maxima of CN and CH fall at 3600°K, while OH, H_2O , and TiO increase monotonically to the lowest temperatures. Calculations are made for two abundances of Zr, the normal, i.e., lower abundance (symbols underlined in Fig. 9-3) and a larger value where the zirconium abundance is set equal to the titanium abundance. Notice that ZrO is more prominent than TiO for equal numbers of the two atoms and that the dominance of a spectrum by ZrO does not necessarily mean that zirconium is more abundant than titanium. Titanium and zirconium are mostly ionized until the temperature drops to as low as 3100°K in these supergiants. Hence the formation of ZrO and TiO is controlled largely by the concentration of neutral atoms. The corresponding spectral classes are indicated at the bottom of the figure.

The relative numbers of molecules above the photosphere for supergiants with equal abundance of carbon and oxygen are given in Fig. 9-4. Notice that at the temperatures below 3500° most of the carbon and oxygen are tied up in CO. The CN concentration now reaches a maximum about five times the value it had in the oxygen-rich star. Water increases as T decreases until a temperature of 3400° is reached after which it increases very slowly to a value fifty times smaller than the concentration shown in Fig. 9-3 at $T = 2500^\circ\text{K}$. The general pattern of behavior of most compounds is the same in Fig. 9-4 as in Fig. 9-3 until oxygen gets tied up in CO at approximately 3400°K. At lower temperatures the depletion of oxygen modi-

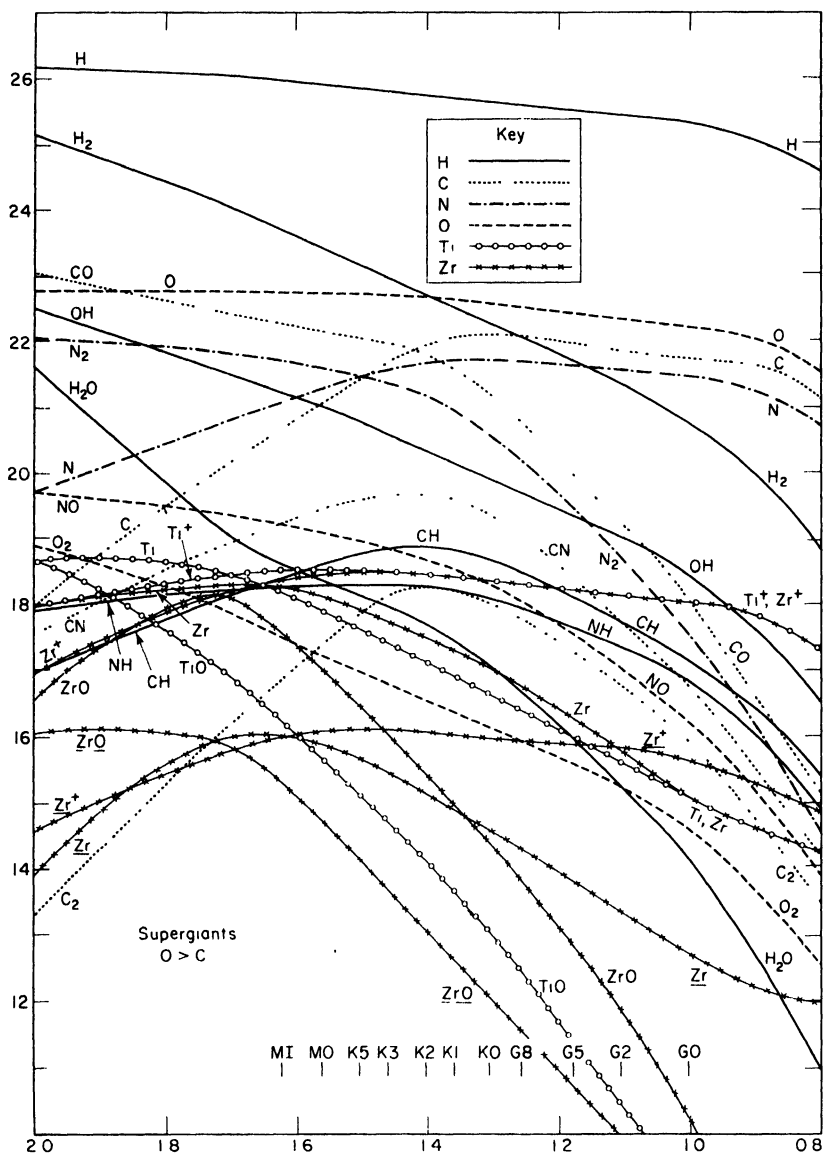
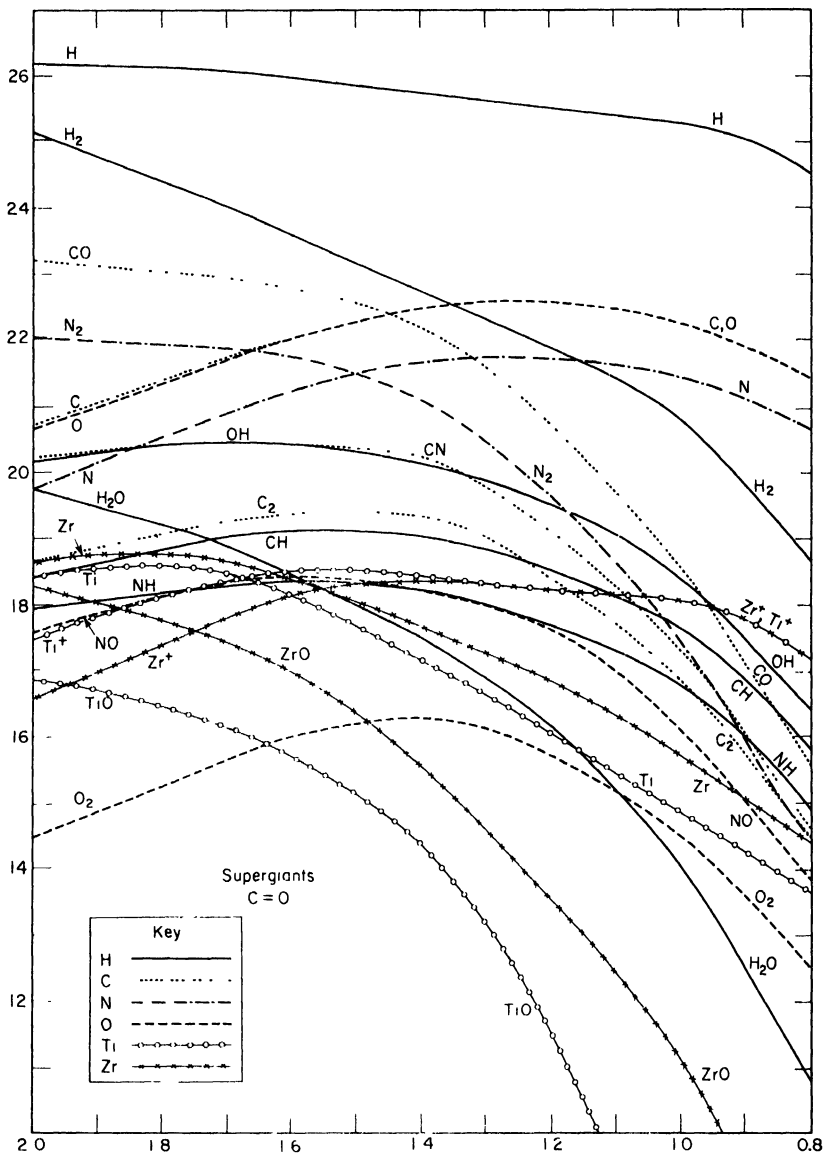


Fig. 9-3. Equilibria of compounds in oxygen-rich supergiants. The logarithm of the number of atoms and molecules above the photosphere is plotted as ordinate against $\theta = 5040/T$ as abscissa. Corresponding spectral classes are also indicated.



fies the dissociative equilibria profoundly. At 2500°K , for example, the amount of TiO is about fifty times smaller than in the oxygen-rich stars.

More pronounced effects are exhibited when carbon is more abundant than oxygen. Then virtually all the oxygen is bound in CO below 3600° and such compounds as OH , H_2O and particularly O_2 are suppressed at the lowest temperatures (see Fig. 9-5). The carbon compounds are naturally all enhanced; CN continues to rise to the lowest temperature and attains a value about two hundred times greater than the maximum reached in the oxygen group, while the CH maximum concentration is of the order of forty times the maximum reached in the O group.

Down to 3900°K , TiO rises at the same rate as in the oxygen stars; thereafter it rises much more slowly to a maximum value at 3100°K after which it levels off. At 2500°K the TiO and ZrO concentrations become thousands and one hundred times smaller, respectively, than in the oxygen stars. Between 3000 and 2500°K , a six-fold increase in the carbon concentration results in a decrease of the amount of TiO by a factor of some thousands. Thus relatively small changes in the abundances of important constituents such as C and O can produce profound changes in the concentrations of spectroscopically important features such as the TiO and ZrO bands. In other words, abundance differences that might lie at or even beyond the limit of detection in hotter stars or gaseous nebulae may produce drastic effects in the appearance of the spectrum of a cool star.

The strengths of the bands of the carbon compounds or of TiO will depend strongly on the composition. Hence the atmospheric opacity will vary with composition (cf. Bidelman 1954) and the structure of the atmosphere can be profoundly affected. In our approximate treatment we have considered the dissociative equilibrium for only one fixed point in the atmosphere. In actual practice the compounds are formed over a range of temperature and pressure, tending to be concentrated in the upper, cooler region of the atmosphere. The atomic lines probably originate over a greater range in depth. Hence one should employ a model atmosphere that takes these characteristics into account.

Our diagrams (Figs. 9-3 through 9-6) illustrate the effects of varying the C/O ratios and the heavy metal/zirconium, in a mixture of "normal" hydrogen content. If the abundance of H with respect to

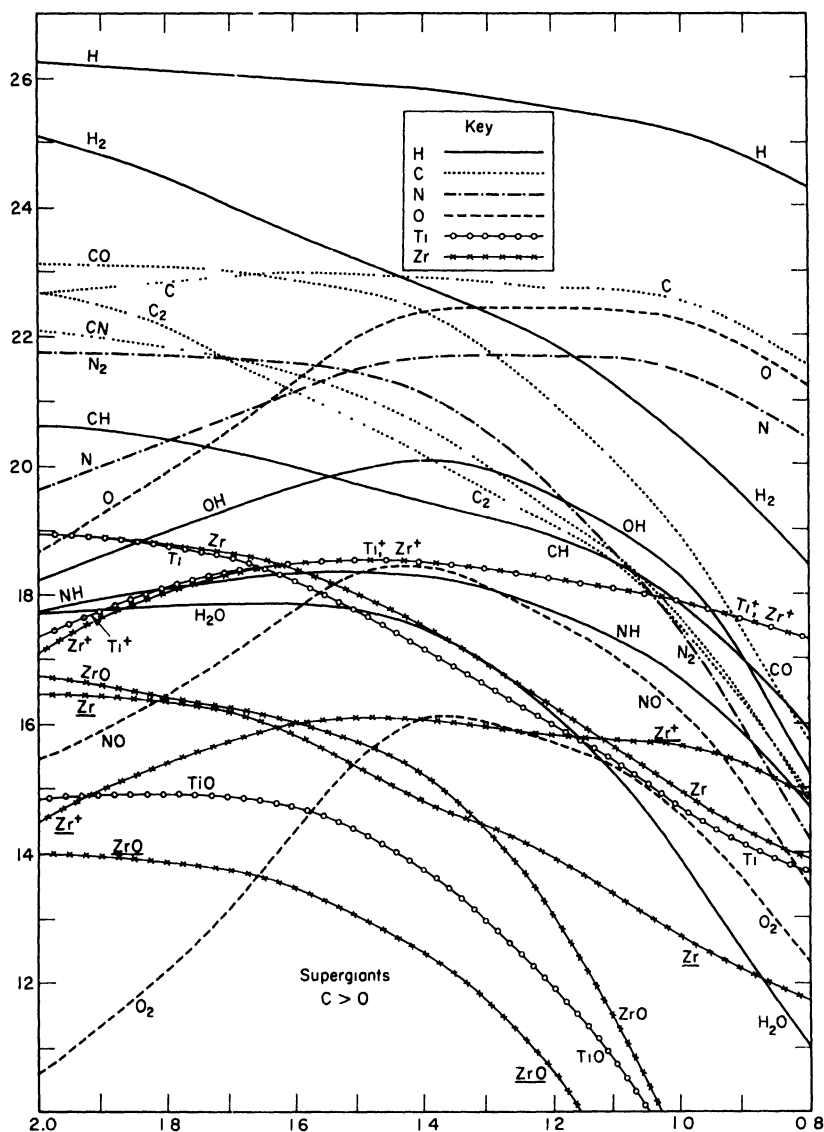


Fig. 9-5. Equilibria of compounds in supergiant carbon stars.

C, N, and O and the metals is greatly increased the result will be that compounds such as CH will remain prominent, but CN, CO, and C_2 will be cut down. On the other hand, if the ratio of H to C, N, and O is decreased, the formation of compounds such as CN will be favored. This situation seems to occur in a few *G* and *K* stars like α Serpentis, where the CN bands are stronger than normal. Some stars with strong CN bands may, of course, be actually nitrogen enriched; quantitative data are lacking.

Now consider the carbon stars that are apparently deficient in hydrogen (cf. Bidelman 1956). The prototype of these objects is the well-known variable R Coronae Borealis. Most of the time this star is at constant light, but it occasionally fades and then recovers slowly. These stars are supergiants with visual absolute magnitudes near -5 . Many years ago, Berman showed that this star contained

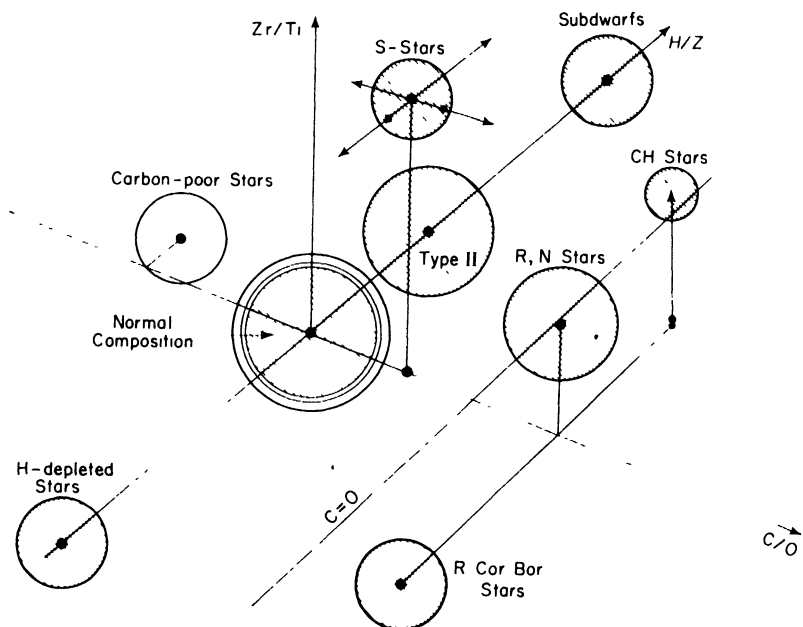


Fig. 9-6. Schematic representation of stars of different composition. Normal stars are placed at the origin. The three composition axes represent carbon/oxygen (C/O), hydrogen/metal (H/Z), and zirconium titanium (Zr/Ti) ratios. The sizes of the circles have no significance. Different composition types grade imperceptibly into one another.

an excess of carbon; O'Keefe attributed the sporadic dimming to a veiling produced by solid carbon particles in its atmosphere. The most recent discussion of the spectrum of R Cor Bor is that by L. Searle, who finds the C/Fe ratio to be twenty-five times greater in this star than in the standard, while the C/H ratio is about 40! No lines of oxygen and nitrogen are observed and if it is assumed that their abundances are the same as in the sun, the abundances of H, He, and carbon are, respectively, 0.00014, 0.92, and 0.07 *by weight*.

The hydrogen-deficient carbon stars show weak hydrogen lines. The cooler members show bands of CN and C₂ although the CH bands characteristic of ordinary carbon stars are missing. The spectrum of nova DQ Herculis shortly after maximum (December 23 to 26, 1934) resembled those of these stars (cf. Bidelman 1954*b*). The C¹³ isotope, prominent in so many carbon stars, (cf. Chap. 7) is not featured in the H-deficient carbon stars; possibly they have the same C/O ratio as the earth. These stars may represent a continuation of the hydrogen-deficient group into the cooler objects.

At the other extreme of the composition gamut are the population II CH stars (cf. McKellar 1948; Keenan 1942, 1958; and Bidelman 1956). These giant stars fall in the temperature range 3500 to 4500°K, and are characterized by such strong CH bands that the normally intense broad resonance 4227 CaI line is smothered into insignificance. Bands of C₂ and CN also appear with intensities that suggest a C/O ratio typical of the carbon stars in an atmosphere where the H/C+O ratio is greatly increased. In HD26, the C₂ bands and most metals are weak and the strongest lines are those of the rare-earth elements. The star seems to be related to the BaII stars. Keenan (1958) concludes that there is a close relationship between the BaII stars and the CH stars, since the former show an enhancement of the CH bands even though the C₂ and CN bands are fainter than in the carbon stars.

The best known carbon stars are the cool objects of spectral classes *R* and *N*. It was recognized long ago that the atomic lines present in these stars were similar to those observed in the oxygen-rich *M* stars, but that the molecular spectra were entirely different, being dominated by the bands of carbon compounds. The empirical *RN* classification should be discarded in favor of the *C* designation proposed by Morgan and Keenan (1941). The stars which show the strongest ultraviolet absorption are not necessarily the coolest. R. Bouigue

(1954) measured the intensities of the vibration bands of C_2 and CN and of the D lines of sodium in a hundred stars of classes *R* and *N*. He obtained the temperature T_{vib} from the excitation of the vibration bands and found a clearcut relation between T_{vib} and the D-line intensity consistent with the spectral class arrangement proposed by Keenan and Morgan. Bouigue showed that the carbon stars of class *C* are giants with temperatures and pressures but little different from those of red *M*-type giants. The C_2 -CN temperature relationship analyzed in connection with the atmosphere state indicates a C^{12} abundance in the carbon stars only slightly in excess of that of oxygen.

The bolometric magnitudes of the carbon and *M* stars are probably closely comparable; hence the principal difference is an enhancement of the carbon content of their atmospheres. The carbon/oxygen ratio varies from star to star. For example, the three variables W Cass, R Ori, and R C Mi show C_2 bands that are very much weaker than in normal carbon stars, indicating that they are of the intermediate type (Bidelman 1954). Most carbon stars seem to have a normal hydrogen content in their atmospheres. Probably the content of heavy metals is greater than in *M* stars, although it is not as great as in the heavy metal stars. The greatly enhanced C^{13}/C^{12} ratio has already been mentioned (Chap. 7). The high C^{13}/C^{12} ratio suggests that the C^{12} has been cycled in a hydrogen-burning shell and then transported to the surface, in which case stars rich in C^{13} should likewise contain great quantities of nitrogen. Further work on these carbon stars is indicated.

9-9. The Heavy-Metal Stars

From the standpoint of theories of element building in stars, the most engaging objects are the *S*-type variables and the barium stars. The *S*-type stars are dominated by bands of ZrO instead of TiO, although most of them such as R Andromedae show bands of both ZrO and TiO.

The ZrO molecule has a greater binding energy than has the TiO molecule. Hence an enhancement of the ZrO bands could sometimes be a physical effect caused by variations of the pressure (Wurm 1940) or the C/O ratio (Fujita 1939, 1940). The inadequacy of this explanation is shown by the fact that in the stars showing the ZrO bands, the lines of atomic zirconium (and neighboring elements in the periodic table as well) are intensified as compared with the same

lines in normal stars (Merrill 1947; Keenan and Aller 1951; Bidelman 1953; Merrill and Greenstein 1956). Buscombe and Merrill (1952) compared atomic-line intensities in the three long-period variable stars, R Andromedae (Se), O (Mira) Ceti (*M6e*), and R Leonis (*M8e*). They found that per unit number of iron atoms, there are several times as many atoms of the heavier elements Y, Zr, and Nb (Cb) in the atmosphere of the *S* star, R Andromedae, as in that of R Leonis. Mira has an intermediate composition. The *S* stars appear to have a C/O ratio intermediate between that of the carbon and oxygen stars [cf. the discussion of F U Monocerotis, the peculiar *S* star, by R. G. Teske (1956)]. As pointed out by Bidelman, there is some difficulty in making quantitative comparisons between *M*, *S*, and carbon stars, since the atmospheres of the *S* stars have a much lower opacity than do those of the *M* or carbon stars because the TiO and carbon bands in the latter are effective in blocking the outgoing radiation.

Thus the carbon stars embrace objects with a great range in intensities of the C₂ bands, whereas the *S* stars show a large range in the strengths of the ZrO bands. It is possible to identify a sequence of stars involving both carbon, *S* stars, and *M* stars in which the only parameter is the carbon/oxygen ratio which decreases monotonically from one to the other. Bidelman and others have noted that the spectra of stars with the weakest C₂ bands closely resemble those having the weakest bands of ZrO and other oxides. These stars approach the situation depicted in Fig. 9-4; Bidelman (1954) has proposed that the irregular variable, GP Orionis, falls in this category. It has strong Na "D" and SrI lines. C₂ bands are not certainly present while those of ZrO are faint. The strongest visible bands are those of MgII and CN, and although the star is very cool, it does not show the strong bands usually found in such low-temperature objects.

The outstanding characteristic of the *S*-type stars, therefore, is the enhanced abundance of heavy metals such as those of the "zirconium" row of the periodic table. More particularly, elements with magic-number nuclei, i.e., strontium, yttrium, zirconium, barium, lanthanum, cerium, praseodymium, and neodymium are increased in abundance with respect to the *M* stars. Keenan, for example, has estimated that zirconium is five times as abundant in the *S* stars as in the *M* stars. The most striking phenomenon, however, is the presence of the lines of the unstable element, num-

ber 43, technetium, in the spectra of the *S*-type stars (Merrill 1952). The longest-lived isotope Tc^{99} which can be formed by neutron capture has a half-life of 210,000 yr. If neutron capture can be regarded as the mechanism for the formation of technetium in cool stars, the products of these neutron reactions must have been mixed into the surface layers relatively recently, since the abundance of Tc in the *S* stars seems comparable with that of some of the neighboring elements. In this way a time limit can be placed on the formation and lifetime of a star in the *S* stage (E. and G. Burbidge 1957). Since the *S* stars are about one per cent as abundant as *M* stars, it follows that if all red giants pass through an *S*-star stage and endure as *M* giants for about ten million years as suggested by the stellar evolution arguments, the lifetime in the *S* stage would be about one hundred thousand years. Bidelman, however, has suggested that the unusual elemental abundances observed in *S* stars might be characteristic to some degree of *M* and carbon stars as well. He cites Merrill's (1952) discovery of weak technetium lines in the spectrum of Mira as support for this suggestion. These examples serve to illustrate the great complexities exhibited in the atmospheres of late-type stars.

More recently, Cameron (1959) has proposed that under equilibrium conditions in stellar interiors, photo-beta reactions may occur involving the excited states of various atomic nuclei. By such effects Mo^{97} may be transformed to Tc^{97} with an abundance comparable with that of Mo . Subsequently, the Tc^{97} is brought to the surface where it decays with its characteristic half-life of 2,600,000 yr. At the same time the formation of Nb^{93} is greatly favored.

The barium stars probably represent an extension of the heavy metal anomalies to higher temperatures (Bidelman 1950) and different atmospheric pressures. They correspond to spectral classes *G* and *K*. The most detailed study is that carried out for HD46407 by the Burbidges. They derived abundance ratios differentially by comparing this star with the *G8III* giant κ Geminorum which has a closely similar luminosity and temperature and which in turn had been compared with the sun. Except for carbon, which appeared to have a slightly greater abundance than normal, all the elements up to germanium appeared to have their customary abundances. The observable elements from strontium on appeared to have abundances of the order of ten times the normal. The Burbidges showed that the

abundance anomalies could easily be understood in terms of theories of element building on the slow neutron-capture process in red giant stars (cf. Chap. 10). As in the *S* stars, abundance peaks appear at those nuclei with the magic number of neutrons, but the greater accuracy of the analysis permits more reliable values to be assigned. Those elements, such as europium, that are not built predominantly by the slow neutron-capture process, did not show any overabundances. Technetium is not observed in either HD46407 or in ζ Capricorni which was studied by Greenstein. Hence the barium stars may represent a later stage in the evolution of a star than the *S* stars, or the stars may have evolved in such a way that the technetium was destroyed before it reached the surface. A more accurate determination of the abundances of the elements near Tc may answer this question.

The "heavy-metal" stars, as we have called them, pose a host of problems to which we can at the present time give only a few sketchy answers. We will consider some of these questions in Chap. 10 in connection with theories of nucleogenesis.

Metallic-abundance anomalies are not confined to the *S* and BaII stars, however, but appear in earlier spectral classes as well where we are concerned with a number of curious enhancements of particular elements or groups of elements.

9-10. The Peculiar *A* Stars

The peculiar *A* stars show anomalously strong lines of selected metals; particularly ionized silicon, chromium, strontium, europium, and certain other lanthanides (rare earths). The *K* line of ionized calcium is usually too weak, while the lines of iron are normal. Some stars, of which $\alpha 2$ Canum Venaticorum is the best known example, are spectrum variables in which the lines of CrI, CrII, SrII vary in phase with one another, but out of phase with respect to the rare-earth element lines. These peculiarities have been interpreted in terms of hydromagnetic oscillations of the stars or in terms of an oblique rotator in which different ions are concentrated at different points on the surface (cf. the discussion by Deutsch 1958).

Early analyses made with relatively low dispersion (cf. Aller 1947) suggested that the metals were about ten times as abundant in these stars as in normal *A* stars. The definitive study was that carried out by the Burbidges (1955, 1956) with high dispersion material. They

studied the three stars, $\alpha 2$ C Vn, HD133029, and HD151199, deriving abundances by comparison with a standard star using empirical line strengths. The analysis was difficult because of the effects of blending, magnetic intensification, and inadequacies of the spectroscopic analyses of certain elements. Not only are the partition functions unknown for the rare-earth ions, but the second ionization potentials are not as yet determined for Ce, Pr, Nd, Gd, and Dy. The correction is not unimportant because about 80 per cent of the rare-earth elements are doubly ionized so a small error in the assumed ionization potential can lead to large errors in the total abundances. Finally, a complication is added by the fact that in $\alpha 2$ C Vn the intensities of most of the lines change with phase and averages have to be taken over a whole cycle. For example, the abundances of the rare earths change with phase. The overabundance factors range between 5 and 30.

In some respects the results are similar to those obtained for HD46407, in the sense that elements with neutron magic numbers are overabundant, but there are significant differences in that while barium is overabundant in HD46407, it is normal in the Ap stars, while europium is strongly overabundant in the Ap stars and normal in HD46407! The Burbidges list additional effects for the Ap stars as follows:

1. Oxygen and calcium are underabundant, the latter by a factor of 30!
2. Silicon is overabundant by a factor of 15.
3. The iron peak is overabundant by about a factor of 6. The enhancement is greatest for manganese and chromium, but only about 2 for iron.
4. Sr, Y, and Zr are overabundant by a factor of about 25.
5. The abundances of La, Ce, Pr, Nd, Sm, Eu, Gd, and Dy are increased by a factor of about 600; lead is overabundant by a factor of 1500.

Uranium may be present. Some of the apparent abundance differences between HD133029 and $\alpha 2$ C Vn seem to be real, while the only notable effects in HD151199 are the overabundances of Mn, Sr, and Eu. The A pec stars appear to fall on the population I main sequence, i.e., they are young stars in which the energy is still supplied by the hydrogen-burning reactions. They are sometimes found

in relatively young galactic clusters, e.g., the Coma cluster and the Ursa Major stream.

Fowler and the Burbidges (cf. Chap. 10) concluded that the clue to the abundance anomalies was to be sought in the strong magnetic fields of these stars. In small regions of the surface, analogous to solar flares, acceleration of particles to high energies can take place. In the ensuing reactions, neutrons are produced, captured by the atoms in the iron peak, and lead to the final abundances.

9-11. Metallic-Line Stars

Abundance anomalies completely different from those exhibited by the magnetic stars are shown by the so-called metallic-line stars, which also fall near the main sequence in the Russell diagram. They show unusually weak CaII *K* lines for their spectral types as measured by the Balmer lines or colors (Morgan and Roman 1948). The other metallic lines would indicate a spectral class a little later than the energy distribution in their spectra. Studies of their spectra have been made by a number of observers (Aller 1947; Greenstein 1948, 1949; Miczaika, Franklin, Deutsch, and Greenstein 1956; and by Mrs. Hack 1956). The apparently brightest stars have been catalogued by Slettebak (1949); an extreme example is τ Ursae Majoris. In his study of this star, Greenstein noticed that atoms whose second ionization potential fell between 12 and 15 eV showed a peculiar abundance deficiency, viz., Ca, Ti, Sc, Zr, and V. On the other hand, the abundances of Zn, Na, and Ni were large, peculiar, but probably real. The stars 8 Comae and 15 Vulpeculae showed the same qualitative effects except that they were less pronounced.

Greenstein suggested that some kind of a spectroscopic peculiarity accounted for this effect, e.g., an excess amount of ionizing energy was liberated, possibly by charge exchange or by some other cause that might liberate energy near the Lyman limit. If an energy source of this type existed we might expect H-emission lines to be produced or at least deformations of the profiles. Yet the profiles of the hydrogen lines look normal. It is difficult to conceive of a source of excess ionization that would not at the same time produce noticeable effects in the observable spectrum.

High atmosphere turbulence seems to be definitely linked with metallicism. The magnitude of the turbulence is appropriate to the atmospheres of giants, yet the stars appear to be on or slightly above

the main sequence in the range corresponding to *A6* to *F8*. Their velocities relative to the sun, frequent membership in clusters, and the presence of a large number of binaries indicate that they are members of population I (cf. Weaver 1952). Abt finds that all metallic-line stars are spectroscopic binaries. Mrs. Hack considered the general characteristics of these stars. From a comparison of 7 metallic and 16 normal stars, she found high turbulent velocities to be characteristic and a deficiency (relative to the sun) for Ca, Ti, Sc, Zr, V, and Mg in essential agreement with the results of Greenstein. She favored the hypothesis of a shell overlying the normal photosphere and an excess of second ionization. Rudkjøbing suggested that the atmospheres of metallic stars were in radiative equilibrium, whereas normal *A* stars are objects whose atmospheres are in convective equilibrium. This suggestion is not supported by the fact that the high turbulence is shown by the metallic stars and that the energy distributions in the normal *A* and *F* stars agree with predictions from model atmospheres in radiative equilibrium. Mrs. Vitense-Böhm concludes that all proposals to account for spectra of metallic-line stars cannot explain the observed results. Possibly the atmospheres are distended by some cause which is not yet identified.

Among the other anomalies found in the late *B*'s and early *A*'s are the silicon stars. We mention one example HD34452, which was studied by Casati and Mrs. Hack. This *B7* star lies slightly above the main sequence and has a temperature near 13,500°K. The lines of SiII show an enormous intensity which they attributed either to an excess abundance or perhaps to a magnetic field. There also exist "manganese" stars in which the MnII lines are intense, e.g., α And B9 p. The connection between the excess abundances of these particular elements and theories of nuclear processes in stars offers some interesting problems. Some of these objects are magnetic variables.

9-12. The Lithium Problem

One of the most interesting problems is that posed by the lithium abundance in different types of cool stars. The lithium nucleus is fragile and is easily destroyed in thermonuclear reactions. Hence it cannot be created in stellar interiors and may be produced only by spallation processes involving heavier nuclei, e.g., neon, magnesium, etc. It is present in the sun to a proportion smaller than in the earth

and meteorites. Indications are that it is destroyed at the bottom of the solar convection zone; the extent of destruction depends on the depth of the zone. (Greenstein and Richardson 1951.) The amount of lithium present thus gives us some idea concerning the depth of the solar convection zone. Weymann's solar model (1957) does not give a high enough temperature at the bottom of the solar convection zone to allow the destruction of any significant amount of lithium in the 5×10^9 yr allotted for the age of the sun. Hence one must conclude that either the convection zone extended to much greater depths during the early history of the sun or the models are somewhat in error in the sense that the convection zone extends to deeper, hotter, and denser layers than Weymann assumed.

In this connection a study by Bonsack is of particular interest. He studied (1959) the ratio of lithium to vanadium in 46 normal stars of spectral classes from *G8* to *M0* and found a range in abundance ratio up to a factor of 100 among stars of similar surface characteristics. No correlation with luminosity is noted, but as one goes to cooler and cooler stars, the maximum observed lithium abundance steadily declines. The explanation is probably to be found in the theory of stellar structure. The cooler a dwarf star, the deeper its convection zone and the higher the temperature and density at the bottom. Thus in the *K* stars the lithium will be more effectively destroyed than in the *G* stars where the turbulent convection does not bring the lithium to such hot dense regions. Why stars of similar surface temperatures and luminosities showed a huge range in lithium abundance remains unexplained.

At the other extreme is the situation found in the T Tauri variables which are believed to be stars in the process of formation from the interstellar medium. That is, they are *proto stars*.

W. K. Bonsack and J. L. Greenstein investigated five of these T Tauri stars where they found that the lithium-to-normal-metal ratio exceeded the solar value by a factor of about 100. Hence the lithium abundance was close to the terrestrial value and indicated that in young stars there were about one lithium atom per thousand million hydrogen atoms. They suggested that the magnetic energy content of such a proto star is large enough so that if it is forced to the surface during the contraction and there dissipated in accelerating protons, the required amount of lithium may be produced by the spallation of heavier atoms.

Most curious of all, however, is the anomalous lithium abundance found in certain *N*-type variables. Since these carbon stars supposedly exhibit the effects of thermal nuclear processes in their deep interiors, it is difficult to understand why lithium should appear in their spectra unless it is actually manufactured in the atmosphere or protected in some fashion against thermonuclear destruction.

The lithium resonance line appears only in the coolest carbon stars. In most *N* stars it is very weak as the investigations by McKellar and Stilwell (1944) and by Feast (1954) demonstrate. Only in three stars, WZ Cassiopeiae (McKellar 1941), WX Cygni (Sanford 1944), and T Arae (Feast 1954), does the line appear with great strength. It would be of great interest to see if these stars also have strong magnetic fields. Lithium is also present in *S* stars (Teske 1956), and in *M* giants.

The Burbidges, Fowler, and Hoyle (1957) point out that lithium does not react thermally with He as rapidly as it does with H, and possibly it can last long enough in a helium-burning zone to be able to reach the surface. Hence these stars must not only have no hydrogen-burning zones, but the hydrogen can extend only to depths when the temperature is less than about a million degrees.

In summary, the abundance anomalies found in cool giant and supergiant stars and in hot stars of unusual composition are extremely useful in that they supply important information concerning nuclear processes in stars and the problems of stellar evolutions. The Burbidges, Fowler, and Hoyle (1957) and Cameron (1957) have discussed this problem extensively. We summarize their results briefly in Chap. 10.

9-13. Abundance Differences between Stellar Systems

Qualitatively the composition of the most distant regions of the universe yet observed with the spectrograph resembles that of our local region. In the galaxies of our local group, it is possible to go further and observe the integrated spectra of the elliptical galaxies near M31, the nucleus of M31 and M33 and the Magellanic Clouds. These integrated spectra which have been studied by de Vaucouleurs and particularly by W. W. Morgan (1956) show the same type of spectra as would be expected from groups of abundant star types in our own galaxy. The spectra of the brightest stars in the Magellanic Clouds can also be observed, but so far no quantitative analyses

have been attempted. From the data obtained from the integrated spectra and from the spectra of individual stars, no evidence of abundance differences between our own and other galaxies has been obtained so far.

The diffuse nebulae observed in external galaxies offer another possibility. In M33 there are a number of emission nebulosities whose spectra closely resemble those of similar objects in our own galaxy. A number of bright emission knots appear in the Large Magellanic Cloud. Two such objects are sufficiently bright for a fairly detailed study; NGC604 in M33 and 30 Doradus in the Large Magellanic Cloud. So far only the hydrogen/helium ratios have been measured in these nebulosities by Mathis and by Johnson (1959) respectively. Johnson finds the same H/He ratio in 30 Doradus as Mathis had found for the Orion nebula, i.e., about eight to one. Very recently, D. J. Faulkner and the present writer have measured the hydrogen/helium ratio in both Magellanic Clouds with a spectrum scanner. This ratio seems slightly larger in the Small Cloud than in the larger one. The intensities of the forbidden lines of neon, oxygen, and sulfur with respect to the hydrogen lines seems to be about the same as in diffuse nebulae in our own galaxy, suggesting that the relative abundances of these elements in these three systems of the local group are about the same.

Selected References

- Abt, H., *Ap. J.* **131**, 99, 1960.
Aller, L. H., *Ap. J.*, **97**, 135, 1943; *Ap. J.*, **106**, 76, 1947; *Atmospheres of the Sun and Stars*, Ronald, New York, 1953; *Nuclear Transformations, Stellar Interiors, and Nebulae*, Ronald, New York, 1954; *Gaseous Nebulae*, Chap. 6, Chapman and Hall, London, 1956.
Aller, L. H., and J. L. Greenstein, *Ap. J. Suppl.*, **46**, 1960.
Baschek, B., *Z. Astrophys.*, **48**, 95, 1959.
Baum, W. A., W. A. Hiltner, H. L. Johnson, and A. R. Sandage, *Ap. J.*, **130**, 749, 1959.
Bidelman, W. P., *Ap. J.*, **112**, 219, 1950; *Ap. J.*, **116**, 227, 1952; *Ap. J.*, **117**, 377, 1953; *Mem. Roy. Soc. Liege* **14**, 307, 1954; *Trans. I.A.U.*, **8**, 852, 1954b; *Views in Astronomy*, A. Beer, ed., 1956, Vol. II, p. 1428.
Bonsack, W. K., *Ap. J.*, **130**, 843, 1959.
Bonsack, W. K., and J. L. Greenstein, *Ap. J.*, **131**, 83, 1960.
Bouigue, R., *Ann d'Ap.*, **17**, 104, 1954.
Burbidge, E. M., and G. R. Burbidge, *Ap. J. Suppl.*, **1**, 431, *Ap. J.*, **122**, 396, 1955; *Ap. J.*, **124**, 116, 130, 655, 1956; *Ap. J.*, **126**, 357, 1957.

- Burbidge, E. M., G. R. Burbidge, A. Sandage, and Wildey, *Mem. Royal Soc. Liege*, [5] 3, 427 1960.
- Burbidge, E. M., W. A. Fowler, and F. Hoyle, *Revs. Modern Phys.*, 29, 547, 1957.
- Buscombe, W., and P. W. Merrill, *Ap. J.*, 116, 525, 1952.
- Cameron, A. G. W., *Chalk River Report PD 308*, 1959.
- Chamberlain, J. W., and L. H. Aller, *Ap. J.*, 111, 353, 1951.
- de Jager, C., and L. Neven, "Les Molecules dans les Astres," *Mem. Roy. Soc. Liege*, 18, 357, 1957.
- Deutsch, A. J., *Handbuch der Physik*, 51, 689, 1958.
- Feast, M. W., *Mem. Roy. Soc. Liege*, 14, 413, 1954.
- Fujita, Y., *Japan. J. Astron. Geophys.*, 17, 17, 1939; 18, 45, 1940.
- Gamow, G., *Ap. J.*, 98, 500, 1943.
- Gratton, L., *Liege Conference on Nuclear Processes in Stars*, P. Swings, ed., 1953, p. 419.
- Greenstein, J. L., *Ap. J.*, 91, 438, 1940; *Ap. J.*, 106, 339, 1947; *Ap. J.*, 107, 151, 1948; *Ap. J.*, 109, 121, 1949; *Mem. Roy. Soc. Liege*, 14, 307, 1954. *Handbuch der Physik*, 50, 161, 1958.
- Greenstein, J. L., and R. S. Richardson, *Ap. J.*, 113, 536, 1951.
- Hack, M., *Contr. Obs. Milano-Merate*, Nos. 60, 65, 82, 92, 1956.
- Helfer, H. L., G. Wallerstein, and J. L. Greenstein, *Ap. J.*, 129, 700, 1959.
- Johnson, Hugh, *Publ. Astron. Soc. Pacific*, 71, 425, 1959.
- Keenan, P. C., *Ap. J.*, 96, 101, 1942; *Ap. J.*, 120, 484, 1954, *Handbuch der Physik*, 50, 93, 1958.
- Keenan, P. C., and L. H. Aller, *Ap. J.*, 113, 72, 1951.
- Keenan, P. C., and G. Keller, *Ap. J.*, 117, 241, 1953.
- McKellar, A., *Observatory*, 64, 4, 1941; *Publ. Dominion Astrophys. Observatory*, Victoria, B. C., 7, 395, 1948.
- McKellar, A., and W. H. Stilwell, *J. Roy. Astron. Soc. Can.*, 38, 237, 1944.
- Melbourne, *Ap. J.*, 132, 101, 1960.
- Merrill, P. W., *Ap. J.*, 105, 360, 1947; *Science*, 115, 484, 1952; *Ap. J.*, 116, 21, 1952.
- Merrill, P. W., and J. L. Greenstein, *Ap. J. Suppl.*, 2, 225, 1956.
- Miczaika, G. R., F. A. Franklin, A. J. Deutsch, and J. L. Greenstein, *Ap. J.*, 124, 134, 1956.
- Morgan, W. W., *Publ. Astron. Soc. Pacific*, 68, 513, 1956.
- Morgan, W. W., and P. C. Keenan, *Ap. J.*, 94, 501, 1941.
- Popper, D. M., *Publ. Astron. Soc. Pacific*, 54, 160, 1942; *Ap. J.*, 105, 204, 1947a; *Publ. Astron. Soc. Pacific*, 59, 320, 1947b.
- Pottasch, S. R., *Ann d'Ap.*, 22, 297, 1958.
- Roman, N., *Ap. J.*, 112, 554, 1950; *Astron. J.*, 59, 307, 1954.
- Roman, N., and W. W. Morgan, *Ap. J.*, 107, 107, 1948.
- Russell, H. N., *Ap. J.*, 79, 317, 1934.
- Salpeter, E. E., *Ann. Rev. Nuclear Sci.*, 2, 41, 1953.
- Sanford, R. F., *Ap. J.*, 99, 145, 1944.

- Santirocco, R. A., and M. P. Savedoff, Unpublished thesis by Santirocco, University of Rochester, 1959.
- Schwarzschild, M., and B. Schwarzschild, *Ap. J.*, **112**, 248, 1950.
- Schwarzschild, M., B. Schwarzschild, L. Searle, and A. Meltzer, *Ap. J.*, **125**, 123, 1956.
- Schwarzschild, M., B. Schwarzschild, L. Spitzer, and R. Wildt, *Ap. J.*, **114**, 398, 1951.
- Slettebak, A. A., *Ap. J.*, **109**, 549, 1949.
- Sliusarev, S. G., *Russian Astronomical J.*, **32**, 346, 1955.
- Stewart, J. C., *Astron. J.*, **61**, 13, 1956.
- Stromgren, B., In *Stellar Populations*, D. J. K. O'Connell, S.J., ed., Interscience, New York, 1958.
- Swihart, T., *Ap. J.*, **123**, 151, 1956; *Ap. J. Suppl.*, **49**, 1960.
- Teske, R. G., *Publ. Astron. Soc. Pacific*, **68**, 520, 1956.
- Thackeray, A. D., *Monthly Notices Roy. Astron. Soc.*, **114**, 95, 1954.
- Underhill, A., *Publ. Dom. Ap. Obs.*, **11**, 209, 1959.
- Wallerstein, G., and H. L. Helfer, *Ap. J.*, **129**, 347, 1959.
- Weaver, H. F., *Ap. J.*, **116**, 612, 1952.
- Weymann, R., *Ap. J.*, **126**, 208, 1957.
- Weidemann, V., *Ap. J.*, **131**, 638, 1960.
- Woltjer, L., *Bull. Astron. Inst. N.*, **14**, 40, 1958.
- Wurm, K., *Ap. J.*, **91**, 103, 1940.

Theories of the Origin of the Elements

10-1. Introduction

That the relative abundances of the elements contain some clues as to their origin long has been suspected. Various theories to account for the distribution have been proposed and some of these will be reviewed here. All of them start from hydrogen atoms or neutrons as the basic building blocks.

If we examine a plot of the atomic abundances, e.g., that by Suess and Urey (1956), we notice a number of features that must be explained by any theory of the origin of elements.

1. The abundances decrease with a roughly exponential dependence on A until $A \sim 100$; there is a much slower decrease thereafter which is at least partially masked by marked abundance fluctuations.

2. There is a pronounced abundance peak at iron.

3. Deuterium, lithium, beryllium, and boron are rare compared with the neighboring elements H, He, C, N, and O.

4. Among the lighter nuclides (up to scandium), those whose atomic weights are multiples of 4, e.g., O^{16} , Ne^{20} , Na^{23} , Mg^{24} , and Si^{28} tend to be more abundant than their neighbors (rule of Oddo). Also, atoms of even atomic weight tend to be more abundant than those of odd atomic weight.

5. There is a tendency for heavy atoms to be neutron-rich. Heavy proton-rich nuclides are rare. In the Suess-Urey compilation there appear abundance maxima at $A = 80$ and 90 , 130 and 138 , and at 196 and 208 . The characteristics of the abundance curve are complex so it is not surprising, as we shall see, that apparently no one mechanism can explain the origin of all the stable nuclides observed in nature.

10-2. Earlier Theories of Element Formation

The earlier work on element formation concentrated on such problems as explaining why heavy elements such as lead or bismuth existed at all, why there was a maximum at iron, why the atomic abundances

fell off exponentially below $A \leq 100$, or on some other special features without giving an account of the whole picture. See, for example, the summarizing account by Podolawski and Ter Haar (1954) or by Alpher and Herman (1953). The polynutron theory (Mayer and Teller 1949) envisaged a cold primordial body consisting mostly of neutrons. Small droplets of the cold nuclear fluid disintegrated by spontaneous fission into fragments that underwent further β -decay to produce nuclei of heavy elements such as the rare earths, lead, etc. This speculative theory offered some advantages for the heavier elements but failed for light and intermediate elements and was never developed in sufficient detail to permit definitive comparisons with abundance data. Beskow and Treffenberg (1947) considered a hypothetical star, whose core consisted of a hot nuclear fluid. Surrounding this core was a region containing excess quantities of neutrons and presumably neutron-rich heavy nuclei. Light elements could be produced in the outer parts of this object.

The equilibrium theories (Chandrasekhar and Henrich 1942; Klein, Beskow, and Treffenberg 1946) postulate that the distribution of the elements was formed under conditions of very high temperature and density and then "frozen in." Subsequently, the material was spread about by some violent explosion in such a way that there was no time for the nuclei to react to form new equilibria. The final distribution was finally established by subsequent β -decays. At densities of a hundred or a thousand million times that of water and at temperatures in excess of a thousand million degrees, nuclear reactions are so violent that relative concentrations of the different nuclides, neutrons, protons, β -rays, and the density of γ -rays will depend on the temperature and density, binding energies of the various nuclides, statistical weights of different isomeric stages, etc. In an equilibrium situation detailed nuclear processes need not be known, any more than the particular collisional and radiative mechanisms need be known to calculate the ionization equilibrium of a stellar interior. The relevant equations are straightforward expressions obtained from statistical mechanics, and can be applied as soon as the nuclear energy states are known. [See Hoyle (1946).] At the present time, most of the energy levels of light nuclei have been established experimentally, and the energy levels of the nuclei of the intermediate elements can be estimated with the aid of the shell model, guided by experimental data.

The greatest objection to the equilibrium theory is that if density and temperature are chosen to explain the distribution of nuclides between oxygen and argon, for example, there will be a deficiency of heavier elements. One might imagine heavy elements being built at one temperature and density and lighter elements at another, perhaps in super-massive primordial stars which subsequently blew up with such suddenness that the nuclide distribution was not affected. The difficulty is that one cannot account for detailed features of the abundance distribution in this way. Although by postulating a number of primordial stars with an appropriate range in central temperatures and densities one might reproduce the broad features of the abundance distribution, the result would be that the individual isotopic abundances would not agree with the observations. The abundance of a nuclide would depend only on its stability and atomic weight. The equilibrium theory does reproduce the features of the abundance curve in the neighborhood of the iron peak but it fails both for heavier and lighter elements.

The failure of the equilibrium theories led Gamow and his co-workers to suggest a non-equilibrium theory for the formation of the elements. It is supposed that at the beginning of the expansion of the universe all the material was compressed into a neutron gas, called the *ylem*. As the gas expanded, neutrons decayed into protons and electrons, the protons collected neutrons and built up complex nuclei by successive neutron captures and β -decay. The entire process of element building took place in less than a couple of hours. Detailed calculations have been made by Alpher and Herman (1950) who have pointed out the difficulties as well as the successes of the theory.

In this theory, the abundance of a nuclide will depend inversely on its cross section for neutron capture. If a nucleus captures a neutron easily it will be transformed rapidly into one of another nuclide. In any steady-flow situation, the following equality will hold, viz.,

$$n(A)\sigma(A) = n(A + 1)\sigma(A + 1)$$

where σ is the cross section for neutron capture and n is the concentration. Consequently, nuclides with low-capture cross sections will tend to build up in larger concentrations and vice versa. This prediction of the neutron-capture theory is substantiated by the high abundances of nuclides with low neutron-capture cross sections.

At room temperatures, neutron cross sections vary capriciously

with Z , but at the energies of many kev believed to have prevailed in the ylem, the cross sections rise uniformly with A up to about $A = 100$. Thereafter, the cross sections remain roughly constant with A . There are, however, certain conspicuous exceptions. At neutron numbers 50, 82, and 126, corresponding to the closure of neutron shells, the cross sections drop to very low values. These magic-number atoms show high abundances, whereas, according to Suess and Urey, the nuclei which correspond to the closure of proton shells show no such abundance maxima.

In spite of these attractive features of the Gamow theory, a number of serious objections must be raised against it.

1. There is no mechanism for producing the so-called shielded isobars. Initially, only neutron-rich nuclei would be formed and these would decay by β -emission to the first stable neutron-rich isobar. The so-called shielded isobars which have fewer neutrons could not be formed. Thus, the Gamow theory requirement of a very rapid neutron capture does not permit the formation of nuclides with small neutron numbers.

2. The iron peak cannot be explained by a neutron-capture theory. Nuclides which are built up by neutron capture and which subsequently decay into iron isotopes do not have unusually small neutron cross sections. Some version of the equilibrium theory must be invoked to explain the iron peak. Difficulties 1 and 2 are inherent in any neutron-capture theory and are not confined to the Gamow version.

3. The fatal objection to the Gamow theory lies in the fact that masses 5 and 8 are unstable. A neutron cannot be added to helium to form a stable nucleus, for example. It would require three-body collisions to bridge this gap and these cannot occur at the densities supposed to have existed in the primordial ylem.

Hence the Gamow theory must be abandoned although certain essential features of both it and the equilibrium theory are retained in the necessarily more elaborate theories that have replaced them.

10-3. Formation of Elements in Stars

The only theory of the origin of elements which offers any promise of success is that elements have been manufactured by a variety of nuclear reactions occurring in stars. Although attempts were made as early as 1930 by Atkinson, modern work on the subject was initiated

by Hoyle (1946, 1954). This hypothesis has been developed particularly by the Burbidges, Fowler, and Hoyle (1957) and by Cameron. An impressive array of evidence (cf. Chaps. 7, 9) has been assembled to substantiate this idea. Younger stars tend to have a higher ratio of metals and heavy elements than do the older stars, while many stars in advanced stages of evolution show the influence of nuclear reactions at work in their interiors.

It is supposed that the first stars may have consisted only of hydrogen. They functioned by converting hydrogen into helium by the proton-proton chain. When the hydrogen was all gone in the deep interior the star may have burned helium into carbon and built up the elements O, Ne, Na, and Mg. Subsequently, the star evolved either smoothly or catastrophically into the white-dwarf stage. If the material of the envelope becomes mixed with the core in the course of the evolution, protons can be captured by C, Ne, etc., to form nuclides like C^{13} and Ne^{21} and if the star is sufficiently massive, heavier elements can be built, perhaps many of them in a last catastrophic moment if the star becomes a supernova.

In any event, when a sufficiently massive star evolves from the main sequence through the giant stage into the final white-dwarf phase, some of its mass is returned to the interstellar medium. The actual amount of material returned and its composition will depend presumably on the mass of the star. More massive stars will not only return a larger fraction of their mass to the interstellar medium, but the material returned will contain probably a greater proportion of heavy elements.

As the material is circulated between the stars and the interstellar medium, more and more heavy atoms are added but the proportions of elements heavier than helium remains very small. Extreme population type II stars, particularly subdwarfs, were formed at an early stage when the proportion of metals was much smaller than it is at present. On this view, even the oldest stars are still second generation objects unless they were formed out of material which was already seeded with heavy nuclei. The sun is then presumed to be at least a third generation star and we must postulate that many stars must have lived and died before the origin of the solar system. If some of the present estimates of the ages of the older clusters (i.e., greater than $\sim 10^{10}$ yr) is accepted, there appear to have been several million millennia between the formation of the oldest stars in the galactic system and the birth of the solar system.

If we accept the hypothesis that all elements have been built from hydrogen, the Burbidges, Fowler, and Hoyle (1957) find that eight different processes must be postulated to account for the observed features of the abundance curve:

1. Hydrogen burning to produce helium
2. Helium burning to produce C, O, Ne, and perhaps Mg
3. α -particle processes in which Mg^{24} , Si^{28} , S^{32} , Ar^{36} and Ca^{40} are produced by successive additions of helium nuclei to O^{16} and Ne^{20} , the α -particles being freed by heavy particle reactions, however
4. The equilibrium *e process* which was suggested to account for the iron peak
5. The *s process* in which neutrons are produced and captured at a relatively slow rate
6. The *r process* in which neutrons are captured on a fast time scale ~ 0.01 to 10 sec
7. The *p process* in which proton-rich isotopes are produced
8. The *x process* which is invoked for the production of the temperature-vulnerable light elements (Fig. 10-1).

The initial contraction from a pre-stellar state is halted at the main sequence when hydrogen burning starts. When all the hydrogen in the core has been converted to helium, a shell source is developed and the core continues to contract until the temperature and density are raised high enough for helium to burn.¹ Then when the helium has been burned into carbon, oxygen, and neon, a further gravitational contraction will take place. Reactions involving carbon, oxygen, and neon will occur and a host of nuclides will be built. The star can continue to extract energy until the elements of the iron peak are built, beyond which point no further energy can be obtained by nuclear reactions. Henceforth the star can obtain radiative energy only by a gravitational contraction which may produce instability. During the course of these events, neutrons are produced slowly during the orderly evolution of the star and perhaps very rapidly during its final catastrophic phases. These particles play an important role in element building, although not in energy production.

¹ Discussions have been given recently by Reeves and Salpeter (1959) and by Hayashi and his associates (1958).

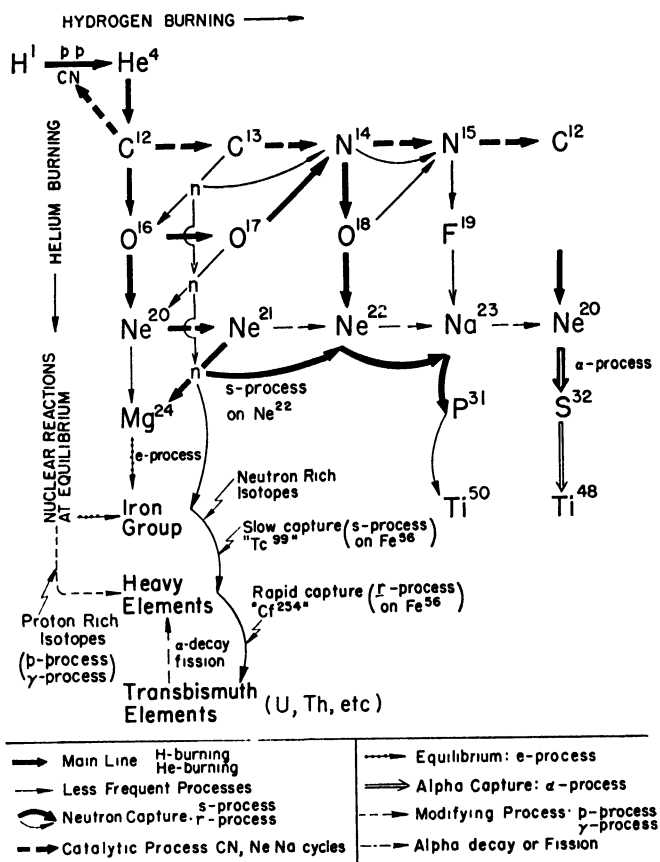
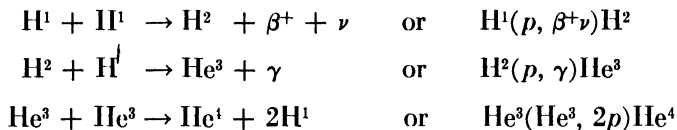


Fig. 10-1. Schematic diagram of nuclear processes by which synthesis of elements in stars takes place. (Reproduced from E. M. Burbidge, G. R. Burbidge, W. A. Fowler, and F. Hoyle, *Revs. Modern Phys.*, 29, p. 552, 1957.)

10-4. Hydrogen Burning

Throughout most of its life, a star shines by converting hydrogen into helium. In terms of the energy output per unit mass, hydrogen burning is by far the most productive nuclear process a star may experience. All other exothermic reactions are far less efficient energy producers, even though they may be of greater interest in connection with the problems of element building.

Consider first the reactions involved in a pure hydrogen composition. The helium can be produced only by the proton-proton chain. At lower temperatures and at a stage when little He^4 has yet been produced, the energy producing chain of events is

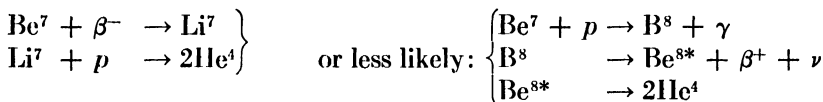
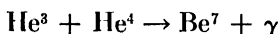


The total energy yield, Q , is 26.2 Mev. There is a 2-per-cent energy loss to the production of the neutrino, ν , when it and the positive electron β^+ are formed along with the deuteron, H^2 .

This first step of the proton-proton chain, $\text{H}^1(p, \beta^+\nu)\text{H}^2$, has never been verified experimentally because of its extremely low cross section. The reaction rate is computed by theory, but our confidence in the theory is greatly enhanced by the discovery of the free neutrino by C. L. Cowan, F. Reines, F. B. Harrison, H. W. Kruse, and A. D. McGuire (1956). The β -decay coupling constant and the free neutron lifetime have been determined with greater accuracy so that the rate of helium building now can be computed with increased confidence.

The deuteron captures a proton to form He^3 and then two He^3 nuclei collide to form an α -particle and two protons.

At high temperatures (i.e., $T > 1.3 \times 10^7^\circ\text{K}$) and large helium concentrations, the pp chain is completed in a different manner, viz.:



$$\bar{Q} = 25.6 \text{ Mev}$$

$$\bar{Q} = 19.1 \text{ Mev}$$

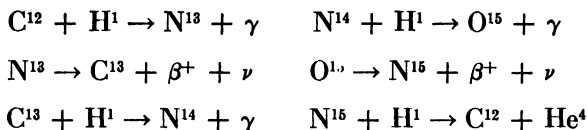
4 per cent loss

29 per cent loss

Notice that the Be^7 atoms are promptly destroyed by electron capture or by proton capture. If the central temperature of the hydrogen star is greater than 20 million degrees, the proton capture which produced B^8 will probably prevail and the star will lose much energy in the form of neutrinos (Fowler 1958). If the temperature is low enough ($< 8,000,000^\circ\text{K}$), the process ends at He^3 and no He^4 is formed. The

proton-proton reaction depends on the temperature less steeply than does the other principal H-burning reaction, the carbon cycle. The sun derives its energy mainly from the *pp* chain although some contribution comes from the carbon cycle.

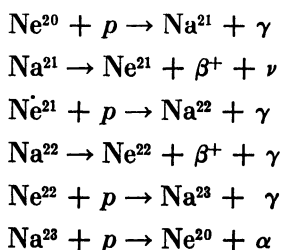
If carbon is present in the original mixture, H may be consumed by the well-known carbon-nitrogen cycle (Bethe 1939; Von Weizsäcker 1938).



By repeated proton capture, the C^{12} is transmuted successively to C^{13} , N^{14} , N^{15} , and finally reappears as C^{12} , the net result of the process being the conversion of four protons into one helium atom. From the standpoint of element building it is of interest to note that if C^{12} alone is initially present, C^{13} , N^{14} , and N^{15} will be produced. The relative proportions of C^{12} , C^{13} , and N^{14} depend on the temperature; a prediction of precise numerical values depends on the actual values of the cross sections for proton captures. The two slowest steps in the CN cycle are the $\text{C}^{12}(p, \gamma)$ and $\text{N}^{14}(p, \gamma)$ reactions whose rates have to be measured experimentally at energies much higher than those at which reactions can occur in the stars. Then the rates are extrapolated to low energies.

At such high temperatures as appear to occur in hydrogen-burning shells of red giant stars, O^{17} is produced by $\text{O}^{16} + \text{H}^1 \rightarrow \text{F}^{17} + \gamma$; $\text{F}^{17} \rightarrow \text{O}^{17} + \beta^+ + \nu$, but most of the O^{17} is destroyed by the exothermic reaction $\text{O}^{17} + \text{H}^1 \rightarrow \text{N}^{14} + \alpha + 1.20 \text{ Mev}$. A small amount must remain to explain the observed $\text{O}^{17}/\text{O}^{16}$ ratio observed on the earth.

It is of interest that Ne^{21} can be built in a neon-sodium cycle analogous to the carbon cycle.



The temperatures required for the operation of the neon-sodium cycle are so high that by the time these temperatures were reached in any star, we would anticipate that all the hydrogen would have been used up. Fowler and the Burbidges suggested that a resonance may favor the formation of Ne^{21} and that this nuclide may be built up in substantial quantities in the cores of certain stars. Indeed a level in Na^{21} , corresponding closely to the energy of $\text{Ne}^{20} + p$ has been discovered and its properties seem adequate to permit a large build-up of Ne^{21} (Marion and Fowler 1957). If protons are introduced into a hot region ($T \sim 100,000,000^\circ\text{K}$) at late stages in stellar evolution, they will react very quickly in all kinds of nuclear reactions. In fact such mixing is sometimes introduced to explain the formation of certain isotopes that cannot be accounted for by quieter reactions.

10-5. Helium-Burning and Alpha-Particle Reactions

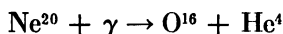
After the hydrogen in the core of a star has all been converted into helium, no further nuclear transformations can take place until the temperature and density both have greatly increased. Then occurs the phenomenon of helium "burning" to form carbon, oxygen, and other heavy elements. We might suppose that we could ram two α -particles together to form Be^8 , but Be^8 is unstable. Experiments have shown that whenever it is produced artificially in nuclear reactions it promptly decays into two α -particles although with a release of 94 kev of energy. In 1952, Edwin Salpeter suggested that at temperatures of the order of a 10^8°K and a density of about 10^5 g/cm^3 near the centers of dense cores of stars, a sufficient number of α - α impacts would take place for a small but not utterly negligible concentration of Be^8 to be built up. Before a given Be^8 nucleus disintegrated, it might capture another α -particle and form C^{12} . Hoyle (1954) suggested that the process might assume considerable importance if the so-formed compound C^{12} nucleus possessed a low-lying resonance. The existence of such a resonance in the form of an excited state of C^{12} was soon thereafter conclusively demonstrated in an experiment carried out at the California Institute of Technology. Fowler and his associates (1956) accelerated deuterons to a high energy in an electrostatic accelerator and fired them at boron, B^{11} , to produce B^{12} with the emission of a proton. The B^{12} undergoes β^- decay with a half-life of 0.020 sec to an excited state of C^{12} . This C^{12*} nucleus forthwith breaks down into three α -particles or (less

frequently) decays to the stable ground state of C^{12} . If the C^{12*} can decay to three α -particles, then conversely the ramming together of three α -particles to form C^{12*} is possible and since some of these C^{12*} nuclei will decay to those of normal C^{12} there exists a means of element synthesis for bridging the substantial gap between helium and carbon in the hot, dense cores of certain stars. During the red-giant phase of a star's evolution, this helium burning may be an important source of energy generation (Salpeter 1952, 1953, 1957; Opik 1951, 1954). The helium-burning phase probably takes 10^7 to 10^8 yr.

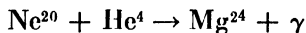
Subsequent α -particle captures can produce O^{16} , Ne^{20} , and perhaps a small amount of Mg^{24} . It is difficult to predict the anticipated amounts of these nuclides because none of the cross sections are known to better than a factor of 10. The rates depend markedly upon temperature. Hence different stars may produce very different ratios of carbon, oxygen, neon, and magnesium. Detailed calculations by Cameron (1959), for example, show that if helium is destroyed quickly at high temperatures and densities as might be expected in a massive star, C^{12} will be the main result, whereas in less massive stars, O^{16} and Ne^{20} are the principal nuclides formed.

In Chap. 9 we described a number of stars believed to be in late stages of their evolution where hydrogen burning had terminated and helium was being consumed. This group included such objects as Bidelman's star, HD140160, the binary ν Sagittarii where perhaps the outer layers had been stripped off in the course of the evolution, the variable carbon star, R Coronae Borealis, the Wolf-Rayet stars, and a number of other objects.

Eventually, when all of the helium has been burned into carbon, oxygen, and neon, the core of the star contracts yet further. At a temperature of about $1.3 \times 10^9 K$, the neon, carbon, and oxygen will be destroyed. The first reaction to occur is the photo-disintegration of Ne^{20} by the high-energy γ -rays then present, viz.,



and the α -particles so produced may build Mg^{24} by the reaction

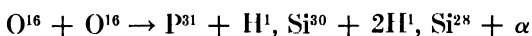
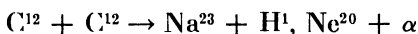
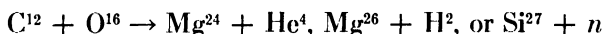


Although energy is absorbed from the gas in the production of the α -particles, it is released in the production of Mg^{24} so that there is a net output of energy. At these temperatures the α -particles can

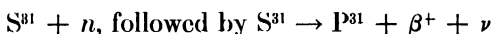
build Mg^{24} into Si^{28} and into S^{32} . Each nuclide produced in the α -process depends on the concentration of its predecessor and hence the abundances of the corresponding nuclei decline with increasing Z .

At high temperatures, other reactions will destroy the neon, carbon, and oxygen, and many light particles (α -particles, protons, and neutrons) will be produced.

For example:



and



Cameron (1959) has considered the reactions involving oxygen and neon in particular detail, estimating the cross section for the interactions and taking into account photo-beta and photo-neutron reactions. He assumed different initial composition mixtures and found that the principal effect of the oxygen and neon burning was to produce large quantities of Mg^{24} , Si^{28} , and S^{32} . If the star contained an initial "solar mixture" he found no increase in the abundances of the nuclei in the heavy-element region. Somewhat more detailed calculations have been carried out by Reeves and Salpeter (1959). In a gas consisting of C^{12} , O^{16} , Ne^{20} at densities of 10^4 g/cm^3 and temperatures 6×10^8 to $8 \times 10^8 \text{ K}$, they find C^{12} to be destroyed in $\text{C} + \text{C}$ collisions. Some O^{16} and Ne^{20} are produced as are appreciable amounts of Na^{23} and Mg , although the $\text{Na}^{23}/\text{Mg}^{24}$ ratio is significantly larger than the solar-system ratio. Below $7 \times 10^8 \text{ K}$, many neutrons are produced which may influence the formation of heavier elements if iron is present in quantity.

The Burbidges, Fowler, and Hoyle (1957) suggest that the peculiar white-dwarf Ross 640, which has strong Mg and Ca lines, may exhibit the operation of the α -process. Other white-dwarf stars may offer examples of α -process element building (Burbidge 1954).

Detailed calculations of element building at this stage can at best be only approximate since the relevant cross sections for so many of the processes are as yet unknown. We can expect that in the stages involving the destruction of oxygen and neon, elements such as F ,

Na, Al, P, Cl, and K will likewise be built up and in quantities that we cannot yet predict precisely. The time scale of the α -process is of the order of 100 to 10,000 yr.

If the initial mass and angular momentum of the star permit, the core will contract further until finally T exceeds 3×10^9 K. Detailed reactions can then no longer be followed.

10-6. The "Equilibrium" Process

The evolution of the star beyond the point where the central temperature reaches 3×10^9 K is very rapid. At this time the rate of nuclear processes is greatly enhanced and a statistical equilibrium between the nuclei, free protons, and neutrons is attained. Hoyle (1946, 1954) showed that elements in the iron peak could be synthesized under such conditions and later the Burbidges, Fowler, and Hoyle gave a more detailed and accurate treatment which we shall now describe.

The procedure is similar to that applied in equilibrium theories of the origin of the elements except that one attempts to account only for nuclides over a short mass-range $46 < A < 66$. At any temperature and density the concentration of nuclides will depend on their binding energies, the number and distribution of excited states, and appropriate statistical weights in accordance with well-established formulac. When the time scale is long enough the β -processes will occur sufficiently rapidly to establish an equilibrium between protons and neutrons. At densities and temperatures relevant to element-building processes in stars, free-neutron decay does not much influence the equilibrium.

If the time scale of the events is so short that neutrons and protons cannot attain an equilibrium, then the ratio of the total density of bound plus free neutrons to the total density of protons must have a fixed value determined by the state of the gas at the outset of the final stage. During these terminal stages, most of the β -decays do not have time to take place. On the other hand, those nuclides whose abundances are fixed by prompt nuclear reactions continue to maintain equilibrium abundances.

The temperature of the gas rises as the explosion point is approached and the equilibrium equations continue to hold. After the explosion of the core, the gas cools rapidly and the abundances are affected for a short time. The density of γ -radiation diminishes at such a rate that free α -particles, neutrons, and protons are produced by photo-

ejection reactions in too few numbers to affect seriously the abundances of the heavy nuclides. These become "frozen in" at a temperature and density that differ from one nuclear species to another. Many of these nuclei which are left behind are unstable against β -decay and the final abundance distribution is determined after these processes are taken into account. Thus the stars which produce these elements are presumed to explode as supernovae and distribute the reaction products throughout space. In any event, an explanation of the iron peak seems to require that some kind of an equilibrium situation existed somewhere in the universe before the solar system was formed.

The Burbidges, Fowler, and Hoyle assumed a series of different densities and temperatures, calculated relative abundances of the various nuclides, and compared them with the solar abundances determined by the Michigan group (cf. Chap. 5). The results are given in Fig. 10.2 where the theoretical predictions for $T = 3.78 \times$

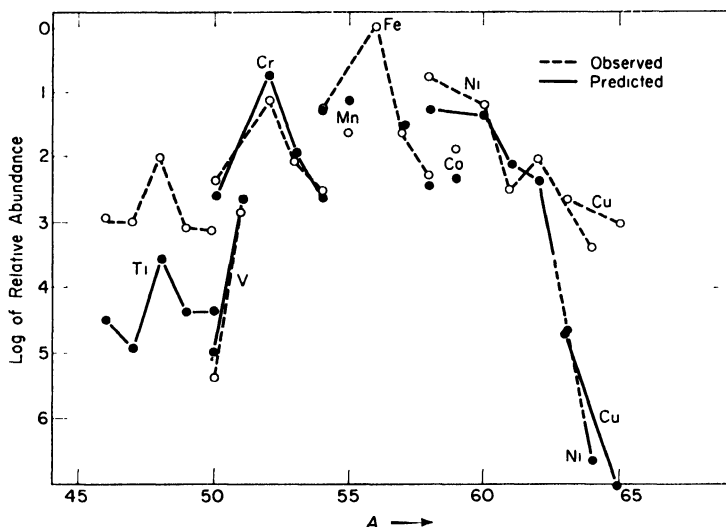
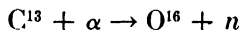


Fig. 10-2. Representation of the abundances of nuclides in the iron group. (—values predicted by E. M. Burbidge, G. R. Burbidge, W. A. Fowler, and F. Hoyle, *Revs. Modern Phys.*, **29**, p. 580, Table IV-1, 1957); —observed values for the sun, Goldberg-Müller-Aller. The figure is similar to Figure IV-1 in the Burbidge, Burbidge, Fowler, and Hoyle article except that the revised rather than preliminary values of the solar abundances are used.

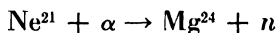
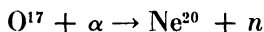
10^{10}K , $n_p/n_n = 30$, and $\rho \sim 10^5 \text{ g/cm}^3$ are plotted with the solar data. It is assumed that the isotope ratios in the sun and earth are the same. For the nuclides falling in the range $50 \leq A \leq 62$, the representation of the observed data is good and might be improved if the solar abundance data were more accurate and if the binding energies of the various nuclides were better known. Copper, nickel, and titanium show large discrepancies in the sense that equilibrium theory predicts abundances that are too small. The copper and nickel nuclides are probably mostly produced by neutron capture on a slow time scale (see Sec. 10-7), whereas titanium isotopes are produced partly by the α -process and partly by neutron capture.

10-7. Neutron-Capture Processes

Of enormous importance to the process of element building is the production of neutrons in stars during the advanced stages of their evolution. J. L. Greenstein and also A. G. W. Cameron (1955) have suggested specific mechanisms whereby intermediate and heavy elements could be manufactured in stars if neutrons could be produced in sufficient quantities. Consider a reaction between C^{13} and an α -particle, viz.,



Similarly, O^{17} and Ne^{21} can liberate neutrons by the reactions



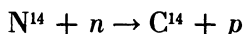
This last mentioned reaction is the one favored by Fowler and his associates as the principal source of neutrons in stars. The O^{17} reaction is not likely to be important because of the rarity of this isotope, but Ne^{20} is formed in large supply by helium burning. Then, in the hydrogen-burning shells surrounding the inert helium cores of red-giant stars the temperature rises so high that the neon-sodium cycle occurs and a substantial fraction of Ne^{21} is produced. As the hydrogen in the H-burning shell is converted into helium and passed into the inert core, the Ne^{21} interacts with the α -particles to produce neutrons. This mechanism has the advantage that it is not necessary to mix hydrogen into a zone containing C^{12} to produce C^{13} by the proton-capture mechanism as Cameron had originally suggested.

There are difficulties in that neutrons tend to be captured by N^{14} and lost to the element-building mechanisms over a considerable range of temperature and density likely to be encountered in stars.

The neutrons which are released cannot combine with the α -particles to form a stable nucleus. They take up kinetic energies appropriate for the local temperature (corresponding to about 10 kev) and are captured predominantly by heavier nuclei at a rate that depends on their abundance and on their cross sections for neutron capture. Under the conditions anticipated in the interiors of red-giant stars, the time interval that will elapse between successive neutron captures by a given heavy nucleus will be of the order of five or ten years to thousands of years. Consequently, nuclei with short lifetimes, of the order of days or a few years, will undergo β -decay, and isobars with large neutron excesses will not be built up; the nuclides will tend to lie in the bottom of the valley of the isobaric mass curves (Chap. 7, Fig. 2). Likewise, the "proton-rich" isotopes cannot be built by any neutron-capture process.

Consider two isobars ($Z + 2, A + 2$) and ($Z, A + 2$). The latter can be formed from neutron-rich nuclides that have evolved through β -decay. It is called an *unshielded isobar*, and on the slow time scale just discussed, its formation from the nuclide (Z, A) would require that the nuclide ($Z, A + 1$) formed by neutron capture would last long enough (several years) for it to capture another neutron. Usually this will not happen. The nuclide ($Z, A + 1$) undergoes β -decay to ($Z + 1, A + 1$), which is stable and then captures another neutron to form the shielded isobar ($Z + 2, A + 2$). Certain types of isobars called *excluded isobars* cannot be formed by neutron capture at all.

Cameron's calculations show that an optimum release of neutrons for heavy-element production occurs if only a very small amount of hydrogen is mixed with helium which has evolved to form some C^{12} . If hydrogen is introduced in any quantity in a medium containing helium and neutrons, the formation of deuterium will quickly use up all the neutrons. Also, if N^{14} is present to any appreciable extent, it will act to reduce the neutron density by converting the neutrons to protons by the reaction:



The most favorable conditions are found when the amount of N^{14} left over from the carbon cycle reactions is small. The protons formed

in this way would undergo the carbon cycle changes and some would produce C^{13} . Cameron finds that if 12 per cent of the helium nuclei are converted into carbon nuclei, the optimum amount of hydrogen to be mixed in the core is only three parts in a thousand.

Suppose that the interior of a star contained the elements in their "standard" abundances and that to this mixture neutrons were added in varying amounts. The nuclei of existing elements would be built into yet heavier ones; the enhancement in the numbers of these heavier elements would depend on capture cross sections and numbers of neutrons. Only relatively small changes occur in the elements below iron because their abundances are already roughly in inverse proportion to their neutron-capture cross sections. Furthermore, many of them are so abundant already that only a small fraction of the atoms are affected by neutron capture.

Cameron carried out some illustrative calculations for 5, 10, 15, 20, 30, 50, 80, and 125 neutrons injected per initial silicon atom. With only five neutrons introduced there is only a small effect, but thereafter there is a rapid growth of heavy element abundance with increasing numbers of neutrons. The growth levels off after 20 neutrons, reaches a peak at 50 neutrons, and thereafter it declines since the heavy-element abundances are now maintained by building up nuclei from the neighborhood of sulfur. We examine Cameron's calculations for 20 neutrons (Fig. 10-3). Most of the neutron captures take place in the neighborhood of the iron peak with the consequence that as these elements are transmuted up into heavier ones, abundances of the heavy atoms may be enhanced by several hundred-fold. Lead is also built up to a high abundance. Notice that the iron peak is shifted over to an atomic weight of about 70. The sharp peak at mass number 140 is due to the closed shell of 82 neutrons. Neutron capture on a slow time scale also accounts for the abundance peak in the Suess-Urey compilation at $A = 90$, corresponding to the magic-number nuclei with $N = 50$. As noted previously in our discussion of the Gamow theory, these nuclei have smaller target areas for neutron capture than do other nuclides nearby.

It has been supposed generally that the technetium in the *S*-type stars is produced by neutron capture in the following reaction:



The Mo^{99} has a lifetime of 67 hr. In its turn Tc^{99} can be built up to

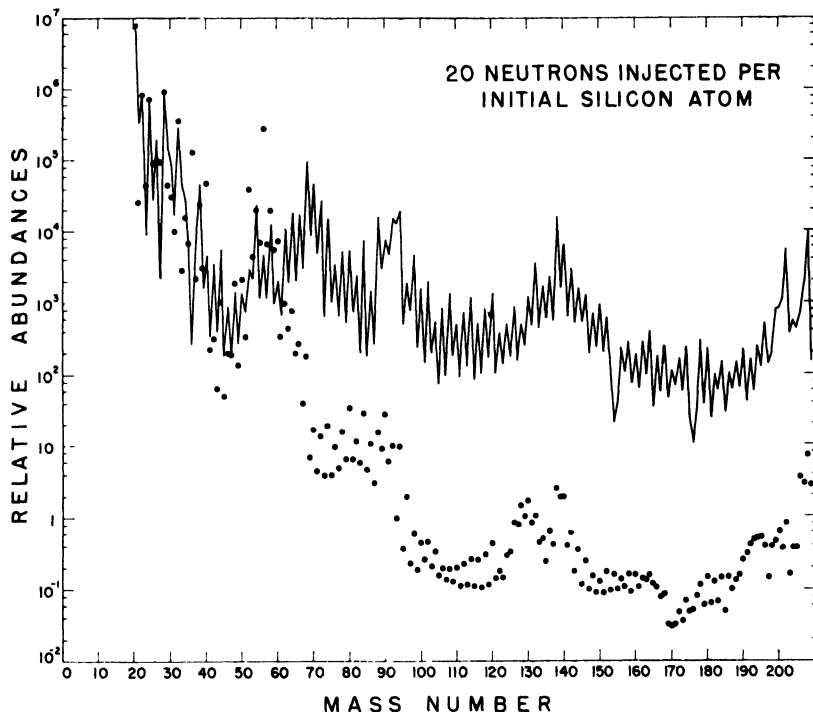


Fig. 10-3. Abundances of heavy elements following neutron capture. The dots give the assumed initial abundances; the solid lines the final abundances. (Reproduced from A. G. W. Cameron, *Atomic Energy of Canada Limited Report* 454, p. 96, Fig. 11.1.4, 1957.)

form Ru^{100} by the capture of a neutron. It is of interest that technetium in S stars appears to have an abundance of the same order of magnitude as the neighboring elements, ruthenium and molybdenum. The implication is that all these heavy elements were built at the same time and in the same spot in the stars, and furthermore considerable mixing must have occurred between the surface layers and the region where the elements were built. Now the length of time an evolving star may spend as an M giant is probably of the order of ten million years. If the S stars evolve from them, it follows that they have lifetimes of the order of 100,000 yr since they are about 1 per cent as numerous. In this time scale, technetium could be built up to an abundance comparable with that of its neighboring elements.

On the other hand, Cameron suggested that the technetium present in *S* stars is not produced by neutron captures but by a mechanism involving photo-disintegration.

The heavy metals whose abundances are enhanced in the *S* stars appear to be those which are built by neutron capture on a slow time scale, the *s*-process. On the other hand, there appear in nature not only the neutron-rich and proton-rich isotopes which cannot be produced by slow neutron capture, but also the radioactive heavy elements, uranium and thorium. Now bismuth is the last element that can be built by the *s*-process. If Bi^{209} captures a neutron to form the unstable isotope Po^{210} , the latter will decay to Pb^{206} by α -particle emission before another neutron can be captured. The Pb^{206} may then be built up again to Bi^{209} , but no uranium or thorium can be produced.

Accordingly, it is necessary to consider what happens if the neutrons are captured on the fast time scale, i.e., the *r*-process. In a slow time scale, each reaction product has time to undergo β -decay before it captures another neutron. Hence the nuclei will tend to stick to the domain of maximum stability (cf. Fig. 2, Chap. 7). On the other hand, if neutron capture can occur at a great rate, a nucleus may capture another neutron before it can undergo β -decay in say 0.1 to 1 sec. Then it will evolve along a different path in which it will retain as many neutrons as it possibly can hold (Figs. 10-4 through 10-6).

The abundances of the nuclides with odd mass numbers, as adopted from the work of Suess and Urey, show broad peaks centered on the mass numbers 80, 130, and 195. These broad peaks are due to the rapid capture of neutrons which cause nuclides to pile up at neutron numbers where the capture cross sections are low (i.e., magic numbers). These nuclides are unstable; they are top-heavy with neutrons and must evolve by β -decay into their final stable forms. Hence nuclides are finally produced with fewer neutrons than the magic numbers, and smaller atomic weights!

Cameron and also Hoyle, Fowler, and the Burbidges (1956) have examined in detail the mechanisms by which various nuclides are formed. Some can be formed by slow neutron capture, some by fast neutron capture, some by both, and yet others by neither. As an illustration, Hoyle, Fowler, and the Burbidges (1956) mention the example of tellurium which has eight isotopes. The light isotopes,

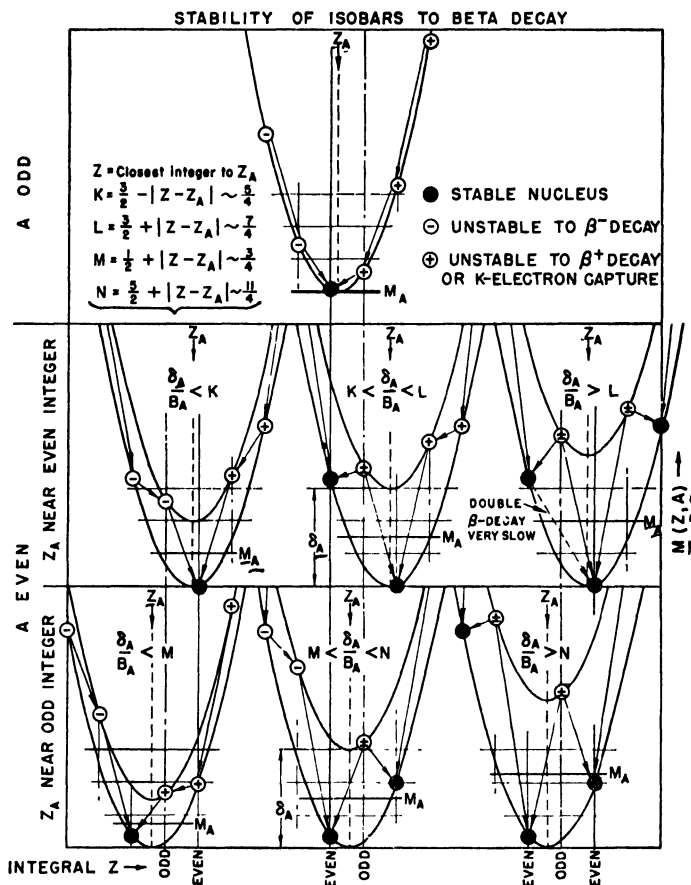


Fig. 10-4. Stability of nuclear isobars to β -decay. (Reproduced from E. M. Burbidge, G. R. Burbidge, W. A. Fowler, and F. Hoyle, *Revs. Modern Phys.*, 29, p. 581, Fig. V-2, 1957.)

Te^{122} , Te^{123} , and Te^{124} can be produced only in the slow neutron-capture process. In the rapid-capture process, the neutron-rich isobars with masses 122, 123, and 124, undergo decay into the stable isotopes of tin and antimony, viz., Sn^{122} , Sn^{124} , and Sb^{123} . The heaviest tellurium isotopes, Te^{130} , can be produced only in the rapid neutron-capture process since it is the stable product of the decay of the neutron-rich isobars of mass 130. In the slow-capture process, Xe^{130}

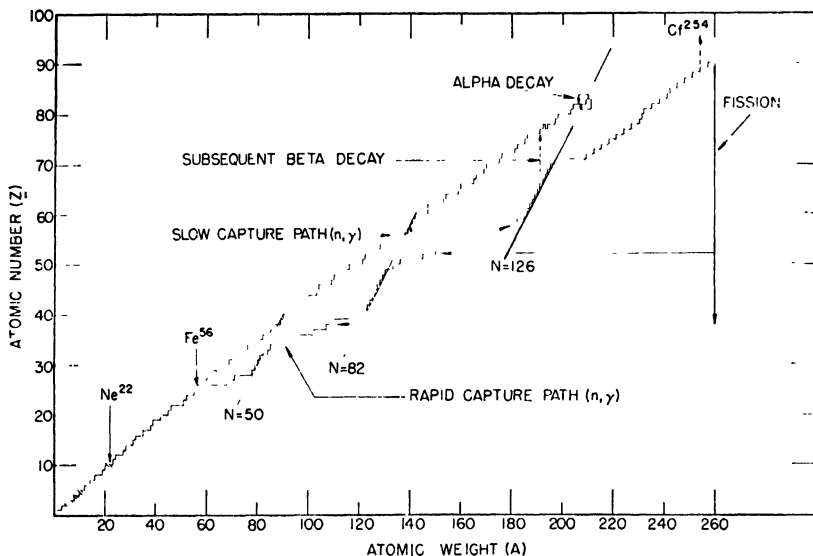


Fig. 10-5. Neutron capture paths of *s*-process and *r*-process. (Reproduced from E. M. Burbidge, G. R. Burbidge, W. A. Fowler, and F. Hoyle, *Revs. Modern Phys.*, 29, p. 582, Fig. V-2, 1957.)

is built instead of Te^{130} . The intermediate isotopes, Te^{125} , Te^{126} and Te^{128} , can be built in either process, although Te^{128} is formed predominantly by the rapid process. The abundance of Te^{126} is comparable with that of Te^{128} and Te^{125} and follows the trend of the rapid-capture process; all are assigned to the rapid neutron-capture mechanism. The rare, light isotope of tellurium, Te^{120} , can be built neither by the slow nor the fast neutron-capture process. It is an example of a class of isotopes that have an excess of protons. Either a small proportion of the heavier elements produced are introduced into a hydrogen-rich region or the heavier nuclides are photo-dissociated in reactions that involve the absorption of γ -rays and the emission of neutrons. From $A = 70$ to $A = 200$, these proton-rich isotopes are approximately 1 per cent as abundant as neighboring isotopes that are produced by the neutron capture processes.

An intense flux of neutrons cannot be produced during the orderly stages of stellar evolution, but apparently originates during the rapid collapse of the star following the formation of the elements in the iron peak. According to the Burbidges, Fowler, and Hoyle, as the

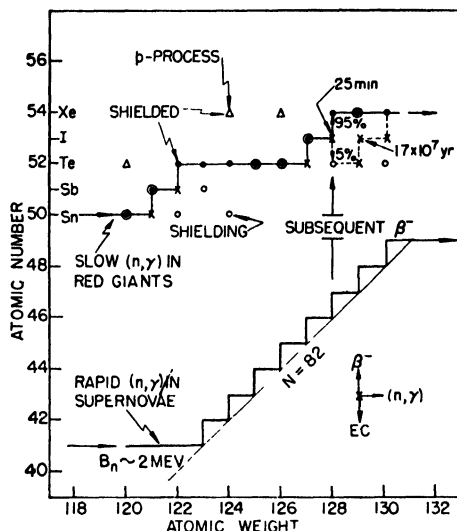


Fig. 10-6. Detail of neutron capture process tracks. (Reproduced from E. M. Burbidge, G. R. Burbidge, W. A. Fowler, and F. Hoyle, *Revs. Modern Phys.*, **29**, Fig. V-3, 1957.)

temperature rises beyond the point where the iron metals are formed under conditions of statistical equilibrium, the energy density in the γ -rays becomes so great that a photo-disintegration of elements of the iron group appears. These nuclei become broken down into α -particles in endothermic reactions that may absorb huge quantities of energy from the surroundings. Furthermore, no additional sources of nuclear energy are available to the star. As a consequence, the core of the star collapses suddenly as the gravitational force is no longer compensated by the pressure of the hot gas and radiation in the stellar interior. A considerable amount of gravitational potential energy is liberated suddenly. Hoyle estimated that the collapse would take place in the order of a minute. This implosion produces some mixing of the outer layers which contain great quantities of hydrogen and other "volatile" nuclei into the still hot gases of the interior. The result is a violent explosion. Under certain circumstances much energy may also be carried off by neutrinos.

If the number of protons is comparable with the number of heavier nuclei, they will be captured to form nuclides like N^{13} , F^{17} , Na^{21} ,

Al^{26} , which undergo β -decay to C^{13} , O^{17} , Ne^{21} , Mg^{25} , respectively. Subsequent α -particle captures by these nuclei may take place very quickly to release great quantities of neutrons in (α, n) reactions. Many of these neutrons will be captured by heavy nuclei to form yet heavier neutron-rich nuclides. The time interval between successive neutron captures is now of the order of a second rather than of a year or a century. Consequently, a given nucleus will have no time in which to undergo a β -decay before another neutron is captured. Nuclides will be built up, therefore, high on the neutron-rich side of the energy valley. If the source of neutrons is sufficiently copious, elements will be built up to the massive unstable elements such as Cf^{254} which decays by spontaneous fission with a half-life of 55 days. The fission products in their turn are built into heavier elements and the process ends when the temperature falls and the supply of neutrons is exhausted.

The connection between supernovae and nucleogenesis seems further strengthened by the remarkable character of the light curves of the former. Supernovae differ in their characteristics. The more modest type (called type II) attain maximum luminosities about ten million times that of the sun. They appear to be associated with the spiral-arm population (type I) and therefore consist of stars enriched in heavy elements by an amount comparable with the sun. The more spectacular type I supernovae, associated with the type II stellar population, attain maximum luminosities of the order of 10^8 that of the sun. They are comparable in brightness with the galaxies in which they are found. After a couple of months, the star's brightness falls off exponentially with a half-life of 55 ± 1 days. The Burbidges, Hoyle, Christy, and Fowler called attention to the fact that this half-life is closely coincident with that of Cf^{254} . Substantial quantities of californium are produced in H-bomb detonations when the U^{238} in the material is exposed to an intense neutron flux during the explosion. The Cf^{254} decays by spontaneous fission with a half-life of 56 days, liberating 200 Mev per nucleus, whereas the Cf^{252} decays at a slower rate, mostly by α -particle decay. The mechanism invoked to explain the light curve is the following.

When the implosion occurs, great quantities of neutrons and γ -rays are produced. The intense flux impinges on the mixture of heavy elements building these into heavier neutron-rich nuclei. If neutrons are added on a fast time scale, the path of a given nucleus

in the (Z - A) diagram will fall below that of the slow neutron-capture (s -process) path. In particular, the region of lead and bismuth will be by-passed and the addition of neutrons will cease near $A \sim 260$ when the nuclides become unstable against fission. Some of the nuclides will decay directly to thorium, uranium, or their progenitors. Thus the natural radioactive elements are produced by r -process events. The Burbidges, Fowler, and Hoyle were able to estimate the original abundances of U^{235} and U^{238} . In the r -process the formation of U^{235} is favored over that of U^{238} by a factor of 1.6 since it has a greater number of progenitors. Hence the initial abundance of the lighter isotope should exceed that of the heavier isotope by this factor and if we suppose that the terrestrial uranium was produced by a single supernova event we can calculate when it occurred given that today $N(\text{U}^{238})/N(\text{U}^{235}) = 140$ and that the half-lives of U^{238} and U^{235} are 4.5×10^9 and 7.1×10^8 yr, respectively. In this way, an "age" of the uranium of 6.6×10^9 yr is obtained. Alternatively, if many supernovae distributed uniformly in time contributed to the formation of the r -process nuclides in the solar system, the Burbidges, Fowler, and Hoyle found that the process had to start 10^{10} yr ago. In any event, the elements appear to have been formed long before the formation of the solar system. A more recent consideration of the decay of the radioactive isotopes Th^{232} , U^{235} , U^{238} by Fowler and Hoyle leads to the conclusion that the age of the galaxy lies between 12×10^9 and 20×10^9 yr. This model assumes that no material has been added from intergalactic space since the formation of the galaxy.

Clearly, detailed abundances cannot be calculated quantitatively, but the qualitative features appear to be well enough reproduced. The rarity of proton-rich nuclides which are produced by photoejection of neutrons by γ -rays or by proton captures during the supernova explosion are easily understood. One minor difficulty may be the apparent discordance between the predicted and observed abundance of lead. Calculations based on theories of nucleogenesis (cf. particularly Cameron 1959) predict a high abundance of lead compared with its neighboring elements not in complete agreement with the meteoritic and the solar values (cf. Chap. 8). More recent work by Fowler and his associates tends to lessen this discrepancy and perhaps remove it entirely.

The type II supernovae (associated with population type I stars) apparently show no indication in their light curves of the decay of

Cf²⁵⁴. Cameron and also the Burbidges, Fowler, and Hoyle suggest that in these stars, envelopes containing great quantities of hydrogen are mixed with hotter layers and protons are added more readily than in type I supernovae to heavy elements to produce proton-rich nuclei.

Recently Anders (1959) has suggested that the exponential decline of type I supernovae is due to the decay of Fe⁵⁹ (with half-life 45 days) rather than to the decay of Cf²⁵⁴. In spite of the advantages claimed for this model, the Cf²⁵⁴ hypothesis appears to give a better internally consistent picture of the building of the *r*-process and the heavy elements.

10-8. The Problem of the Synthesis of Deuterium, Lithium, Beryllium, and Boron

The light elements, deuterium, lithium, boron, and beryllium, cannot be produced by thermonuclear reactions in stellar interiors since they (H²) are inevitably built up into or (B, Be, Li) broken down into α -particles. We have seen that the abundance of deuterium on the earth is probably very much higher than in the sun. Lithium appears to be three hundred times rarer in the sun than on the earth, while Bonsack (1959) has found even higher ratios in the late-type dwarfs. Evidently this element is destroyed by nuclear reactions occurring at the bottom of the convection zone. In the interstellar medium, Spitzer found an upper limit of 0.1 for the Li/Na ratio which is well within the range of normal lithium abundance. On the other hand, certain late-type carbon stars and the T Tauri variables have lithium abundances that approach the terrestrial value.

The Be/H ratio in the sun is 2×10^{-10} which is somewhat smaller than the Suess-Urey value. Fowler and the Burbidges (1955) found a similar result for the magnetic star, α_2 Can Ven, whereas Spitzer found an upper limit to the beryllium abundance in the interstellar medium about twenty times smaller than that found in the sun, and suggested that some of it may be incorporated into the interstellar solid particles.

The Burbidges, Fowler, and Hoyle have examined the conditions for the formation of these elements in our galaxy. Since these nuclei are so easily destroyed in stellar interiors, it is generally suggested that they are produced in stellar atmospheres or under other conditions of low density and temperatures. The following possibilities

are assessed: (1) nuclear reactions in magnetic stars and in red dwarf stars; (2) spallation processes in certain non-thermal mechanisms in gaseous nebulae and T Tauri stars and (3) neutron-capture and spallation processes in the expanding shells of supernovae.

The large magnetic fields found in such stars as α_2 Can Ven may produce accelerations of particles that will create light elements by spallation. The difficulty with this hypothesis is that a deuterium/hydrogen ratio of only less than 10^{-10} can be produced in this way even if the entire output of the mechanism is ejected into the interstellar medium. Likewise, if we suppose that all the Li, Be, and B are produced by spallation processes high in the atmospheres of magnetic stars, negligible quantities of these elements will be supplied to the interstellar medium. If similar processes occur in red dwarf stars and the products are supplied to the medium, metal/H ratios as great as 10^{-10} can be confidently predicted. On the other hand, the recent data of Bonsack would suggest that the lithium produced in a red dwarf star would be destroyed at the bottom of its convection zone.

It is possible, of course, that these light elements are manufactured with their terrestrial abundances during the formation of the star as suggested by Greenstein and Bonsack who proposed that the magnetic energy in a proto star was used to accelerate protons and build up lithium in T Tauri stars presumably by spallation processes.

The radio-frequency radiation from a number of galactic nebulae and rf sources is of a non-thermal type. Probably it is synchrotron-type radiation produced by high-energy electrons moving in a magnetic field. There appears to be sufficient energy present to permit the production of particles capable of inducing nuclear transformations such as stripping reactions. The densities are so low that the amount of H^2 , Li, B, and Be produced in this way must be very small, although perhaps in the early stages of their development these sources may have been capable of producing such atoms.

Many, perhaps all, of these rf sources are ex-supernovae. Hence, the light elements may have been created in an expanding shell of a supernova, e.g., by exposing a shell of hydrogen to an intense neutron flux, deuterium may be produced. Similarly, an intense flux of high-energy neutrons or protons might produce Be, Li, and B from atoms of C, N, and O by spallation. The problem of forming these light elements in sufficient quantities remains one of the out-

standing difficulties in current theories of nucleogenesis. Possibly they were created early in the history of the solar system in low-density regions subject to large magnetic fields that accelerated particles to high energy. Flare activity may have been very great in the proto sun as the T Tauri star data suggest.

Some details of the reaction cross sections appropriate to this situation have been considered (Bashkin and Peaslee 1961). It appears that the isotopic ratios of Li^6/Li^7 and $\text{B}^{10}/\text{B}^{11}$ from spallation reactions are of the order of 0.1 to 0.2, in good agreement with terrestrially observed values. It seems extremely difficult to find a mechanism for producing H^2 in terrestrially observed abundances, and one is lead to postulate some mechanism of relative H^2/H^1 concentration in the early stage of planet formation.

10-9. Element Building in the Atmospheres of Magnetic Stars

Fowler and the Burbidges (1955) suggested that the high abundances of certain heavy elements in the magnetic *A* stars were produced in the atmospheres themselves, rather than in their interiors, since these stars did not seem to differ very much from normal main-sequence *A* stars.

The detailed mechanisms are not known, but clues are suggested by radio bursts of the type first observed by Wild in Australia and found to be sometimes associated with solar flares. The type III bursts which are associated with the highest velocities are believed to be due to the coherent upward motion of rapidly moving (30,000 to 100,000 km/sec) charged particles in the solar atmosphere. The corresponding energies of the protons are 5 to 50 Mev. The duration of the bursts is of the order of 10 sec, but they sometimes occur in groups. Certain very brilliant flares are also associated with enhancements in cosmic rays of low energy. Fowler and the Burbidges supposed that in regions where the magnetic field changes rapidly the particles are accelerated by the Swann-Betatron mechanism with due allowance for collision processes, etc., in the gas. They had to assume local magnetic fields of the order of a million gauss, and spot regions with diameters of about 20,000 miles and densities of 10^{-7} to 10^{-8} g/cm³. They estimated that between 1 and 50 per cent of the magnetic energy could be converted to kinetic energy. In some instances the acceleration mechanism might operate for only a few seconds at a time.

In the region of acceleration, (p , n) reactions would enable a ratio of neutrons to protons of the order of 0.01 to 0.001 to be built up. Most of these neutrons will escape from the "hot spots" and be captured by protons to form deuterium in the surrounding regions. Eventually, as hot spots break out at various regions over the surface of the star, a greater and greater concentration of deuterium is built up. Subsequently, these deuterons are themselves accelerated and serve to build up heavy elements from the iron peak by stripping collisions (d , p and d , n). Also, the release of neutrons that are captured by heavy elements to build up yet heavier ones, such as the rare earths, may account for anomalous abundances found in magnetic stars. They found that if they assumed that the process had operated for about 500 million years, they could account plausibly for the overabundances of Sr, Y, Zr, La, and rare earths.

The high concentration of these substances in the magnetic stars is favored not only by the presence of huge magnetic fields, but also by the fact that the convection zone is very shallow. Hence, the synthesized elements are predominantly confined to the superficial layers of the star. One interesting by-product of the reactions is that He^3 may be built up by the well-known reaction $\text{H}(d, \gamma) \text{He}^3$, i.e., by the capture of protons by deuterons. Under certain conditions, the concentration of He^3 may become comparable with that of He^4 , a situation which the Burbidges find probably exists in the magnetic star, 21 Aquilae.

Serious difficulties in this Fowler-Burbidge theory have been pointed out by Bashkin and Peaslee (1961) who note that production of the excess abundances of heavy elements by any combination of mechanisms would entail complete destruction of C, N, and O in the same atmospheric strata.

10-10. Concluding Remarks

The theory of nuclide building in stars seems to account for all principal features of the abundance distribution of the elements. It is shown that it is possible to start with a star of pure hydrogen that will burn hydrogen into helium and eventually helium into carbon, oxygen, neon, and magnesium. In the next generation, nitrogen and other light elements may be built, and if the star is massive enough to evolve an iron-making core or undergo a supernova expansion, all of the elements can be built. The oldest known stars,

the subdwarfs, all contain iron and heavier metals although in much smaller quantities than does the sun. Apparently, these elements were built in massive stars or supernovae that preceded them. The age of the oldest stellar systems appears to be of the order of 10^{10} yr, or twice the age of the solar system which was itself built out of the debris of longdead stars. Each star that evolves from the main sequence into the giant or supergiant phase returns some of its substance to the interstellar medium. In spiral and irregular galaxies, new stars are continually being born from the interstellar gas and dust. In the type II population, globular clusters, and elliptical systems, the stars appear to die off gradually; there is no efficient mechanism whereby the gas which is returned to interstellar space leads to formation of new stars. In some elliptical systems such formation may occasionally occur, but is so rare as to have no great effect on the general evolution. In the spiral-arm population, the building of heavy elements seems to be continuing as recycling continues between stars and gas.

Thus, the evolution of the observable universe results in a gradual transformation of hydrogen into helium and heavier elements, but many, perhaps most, of these heavy atoms are sealed forever in the dense, white-dwarf stars from which they can never be extracted. Only the material scattered into the interstellar medium lives on in the main stream of the evolution of stars and nebulae.

Selected References

- Alpher, R. A., and R. C. Herman, *Revs. Modern Phys.*, **22**, 153, 406, 1950.
Anders, E., *Ap. J.*, **129**, 327, 1959.
Bashkin, S., and D. C. Peaslee, *Ap. J.*, in press, 1961.
Beskow, G., and L. Treffenberg, *Ark. Mat. Astron. Fysik A* **34**, Nos. 13, 17, 1947.
Bethe, H. A., *Phys. Rev.*, **55**, 103, 434, 1939.
Bonsack, W. K., *Ap. J.*, **130**, 843, 1959.
Burbidge, E. M., and G. R. Burbidge, *Publ. Astron. Soc. Pacific*, **66**, 308, 1954.
Burbidge, E. M., G. R. Burbidge, W. A. Fowler, and F. Hoyle, *Revs. Modern Phys.*, **29**, 547, 1957.
Cameron, A. G. W., *Ap. J.*, **121**, 144, 1955; *Chalk River Reports* 652, 1956; "Stellar Evolution, Nuclear Astrophysics, and Nucleogenesis," *Chalk River Project CRL-41*, 1958; *Ap. J.*, **130**, 429, 895, 1959.
Chandrasekhar, S., and L. R. Henrich, *Ap. J.*, **95**, 288, 1942.
Cowan, C. L., F. Reines, F. B. Harrison, H. W. Kruse, and A. D. McGuire, *Science* **124**, 103, 1956.
Fowler, W. A., *Ap. J.*, **127**, 551, 1958.
Fowler, W. A., et al., *Bull. Am. Phys. Soc.*, **1**, 191, 1956.

- Fowler, W. A., G. R. Burbidge, and E. M. Burbidge, *Ap. J. Suppl.*, **2**, 167, 1955.
- Fowler, W. A., and J. L. Greenstein, *Proc. Nat'l Acad. Sci.* **42**, 173, 1956.
- Greenstein, J. L., *Mem. Roy. Soc. Liege* **14**, 307, 1954.
- Hayashi, C. et al., *Progr. Theoret. Phys.* (Kyoto) **20**, 110, 1958.
- Hoyle, F., *Monthly Notices Roy. Astron. Soc.*, **106**, 343, 1946; *Ap. J. Suppl.*, **1**, 121, 1954.
- Hoyle, F., W. A. Fowler, E. M. Burbidge, and G. R. Burbidge, *Science*, **124**, 611, 1956.
- Klein, O., G. Beskow, and L. Treffenberg, *Ark. Mat. Astron. Fysik*, **B 33**, no. 1, 1946.
- Opik, E. J., *Proc. Roy. Irish Acad.*, **A 54**, 49, 1951; *Mem. Roy. Soc. Liege* **14**, 131, 1954.
- Marion, J. B., and W. A. Fowler, *Ap. J.*, **125**, 221, 1957.
- Mayer, M. G., and E. Teller, *Phys. Rev.*, **76**, 1226, 1949.
- Podolanski, J., and D. Ter Haar, *Mem. Roy. Soc. Liege*, **14**, 19, 1954.
- Reeves, H., and E. E. Salpeter, *Phys. Rev.*, **116**, 1505, 1959.
- Salpeter, E. E., *Ap. J.*, **115**, 326, 1952; *Ann. Rev. Nuclear Sci.*, **2**, 41, 1953; *Phys. Rev.*, **107**, 516, 1957.
- Spitzer, L., *Ap. J.*, **109**, 548, 1949.
- Spitzer, L., and G. B. Field, *Ap. J.*, **121**, 300, 1955.
- Suess, H., and H. C. Urey, *Revs. Modern Phys.* **28**, 53, 1956.
- Von Weizsäcker, C. F., *Z. Physik*, **39**, 633, 1938.

Author Index

- Abt, H., 211, 237
Adams, W. S., 207
Adgie, R. L., 162, 169
Ahrens, L. H., 30, 31, 32, 33
Aizu, H., 146, 147, 149
Alfvén, H., 142, 149
Allen, C. W., 93, 95, 119, 124, 127, 128,
129, 131, 132, 133, 134, 135, 197
Alpher, R. A., 241, 242, 268
Anders, E., 264, 268
Appo Rao, M. V. K., 144, 145, 150
Arp, H. C., 15, 206
Asaad, A. S., 124, 127, 128, 129, 131,
132, 133

Baade, W., 219
Baker, J. G., 65
Barbier, D., 119
Baschek, B., 208, 237
Bashkin, S., 163, 266, 267, 268
Bate, G., 44, 53, 189, 198
Bates, D., 94, 100, 124, 131, 133, 134,
135, 140
Bauer, C., 47
Baum, W., 204, 206
Beals, C. S., 215
Bell, G. D., 92, 95, 124, 133, 141
Berman, L., 226
Beskow, G., 241, 268
Bethe, H., 248, 268
Bidelman, W., 21, 164, 167, 169, 212,
213, 226, 227, 228, 229, 230
Biermann, L., 18, 124, 131
Birch, F., 34, 38
Biswas, S., 144, 145, 150
Boato, G., 57, 58
Bobrovnikoff, N. T., 164
Böhm, K. H., 118, 136, 140
Böhm-Vitense, E., 234
Boisse, A., 41

Boldt, G., 124, 131
Bonsack, W. K., 235, 237, 264, 265, 268
Bouigne, R., 227, 228, 237
Boury, A., 114
Bowen, I. S., 63, 75, 77, 119, 140
Brandenburg, W. J., 70, 78
Brandt, H. L., 142, 150
Bretz, M., 136
Brewer, L., 96
Brown, Harrison, 45, 49, 53, 58, 173,
175
Burbridge, E. M., 24, 162, 163, 166, 169,
198, 200, 207, 208, 216, 230, 231, 232,
233, 236, 238, 244, 245, 251, 252, 253,
258, 259, 260, 261, 262, 263, 264,
266, 267
Burbridge, G. R., 24, 162, 163, 166, 169,
189, 198, 200, 207, 208, 216, 230, 231,
232, 233, 236, 238, 244, 245, 251,
252, 253, 258, 259, 260, 261, 262,
263, 264, 266, 267
Burgess, A., 65, 66, 77
Buscombe, W. P., 229, 238

Cabannes, J., 119, 125, 140
Cameron, A. G. W., 24, 159, 166, 170,
173, 180, 189, 193, 195, 198, 200,
207, 230, 236, 238, 244, 250, 251,
254, 255, 256, 257, 258, 263, 264
Campbell, W. W., 214
Casati, 234
Cayrel, R., 106, 114, 115, 140
Cester, R., 145, 150
Chandrasekhar, S., 103, 140, 241, 268
Chamberlain, J. W., 207, 238
Chapman, S., 138, 140
Chodos, A., 49, 58
Christy, R., 262
Claas, W. J., 118, 119
Clarke, F. W., 29, 38, 30, 170

- Climenhaga, J., 165-167
 Condon, E. U., 160, 169
 Cook, A. F., 57, 58
 Cowan, C. L., 247, 268
 Czyzak, S., 194

 Damgaard, A., 94, 100, 124, 130, 131, 133, 134, 135, 140
 Daniel, R. R., 144, 145, 150
 d'Atkinson, R., 243
 Davis, M. N., 92, 95, 124, 141
 Debenedetti, A., 145, 150
 de Jager, C., 114, 221, 238
 de Marcus, W. C., 36, 37, 38
 Deutsch, A. J., 231, 233, 238
 de Vaucouleurs, G., 236
 Dieke, G. H., 127, 129
 Donn, B., 50, 59
 Dubov, D. E., 119, 125, 140
 Dufay, J., 119, 125, 140

 Eddington, A., S., 97, 104
 Edlén, B., 215
 Edwards, G., 44
 Elsasser, W., 156
 Elste, G., 109, 114, 115, 119, 121, 126, 140
 Engler, D., 143, 150
 Estabrook, F. B., 127, 128, 129

 Farrington, O. C., 45, 58
 Faulkner, D. J., 237
 Feast, M. W., 236, 238
 Fermi, E., 149
 Finnegan, B. J., 41, 58
 Fleischer, M., 31, 38
 Fowler, W., 162, 166, 169, 198, 200, 216, 233, 236, 238, 244, 245, 247, 249, 251, 252, 253, 258, 259, 260, 261, 262, 263, 264, 266, 267
 Franklin, F. A., 233, 238
 Freier, P., 142, 145, 150
 Fujimoto, Y., 146, 147, 149
 Fujita, Y., 228, 238

 Gamow, G., 20, 216, 238, 242, 243, 256
 Garelli, C. M., 145, 150

 Gerling, E. K., 47, 58
 Goldberg, E., 175, 198
 Goldberg, L., 94, 119, 121, 132, 140, 162, 193
 Goldschmidt, V. M., 26, 29, 38, 45, 53, 58, 171
 Gratton, L., 210, 238
 Green, J., 29, 38
 Greenstein, J. L., 119, 125, 140, 163, 169, 206, 208, 212, 216, 229, 231, 233, 234, 238, 254, 265
 Griem, H., 88, 116, 208

 Hack, M., 233, 234, 238
 Hamaguchi, H., 189, 198
 Harris, D., 90, 141
 Harrison, F. B., 247, 268
 Hase, V., 165, 169
 Hasegawa, S., 146, 147, 149
 Hawkins, G. S., 57
 Hayashi, C., 245, 269
 Hayden, R. J., 47, 59
 Hebb, M. H., 66
 Heid, R. L., 127, 129
 Helfer, H. L., 205, 206, 239
 Henrich, L., 241, 268
 Herbig, G., 168, 169
 Herman, R. C., 241, 242, 268
 Hey, Max, 41, 45
 Hill, A., 124, 128
 Hiltner, W. A., 204
 Hjerting, F., 90, 141
 Hoyle, F., 18, 166, 198, 200, 216, 236, 238, 241, 244, 245, 251, 252, 253, 258, 259, 260, 261, 262, 263, 264
 Hughes, D. J., 157
 Huizenga, J. R., 189, 198
 Hunaerts, J., 119, 125, 139, 141
 Hunger, K., 106, 113, 114, 141

 Jensen, H., 157, 169
 Jesse, W. P., 142, 150
 Johnson, Harold, 14, 15, 201, 204, 206
 Johnson, Hugh, 237, 238
 Joy, A. H., 207
 Jugaku, J., 109, 114, 115, 140
 Jurgens, J., 124, 130

- Kandel, R. S., 135
Kaplon, M. F., 143, 145, 150
Keenan, P. C., 206, 209, 227, 228, 229, 238
Keller, G., 206, 209, 238
Kersten, J. A., 131
Khoklov, M. Z., 125, 135
Kigoshi, V., 44, 52, 190, 198
King, R. B., 92, 95, 124, 128, 129, 131, 132, 141, 164
Kingsbury, R. F., 125, 130
Kinman, T. D., 161
Klarmann, J., 143, 145, 150
Klein, O., 241, 269
Kolb, A. C., 88, 116, 208
Kopfermann, H., 92, 141
Koshiba, M., 146, 147, 148, 149, 150
Koslovskaya, S. V., 53, 54, 55, 58
Kristiansson, K., 145
Kruse, H. W., 247, 268
Kuiper, G. P., 41, 164

Ladenburg, R., 88
Laporte, O., 93
Lasch, J. E., 196, 198
Leonard, F. C., 41, 42, 58
Levi, H., 30, 38
Levin, B. Yu., 34, 39, 53, 54, 55, 58
Liller, W., 76, 77, 193
Lipson, J. I., 56, 58
Lochte-Holtgreven, W., 92, 131, 144
Lofgren, E. J., 142, 150
Lohrmann, E., 145, 150
Lovell, B., 41
Lovering, J. F., 42, 49, 58
Lubeck, K., 124, 131
Lynds, B., 24

McDonald, F. B., 145, 150
MacDonald, G. F., 34, 39
McDonald, J. K., 106, 111, 112, 113, 141
McGuire, A. D., 247, 268
McKellar, A., 165, 167, 168, 169, 227, 236, 238
McKinney, C. R., 49, 58

Maecker, H., 125, 130
Marion, J. B., 249, 269
Mason, B., 26, 34, 35, 39, 50, 58
Mathiesen, O., 145
Mathis, J., 66, 70, 77, 117, 237
Mayer, M., 157, 169, 241, 269
Mayne, K. I., 47, 59
Meinke, W. W., 30, 39
Melbourne, W., 208, 238
Melzer, A., 210, 239
Menzel, D. H., 63, 65, 66, 78, 97, 98, 125, 141
Merrill, P. W., 21, 229, 230
Miczaika, G. R., 233, 238
Milligan, J., 106, 111, 112, 113
Millman, P., 41, 57, 58
Milne, E. A., 97, 104
Mina, mi, E., 178, 188, 196
Minkowski, R., 77
Minnaert, M., 98, 105, 118, 141
Mito, I., 146, 147, 149
Mohler, O. C., 119, 141, 162, 169
Moore, C. E., 100, 120, 144
Morgan, W. W., 201, 206, 227, 228, 233, 236, 238
Moseley, 159
Mosen, A. W., 195, 198
Mugglestone, D., 130, 141
Müller, E. A., 119, 121, 132, 135, 140, 162, 193
Münch, G., 212
Mutschlechner, P., 197

Neelakatan, K. A., 144, 145, 150
Neven, L., 114, 221, 238
Newkirk, G., 139, 141
Ney, 145
Nichiporuk, W., 49, 58
Niggli, P., 34, 39
Nininger, H. H., 43, 45, 46, 58
Nishimura, J., 146, 147, 149
Noddack, I., 178, 188, 196
Noon, J. H., 145, 150

Odishaw, H., 160, 169
O'Keefe, J. A., 227
Olehy, D. A., 196, 198

- Olsen, H. N., 92
 Olsen, K. H., 125, 131
 Oort, J., 204
 Opik, E. J., 250, 269
 Oppenheimer, F., 142, 150
 Ornstein, L. S., 131
 Osawa, K., 106
 Osterbrock, D., 72, 76, 78
 Ostrovsky, Yu I., 125, 128, 132, 133, 134

 Patterson, C., 47, 49, 58
 Pavlova, T. G., 47, 58
 Payne, C. H., 215
 Peaslee, D. C., 163, 266, 267, 268
 Pecker, J. C., 106, 109, 110, 116, 135, 141
 Penkin, N. P., 125, 128, 132
 Peters, B., 142, 144, 145, 147, 150
 Phillips, J. G., 96
 Pierce, A. K., 119
 Pillans, H., 24
 Podolawski, J., 241, 269
 Poldervaart, A., 29, 31, 38
 Popper, D. M., 21, 206, 212
 Potratz, H. A., 189, 198
 Pottasch, S. R., 218, 238
 Prior, G. T., 41, 42, 45, 58
 Prokofjew, W. K., 125, 131
 Przybylski, A., 106, 213

 Quassiat, B., 145, 150

 Rankama, K., 26, 29, 31, 39, 57, 58, 151, 152, 158
 Ramsey, H. W., 37, 39
 Reed, G. W., 47, 48, 52, 58, 189, 195, 198
 Reeves, H., 245, 251, 269
 Reines, F., 247, 268
 Reynolds, J. H., 56, 58
 Richardson, R., 119, 163, 169, 235
 Richter, J., 125, 130
 Righini, G., 152, 164, 169
 Ringwood, A. E., 34, 37, 39, 45, 50, 51, 58

 Rohrllich, F., 94, 141
 Roman, N., 207, 210, 233, 238
 Routly, P., 92, 95, 124, 125, 131, 141
 Rudkjöbing, M., 106, 234
 Russell, H. N., 118, 130, 141, 221
 Russell, J. A., 57

 Sahade, J., 216
 Sahama, S., 26, 29, 39
 Saito, S., 106
 Salpeter, E., 216, 238, 249, 250, 269
 Sandage, A., 14, 15, 204, 206, 207
 Sandell, E. B., 30, 39
 Sanford, R. F., 207, 238
 Santirocco, R. A., 205, 239
 Savedoff, M. P., 205, 239
 Schein, M., 142, 145, 148, 150
 Schindewolf, U., 44, 53
 Schmitt, R. A., 190, 196, 198
 Schopp, J. D., 167, 169
 Schultz, 148, 150
 Schuster, A., 96, 97, 103, 104
 Schwarzschild, B., 210, 239
 Schwarzschild, K., 96, 97, 103, 104
 Schwarzschild, M., 18, 24, 203, 210, 230
 Searle, L., 210, 227
 Seaton, M. J., 65, 66, 67, 68, 72
 Severney, A. B., 162
 Sahj, G. A., 165, 169
 Sharp, R. A., 196, 198
 Sherman, D., 157
 Slettebak, A., 233, 239
 Sliusarev, S. G., 216, 239
 Spitzer, L., 210, 239, 264
 Starkova, A. G., 53, 54, 55, 58
 Stewart, J. C., 212, 239
 Stibbs, D. W. N., 136, 141
 Strömgren, B., 80, 118, 125, 141, 201
 Struve, O., 24
 Suess, H., 2, 24, 26, 27, 39, 53, 159, 170, 171, 173, 174, 175, 178, 187, 191, 192, 193, 194, 195, 197, 198, 240, 256, 258, 264
 Suffredini, C. S., 196, 198
 Swihart, T. L., 106, 207, 208, 239
 Swings, P., 164

- Tallone, L., 145, 150
Tandberg, Hanssen, E., 119, 125, 140
Taylor, S. R., 30, 31, 32, 33, 198
Teller, E., 241, 269
ter Haar, D., 241, 269
Teske, R. G., 229, 236, 239
Teucher, M. W., 145, 150
Thackeray, A. D., 212, 239
Thomson, S. J., 47, 59
Traving, G., 106, 114, 115, 141
Treffenberg, L., 241, 268
Treffitz, E., 125, 131
Turkevich, A., 47, 48, 52, 58, 189, 190, 198

Ueno, S., 106
Underhill, A., 106, 112, 116, 141, 216, 239
Unsöld, A., 97, 105, 114, 125, 136, 141, 208
Urey, H. C., 2, 24, 25, 26, 27, 37, 39, 45, 50, 51, 53, 56, 59, 140, 141, 159, 170, 173, 174, 175, 178, 187, 191, 193, 194, 195, 197, 198, 240, 243, 256, 258, 264

van den Bold, H. J., 125, 133
Vigone, M., 145, 150
Villars, D., 125, 131
Vinogradov, A. P., 31, 32, 33, 39, 56, 57, 59
Voigt, H. H., 114, 115, 141
von Hevesy, G., 30, 38
Von Weizsacker, C. F., 248, 269

Waddington, C. J., 145, 147, 150
Wahl, W. A., 49
Waldeskog, B., 145
Walker, M. F., 206
Wallerstein, G., 205, 206, 239
Wardani, E. W., 49, 59
Washington, H. S., 29, 30, 34, 38, 39
Wasserburg, G. J., 47, 59
Webber, W. R., 145, 150
Weidemann, V., 119, 125, 141, 214, 239
Wessel, G., 92, 141
Weymann, R., 137, 141, 235, 239
Whipple, F. L., 40
White, H. E., 94, 141
White, M. L., 68, 78
Wickman, F. E., 29, 39
Wiik, H. B., 44, 59, 175, 198
Wild, P., 266
Wildey, 207, 238
Wildt, R., 210, 239
Wilson, O. C., 71, 78, 168, 169
Wollan, E. O., 142, 150
Woltjer, L., 218, 220, 239
Woolley, R.v.d.R., 136, 141
Wright, K. O., 131
Wrubel, M., 97, 141
Wurm, K., 77, 228
Wyller, A. A., 165, 169
Wyse, A. B., 75, 76, 77, 78

Yates, G. K., 145
Yokoi, K., 146, 147, 149

Zanstra, H., 63, 70, 78

Subject Index

- Achondrites, 44, 46, 47, 48
Actinide elements, 26, 52, 262, 263
Aerolites (stony meteorites) (*see also* Chondrites, Achondrites), 4, 42, 43, 45, 48
Allegan chondrite, 190
Amperometric titration, 30
Andromeda nebula, 13, 206
Anomalous dispersion, 91
Anorthite, 46
Antares, 13
Argonne Laboratory, 163
Arizona (Barringer) meteor crater, 41
Atomic beam, 91, 92
Atomic number, 2
Atomic weight, 2
Augite, 43
Auroral-type transition, 66, 67
- Balmer lines of hydrogen (*see* Hydrogen)
Barium stars (*see* Heavy metal stars)
Beta decay, 47, 155, 156, 247, 248, 252, 255, 256, 259, 262
Betelgeuse, 13
Blanketing effect, 206
Bolometric correction, 11
Boltzmann equation, 9, 102, 110
Bright line spectra of nebulae, 63
Broadening of spectral lines, 87, 107
 by collisions, 88, 95, 96
 by Doppler effect, 89
 of hydrogen, 116
 by natural damping, 87
Bronzite, 43
- California Institute of Technology, 249
Californium, 262
Carbon
 isotopes of, 152, 160, 164–168
 resonance, 249
 stars, 164–168, 213, 220–228, 250
 in sun, 130
Carbon cycle, 18, 22, 166, 248
Carbonaceous chondrites, 43, 51, 197
 ages of, 52
 analyses of, 44
 deuterium in, 57
 as samples of solar system composition, 53, 189
Cerenkov radiation, 142
Ceres, 41
Chalcophile elements, 25, 35
Chondrites, 4, 171, 174, 178
 ages of, 47, 48
 carbonaceous (*see* Carbonaceous chondrites)
 compared with earth's crust, 56
 compositions of, 53, 54, 55
 enstatite, 43, 44
 and mantle of earth, 28
 minerological features of, 46, 49
 origins of, 41, 49, 50
 types of, 43, 45
Chondrules, 43
Chromosphere, 106, 116, 117, 139
Cloud chambers, 142
Collisional damping constant, 88, 95, 96
Collisional excitation of nebular lines, 63, 66, 67, 72, 194
Color index of stars
 defined, 7
 related to stellar composition, 206
 related to spectral class, 10, 201
Color-luminosity diagram for stars, 10, 11, 13, 15–17, 205
Coma Berenices, 13
Comets, 57, 164
Compounds in stellar atmospheres, 8, 9, 221, 228
Continental shield, 29
Continuous stellar absorption coefficient

- cient, 84–86, 103, 106
- Continuous stellar spectra, 82, 85
 - influence of metal-hydrogen ratio on, 201
- Contribution function, 110, 111, 112
- Convection
 - in cores of stars, 18
 - in parent bodies of meteorites, 51
 - in stellar atmospheres, 84, 106, 137, 191, 235, 267
- Core of earth, 28
- Corona, 106
- “Cosmic” abundances, 60, 170, 192
- Cosmic rays
 - abundances from, 146, 147
 - and ages of meteorites, 48, 49
 - charge distribution spectrum of, 144
 - effects on meteoritic isotope ratios, 56
 - energy spectrum of, 143
 - showers, 144
- Crab nebula, 193, 219
- Crust of earth, 25–29
 - chemical composition of, 29–33, 170, 196
 - isotope ratios, 57
 - relation to mean composition of earth, 35
- Curve of growth
 - comparison of stars by means of, 104, 200
 - effects for molecular bands, 165
 - modified for model atmospheres, 108, 113, 118
 - practical example of, 100
 - theory of, 97
- Daubriéllité, 46
- Deuterium, 160–162, 240
 - formation of, 163, 264, 266
 - in meteorites, 57
 - in sun, 152
- Diffusion, influence on composition of stellar atmospheres, 5, 136
- Disk population of galaxy, 209
- Doppler effect on spectral lines, 88–91
- Dunite, 28, 34
- Dwarf sequence, 11
- Dynamo theory of earth’s magnetic field, 28
- Eclogite, 28, 34
- Electric quadrupole transitions, 63
- Electron densities in gaseous nebulae, 71, 72
- Electron temperatures in gaseous nebulae, 72
- Electron scattering in stellar atmospheres, 87, 106
- Elliptical galaxies, 236, 268
- Enstatite, 43
- Equilibrium nuclear reactions, 23, 245, 252–254
- Equilibrium theory of element building, 241–242
- Equivalent width of spectral lines
 - accuracy of, 120
 - defined, 82
 - interpreted, 97
- Evolution, stellar, 16–20, 244 et seq.
- Exothermic reactions, 246, 248
- Fermi cosmic ray mechanism, 149
- Flares, solar, 266
- Fission, 153, 262
- Forbidden lines
 - in gaseous nebulae, 61, 63, 66–68, 194
 - types of, 66, 67
- Fractionation of elements
 - effects on isotope ratios, 57
 - in crust of earth, 25, 26, 29, 34, 35, 175
 - in meteorites, 51, 52
- f*-value
 - defined, 88
 - experimental determination of, 91
 - in molecular spectra, 96
 - solar line data, 121, 124, 125, 138
 - sum rules, 94–95
 - theoretical calculation of, 94
- Galactic clusters, 13, 202, 204, 205
- Gaseous nebulae

- chemical compositions of, 73–75, 194, 237
- ionic concentrations in, 69, 70, 71, 72–75
- spectra of, 60, 63–65
- stratification in, 70
- Gaunt factor, 65
- Geiger counters, 142
- Geochemical affinity, 26, 27, 35
- Giant stars, 12, 205, 206, 250, 255
- Globular clusters, 14, 15, 202, 204–206
- Globules, 16
- Grobanalyse, 105
- Halo
 - of galaxy, 194
 - stars, 204–206
- Harkins' rule, 171
- Heavy metal stars, 200, 228–231, 258
- Helium
 - ages for meteorites, 47
 - in gaseous nebulae, 64, 77, 237
 - in stars, 117, 120, 130, 216, 218, 267
 - isotopes, 152, 163
 - stars, 21, 211–213
 - thermonuclear destruction of, 19, 22, 245, 249, 250
- Hertzsprung-Russell diagram, 10, 12, 14, 15
- Holbrook chondrite, 48
- Holtmark theory of line broadening, 116
- Hyades, 13, 14
- Hydrogen
 - continuous absorption by, 85, 86
 - deficient stars, 21, 200, 211, 212, 213, 226, 227
 - in gaseous nebulae, 64, 65
 - heavy (*see* Deuterium)
 - negative ion of, 84, 103
 - thermonuclear destruction of, 18, 19, 245–248
- Hydromagnetic oscillations, 231
- Hydrostatic equilibrium, 82
- Hyperfine structure, 152
- Hypersthene, 43
- Interstellar medium, 16, 17, 23, 60, 115, 199, 204, 205, 211, 244, 265, 268
 - composition of, 76
- Ionization
 - in gaseous nebulae, 71
 - Saha equation for, 99, 103, 110
- Iron
 - abundance peak of, 173, 240, 243, 252, 261
 - in core of earth, 28
 - in cosmic rays, 148
 - in meteorites, 42, 49
 - in sun 133
 - sun-meteorite discordance 194, 195
- Iron-nickel meteorites (*see also* Siderites), 4, 51
- Isobars, 2, 3, 151, 155, 171, 187
 - excluded, 255
 - proton-rich, 23, 260
 - shielded, 187, 243, 255
 - unshielded, 23, 255
- Isodiaspheres, 2, 3
- Isomer, 2
- Isotones, 2, 3, 151
- Isotopes (*see* Chapter 7)
 - abundances of, 26, 151
 - defined, 2, 3
 - in earth's crust, 158
 - in meteorites, 53, 56, 57, 151
 - in molecular spectra, 152
 - shifts in atomic spectra, 152
 - in stars, 152 *et seq.*
- Jamin interferometer, 91
- jj coupling, 157
- Kamacite, 43
- Kelvin contraction, 18
- Kirchhoff's law, 83, 87, 106
- Kramer's formula, 65, 85
- Lanthanide elements
 - abundances not measurable in sun, 196
 - excess abundance in certain stars, 23, 229, 232

- in earth's crust, 26, 30, 196, 198
- in meteorites, 174, 188, 190, 196
- Lead, 170, 173, 175, 178, 189, 263
 - abundance in meteorites, 52, 178, 189
 - abundance in sun, 135, 138, 190, 197
 - isotopes of, and meteorite ages, 47, 52
- Lick Observatory, 85
- Limb darkening in sun and stars, 84
- Linde Company, 92
- Lithium, 130, 137, 147, 175, 191
 - abundance problems involving 234–236, 264–266
 - isotopes of, 160, 163
- Lithophile elements, 25, 35, 171
- Local thermodynamic equilibrium, deviations from, 83, 106, 107, 110
 - in gaseous nebulae, 61, 65, 67
 - in stellar atmospheres, 106, 116, 135, 199
- LS coupling, 157
- McMath-Hulbert Observatory, 80, 81, 119, 121, 130, 134, 161, 197
- Mafic rocks, 31
- Magellanic clouds, 237
- Magnetic dipole transitions, 63
- Magnetic stars, 231, 265–267
- Magnitudes of stars, 6, 7
- Main sequence of stars, 11, 17
- Mantle of earth, 4, 27
 - chemical composition of, 34
 - relation to chondrites, 28, 34
 - rigidity of, 31
- Mass defect, 154
- Mass spectrograph, 151
- Meson, 142
- Metallic line stars, 223
- Metastable levels, 63, 67
- Meteor, 40, 41, 57, 58
- Meteorite (*see* Achondrites, Chondrites, Iron-nickel meteorites, Siderites, Siderolites (stony-iron meteorites))
- Milne-Eddington approximation, 97, 104
- Model stellar atmospheres, 83, 105, 113, 118
- Mohorovicic discontinuity, 4, 27, 29
- Mount Wilson Observatory, 119, 208
- Nebulae, (*see* Gaseous nebulae)
- Nebular-type transitions, 66, 67
- Neumann lines, 42
- Neutrino, 247
- Neutron
 - activation, 30, 53, 196, 197
 - capture hypotheses, 20, 23, 242–245, 254–262
 - cross section, 157
 - excess, 153, 187
- Nickel
 - in meteorites, 175
 - in sun, 127
- Norton County achondrite, 44
- Novae, 216–218
- Nuclear emulsions, 142
- Nuclei (of atoms)
 - abundances of individual, 176, 177, 179–186
 - binding energy of, 153, 154
 - magic number, 156, 157, 173, 187, 243
 - shell model, 157, 171, 241
 - stability of, 153
- Nuevo Laredo chondrite, 48
- Nutation, 31
- Oblique rotator, 231
- Oddo's rule, 171
- Oldhamite, 46
- Oligoclase, 46
- Olivine, 43, 46
- Optical depth, 82, 83, 103, 105
- Orion nebula, 61, 62, 76, 77, 172, 189, 191, 194
- Orthopyroxene nickel-iron, 46
- Oscillator strength (*see* f -value)
- Oxysphere, 29
- Packing fraction, 154
- Pairing energy, 155
- Parsec, defined, 6
- Pasamonte, achondrite, 47

- Peridotite, 28, 34
 Periodic table, 170
 Phase shift theory of line broadening, 88
 Photo-disintegration, 258, 261
 Photosphere, 96, 106, 117, 139
 Plagioclase, 43, 46
 Planets, 35, 37, 38, 164
 Planetary nebulae (*see* Gaseous nebulae)
 Planetary nebulae nuclei, 214
 Planetoids, 50
 Pleiades, 13, 14
 Plessite, 43
 Polynutron theory, 241
 Potassium-argon ages, 47
 Poynting-Robertson effect, 58
 Precession of equinoxes, 27, 31
 Primary mechanism for excitation of nebular lines, 63, 64
 Promethium, 159
 Proper motions of stars, 6
 Proton-proton reaction, 18, 22, 244, 247
 Proto stars, 235

 Quadratic Stark Effect, 88
 Quartz, 46
 Quebec crater, 41

 R Corona Borealis stars, 165, 213
 Radiative equilibrium, 84
 Rare earths (*see* Lanthanide and Actinide elements)
 Recombination spectra in gaseous nebulae, 64
 Richardton chondrite, 190

 S-type stars (*see* Heavy metal stars)
 Saturation function, 110, 111
 Serpentine, 46
 Schriebersite, 46
 Schuster-Schwarzschild approximation, 96, 97, 100, 103, 104, 126

 Scintillation counters, 142
 Shock tube, 91, 93
 Siderites, 42, 45, 49
 Siderolites (stony-iron meteorites), 42, 45
 Siderophile elements, 25, 35
 Silicon, 112, 113, 116, 131
 Silicon stars, 234
 Snow Telescope, 119
 Solar system, abundances for, 192
 Space probes, 140, 198
 Spallation effects, 143, 148, 163, 235, 265
 Spectral lines, broadening of, 87-91
 Spectral stellar classification, 8, 220
 Spectrum luminosity diagram, 10-12, 14
 Spectrum variable stars, 231
 Spiral arm stars, 203-205
 Standard chemical composition, adapted as that of sun, 5
 Stars
 associations of, 16
 colors of, 6, 7, 79, 201, 206, 208
 evolution of, 16-20, 244
 formation of, 16, 17, 244
 luminosities, 6, 12-15
 population types, 202, 203
 spectra of, 8, 9, 81, 82
 spectral energy curves of, 80, 85
 Subdwarfs, 20, 23, 201, 202, 244, 268
 colors of, 208
 compositions of, 207
 Subgiants, 12
 Sun, 81, 100, 106, 113, 148
 composition of, 118
 flares and cosmic rays, 266
 limb darkening, 84
 sunspots, 139
 Supergiants, 13, 202
 Supernovae, 19, 193, 194, 218-220, 244, 253, 261-265, 267
 Swann-Betatron mechanism, 266
 Synchrotron radiation, 194, 266, 265

 Taenite, 43

- Technetium, 22, 159, 160, 230, 256-258
Transition probability (*see f-value*)
Tridymite, 46
Trifid nebula, 60
Trigonometric parallaxes, 6
Troilite, 46, 49
Turbulence in stellar atmospheres, 99, 233

Ultramafic rocks, 28, 31, 57
Uranium, 153, 178, 189, 232
 in earth's crust, 34
 in meteorites 48, 50, 189
 not detected in sun, 120, 196
Utrecht Observatory, 119

Van Allen belt, 152
Van der Waals interaction, 88
Variation of latitude, 31

Weighting function, 110
White dwarfs, 13, 16, 213, 214, 244
Widmanstätten figures, 42
Wolf-Rayet stars, 21, 215, 216

Ylem, 20, 242, 243

Zeeman effect, 140, 200
Zirconium oxide, 21, 228
Zodiacal light, 58

Index of Stars, Clusters, and Nebulae

- R Andromedae, 229
 14 Andromedae, 211
 Antares (α Scorpii), 13
 21 Aquilae, 163
 T Arae, 236
 Arcturus (α Bootis), 210, 211
 AE Aurigae, 16
 ϵ Aurigae, 217
 Betelgeuse (α Orionis), 13
 RU Camelopardis, 165, 166
 R Canis Minoris, 228
 α_2 Canum Venaticorum, 231, 232, 264
 20 Canum Venaticorum, 205
 ζ Capricorni, 231
 W Cassiopeia, 238
 WZ Cassiopeia, 236
 o Ceti, 168, 229, 230
 ω Centauri, 206
 μ Columbae, 16
 8 Comae, 223
 R Coronae Borealis, 226, 227
 θ Crateris, 85
 ϵ Cygni, 210
 29 Cygni, 113, 114
 55 Cygni, 207
 WX Cygni, 236
 30 Doradus, 237
 κ Geminorum, 230
 DQ Herculis, 227
 89 Herculis, 211
 Hyades, 13, 14
 Krueger 60, 17
 10 Lacertae, 114
 ζ Lacertae, 16
 γ Leonis A, 210
 R Leonis, 229
 α Lyrae, 113
 RR Lyrae, 205
 FU Monocerotis, 229
 ϕ^2 Orionis, 211
 R Orionis, 228
 GP Orionis, 229
 22 Orionis, 113, 114, 117
 γ Pegasi, 113, 114, 117, 194
 h and χ persei, 14
 ζ Persei, 114, 115
 Pleiades, 13, 14
 Rigel, 7
 Ross, 640, 214
 ν Sagittarii, 212, 213
 τ Scorpii, 114, 115
 α Scutum, 211
 Nova Scutum, 217
 β Serpentis, 210
 Sirius, 7
 114 Tauri, 113, 114
 Trifid Nebula, 60
 α Ursae Majoris, 210
 τ Ursae Majoris, 223
 Vega, 113
 Van Maanen 2, 214
 BD + 30°3639, 214, 215
 BD + 35°4013, 216
 HD26, 227
 HD2454, 205
 HD5223, 166
 HD19445, 207
 HD30353, 212, 213
 HD34452, 234
 HD36972, 166
 HD39853, 211
 HD46407, 230, 231, 232
 HD76846, 116
 HD101063, 213
 HD106223, 207, 208
 HD124448, 21, 212
 HD133029, 232
 HD135485, 212
 HD140283, 207, 209
 HD151119, 232

- HD154733, 211
HD156074, 166
HD160641, 21, 212
HD161796, 211
HD161817, 207
HD168476, 212
HD182040, 167
HD192163, 216
HD197604, 166
HD209621, 166
HD219617, 208, 209
HD223392, 166
HDE232078, 206
HZ44, 212
M3, 206
M5, 206
M8, 17, 76
M13, 14, 204, 206
M15, 206
M31, 206, 207, 236
M32, 13
M33, 236, 237
M41, 206
M53, 206
M67, 14, 15
M92, 206
NGC205, 13
NGC246, 214
NGC604, 237
NGC1535, 74
NGC2022, 74
NGC2165, 74
NGC2264, 17
NGC2362, 14
NGC2392, 70, 74
NGC6229, 206
NGC6356, 206, 207
NGC6440, 206
NGC6637, 206
NGC6741, 74
NGC7009, 71, 73
NGC7027, 70, 74, 194
NGC7662, 74
NGCII(IC)5217, 74

